

Diesel engine exhaust emission fractions: clastogenic effects *in vitro*

by

Rachael Ann Whittington

A thesis submitted to the University of Plymouth
in partial fulfilment for the degree of

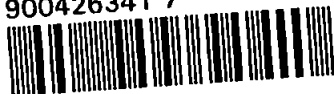
Doctor of Philosophy

Department of Biological Sciences
Faculty of Science

July 1999

UNIVERSITY OF PLYMOUTH	
Item No.	900 426341 7
Date	18 MAY 2000 S
Class No.	7 629.25 WHI
Cont. No.	X70406912-2
LIBRARY SERVICES	

900426341 7



REFERENCE ONLY

LIBRARY STORE

Diesel engine exhaust emission fractions: clastogenic effects *in vitro*

Rachael Ann Whittington

Abstract

Despite being hailed as a green fuel, emissions from diesel engines including particulate matter (PM₁₀ and PM_{2.5}) have been implicated in a range of adverse human health effects from lung and bladder cancers to premature mortality. In this study diesel engine exhaust emissions were collected from a light duty direct injection diesel engine on a standard test bed. Engine conditions of speed and load were altered to provide a set of total emission samples from over the engine's operating range. Diesel emission samples collected were fractionated on a silica column into aliphatic, aromatic, and polar groups of compounds, which were tested for their genotoxicity in the chromosome aberration assay in Chinese hamster ovary CHO-K1 cells both with and without metabolic activation (rat liver S9 fraction).

The aliphatic fractions did not exhibit cytotoxicity up to the maximum concentration assayed, and one emission sample (3000 rpm speed and 5 Nm load) assayed for effect on chromosome aberrations was not clastogenic (up to 600 µg/ml). The aromatic fractions of all engine emission samples assayed and of the fuel were not clastogenic, but did show high levels of cytotoxicity at relatively low doses, raising concern that any genotoxic effect was masked by the toxicity of certain chemicals within the fraction. Further fractionation, using HPLC, was therefore performed which separated the aromatics into various ring sizes. Assay of the ring fractions showed evidence of increasing clastogenicity with increasing ring size, with the 3+ -ring fractions of both the fuel and one emission sample clearly clastogenic when assayed with metabolic activation (evidence of the presence of indirect-acting genotoxic compounds within both samples).

The final fractions to be assayed, the polar fractions, were clastogenic when assayed both with and without metabolic activation. All seven fractions from emission samples collected over a range of speed and load conditions caused highly significant increases in chromosome aberrations at concentrations as low as 20 µg/ml. An engine running for less than 30 minutes at 1000 rpm speed and 55 Nm load (urban driving conditions for a heavily laden vehicle) would emit 148 mg of polar group compounds for every litre of fuel consumed. Polar compounds have been shown to be a highly mutagenic fraction of air particulate samples, and as diesel emissions contribute up to 80 % of the particulate matter in urban air in some areas, diesel emissions and the polar compounds in particular are of real concern to human health.

Contents

Abstract.....	3
List of figures.....	10
List of tables.....	19
List of abbreviations.....	27
Acknowledgements.....	29
Declaration.....	30
1. INTRODUCTION.....	31
1.1 Introduction to the diesel engine.....	32
1.2 A comparison of diesel with petrol powered vehicles.....	32
1.3 Diesel composition.....	35
1.3.1 Diesel particulates.....	35
1.3.2 Polycyclic aromatic compounds and diesel chemistry.....	37
1.3.3 Nitro emissions – nitro-polycyclic aromatic compounds (nitro-PAC) and oxides of nitrogen (NO _x).....	40
1.4 Environmental and human impact of diesel emissions.....	41
1.4.1 Gaseous emissions.....	41
1.4.2 The environmental and health impact of diesel particulate matter.....	42
1.4.3 The potential affects of airborne particulate matter.....	45
1.5 Legislation for diesel emissions and related ambient air pollution.....	48
1.6 Reduction in diesel engine emissions.....	51
1.6.1 Improvements in engine performance to reduce emissions.....	51
1.6.2 Post-combustion treatment devices.....	52
1.6.3 Alternative fuels.....	53
1.7 Assessing the mutagenicity of chemical species.....	53
1.7.1 What is mutagenicity?.....	53
1.7.2 Action of mutagens.....	55
1.7.3 The significance of mutagens.....	56
1.8 The testing of compounds for their mutagenicity.....	58
1.8.1 Carcinogenicity and mutagenicity testing in vivo.....	58
1.8.2 Short term in vitro mutagenicity assays.....	59
1.8.3 Mammalian cell assays.....	59
1.8.4 Metabolic activation.....	60
1.8.5 Assessment of cytotoxic effect of unknown compounds.....	61
1.9 The assessment of mutagenicity through the chromosome aberration assay.....	62
1.9.1 Overview.....	62
1.9.2 The significance of chromosome aberrations.....	63

1.9.3 Mechanism of chromosome aberration induction	65
1.9.4 The chromosome aberration assay method	67
1.9.4.1 Introduction.....	67
1.9.4.2 Mammalian cell lines used to assay for chromosomal aberrations.....	67
1.9.4.3 The CHO cell line	69
1.9.4.4 Aberration assay control	70
1.9.4.5 Sampling time.....	70
1.9.4.6 Culture conditions and choice of concentrations.....	71
1.9.4.7 Scoring of aberrations, statistical analysis and interpretation of results	72
1.10 Mutagenicity of diesel emissions, PAH, and airborne particulates.....	72
1.10.1 Mutagenicity testing of complex samples.....	73
1.10.2 Mutagenicity testing of whole diesel emissions.....	75
1.10.2.1 Assay of whole diesel emission organic extracts in short term assays.....	77
1.10.2.2 Assay of whole diesel emission extracts in vivo.....	77
1.10.3 Mutagenicity and carcinogenicity of fractionated diesel emissions	79
1.10.4 Mutagenicity of fractions of airborne particulates	80
1.10.5 Mutagenicity and carcinogenicity of polycyclic aromatic compounds	80
1.10.5.1 Introduction	80
1.10.5.2 Mutagenicity of polycyclic aromatic hydrocarbons.....	80
1.10.5.3 Mutagenicity of nitro-PAH species	82
1.11 Aims of the investigation	84
 2. MATERIALS AND METHODS	 86
2.1 Collection and preparation of diesel samples.....	87
2.1.1 Diesel engine set up and fuel description.....	87
2.1.2 The Total Exhaust Solvent Stripping Apparatus (TESSA)	89
2.1.3 Collection of emission samples	89
2.1.4 Engine runs performed and emission samples collected.....	91
2.1.5 Sample preparation.....	93
2.2 Fuel and engine emission sample fractionation	93
2.2.1 Silica gel column fractionation of fuel and whole emission samples.....	94
2.2.2 Fractionation of the aromatic group of compounds by HPLC	96
2.3 Mammalian cell line characterisation	98
2.3.1 CHO-K1 cell line details	98
2.3.2 Cytogenetic characterisation of the cell line	98
2.4 Cell line handling and maintenance	99
2.4.1 Routine sub-culture.....	99
2.4.2 Freezing and resuscitation of cells.....	99
2.4.3 Sterility checking of media and cell cultures	101

2.5	Cytogenetic techniques	102
2.5.1	Cell harvesting.....	102
2.5.2	Slide preparation and staining.....	103
2.5.3	Giemsa banding.....	103
2.5.4	Microscopy and photomicrography	104
2.6	Mutagenicity Testing.....	104
2.6.1	Cytotoxicity testing.....	104
2.6.2	Chromosome aberration testing	105
2.6.3	Assessment of mitotic rate.....	106
2.6.4	Scoring metaphase preparations for chromosome aberrations	106
2.6.5	Chromosome aberration assay of a known mutagen in the CHO-K1 cell line	108
2.7	Metabolic activation.....	108
2.7.1	Introduction	108
2.7.2	Preparation of rat liver S9 fraction.....	109
2.7.3	Sterility checking of S9 mix	109
2.7.4	Determination of cytochrome P450.....	110
2.7.5	Composition of S9 mix.....	110
2.7.6	Characterisation of S9 activity in chromosome aberration assays	111
2.7.7	Cytotoxicity testing with metabolic activation.....	112
2.7.8	Chromosome aberration assay with metabolic activation	113
2.8	Summary of cytotoxicity and chromosome aberration assays performed	114
2.9	Statistical analyses.....	114
2.9.1	Variation between replicate cultures in percentage of cells with aberrations.....	115
2.9.2	Chromosome aberration data	116
3.	RESULTS.....	118
3.1	Engine runs performed and emission samples collected.....	119
3.1.1	Mass of total engine emission samples collected.....	119
3.1.2	Fuel consumption of the test engine during sample collection.....	120
3.2	Fuel and emission sample fractionation.....	122
3.2.1	Silica gel column fractionation of fuel and whole emission samples.....	122
3.2.2	Fractionation of the aromatic group of compounds by HPLC	126
3.3	Chinese hamster ovary cell line characterisation	128
3.3.1	Karyotype of CHO-K1 cell line after sub-culture at Plymouth	128
3.3.2	Assessment of chromosome number and polyploidy of CHO-K1 cell line after sub-culture at Plymouth.....	132
3.3.3	Assessment of basal chromosome aberration rate of untreated CHO-K1 cells	134
3.3.4	Chromosome aberration assay of known mutagens in the CHO-K1 cell line	134
3.4	Types of chromosome aberration observed in CHO-K1 cells	135
3.4.1	Polyploidy and endoreduplication	135

3.4.2 Chromosome gaps and 'simple' aberrations	136
3.4.3 Complex chromosome aberrations	136
3.5 Metabolic activation.....	141
3.5.1 Fractions of S9 collected	141
3.5.2 Cytochrome P450 in preparations of S9 collected	141
3.5.3 Characterisation of S9 activity with a known indirect acting mutagen, cyclophosphamide 143	
3.6 Cytotoxicity testing	144
3.6.1 Cytotoxicity of aliphatic fractions of diesel engine emission samples	145
3.6.1.1 The aliphatic fraction of diesel fuel.....	145
3.6.1.2 The aliphatic fraction of diesel emission sample collected at 3000 rpm and 5 Nm .	146
3.6.1.3 The aliphatic fraction of diesel emission sample collected at 1000 rpm and 55 Nm	147
3.6.1.4 The aliphatic fraction of diesel emission sample collected at 1000 rpm and 5 Nm .	148
3.6.2 Cytotoxicity of the aromatic fractions of diesel fuel and engine emissions	148
3.6.2.1 The aromatic fraction of diesel fuel.....	149
3.6.2.2 The aromatic fraction of diesel emission sample collected at 3000 rpm and 5 Nm .	150
3.6.2.3 The aromatic fraction of diesel emission sample collected at 1000 rpm and 55 Nm	151
3.6.2.4 The aromatic fraction of diesel emission sample collected at 1000 rpm and 5 Nm .	152
3.6.3 Cytotoxicity of the 1-ring aromatic fractions of diesel fuel and engine emission samples	153
3.6.3.1 The diesel fuel 1-ring aromatic fraction	153
3.6.3.2 The 1-ring aromatic fraction of the diesel emission sample collected at 3000 rpm speed and 5 Nm load.....	154
3.6.3.3 The 1-ring aromatic fraction of the diesel emission sample collected at 1000 rpm speed and 55 Nm load.....	154
3.6.4 Cytotoxicity of the 2-ring aromatic fractions of diesel fuel and engine emission samples.....	155
3.6.4.1 The diesel fuel 2-ring aromatic fraction	155
3.6.4.2 The 2-ring aromatic fraction of the diesel emission sample collected at 3000 rpm speed and 5 Nm load.....	156
3.6.4.3 The 2-ring aromatic fraction of the diesel emission sample collected at 1000 rpm speed and 55 Nm load.....	157
3.6.5 Cytotoxicity of the 3+ -ring aromatic fractions of diesel fuel and engine emission samples	158
3.6.5.1 The diesel fuel 3+ -ring aromatic fraction	158
3.6.5.2 The 3+ -ring aromatic fraction of the diesel emission sample collected at 3000 rpm speed and 5 Nm load.....	159
3.6.6 Cytotoxicity of the polar fractions of diesel engine emission samples collected during June 1996	160
3.6.6.1 The polar fraction of diesel emission sample collected at 3000 rpm and 5 Nm.....	160
3.6.6.2 The polar fraction of diesel emission collected at 1000 rpm and 55 Nm	161
3.6.6.3 The polar fraction of diesel emission sample collected at 1000 rpm and 5 Nm	162
3.6.7 Cytotoxicity of polar fractions of diesel engine emissions collected in January 1997.	163

3.7 Overview of the cytotoxicity of diesel engine emission sample fractions.....	164
3.7.1 Cytotoxicity of the aliphatic fractions.....	164
3.7.2 Cytotoxicity of the aromatic fractions	166
3.7.3 Cytotoxicity of the 1-ring aromatic fractions	166
3.7.4 Cytotoxicity of the 2-ring aromatic fractions	169
3.7.5 Cytotoxicity of the 3-ring aromatic fractions	169
3.7.6 Cytotoxicity of the polar fractions collected in June 1996.....	172
3.7.7 Summary of the cytotoxicity of the polar fractions collected in January 1997	172
3.7.8 Summary of cytotoxic assays performed without metabolic activation	175
3.7.9 Summary of cytotoxic assays performed with metabolic activation (rat liver S9).....	177
3.8 Chromosome aberration assay results.....	179
3.8.1 The aliphatic fraction.....	179
3.8.1.1 The aliphatic fraction without metabolic activation	179
3.8.1.2 The aliphatic fraction with metabolic activation	181
3.8.2 The aromatic fractions.....	183
3.8.2.1 The aromatic fractions without metabolic activation.....	183
3.8.2.2 The aromatic fractions assayed with metabolic activation.....	189
3.8.3 The 1-ring aromatic fractions	195
3.8.3.1 Clastogenicity of the 1-ring aromatic fractions without S9	195
3.8.3.2 Clastogenicity of the 1-ring aromatic fraction with metabolic activation.....	200
3.8.4 The 2-ring aromatic fractions	205
3.8.4.1 The 2-ring aromatic fractions assayed without metabolic activation.....	205
3.8.4.2 The 2-ring aromatic fractions assayed with metabolic activation.....	210
3.8.5 The 3+ -ring aromatic fractions	216
3.8.5.1 The 3+ -ring aromatic fractions assayed without metabolic activation.....	216
3.8.5.2 The 3+ -ring aromatic fractions assayed with metabolic activation.....	220
3.8.5.3 Summary of the 3+ -ring fractions	224
3.8.6 The polar fractions.....	225
3.8.6.1 The polar fractions collected during June 1996, assayed without metabolic activation	226
3.8.6.2 The polar fractions collected during January 1997, assayed without metabolic activation.....	231
3.8.6.3 The polar fractions assayed with metabolic activation	238
3.9 Summary of diesel engine emission fraction clastogenicity in CHO-K1 cells.....	244
3.10 Overview of chromosome aberration type observed in CHO-K1 cells in response to diesel emission fraction exposure	244
3.10.1 Aberration types observed in clastogenic fractions.....	246
3.10.2 Centromeric disruption after exposure to the polar fractions of diesel engine emissions	247

4. DISCUSSION	250
4.1 Methodology variations and issues raised during the investigation.....	251
4.1.1 The diesel engine emission sampling method.....	251
4.1.2 Emission sample work up and collection during this study	254
4.1.3 Chinese hamster ovary CHO-K1 cell line freezing.....	255
4.1.4 Cytotoxicity assay methodology.....	256
4.1.5 Chromosome aberration assay methodology	256
4.2 Overview of testing	258
4.3 Cytotoxicity of fuel and engine emission sample fractions	259
4.4 Clastogenicity of diesel fuel and engine emission sample fractions.....	262
4.4.1 The aliphatic fraction of diesel engine emissions	262
4.4.2 The aromatic fractions of diesel engine emissions.....	263
4.4.3 Aromatic ring fractions.....	265
4.4.3.1 1-ring aromatic diesel emission sample fractions.....	265
4.4.3.2 2-ring aromatic diesel emission sample fractions.....	266
4.4.3.3 3+ -ring aromatic diesel emission sample fractions.....	269
4.4.4 The polar fractions of diesel engine emission samples	271
4.5 Mass of emission sample fraction obtained during standard sampling.....	274
4.6 Type of chromosome aberrations observed	275
4.7 Implications of the results for health and the environment.....	276
4.8 Conclusions	277
 Appendix A.....	 280
Appendix B.....	302
Appendix C.....	325
Appendix D.....	327
References.....	329

List of Figures

Figure 1. Chemical structures of sixteen polycyclic aromatic hydrocarbons identified as priority pollutants by the World Health Organisation, the European Economic Community, and the US Environmental Protection Agency.....	38
Figure 2. Bioassay directed chemical analysis scheme for identification of mutagenic agents in complex mixtures.....	74
Figure 3. The diesel engine test bed set up at Plymouth.....	88
Figure 4. The Total Exhaust Solvent Scrubbing Apparatus (TESSA) for engine emission sampling.....	90
Figure 5. Scheme of fractionation for diesel fuel and engine emission samples collected over a range of engine speeds (1000 – 3000 rpm) and loads (5 to 75 Nm).....	97
Figure 6. Average mass of total emission sample obtained from six consecutive 2 minute engine emission sampling sessions at each set of engine speed and load conditions.....	120
Figure 7. The average mass of aliphatic, aromatic and polar group compounds, expressed as a percentage of the total mass recovered, from silica column separation of combined samples of diesel fuel and engine emission samples collected at 3000 rpm/5 Nm, 1000 rpm/55 Nm and 1000 rpm/5 Nm.....	125
Figure 8. The average mass of 1-ring, 2-ring, and 3+ -ring compounds, expressed as a percentage of the total aromatic mass recovered, from HPLC separation of samples of diesel fuel and engine emission samples collected at 3000 rpm/5 Nm, and combined emission samples collected at 1000 rpm/5 Nm.....	127
Figure 9. Karyotype of a Chinese hamster ovary CHO-K1 cell and the metaphase spread preparation from which it was derived.....	129
Figure 10. Ideogram of chromosome 1 from the Chinese hamster <i>Cricetulus griseus</i> (a) and photograph of a G-banded chromosome 1 from the Chinese hamster ovary cell line CHO-K1 (b).....	130
Figure 11. Ideogram of chromosome 3 from the Chinese hamster <i>Cricetulus griseus</i> (a) and photograph of a G-banded chromosome 3 from the Chinese hamster ovary cell line CHO-K1 (b).....	131
Figure 12. Ideogram of chromosome 4 from the Chinese hamster <i>Cricetulus griseus</i> (a) and photograph of a G-banded chromosome 4 from the Chinese hamster ovary cell line CHO-K1 (b).....	131
Figure 13. Giemsa banded metaphase preparation of a Chinese hamster ovary CHO-K1 cell.....	132
Figure 14. Chromosome number in 2,000 metaphases of the Chinese hamster ovary CHO-K1 cell line following subculture at Plymouth.....	133
Figure 15. Dose response curve for the direct acting mutagen MNNG showing the number of chromosome aberrations induced in Chinese hamster ovary CHO-K1 cells.....	135

Figure 16. Example of a Giemsa-banded metaphase preparation of a Chinese hamster ovary CHO-K1 cell in which endoreduplication has occurred.....	137
Figure 17. Example of a chromatid gap type aberration observed in Giemsa stained metaphase preparations of Chinese hamster ovary CHO-K1 cells during the study.....	137
Figure 18. Examples of chromosome type aberrations observed in Giemsa stained metaphase preparations of Chinese hamster CHO-K1 cells during the study.....	138
Figure 19. Examples of complex exchange aberrations observed in Giemsa stained metaphase preparations of Chinese hamster CHO-K1 cells during the study.....	139
Figure 20. Examples of Giemsa-banded metaphase preparations of Chinese hamster CHO-K1 cells observed containing multiple aberrations.....	140
Figure 21. Absorbance spectra of reduced cytochrome P450 in two batches (prepared in January 1995 and July 1996) of the S9 fraction of rat livers from male Wistar rats, pre-treated with Aroclor 1254.....	142
Figure 22. Dose response curves for the indirect-acting mutagen cyclophosphamide with two batches of S9 showing the number of chromosome aberrations induced in Chinese hamster ovary CHO-K1 cells.....	143
Figure 23. Cytotoxicity of the aliphatic fractions of diesel fuel and of emission samples collected at 3000 rpm/5 Nm, 1000 rpm/55 Nm and 1000 rpm/5 Nm in the neutral red dye assay in Chinese hamster CHO-K1 cells.....	165
Figure 24. Cytotoxicity of the aromatic fractions of diesel fuel and of emission samples collected at 3000 rpm/5 Nm, 1000 rpm/55 Nm and 1000 rpm/5 Nm in the neutral red dye assay in Chinese hamster CHO-K1 cells.....	167
Figure 25. Cytotoxicity of the 1-ring aromatic fractions of diesel fuel and of emission samples collected at 3000 rpm/5 Nm and 1000 rpm/55 Nm in the neutral red dye assay in Chinese hamster CHO-K1 cells.....	168
Figure 26. Cytotoxicity of the 2-ring aromatic fractions of diesel fuel and of emission samples collected at 3000 rpm/5 Nm and 1000 rpm/55 Nm in the neutral red dye assay in Chinese hamster CHO-K1 cells.....	170
Figure 27. Cytotoxicity of the 3-ring aromatic fractions of diesel fuel and of the emission sample collected at 3000 rpm/5 Nm in the neutral red dye assay in Chinese hamster ovary CHO-K1 cells.....	171
Figure 28. Cytotoxicity of the polar fractions of the emission samples collected at 3000 rpm/5 Nm, 1000 rpm/55 Nm, and 1000 rpm/5 Nm in the neutral red dye assay in Chinese hamster ovary CHO-K1 cells.....	173
Figure 29. Cytotoxicity of the polar fractions of the four emission samples collected at 2000 rpm/30 Nm, 2000 rpm/55 Nm, 3000 rpm/30 Nm, and 3000 rpm/55 Nm in the neutral red dye assay in Chinese hamster ovary CHO-K1 cells, without metabolic activation....	174
Figure 30. Mitotic rate and number of chromosome aberrations induced in Chinese hamster ovary CHO-K1 cells after exposure without metabolic activation to the aliphatic fraction of the diesel engine emission sample collected at 3000 rpm and 5 Nm (ES 40)..	180

Figure 31. Mitotic rate and number of chromosome aberrations induced in Chinese hamster ovary CHO-K1 cells after exposure with metabolic activation (rat liver S9 fraction) to the aliphatic fraction of the diesel engine emission sample collected at 3000 rpm and 5 Nm (ES 40).....	182
Figure 32. Mitotic rate and number of chromosome aberrations induced in Chinese hamster ovary CHO-K1 cells after exposure without metabolic activation to the aromatic fraction of diesel fuel (F 8).....	184
Figure 33. Mitotic rate and number of chromosome aberrations induced in Chinese hamster ovary CHO-K1 cells after exposure without metabolic activation to the aromatic fraction of diesel engine emission sample collected at 3000 rpm and 5 Nm (ES 38+41)..	185
Figure 34. Mitotic rate and number of chromosome aberrations induced in Chinese hamster ovary CHO-K1 cells after exposure without metabolic activation to the aromatic fraction of diesel engine emission sample collected at 1000 rpm and 55 Nm (ES44+47).	186
Figure 35. Mitotic rate and number of chromosome aberrations induced in Chinese hamster ovary CHO-K1 cells after exposure without metabolic activation to the aromatic fraction of diesel engine emission sample collected at 1000 rpm and 5 Nm (ES 50+53)..	187
Figure 36. Summary of the percentage of cells with total aberrations induced in Chinese hamster ovary CHO-K1 cells after exposure without metabolic activation to aromatic fractions of diesel fuel and emission samples ES 38+41 (3000 rpm/5 Nm), ES 44+47 (1000 rpm/55 Nm) and ES 50+53 (1000 rpm/5 Nm).....	188
Figure 37. Mitotic rate and number of chromosome aberrations induced in Chinese hamster ovary CHO-K1 cells after exposure in the presence of metabolic activation (rat liver S9 fraction) to the aromatic fraction of the diesel fuel (F 8).....	190
Figure 38. Mitotic rate and number of chromosome aberrations induced in Chinese hamster ovary CHO-K1 cells after exposure with metabolic activation (rat liver S9 fraction) to the aromatic fraction of the diesel engine emission sample collected at 3000 rpm and 5 Nm (ES 38+41).....	191
Figure 39. Mitotic rate and number of chromosome aberrations induced in Chinese hamster ovary CHO-K1 cells after exposure with metabolic activation (rat liver S9 fraction) to the aromatic fraction of the diesel engine emission sample collected at 1000 rpm and 55 Nm (ES 44+47).....	192
Figure 40. Mitotic rate and number of chromosome aberrations induced in Chinese hamster ovary CHO-K1 cells after exposure with metabolic activation (rat liver S9 fraction) to the aromatic fraction of the diesel engine emission sample collected at 1000 rpm and 5 Nm (ES 50+53)	193
Figure 41. Summary of the percentage of cells with total aberrations induced in Chinese hamster ovary CHO-K1 cells after exposure to aromatic fractions of diesel fuel and emission samples ES 38+41 (3000 rpm/5 Nm), ES 44+47 (1000 rpm/55 Nm) and ES 50+53 (1000 rpm/5 Nm), assayed with metabolic activation (rat liver S9 fraction).....	194

Figure 42. Mitotic rate and number of chromosome aberrations induced in Chinese hamster ovary CHO-K1 cells after exposure without metabolic activation to the 1-ring aromatic fraction of the diesel fuel (R 40)	196
Figure 43. Mitotic rate and number of chromosome aberrations induced in Chinese hamster ovary CHO-K1 cells after exposure without metabolic activation to the 1-ring aromatic fraction of the diesel engine emission sample collected at 3000 rpm and 5 Nm (R 41).....	197
Figure 44. Mitotic rate and number of chromosome aberrations induced in Chinese hamster ovary CHO-K1 cells after exposure without metabolic activation to the 1-ring aromatic fraction of the diesel engine emission sample collected at 1000 rpm and 55 Nm (R 37)	198
Figure 45. Summary of the percentage of cells with total aberrations induced in Chinese hamster ovary CHO-K1 cells after exposure without metabolic activation to 1-ring aromatic fractions of diesel fuel R 40 and emission samples R 41 (3000 rpm/ 5 Nm), and R 37 (1000 rpm/55 Nm)	199
Figure 46. Mitotic rate and number of chromosome aberrations induced in Chinese hamster ovary CHO-K1 cells after exposure with metabolic activation (rat liver S9 fraction) to the 1-ring aromatic fraction of diesel fuel (R 40).....	201
Figure 47. Mitotic rate and number of chromosome aberrations induced in Chinese hamster ovary CHO-K1 cells after exposure with metabolic activation (rat liver S9 fraction) to the 1-ring aromatic fraction of the diesel engine emission sample collected at 3000 rpm and 5 Nm (R 41)	202
Figure 48. Mitotic rate and number of chromosome aberrations induced in Chinese hamster ovary CHO-K1 cells after exposure with metabolic activation (rat liver S9 fraction) to the 1-ring aromatic fraction of the diesel engine emission sample collected at 1000 rpm and 55 Nm (R 37).....	203
Figure 49. Summary of the percentage of cells with total aberrations induced in Chinese hamster ovary CHO-K1 cells after exposure with metabolic activation (rat liver S9 fraction) to 1-ring aromatic fractions of diesel fuel R 40 and emission samples R 41 (3000 rpm/5 Nm), and R 37 (1000 rpm/55 Nm).....	204
Figure 50. Mitotic rate and number of chromosome aberrations induced in Chinese hamster ovary CHO-K1 cells after exposure without metabolic activation to the 2-ring aromatic fraction of diesel fuel (R 26).....	206
Figure 51. Mitotic rate and number of chromosome aberrations induced in Chinese hamster ovary CHO-K1 cells after exposure without metabolic activation to the 2-ring aromatic fraction of the diesel engine emission sample collected at 3000 rpm and 5 Nm (R 32).....	207
Figure 52. Mitotic rate and number of chromosome aberrations induced in Chinese hamster ovary CHO-K1 cells after exposure without metabolic activation to the 2-ring aromatic fraction of diesel engine emission sample collected at 1000 rpm and 55 Nm (R 38).....	208
Figure 53. Summary of the percentage of cells with total aberrations induced in Chinese hamster ovary CHO-K1 cells after exposure without metabolic activation to 2-ring	

aromatic fractions of diesel fuel R 26 and diesel emission samples R 32 (3000 rpm/5 Nm), and R 38 (1000 rpm/55 Nm).....	209
Figure 54. Mitotic rate and number of chromosome aberrations induced in Chinese hamster ovary CHO-K1 cells after exposure with metabolic activation (rat liver S9 fraction) to the 2-ring aromatic fraction of the diesel fuel (R 26).....	212
Figure 55. Mitotic rate and number of chromosome aberrations induced in Chinese hamster ovary CHO-K1 cells after exposure with metabolic activation (rat liver S9 fraction) to the 2-ring aromatic fraction of the diesel engine emission sample collected at 3000 rpm and 5 Nm (R 32).....	213
Figure 56. Mitotic rate and number of chromosome aberrations induced in Chinese hamster ovary CHO-K1 cells after exposure with metabolic activation (rat liver S9 fraction) to the 2-ring aromatic fraction of the diesel engine emission sample collected at 1000 rpm and 55 Nm (R 38).....	214
Figure 57. Summary of the percentage of cells with total aberrations induced in Chinese hamster ovary CHO-K1 cells after exposure with metabolic activation (rat liver S9 fraction) to the 2-ring aromatic fractions of diesel fuel R 26 and the diesel emission samples R 32 (3000 rpm/5 Nm) and R 38 (1000 rpm/55 Nm).....	215
Figure 58. Mitotic rate and number of chromosome aberrations induced in Chinese hamster ovary CHO-K1 cells after exposure without metabolic activation to the 3+ -ring aromatic fraction of diesel fuel (R 27).....	218
Figure 59. Mitotic rate and number of chromosome aberrations induced in Chinese hamster ovary CHO-K1 cells after exposure without metabolic activation to the 3+ -ring aromatic fraction of diesel engine emission sample collected at 3000 rpm and 5 Nm (R 33).....	219
Figure 60. Mitotic rate and number of chromosome aberrations induced in Chinese hamster ovary CHO-K1 cells after exposure with metabolic activation (rat liver S9 fraction) to the 3+ -ring aromatic fraction of diesel fuel (R 27).....	222
Figure 61. Mitotic rate and number of chromosome aberrations induced in Chinese hamster ovary CHO-K1 cells after exposure with metabolic activation (rat liver S9 fraction) to the 3+ -ring aromatic fraction of diesel engine emission sample collected at 3000 rpm and 5 Nm (R 33).....	223
Figure 62. Summary of the chromosome aberrations induced in Chinese hamster ovary CHO-K1 cells after exposure without, and with, metabolic activation (rat liver S9 fraction) to the 3+ -ring fractions of diesel fuel (R27) and the engine emission sample collected at 3000 rpm and 5 Nm (R 33).....	224
Figure 63. Mitotic rate and number of chromosome aberrations induced in Chinese hamster ovary CHO-K1 cells after exposure without metabolic activation to the polar fraction of diesel engine emission sample collected at 3000 rpm and 5 Nm (ES 39).....	228
Figure 64. Mitotic rate and number of chromosome aberrations induced in Chinese hamster ovary CHO-K1 cells after exposure without metabolic activation to the polar fraction of diesel engine emission sample collected at 1000 rpm and 55 Nm (ES 48)....	229

Figure 65. Mitotic rate and number of chromosome aberrations induced in Chinese hamster ovary CHO-K1 cells after exposure without metabolic activation to the polar fraction of diesel engine emission sample collected at 1000 rpm and 5 Nm (ES 51).....	230
Figure 66. Mitotic rate and number of chromosome aberrations induced in Chinese hamster ovary CHO-K1 cells after exposure without metabolic activation to the polar fraction of diesel engine emission sample collected at 2000 rpm and 30 Nm (ES 107)...	233
Figure 67. Mitotic rate and number of chromosome aberrations induced in Chinese hamster ovary CHO-K1 cells after exposure without metabolic activation to the polar fraction of diesel engine emission sample collected at 2000 rpm and 55 Nm (ES 116)...	234
Figure 68. Mitotic rate and number of chromosome aberrations induced in Chinese hamster ovary CHO-K1 cells after exposure without metabolic activation to the polar fraction of diesel engine emission sample collected at 3000 rpm and 30 Nm (ES 119)...	235
Figure 69. Mitotic rate and number of chromosome aberrations induced in Chinese hamster ovary CHO-K1 cells after exposure without metabolic activation to the polar fraction of diesel engine emission sample collected at 3000 rpm and 55 Nm (ES 125)...	236
Figure 70. Number of chromosome aberrations induced in Chinese hamster ovary CHO-K1 cells after exposure without metabolic activation to the polar fractions of seven engine emission samples collected over a range of engine conditions of speed and load.....	237
Figure 71. Mitotic rate and number of chromosome aberrations induced in Chinese hamster ovary CHO-K1 cells after exposure with metabolic activation (rat liver S9 fraction) to the polar fraction of the diesel engine emission sample collected at 3000 rpm and 5 Nm (ES 39).....	240
Figure 72. Mitotic rate and number of chromosome aberrations induced in Chinese hamster ovary CHO-K1 cells after exposure with metabolic activation (rat liver S9 fraction) to the polar fraction of the diesel engine emission sample collected at 1000 rpm and 55 Nm (ES 48).....	241
Figure 73. Mitotic rate and number of chromosome aberrations induced in Chinese hamster ovary CHO-K1 cells after exposure with metabolic activation (rat liver S9 fraction) to the polar fraction of the diesel engine emission sample collected at 1000 rpm and 5 Nm (ES 51).....	242
Figure 74. Number of chromosome aberrations induced in Chinese hamster ovary CHO-K1 cells after exposure with metabolic activation (rat liver S9 fraction) to the polar fractions of three diesel engine emission samples collected at 3000 rpm/5 Nm, 1000 rpm/55 Nm, and 1000 rpm/5 Nm.....	243
Figure 75. Summary of diesel fuel and engine emission samples assayed and their resultant clastogenic activity in the chromosome aberration assay in Chinese hamster ovary CHO-K1 cells, assayed both with and without metabolic activation.....	245
Figure 76. The ratios of simple to complex chromosome aberrations induced in Chinese hamster ovary CHO-K1 cells after exposure to clastogenic fractions of diesel engine fuel and emission samples.....	247

Figure 77. Centromeric disruption of Chinese hamster ovary CHO-K1 cells after exposure to the polar fraction of diesel engine emission samples collected over a range of engine speed and load conditions.....	248
Figure 78. Centromeric disruption of Chinese hamster ovary CHO-K1 cells after exposure to the polar fraction of diesel engine emission samples collected over a range of engine speed and load conditions.....	246
Figure 79. Relative abundance of selected aromatic compounds in the diesel fuel and engine emission 3+ -ring fractions detected by GC/MS.....	271
Figure 80. The extrapolated mass of polar fraction group compounds emitted per minute from the diesel test engine for various engine conditions of speed and load tested.....	275
Figure 81. Cytotoxicity of the aliphatic fraction F 7 of the diesel fuel in the neutral red dye assay in Chinese hamster ovary CHO-K1 cells, without metabolic activation.....	281
Figure 82. Cytotoxicity of the aliphatic fraction F 7 of diesel fuel in the neutral red dye assay in Chinese hamster ovary CHO-K1 cells, with metabolic activation (rat liver S9 fraction)	281
Figure 83. Cytotoxicity of the aliphatic fraction ES 37+40, from diesel engine emission sample collected at 3000 rpm/5 Nm, in the neutral red dye assay in Chinese hamster ovary CHO-K1 cells without metabolic activation.....	282
Figure 84. Cytotoxicity of the aliphatic fraction ES 37+40, from diesel engine emission sample collected at 3000 rpm/5 Nm, in the neutral red dye assay in Chinese hamster ovary CHO-K1 cells with metabolic activation (rat liver S9 fraction).....	282
Figure 85. Cytotoxicity of the aliphatic fraction ES 43+46, from diesel engine emission sample collected at 1000 rpm/55 Nm, in the neutral red dye assay in Chinese hamster ovary CHO-K1 cells without metabolic activation.....	283
Figure 86. Cytotoxicity of the aliphatic fraction ES 43+46, from diesel engine emission sample collected at 1000 rpm/55 Nm, in the neutral red dye assay in Chinese hamster ovary CHO-K1 cells with metabolic activation (rat liver S9 fraction).....	283
Figure 87. Cytotoxicity of the aliphatic fraction ES 49+52, from diesel engine emission sample collected at 1000 rpm/5 Nm, in the neutral red dye assay in Chinese hamster ovary CHO-K1 cells without metabolic activation.....	284
Figure 88. Cytotoxicity of the aliphatic fraction ES 49+52, from diesel engine emission sample collected at 1000 rpm/5 Nm, in the neutral red dye assay in Chinese hamster ovary CHO-K1 cells with metabolic activation (rat liver S9 fraction).....	284
Figure 89. Cytotoxicity of the aromatic fraction F 8 of diesel fuel in the neutral red dye assay in Chinese hamster ovary CHO-K1 cells without metabolic activation.....	285
Figure 90. Cytotoxicity of the aromatic fraction F 8 of diesel fuel in the neutral red dye assay in Chinese hamster ovary CHO-K1 cells with metabolic activation (rat liver S9 fraction)	285

Figure 91. Cytotoxicity of the aromatic fraction ES 38+41, from diesel engine emission sample collected at 3000 rpm/5 Nm, in the neutral red dye assay in Chinese hamster ovary CHO-K1 cells without metabolic activation.....	286
Figure 92. Cytotoxicity of the aromatic fraction ES 38+41, from diesel engine emission sample collected at 3000 rpm/5 Nm, in the neutral red dye assay in Chinese hamster ovary CHO-K1 cells with metabolic activation (rat liver S9 fraction).....	286
Figure 93. Cytotoxicity of the aromatic fraction ES 44+47, from diesel engine emission sample collected at 1000 rpm/55 Nm, in the neutral red dye assay in Chinese hamster ovary CHO-K1 cells without metabolic activation.....	287
Figure 94. Cytotoxicity of the aromatic fraction ES 44+47, from diesel engine emission sample collected at 1000 rpm/55 Nm, in the neutral red dye assay in Chinese hamster ovary CHO-K1 cells with metabolic activation (rat liver S9 fraction).....	287
Figure 95. Cytotoxicity of the aromatic fraction ES 50+53, from diesel engine emission sample collected at 1000 rpm/5 Nm, in the neutral red dye assay in Chinese hamster ovary CHO-K1 cells without metabolic activation.....	288
Figure 96. Cytotoxicity of the aromatic fraction ES 50+53, from diesel engine emission sample collected at 1000 rpm/5 Nm, in the neutral red dye assay in Chinese hamster ovary CHO-K1 cells with metabolic activation (rat liver S9 fraction)	288
Figure 97. Cytotoxicity of the 1-ring aromatic fraction R 40 from diesel fuel in the neutral red dye assay in Chinese hamster ovary CHO-K1 cells, without metabolic activation....	289
Figure 98. Cytotoxicity of the 1-ring aromatic fraction R 40 from diesel fuel in the neutral red dye assay in Chinese hamster ovary CHO-K1 cells, with metabolic activation (rat liver S9 fraction)	289
Figure 99. Cytotoxicity of the 1-ring aromatic fraction R 41, from diesel engine emission sample collected at 3000 rpm and 5 Nm, in the neutral red dye assay in Chinese hamster ovary CHO-K1 cells without metabolic activation.....	290
Figure 100. Cytotoxicity of the 1-ring aromatic fraction R 41, from diesel engine emission sample collected at 3000 rpm and 5 Nm, in the neutral red dye assay in Chinese hamster ovary CHO-K1 cells with metabolic activation (rat liver S9 fraction)	290
Figure 101. Cytotoxicity of the 1-ring aromatic fraction R 28+37, from diesel engine emission sample collected at 1000 rpm and 55 Nm, in the neutral red dye assay in Chinese hamster ovary CHO-K1 cells without metabolic activation.....	291
Figure 102. Cytotoxicity of the 1-ring aromatic fraction R 28+37, from diesel engine emission sample collected at 1000 rpm and 55 Nm, in the neutral red dye assay in Chinese hamster ovary CHO-K1 cells with metabolic activation (rat liver S9 fraction).....	291
Figure 103. Cytotoxicity of the 2-ring aromatic fraction R 26 from diesel fuel in the neutral red dye assay in Chinese hamster ovary CHO-K1 cells, without metabolic activation.....	292
Figure 104. Cytotoxicity of the 2-ring aromatic fraction R 26 from diesel fuel in the neutral red dye assay in Chinese hamster ovary CHO-K1 cells, with metabolic activation (rat liver S9 fraction).....	292

Figure 105. Cytotoxicity of the 2–ring aromatic fraction R 32, from diesel engine emission sample collected at 3000 rpm and 5 Nm, in the neutral red dye assay in Chinese hamster ovary CHO-K1 cells without metabolic activation.....	293
Figure 106. Cytotoxicity of the 2–ring aromatic fraction R 32, from diesel engine emission sample collected at 3000 rpm and 5 Nm, in the neutral red dye assay in Chinese hamster ovary CHO-K1 cells with metabolic activation (rat liver S9 fraction).....	293
Figure 107. Cytotoxicity of the 2–ring aromatic fraction R 29+38, from diesel engine emission sample collected at 1000 rpm and 55 Nm, in the neutral red dye assay in Chinese hamster ovary CHO-K1 cells without metabolic activation.....	294
Figure 108. Cytotoxicity of the 2–ring aromatic fraction R 29+38, from diesel engine emission sample collected at 1000 rpm and 55 Nm, in the neutral red dye assay in Chinese hamster ovary CHO-K1 cells with metabolic activation (rat liver S9 fraction).....	294
Figure 109. Cytotoxicity of the 3–ring aromatic fraction R 27 from diesel fuel in the neutral red dye assay in Chinese hamster ovary CHO-K1 cells, without metabolic activation.....	295
Figure 110. Cytotoxicity of the 3–ring aromatic fraction R 27 from diesel fuel in the neutral red dye assay in Chinese hamster ovary CHO-K1 cells, with metabolic activation (rat liver S9 fraction)	295
Figure 111. Cytotoxicity of the 3–ring aromatic fraction R 33, from diesel engine emission sample collected at 3000 rpm and 5 Nm, in the neutral red dye assay in Chinese hamster ovary CHO-K1 cells without metabolic activation.....	296
Figure 112. Cytotoxicity of the 3–ring aromatic fraction R 33, from diesel engine emission sample collected at 3000 rpm and 5 Nm, in the neutral red dye assay in Chinese hamster ovary CHO-K1 cells with metabolic activation (rat liver S9 fraction).....	296
Figure 113. Cytotoxicity of the polar fraction ES 39+42, from diesel engine emission sample collected at 3000 rpm and 5 Nm, in the neutral red dye assay in Chinese hamster ovary CHO-K1 cells without metabolic activation.....	297
Figure 114. Cytotoxicity of the polar fraction ES 39+42, from diesel engine emission sample collected at 3000 rpm and 5 Nm, in the neutral red dye assay in Chinese hamster ovary CHO-K1 cells with metabolic activation (rat liver S9 fraction)	297
Figure 115. Cytotoxicity of the polar fraction ES 45+48, from diesel engine emission sample collected at 1000 rpm and 55 Nm, in the neutral red dye assay in Chinese hamster ovary CHO-K1 cells without metabolic activation.....	298
Figure 116. Cytotoxicity of the polar fraction ES 45+48, from diesel engine emission sample collected at 1000 rpm and 55 Nm, in the neutral red dye assay in Chinese hamster ovary CHO-K1 cells with metabolic activation (rat liver S9 fraction).....	298
Figure 117. Cytotoxicity of the polar fraction ES 51+54, from diesel engine emission sample collected at 1000 rpm and 5 Nm, in the neutral red dye assay in Chinese hamster ovary CHO-K1 cells without metabolic activation.....	299

Figure 118. Cytotoxicity of the polar fraction ES 51+54, from diesel engine emission sample collected at 1000 rpm and 5 Nm, in the neutral red dye assay in Chinese hamster ovary CHO-K1 cells with metabolic activation (rat liver S9 fraction).....	299
Figure 119. Cytotoxicity of the polar fraction ES 107, from diesel engine emission sample collected at 2000 rpm and 30 Nm, in the neutral red dye assay in Chinese hamster ovary CHO-K1 cells without metabolic activation.....	300
Figure 120. Cytotoxicity of the polar fraction ES 116, from diesel engine emission sample collected at 2000 rpm and 55 Nm, in the neutral red dye assay in Chinese hamster ovary CHO-K1 cells without metabolic activation.....	300
Figure 121. Cytotoxicity of the polar fraction ES 119, from diesel engine emission sample collected at 3000 rpm and 30 Nm, in the neutral red dye assay in Chinese hamster ovary CHO-K1 cells without metabolic activation.....	301
Figure 122. Cytotoxicity of the polar fraction ES 125, from diesel engine emission sample collected at 3000 rpm and 55 Nm, in the neutral red dye assay in Chinese hamster ovary CHO-K1 cells without metabolic activation.....	301
Figure 123. GC/MS trace for the 3+ -ring aromatic fractions, obtained by HPLC fractionation of the diesel fuel and engine emission sample collected at 3000 rpm and 5 Nm, showing relative abundance of peak compounds.....	326
Figure 124. Measured outputs of smoke, hydrocarbons, NO _x , and carbon monoxide for the diesel test engine used during this study measured at each condition of speed and load used for emission sampling.....	328

List of Tables

Table 1. Chemical compounds and species groups found in diesel engine exhaust emissions.....	36
Table 2. The IARC carcinogenic classification of selected polycyclic aromatic compounds from diesel engine particulate emissions.....	39
Table 3. Selected European Community Directives relating to the regulation of emissions from diesel vehicles.....	49
Table 4. Summary of specific objectives for eight pollutants proposed by the UK National Air Quality Strategy.....	49
Table 5. Major variations in materials and methodology affecting chemical make up of diesel engine emissions and emission fractions assessed for mutagenicity in different studies.....	76
Table 6. Properties of the low sulphur No.2 DERV diesel fuel used throughout this research work (figures provided by the fuel refiner)	87

Table 7. Diesel engine runs performed, fuel consumption, and sample masses achieved from each consecutive 2 minute sampling session.....	92
Table 8. Constituents of alternative freezing media used to store Chinese hamster ovary CHO-K1 cells at -70°C and in liquid nitrogen (-196°C)	100
Table 9. Classification of structural chromosome aberrations.....	107
Table 10. Composition of S9 mixes used in cytotoxicity and chromosome aberration assays requiring metabolic activation.....	111
Table 11. Summary of all fuel and emission samples assayed for their cytotoxic effect in the neutral red dye assay in CHO-K1 cells, and subsequently for their clastogenicity in the chromosome aberration assay in CHO-K1 cells.....	114
Table 12. Criteria for classification of results of statistical analyses of data produced from chromosome aberration assays.....	117
Table 13. Engine diesel fuel consumption (litres/min) recorded during sample collection for each set of engine conditions of speed and load.....	121
Table 14. Summary of the silica column fractionation of fuel and diesel engine emission samples collected during 2 minute sampling over a range of engine conditions of speed and load, the fraction masses achieved, and percentage recovery of the original sample.....	124
Table 15. Fuel and diesel engine emission samples collected during 5 minute sampling at three different engine conditions of speed and load, their total mass and the masses of aromatic ring fractions obtained after separation by HPLC.....	126
Table 16. Cytotoxic effect of diesel fuel and engine emission sample fractions, collected over a range of engine speed and load, on the viability of Chinese hamster ovary CHO-K1 cells measured in the neutral red dye assay.....	176
Table 17. Cytotoxic effect of diesel fuel and engine emission sample fractions, collected over a range of engine speed and load, on the viability of Chinese hamster ovary CHO-K1 cells measured in the neutral red dye assay with metabolic activation.....	178
Table 18. Chromosome aberrations induced in Chinese hamster ovary CHO-K1 cells exposed without metabolic activation to the aliphatic fraction of the diesel engine emission sample collected at 3000 rpm and 5 Nm (ES 40)	180
Table 19. Chromosome aberrations induced in Chinese hamster ovary CHO-K1 cells exposed with metabolic activation (rat liver S9 fraction) to the aliphatic fraction of the diesel engine emission sample collected at 3000 rpm and 5 Nm (ES 40).....	182
Table 20. Chromosome aberrations induced in Chinese hamster ovary CHO-K1 cells exposed without metabolic activation to the aromatic fraction of the diesel fuel (F 8)....	184
Table 21. Chromosome aberrations induced in Chinese hamster ovary CHO-K1 cells exposed without metabolic activation to the aromatic fraction of the diesel engine emission sample collected at 3000 rpm and 5 Nm (ES 38+41)	185

Table 22. Chromosome aberrations induced in Chinese hamster ovary CHO-K1 cells exposed without metabolic activation to the aromatic fraction of the diesel engine emission sample collected at 1000 rpm and 55 Nm (ES 44+47)	186
Table 23. Chromosome aberrations induced in Chinese hamster ovary CHO-K1 cells exposed without metabolic activation to the aromatic fraction of the engine emission sample collected at 1000 rpm and 5 Nm (ES 50+53)	187
Table 24. Chromosome aberrations induced in Chinese hamster ovary CHO-K1 cells exposed in the presence of metabolic activation (rat liver S9 fraction) to the aromatic fraction of diesel fuel sample F 8.....	190
Table 25. Chromosome aberrations induced in Chinese hamster ovary CHO-K1 cells exposed with metabolic activation (rat liver S9 fraction) to the aromatic fraction of the diesel engine emission sample collected at 3000 rpm and 5 Nm (ES 38+41).....	191
Table 26. Chromosome aberrations induced in Chinese hamster ovary CHO-K1 cells exposed with metabolic activation (rat liver S9 fraction) to the aromatic fraction of the diesel engine emission sample collected at 1000 rpm and 55 Nm (ES 44+47).....	192
Table 27. Chromosome aberrations induced in Chinese hamster ovary CHO-K1 cells exposed with metabolic activation (rat liver S9 fraction) to the aromatic fraction of the diesel engine emission sample collected at 1000 rpm and 5 Nm (ES 44+47).....	193
Table 28. Chromosome aberrations induced in Chinese hamster ovary CHO-K1 cells exposed without metabolic activation to the 1-ring aromatic fraction of the diesel fuel (R 40)	196
Table 29. Chromosome aberrations induced in Chinese hamster ovary CHO-K1 cells exposed without metabolic activation to the 1-ring aromatic fraction of the diesel engine emission sample collected at 3000 rpm and 5 Nm (R 41)	197
Table 30. Chromosome aberrations induced in Chinese hamster ovary CHO-K1 cells exposed without metabolic activation to the 1-ring aromatic fraction of the engine emission sample collected at 1000 rpm and 55 Nm (R 37)	198
Table 31. Chromosome aberrations induced in Chinese hamster ovary CHO-K1 cells exposed with metabolic activation (rat liver S9 fraction) to the 1-ring aromatic fraction of the diesel fuel (R 40)	201
Table 32. Chromosome aberrations induced in Chinese hamster ovary CHO-K1 cells exposed with metabolic activation (rat liver S9 fraction) to the 1-ring aromatic fraction of the diesel engine emission sample collected at 3000 rpm and 5 Nm (R 41).....	202
Table 33. Chromosome aberrations induced in Chinese hamster ovary CHO-K1 cells exposed with metabolic activation (rat liver S9 fraction) to the 1-ring aromatic fraction of the diesel engine emission sample collected at 1000 rpm and 55 Nm (R 37).....	203
Table 34. Chromosome aberrations induced in Chinese hamster ovary CHO-K1 cells exposed without metabolic activation to the 2-ring aromatic fraction of diesel fuel (R 26).....	206

Table 35. Chromosome aberrations induced in Chinese hamster ovary CHO-K1 cells exposed without metabolic activation to the 2-ring aromatic fraction of the diesel engine emission sample collected at 3000 rpm and 5 Nm (R 32)	207
Table 36. Chromosome aberrations induced in Chinese hamster ovary CHO-K1 cells exposed without metabolic activation to the 2-ring aromatic fraction of the diesel engine emission sample collected at 1000 rpm and 55 Nm (R 38)	208
Table 37. Chromosome aberrations induced in Chinese hamster ovary CHO-K1 cells exposed with metabolic activation (rat liver S9 fraction) to the 2-ring aromatic fraction of the diesel fuel (R 26)	212
Table 38. Chromosome aberrations induced in Chinese hamster ovary CHO-K1 cells exposed with metabolic activation (rat liver S9 fraction) to the 2-ring aromatic fraction of the diesel engine emission collected at 3000 rpm and 5 Nm (R 32)	213
Table 39. Chromosome aberrations induced in Chinese hamster ovary CHO-K1 cells exposed with metabolic activation (rat liver S9 fraction) to the 2-ring aromatic fraction of the diesel engine emission collected at 1000 rpm and 55 Nm (R 38)	214
Table 40. Chromosome aberrations induced in Chinese hamster ovary CHO-K1 cells exposed without metabolic activation to the 3+ -ring aromatic fraction of diesel fuel (R 27)	218
Table 41. Chromosome aberrations induced in Chinese hamster ovary CHO-K1 cells exposed without metabolic activation to the 3+ -ring aromatic fraction of the diesel engine emission sample collected at 3000 rpm and 5 Nm (R 33)	219
Table 42. Chromosome aberrations induced in Chinese hamster ovary CHO-K1 cells exposed with metabolic activation (rat liver S9 fraction) to the 3+ -ring aromatic fraction of diesel fuel (R 27)	222
Table 43. Chromosome aberrations induced in Chinese hamster ovary CHO-K1 cells exposed with metabolic activation (rat liver S9 fraction) to the 3+ -ring aromatic fraction of engine emission sample collected at 3000 rpm and 5 Nm (R 33)	223
Table 44. Chromosome aberrations induced in Chinese hamster ovary CHO-K1 cells exposed without metabolic activation to the polar fraction of diesel engine emission sample collected at 3000 rpm and 5 Nm (ES 39)	228
Table 45. Chromosome aberrations induced in Chinese hamster ovary CHO-K1 cells exposed without metabolic activation to the polar fraction of diesel engine emission sample collected at 1000 rpm and 55 Nm (ES 48)	229
Table 46. Chromosome aberrations induced in Chinese hamster ovary CHO-K1 cells exposed without metabolic activation to the polar fraction of engine emission sample collected at 1000 rpm and 5 Nm (ES 51)	230
Table 47. Chromosome aberrations induced in Chinese hamster ovary CHO-K1 cells exposed without metabolic activation to the polar fraction of the diesel engine emission sample collected at 2000 rpm and 30 Nm (ES 107)	233

Table 48. Chromosome aberrations induced in Chinese hamster ovary CHO-K1 cells exposed without metabolic activation to the polar fraction of the diesel engine emission sample collected at 2000 rpm and 55 Nm (ES 116)	234
Table 49. Chromosome aberrations induced in Chinese hamster ovary CHO-K1 cells exposed without metabolic activation to the polar fraction of the diesel engine emission sample collected at 3000 rpm and 30 Nm (ES 119)	235
Table 50. Chromosome aberrations induced in Chinese hamster ovary CHO-K1 cells exposed without metabolic activation to the polar fraction of the diesel engine emission sample collected at 3000 rpm and 55 Nm (ES 125)	236
Table 51. Chromosome aberrations induced in Chinese hamster ovary CHO-K1 cells exposed with metabolic activation (rat liver S9 fraction) to the polar fraction of the diesel engine emission sample collected at 3000 rpm and 5 Nm (ES 39).....	240
Table 52. Chromosome aberrations induced in Chinese hamster ovary CHO-K1 cells exposed with metabolic activation (rat liver S9 fraction) to the polar fraction of the diesel engine emission sample collected at 1000 rpm and 55 Nm (ES 48).....	241
Table 53. Chromosome aberrations induced in Chinese hamster ovary CHO-K1 cells exposed with metabolic activation (rat liver S9 fraction) to the polar fraction of the diesel engine emission sample collected at 1000 rpm and 5 Nm (ES 51).....	242
Table 54. Chromosome aberrations observed in Chinese hamster ovary CHO-K1 cells after exposure to aliphatic diesel emission sample ES 40 (3000 rpm speed/ 5 Nm load) without metabolic activation.....	303
Table 55. Chromosome aberrations observed in Chinese hamster ovary CHO-K1 cells after exposure to aliphatic diesel emission sample ES 40 (3000 rpm speed/ 5 Nm load) with metabolic activation (rat liver S9 fraction)	303
Table 56. Chromosome aberrations observed in Chinese hamster ovary CHO-K1 cells after exposure to the aromatic fraction F 8 of diesel fuel, without metabolic activation...	304
Table 57. Chromosome aberrations observed in Chinese hamster ovary CHO-K1 cells after exposure to the aromatic fraction F 8 of diesel fuel, with metabolic activation (rat liver S9 fraction)	304
Table 58. Chromosome aberrations observed in Chinese hamster ovary CHO-K1 cells after exposure to aromatic diesel emission sample ES 38+41 (3000 rpm speed/ 5 Nm load), without metabolic activation.....	305
Table 59. Chromosome aberrations observed in Chinese hamster ovary CHO-K1 cells after exposure to aromatic diesel emission sample ES 38+41 (3000 rpm speed/ 5 Nm load), with metabolic activation (rat liver S9 fraction)	306
Table 60. Chromosome aberrations observed in Chinese hamster ovary CHO-K1 cells after exposure to aromatic diesel emission sample ES 38+41 (3000 rpm speed/ 5 Nm load), with 2 x S9 mix metabolic activation (double concentration of rat liver S9 fraction).....	306
Table 61. Chromosome aberrations observed in Chinese hamster ovary CHO-K1 cells after exposure to aromatic diesel emission sample ES 44+47 (1000 rpm speed/ 55 Nm load) without metabolic activation.....	307

Table 62. Chromosome aberrations observed in Chinese hamster ovary CHO-K1 cells after exposure to aromatic diesel emission sample ES 44+47 (1000 rpm speed/ 55 Nm load) with metabolic activation (rat liver S9 fraction)	307
Table 63. Chromosome aberrations observed in Chinese hamster ovary CHO-K1 cells after exposure to aromatic diesel emission sample ES 50+53 (1000 rpm speed/ 5 Nm load) without metabolic activation.....	308
Table 64. Chromosome aberrations observed in Chinese hamster ovary CHO-K1 cells after exposure to aromatic diesel emission sample ES 50+53 (1000 rpm speed/ 5 Nm load) with metabolic activation (rat liver S9 fraction)	308
Table 65. Chromosome aberrations observed in Chinese hamster ovary CHO-K1 cells after exposure to 1-ring aromatic fraction of diesel fuel (R 40) without metabolic activation.....	309
Table 66. Chromosome aberrations observed in Chinese hamster ovary CHO-K1 cells after exposure to 1-ring aromatic fraction of diesel fuel (R 40) with metabolic activation (rat liver S9 fraction)	309
Table 67. Chromosome aberrations observed in Chinese hamster ovary CHO-K1 cells after exposure to 1-ring aromatic diesel emission fraction R 41 (3000 rpm speed/ 5 Nm load) without metabolic activation.....	310
Table 68. Chromosome aberrations observed in Chinese hamster ovary CHO-K1 cells after exposure to 1-ring aromatic diesel emission fraction R 41 (3000 rpm speed/ 5 Nm load) with metabolic activation (rat liver S9 fraction)	310
Table 69. Chromosome aberrations observed in Chinese hamster ovary CHO-K1 cells after exposure to 1-ring aromatic diesel emission fraction R 37 (1000 rpm speed/ 55 Nm load) without metabolic activation.....	311
Table 70. Chromosome aberrations observed in Chinese hamster ovary CHO-K1 cells after exposure to 1-ring aromatic diesel emission fraction R 37 (1000 rpm speed/ 55 Nm load) with metabolic activation (rat liver S9 fraction)	311
Table 71. Chromosome aberrations observed in Chinese hamster ovary CHO-K1 cells after exposure to the 2-ring aromatic fraction R 26 of diesel fuel without metabolic activation.....	312
Table 72. Chromosome aberrations observed in Chinese hamster ovary CHO-K1 cells after exposure to the 2-ring aromatic fraction R 26 of diesel fuel with metabolic activation (rat liver S9 fraction)	312
Table 73. Chromosome aberrations observed in Chinese hamster ovary CHO-K1 cells after exposure to the 2-ring aromatic diesel emission fraction R 32 (3000 rpm speed/ 5 Nm load) without metabolic activation.....	313
Table 74. Chromosome aberrations observed in Chinese hamster ovary CHO-K1 cells after exposure to the 2-ring aromatic diesel emission fraction R 32 (3000 rpm speed/ 5 Nm load) with metabolic activation (rat liver S9 fraction)	313

Table 75. Chromosome aberrations observed in Chinese hamster ovary CHO-K1 cells after exposure to the 2–ring aromatic diesel emission fraction R 38 (1000 rpm speed/ 55 Nm load) without metabolic activation.....	314
Table 76. Chromosome aberrations observed in Chinese hamster ovary CHO-K1 cells after exposure to the 2–ring aromatic diesel emission fraction R 38 (1000 rpm speed/ 55 Nm load) with metabolic activation (rat liver S9 fraction)	314
Table 77. Chromosome aberrations observed in Chinese hamster ovary CHO-K1 cells after exposure to the 3–ring aromatic fraction R 27 from diesel fuel without metabolic activation.....	315
Table 78. Chromosome aberrations observed in Chinese hamster ovary CHO-K1 cells after exposure to the 3–ring aromatic fraction R 27 from diesel fuel with metabolic activation (rat liver S9 fraction)	315
Table 79. Chromosome aberrations observed in Chinese hamster ovary CHO-K1 cells after exposure to the 3–ring aromatic diesel emission fraction R 33 (3000 rpm speed/ 5 Nm load) without metabolic activation.....	316
Table 80. Chromosome aberrations observed in Chinese hamster ovary CHO-K1 cells after exposure to the 3–ring aromatic diesel emission fraction R 33 (3000 rpm speed/ 5 Nm load) with metabolic activation (rat liver S9 fraction)	316
Table 81. Chromosome aberrations observed in Chinese hamster ovary CHO-K1 cells after exposure to the polar diesel emission fraction ES 39 (3000 rpm speed/ 5 Nm load), without metabolic activation.....	317
Table 82. Binomial dispersion test calculated for replicate cultures of the polar emission fraction ES 39 (3000 rpm speed/ 5 Nm load) when assayed in the chromosome aberration assay in CHO-K1 cells without metabolic activation.....	317
Table 83. Chromosome aberrations observed in Chinese hamster ovary CHO-K1 cells after exposure to the polar diesel emission fraction ES 39 (3000 rpm speed/ 5 Nm load), with metabolic activation (rat liver S9 fraction)	318
Table 84. Binomial dispersion test calculated for replicate cultures of the polar emission fraction ES 39 (3000 rpm speed/ 5 Nm load) when assayed in the chromosome aberration assay in CHO-K1 cells with metabolic activation (rat liver S9 fraction)	318
Table 85. Chromosome aberrations observed in Chinese hamster ovary CHO-K1 cells after exposure to the polar diesel emission fraction ES 48 (1000 rpm speed/ 55 Nm load), without metabolic activation.....	319
Table 86. Binomial dispersion test calculated for replicate cultures of the polar emission fraction ES 48 (1000 rpm speed/ 55 Nm load) when assayed in the chromosome aberration assay in CHO-K1 cells without metabolic activation.....	319
Table 87. Chromosome aberrations observed in Chinese hamster ovary CHO-K1 cells after exposure to the polar diesel emission fraction ES 48 (1000 rpm speed/ 55 Nm load), with metabolic activation (rat liver S9 fraction)	320

Table 88. Binomial dispersion test calculated for replicate cultures of the polar emission fraction ES 48 (1000 rpm speed/ 55 Nm load) when assayed in the chromosome aberration assay in CHO-K1 cells with metabolic activation (rat liver S9 fraction)320

Table 89. Chromosome aberrations observed in Chinese hamster ovary CHO-K1 cells after exposure to the polar diesel emission fraction ES 51 (1000 rpm speed/ 5 Nm load), without metabolic activation.....321

Table 90. Binomial dispersion test calculated for replicate cultures of the polar emission fraction ES 51 (1000 rpm speed/ 5 Nm load) when assayed in the chromosome aberration assay in CHO-K1 cells without metabolic activation.....321

Table 91. Chromosome aberrations observed in Chinese hamster ovary CHO-K1 cells after exposure to the polar diesel emission fraction ES 51 (1000 rpm speed/ 5 Nm load), with metabolic activation (rat liver S9 fraction)322

Table 92. Binomial dispersion test calculated for replicate cultures of the polar emission fraction ES 51 (1000 rpm speed/ 5 Nm load) when assayed in the chromosome aberration assay in CHO-K1 cells with metabolic activation (rat liver S9 fraction)322

Table 93. Chromosome aberrations observed in Chinese hamster ovary CHO-K1 cells after exposure to the polar diesel emission fraction ES 107 (2000 rpm speed/ 30 Nm load), without metabolic activation.....323

Table 94. Chromosome aberrations observed in Chinese hamster ovary CHO-K1 cells after exposure to the polar diesel emission fraction ES 116 (2000 rpm speed/ 55 Nm load), without metabolic activation.....323

Table 95. Chromosome aberrations observed in Chinese hamster ovary CHO-K1 cells after exposure to the polar diesel emission fraction ES 119 (3000 rpm speed/ 30 Nm load), without metabolic activation.....324

Table 96. Chromosome aberrations observed in Chinese hamster ovary CHO-K1 cells after exposure to the polar diesel emission fraction ES 125 (3000 rpm speed/ 55 Nm load), without metabolic activation.....324

List of abbreviations

B[a]P	benzo (α) pyrene
CHO-K1	Chinese hamster ovary K1 cell line
CO	carbon monoxide
CO ₂	carbon dioxide
CP	cyclophosphamide
DCM	dichloromethane
DES	diethylstilbestrol
d.f.	degrees of freedom
DI	direct injection
DoH	Department of Health
DMSO	dimethylsulphoxide
DNP	di-nitropyrene
EC	European Community
ECACC	European collection of animal cell cultures
EEC	European Economic Community
EPA	Environmental Protection Agency (US)
ES	Emission sample
G-6-P	glucose-6-phosphate
GC	gas chromatography
GC/MS	gas chromatography/ mass spectrometry
H ₂ O	water
HC	hydrocarbons
HEI	Health Effects Institute
HGV	heavy goods vehicle
HPLC	high performance liquid chromatography
IARC	International Agency for Research on Cancer
IDI	indirect injection
IPCS	International Programme on Chemical Safety
KCl	potassium chloride
MNNG	N-methyl-N'-nitro-N-nitrosoguanidine
MOT	Ministry of Transport test
MR	mitotic rate
1-NP	1-nitropyrene

NADP	nicotinamide adenine diphosphate
nitro-PAC	PAC with nitrogen group substitution
Nm	Newton metres
NO	nitric oxide
NO ₂	nitrogen dioxide
NO _x	oxides of nitrogen
O ₂	oxygen
OECD	Organisation for Economic Co-operation and Development
PAC	polycyclic aromatic compounds
PAH	polycyclic aromatic hydrocarbons
PBS	phosphate buffered saline
PM _{2.5}	particulate matter with diameter less than 2.5 µm
PM ₁₀	particulate matter with diameter less than 10 µm
Ppm	parts per million
QUARG	Quality of Urban Air Review Group
Rpm	revolutions per minute
RTE	rat tracheal epithelial cells
TESSA	Total Exhaust Solvent Scrubbing Apparatus
TSA	tryptone soy agar
UKEMS	United Kingdom Environmental Mutagen Society
UK NAQS	United Kingdom National Air Quality Strategy
US EPA	United States Environmental Protection Agency
UV	Ultra violet
VOC	volatile organic compounds
WHO	World Health Organisation

Acknowledgements

I would like to thank my supervisor Dr Dave J Price for allowing me to undertake the research, and for all his help and encouragement throughout. Thanks to Mike Rhead for help with the chemistry in particular in the early stages, and to Dr Robin Pemberton of the Environmental Sciences team for help with engine sample collection, fractionation and not least of all for performing all HPLC and GC/MS on the aromatic fractions. Don Ryder and Annie Bell also provided invaluable assistance during emission sample collection.

Thanks to Lynne Cooper for teaching me everything about animal cell culture, for being very calm and patient, and more than anything for providing moral support. Thanks also to Dr Christine King for advice with the cell culture, and for being a pleasure to demonstrate for. Jo Carter was a desperately needed extra pair of hands during S9 preparation, and willingly letting me use and clutter up her lab space in one of my desperate searches for somewhere to work. Nick Crocker deserves special mention for help with biochemistry, from provision of all sorts of equipment on very long term loan to innovative ideas when we did not have what was needed. Thanks also to Nick, Lynne, Andy, and others long gone for the sometimes intellectual and often stimulating coffee room chats. Thanks to Chris Coleman and latterly Suzie for ordering all chemicals and equipment, most of which was 'urgent', without batting an eye. Thanks also to all other technical staff for their assistance at various times including Marion and Julie.

Sarah May, Janice Bateson, Angela Watson, and Suzie Bloomfield were colleagues who became close friends and gave much in the way of moral support, especially in my final year. In particular they showed me that any problem, no matter how large, can be cured or forgotten by going shopping. I am especially grateful to Janice for 'words of wisdom' during the writing up.

Finally thanks to my mum and dad for always believing in me, and most of all to Paul for putting up with me and without whom none of this would have been possible.

Authors Declaration

At no time during the registration for the degree of Doctor of Philosophy has the author been registered for any other University award.

This study was financed with the aid of a studentship from the University of Plymouth and was performed in association with the Department of Environmental Sciences at the University of Plymouth.

Membership of the United Kingdom Environmental Mutagen Society, the Genetical Society, and the European Cytogeneticists Association was obtained.

Relevant scientific seminars were regularly attended. Seminars were presented at Departmental Lecture and Seminar Programmes in May 1996 and October 1997. The following meetings and conferences were attended:

UKEMS Annual Meeting, Leicester, 5-7 July 1995*

Molecular aspects of carcinogenesis, York, 5-9 September 1995

UKEMS Annual Meeting, Birmingham, 15-17 July 1996

Genetical Society Spring Meeting, Warwick, 19-21 March 1997*

1st European Cytogenetics Conference, Athens, 22-25 June 1997*

7th International Conference on Environmental Mutagens, Toulouse, 7-12 September 1997*

Aspects of this work were presented in poster form at conferences marked*.

Signed



Date

13th July 1999

1. INTRODUCTION

1.1 Introduction to the diesel engine

In 1892 Rudolph Diesel, a German engineer developed a new type of engine that differed from the standard gasoline engine which had been introduced 30 years earlier. It became known as the diesel engine and was capable of spontaneous combustion of liquid fuel without requiring spark ignition. The first prototype engine actually exploded small coal dust particles rather than using liquid fuel (Morgan *et al.*, 1997).

The use of diesel engines became more widespread during the 1980s as a response to the warnings about petrol powered vehicles and their production of harmful emissions. At this time diesel was hailed as the new green fuel, and Governments and environmental agencies encouraged car companies to develop and produce new diesel models to sell to the public on the basis of their green credentials. In the United Kingdom as recently as 1992, the Treasury and Departments of Environment and Transport joined forces to cut the price of diesel relative to petrol. The owners of fleet cars were also offered tax incentives to run diesel cars (Bown, 1994). The greater fuel economy that was and continues to be achieved through diesel combustion was one of the major factors of its rise in popularity, especially among the fleet trade. Early evidence in the mid 1990s of the drawbacks of diesel combustion lead the Department of Health to shift its position on diesel from neutrality to one advocating a precautionary approach. The rise in popularity has however been sustained by continued improvements in diesel engine performance, and it appears that public reports of possible adverse health effects associated with diesel have yet to impact on the diesel car market.

1.2 A comparison of diesel with petrol powered vehicles

Early diesel vehicles were designed for optimum fuel economy and performance, and provided approximately 15 to 30 % better volumetric fuel efficiency than similar petrol

vehicles (Hammerle *et al.*, 1994). Fuel economy is a major asset of the diesel engine and explains its unrivalled popularity in transportation, particularly buses, vans, and heavy duty trucks, and has been sustained in spite of advances in petrol technology. Because of this fuel economy, and due to recent further improvements in engine performance and in resale values, the UK has seen a substantial increase in the number of new diesel car sales as a proportion of total car sales. Diesel sales in 1990 accounted for 5.4 % of new car sales in the UK, increased to 12.6 % in 1995 (Collier, 1995), and are now approaching 20 % so that they now comprise 6 % of the national total (QUARG, 1996). In some European countries the surge in popularity of the diesel car is even greater, for example France where half of all new cars sold now have diesel engines (Patel, 1995).

As well as its greater fuel efficiency over petrol, diesel continues to be attractive to consumers who are increasingly aware of the 'greenhouse effect' because its combustion produces less of the regulated gaseous emissions such as carbon dioxide (the principal greenhouse gas) per mile travelled. Diesels also emit less of the other greenhouse gases, methane and nitrous oxide, than do similarly powered petrol cars (QUARG, 1993b). Petrol vehicles are responsible for the emission of much higher amounts of VOCs (Volatile Organic Compounds), in particular benzene and 1,3-butadiene, both of which are known human carcinogens (DoE, 1996). In addition to the production of carbon dioxide from petrol combustion, evaporative emissions from petrol cars contribute significantly to hydrocarbons in ambient air from petrol station forecourts, petrol storage depots and oil refineries, and evaporation from the petrol stored in cars, parked and moving. The main environmental significance is their contribution to photochemical ozone formation and its long-range transport (QUARG, 1993b).

The transfer of hot exhaust vapour into a cooler exhaust tailpipe leads to the spontaneous nucleation of 'carbon' particles before emission, forming 'particulates'. For

diesel vehicles, the combustion process is such that they generally emit a much greater mass of this particulate matter than do petrol equivalents (QUARG, 1996). There has been a great deal of recent publicity implicating particulates in a range of possible serious adverse health effects (Pope *et al.*, 1992, 1995; Anderson *et al.*, 1995). Diesel vehicles also emit almost twice as much NO_x (a combination of nitric oxide, NO, and nitrogen dioxide, NO₂) than petrol vehicles with state of the art control systems (Chang *et al.*, 1991). Nitrogen dioxide is a respiratory irritant, and may exacerbate asthma and possibly increase susceptibility to infections. There is considered a general shortfall in information about emissions from diesel powered vehicles, and in particular there has been little on road emissions measurements. With continuous advances in diesel technology, Hammerle *et al.* (1994) felt that more data on current and future diesel vehicles were needed to provide an accurate assessment of the effect of diesel emissions on urban ozone formation, atmospheric particle concentration, and therefore the attendant health risk.

The increased proportion of diesel cars on the roads is therefore associated with an improvement in hydrocarbon and carbon dioxide emissions, a worsening of emissions of nitrogen oxides, and importantly has a major impact on the emission of particulate matter. The lower levels of greenhouse gas emissions from diesel cars does not necessarily imply a lesser impact of such engines on global warming as the carbonaceous particulate emissions from diesels may also act to warm the lower atmosphere (QUARG, 1993b). The question of whether a diesel car is more polluting than a petrol car is difficult to answer as the two have major differences. Ignoring the difficulties of comparing like with like, the question then arises as to which pollutants are most important. Unfortunately there is not a simple answer to this question as the consequences of the different pollutants vary markedly, and indeed are still not fully categorised and understood (QUARG, 1993b).

1.3 Diesel composition

Diesel fuel is known to be an exceptionally complex chemical which on combustion produces an equally complex cocktail of hydrocarbons and polar derivatives (Rhead & Trier, 1992), of which only a small number have been classified. Complete diesel combustion primarily results in the production of CO₂ (13 %), H₂O (13 %), with nitrogen from the air representing 73 %. The emission of CO and compounds formed by incomplete combustion of the diesel fuel or engine oil make up the remaining 1 % (Kingston, 1995). The incomplete combustion products are thought to represent thousands of chemical species in both the vapour and particulate phases of particulate exhaust emissions, of which around 400 have been definitely identified. The distribution of chemicals between the particulate and vapour phases is determined by a number of factors including the vapour pressure of the compound, the temperature of the exhaust stream, and the relative concentration of particular compounds. Table 1 shows some of the compounds and chemical groups readily identified in diesel exhaust emissions.

1.3.1 Diesel particulates

A major drawback of diesel combustion in particular is the emission of a fine carbonaceous particulate matter, produced mainly by the incomplete burning of fuel. Polycyclic Aromatic Compounds (PAC) and other organic components from the diesel exhaust stream are readily adsorbed onto the carbon core, and many of these organics have been shown to be genotoxic (Lewtas, 1988; Scheepers & Boss, 1992) and/or carcinogenic (IARC, 1989). The presence of mutagens and carcinogens adsorbed on to particulates has generated concern about diesel exhaust and its potential for inducing lung cancer (Morgan *et al.*, 1997).

gas phase	particulate phase
acrolein	heterocyclics and derivatives ¹
ammonia	hydrocarbons (C ₁₄ – C ₃₅) and derivatives ¹
benzene	inorganic sulphates and nitrates
1,3-butadiene	metals
formaldehyde	polycyclic aromatic compounds and derivatives ¹ (several hundred chemical species)
formic acid	
heterocyclics and derivatives ¹	
hydrocarbons (C ₁ – C ₁₈) and derivatives ¹	
hydrogen cyanide	
hydrogen sulphide	
methane	
methanol	
nitric acid	
nitrous acid	
oxides of nitrogen	
polycyclic aromatic compounds and derivatives ¹	
sulphur dioxide	
toluene	

¹ derivatives include acids, alcohols, aldehydes, anhydrides, esters, ketones, nitriles, quinones, sulphonates and halogenated and nitrated compounds, and multi-functional derivatives

Table 1. Chemical compounds and species groups found in diesel engine exhaust emissions (adapted from IARC, 1989, and Collier, 1995)

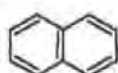
Primary emissions of particulate matter can arise from many sources, including road transport, stationary combustion, and industrial processes (QUARG, 1996). The majority of airborne particulate mass has a diameter of 10 µm or less and has been termed PM10 or coarse particulate matter, which generally deposit in the upper airways. Particles outside of this size are relatively very large in size and have little impact on health. Currently, diesel vehicles, in particular trucks and buses, are a major contributor to such emissions, especially in urban areas. It has been estimated that road transport accounts for a third of atmospheric PM10, rising to as much as 80 % in London (QUARG, 1996). Within the PM10 size range, particles of less than 2.5 µm aerodynamic diameter (PM2.5) are normally described as fine, and are currently the cause of greatest concern as they are capable of reaching the deepest part of the lung. As well as creating dirt, odour, and visibility problems, increased atmospheric burdens of PM10 have been linked with higher

rates of mortality and morbidity (QUARG, 1993b; Pope *et al.*, 1995). Research on airborne particulate matter has lagged behind research on other common air pollutants, possibly because particulate matter was not perceived as a significant threat to health once the extreme pollution characterised by the London smogs was abolished (QUARG, 1996).

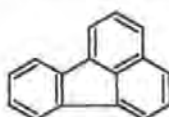
1.3.2 Polycyclic aromatic compounds and diesel chemistry

PAHs (Polycyclic Aromatic Hydrocarbons) are a group of chemicals containing carbon and hydrogen atoms with more than one benzene ring in their structure, and are ubiquitous in nature. The broader class of PAC incorporate a range of substituent groups such as nitrogen, oxygen, or sulphur in the ring structure (QUARG, 1993a). PAHs were first identified in diesel exhaust in 1954 (Kotin *et al.*, 1955), and the suspicion that they played a role in cancer led on to a pronounced research interest in the human health effects over the following 25 years. Many individual PAHs have carcinogenic (White, 1986) or mutagenic potential (Pahlmann and Pelkonen, 1987). Sixteen PAHs have been recommended as priority pollutants by the World Health Organisation (WHO), the European Economic Community (EEC), and the US Environmental Protection Agency (US EPA) (Hellou, 1996). All sixteen of these priority pollutants, shown in Figure 1, have now been quantified in diesel exhaust particles (Pointet *et al.*, 1997). Table 2 lists the International Agency for Research on Cancer (IARC) classifications for a range of PAC that have been found in vehicle exhaust. A significant number of these compounds fall into the IARC group 2 (2A – at least limited evidence of carcinogenicity in humans, 2B – evidence of carcinogenicity in animals) (QUARG, 1993b).

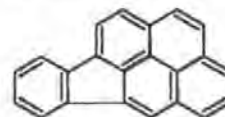
naphthalene



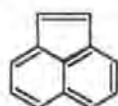
fluoranthene



indeno[1,2,3-*cd*]pyrene



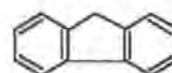
acenaphthylene



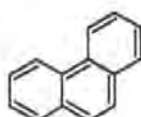
acenaphthene



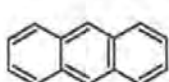
fluorene



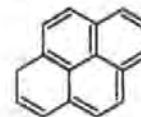
phenanthrene



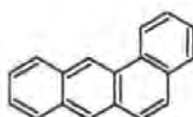
anthracene



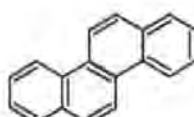
pyrene



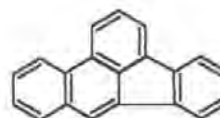
benz[*a*]anthracene



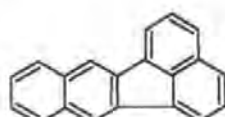
chrysene



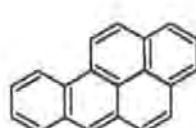
benzo[*b*]fluoranthene



benzo[*k*]fluoranthene



benzo[*a*]pyrene



benzo[*ghi*]perylene



dibenz[*a,h*]anthracene

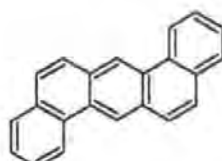


Figure 1. Chemical structures of sixteen polycyclic aromatic hydrocarbons identified as priority pollutants by the World Health Organisation, the European Economic Community, and the US Environmental Protection Agency. All sixteen have been isolated from diesel exhaust emissions (Hellou, 1996; Pointet *et al.*, 1997)

compound class	compound	IARC classification *
olefins	1,3-butadiene	2A
	ethylene	3
aromatics	benzene	1
PAHs	anthracene	3
	benzo[a]anthracene	2A
	benzo[j+k]fluoranthene	2B
	benzo[ghi]perylene	3
	benzo[a]pyrene	2A
	benzo[e]pyrene	3
	chrysene	2B
	coronene	3
	fluoranthene	3
	phenanthrene	3
nitro-PAH	1,3-dinitropyrene	3
	1,6-dinitropyrene	2B
	1,8-dinitropyrene	2B
	6-nitrobenzo(a)pyrene	3
	3-nitrofluoranthene	3
	2-nitrofluorene	2B
	1-nitropyrene	2B

*IARC Group 1 – proven human carcinogens, Group 2A – limited evidence of carcinogenicity in humans, Group 2B – evidence of carcinogenicity in animals, Group 3 – unclassified chemicals (IARC, 1989)

Table 2. The IARC carcinogenic classification of selected polycyclic aromatic compounds from diesel engine particulate emissions (adapted from Scheepers and Boss, 1992 and QUARG, 1993b)

PAC are found in significant masses in diesel exhaust emissions, the majority arising from PAC already present in the fuel which survive combustion and appear in the exhaust (Collier *et al.*, 1995). PAC also arise from other sources including survival from the lubricating oil and from pyrosynthetic formation within the combustion chamber (amounting to no more than 20 %). Pyrosynthetic formation results when molecules of fuel or oil have been transformed into intermediate products under the extreme temperature

and pressure region in the cylinder, but have not proceeded to complete combustion (in part due to a lack of oxygen from poor mixing). These may not have the same structure as PAC surviving combustion (Rhead & Trier, 1992). Research by Collier (1995) has shown that PAC and emissions are sensitive to the engine operating conditions of speed and load, and to the type of diesel engine combustion system (Direct Injection-DI or Indirect Injection-IDI). The greatest PAC combustion efficiencies i.e. the lowest percentage recoveries of PAC, were found at high engine loads and mid speed. Thus, the mutagenicity of diesel engine exhaust is likely to vary depending upon the engine operating conditions.

1.3.3 Nitro emissions – nitro-polycyclic aromatic compounds (nitro-PAC) and oxides of nitrogen (NO_x)

Nitro-PAHs are derivatives of PAH or PAC where nitro-groups replace one or more hydrogens on the ring structure. They are a widespread class of environmental contaminants derived from different environmental combustion sources, including diesel and aeroplane emissions, airborne particulates, coal fly ash, and food, and their presence has been suggested in cigarette smoke (Fu, 1990). A number of nitro-PAH have been identified in diesel engine exhaust extracts (Table 2), and have been widely studied in bacteria since the confirmation of a number of them as potent direct-acting mutagens (Schuetzle *et al.*, 1980). 1-nitropyrene is the most abundant nitro-PAH found in many environmental sources, and is a moderately potent direct-acting mutagen tested in bacteria Fu (1990). The contribution of 1-nitropyrene to the total mutagenic activity of diesel particulates has been estimated at 10 – 40% (Schuetzle *et al.*, 1980; Nakagawa *et al.*, 1983; Veigl *et al.*, 1994). Study of nitro-PAH in mammalian systems has however been minimal, and is particularly relevant as bacteria contain high levels of nitroreductase enzymes which activate nitro compounds to potential mutagens, which does not necessarily reflect nitro compound activation *in vivo* (section 1.10.6.3).

Nitro-PAH are not detected in the diesel fuel nor in the sump oil samples (Collier, 1995), and are produced only through combustion. The nitrating species are oxides of nitrogen, NO_x, which are formed by the thermal decomposition of nitrogen and air in the combustion chamber. The composition of NO_x is key in nitration process (the proportion of NO:NO₂, which is dependent upon engine operating conditions). Once formed, the NO_x may then react with PAH to form nitro-PAH via a free radical mechanism within the combustion chamber (Scheepers & Boss, 1992b). Nitration may also occur by an electrophilic substitution of exhaust PAH by nitrogen dioxide in the presence of nitric acid via the nitronium ion. The present technology for NO_x emission reduction for diesels gives limited benefit and does not approach the performance of three way catalysts (QUARG, 1993b). Nitro-PAH emissions therefore continue to pose a potential threat to health.

1.4 Environmental and human impact of diesel emissions

The exhaust emissions from diesel engines have raised concern since it was first suggested that they have the potential to cause adverse health effects. Their effects may arise from their regulated and unregulated gaseous emissions (1.4.1), from the emission of the fine carbonaceous particulate matter (1.4.2), or more likely a combination of these factors by the addition of a significant burden of particulates to ambient air (1.4.3).

1.4.1 Gaseous emissions

Of the gaseous emissions emitted during diesel combustion, carbon monoxide and nitrogen dioxide can potentially cause the most harm. In European urban areas almost 90 % of CO is produced from road traffic emissions. At levels found in ambient air, carbon monoxide combines with haemoglobin in the blood, reducing the ability of the blood to carry O₂. At higher concentrations, it can aggravate cardiovascular diseases and impair mental function

(QUARG, 1993b). The impact of carbon monoxide is increased by its capacity to survive in the atmosphere for approximately 1 month before its eventual oxidation to carbon dioxide. Of the oxides of nitrogen, only NO₂ is of such toxicity to raise concern at ambient levels (QUARG, 1993b). NO₂ is a respiratory irritant as exposure at high levels can lead to constriction of the airways and an increase in airway resistance, and is therefore linked to asthma. In the presence of sunlight, NO₂ reacts with hydrocarbons to produce photochemical pollutants such as ozone, which have their own environmental and health effects. After their conversion to nitric acid (after approximately 1 day), the oxides of nitrogen can damage vegetation – either directly or indirectly by contributing to the acidification of rainfall. The strict control of these gaseous emissions has therefore been undertaken by Governments throughout the Western world.

1.4.2 The environmental and health impact of diesel particulate matter

Before establishing a direct causal link, an understanding of where diesel emission compounds exert their effects is required. The primary potential route of administration of diesel emissions to the human system is through inhalation of gaseous and particulate extracts. The particulates emitted after diesel combustion are of a size range that is likely to pass through the nose and mouth (PM₁₀), making the respiratory tract the major site of exposure to airborne particulates (Heyder, 1993). The more recently described fine particulates, PM_{2.5}, are capable of lodging deep in the lungs. Once bound to the alveoli, ultrafine particles (< 0.1µm) may induce oxidant production, lung inflammation, and hyperactivity. This may be as a result of the particle-associated organic compounds, PAC, which are then made available in the tissue by being dissolved in physiological fluids, or as more recently suggested by being solubilised or dispersed by pulmonary surfactant compounds (Scheepers and Boss, 1992). Additionally, the absorption of components of diesel emissions through the skin cannot be excluded as PAHs are easily absorbed percutaneously (Jongeneelen *et al.*, 1984). As well as prolonging the residence time of

particulate-associated organic compounds in the lung, particulates may induce the generation of reactive oxygen species, and together with some gas phase components may exert a promoting effect (McClellan, 1986).

Diesel exhaust was classified as 'probably carcinogenic to man (Group 2A)' by the IARC in 1989. People most at risk are thought to be those occupationally exposed to the combustion products of diesel engines, including miners, bridge, tunnel, railroad, loading dock, farm, and maintenance garage workers, and truck and fork-lift drivers (Ensell *et al.*, 1998). The general public, particularly in urban areas, are also potentially at risk. There have been several reviews of the numerous epidemiological papers published so far on occupational exposure, the authors not always concurring in their conclusions. The Health Effects Institute in America published a detailed review in 1995 which concluded that the epidemiologic data were consistent in showing weak associations between exposure to diesel exhaust and lung cancer. They found that long-term exposure to diesel exhaust in a variety of occupational circumstances inferred a 1.2- to 1.5-fold increase in the relative risk of lung cancer compared with workers classified as unexposed. Although the small magnitudes of the increases in these risks make the studies very sensitive to confounding factors and uncertainties of exposure, the HEI felt that the association between increased risk of lung cancer and exposure to diesel emissions persisted after controls for smoking were applied, although in some cases the risk was lower (HEI, 1995). As well as the increase risk of lung cancer described above and in other studies (Bhatia *et al.*, 1998), occupationally exposed bus drivers in Copenhagen were found to be at increased risk of bladder and liver carcinomas (Nielson *et al.*, 1996). An excess of bladder cancer has been previously described in three out of four case-controlled studies (IARC, 1989). In contrast to the HEI report, a review of epidemiological evidence by Morgan *et al.* (1997) concluded that a link between lung cancer and diesel exposure had not been established. Criticism

was made of some studies for failure to assess the smoking habits of individuals, and the way in which occupational exposure was assessed.

The increased risk of certain cancers is not the only proposed direct effect of diesel emission exposure. There have been numerous reports of pulmonary irritation and bronchial hyperactivity in persons persistently exposed to diesel emissions. Wade and Newman (1993) found three non-smoking railroad workers developed asthma following excessive exposure to locomotive emissions following an alteration in working patterns. Further acute effects of diesel exhaust exposure include eye irritations and cardiovascular symptoms (Scheepers and Bos, 1992). There has been little investigation into the detrimental effects of diesel exhaust on heart activity, even though links with air pollution in general have been described. An indication of the genotoxic potential of diesel in humans has been shown by enhanced amount of PAH-DNA adducts found in the lymphocytes, urine and haemoglobin of occupationally exposed bus garage workers (Nielson *et al.*, 1996a; 1996b).

The lung has a natural self-clearing mechanism, but when atmospheric levels of particulates rise this can be overloaded. The question of whether such particle overloading occurs in humans under environmental exposure conditions has been addressed using toxicity and modelling data. Levels of diesel particulate matter alone in ambient settings (1 to 10 $\mu\text{g}/\text{m}^3$) were not sufficiently high to overwhelm lung clearance processes, and hence lead to lung tumour induction by a mechanism driven by inflammation and cell proliferation (HEI, 1995). There may have been an underestimation of environmental exposure as a higher concentration range, of 3 to 29 $\mu\text{g}/\text{m}^3$ in the environment, was described by Lafon *et al.* (1994). Occupational exposure levels of diesel particulate, which can be as high as 164 $\mu\text{g}/\text{m}^3$ (Hammond *et al.*, 1993), were not studied.

At present, there is no clear evidence as to whether health effects of particulate matter are related to certain components such as PAC or whether they represent non-specific effects of inhaled particles. That the transport of chemicals on the surface of particles may be important in the cause of lung inflammation has been shown in recent studies in which iron complexed on the surface of fly ash particles promoted oxidative lung injury, and this effect was reduced after removal of surface iron by washing (Tepper *et al.*, 1994). Diesel exhaust extracts have been suggested as important air pollutants in the activation of airway epithelial cells and thus potentially responsible for allergic airway inflammation (Ohtoshi *et al.*, 1998; Takano *et al.*, 1998; Miyabara *et al.*, 1998). The full extent of the biological activity of particulate matter from diesel vehicles is therefore yet to be determined, and hence the health effects for inhalation of diesel particulate matter remain uncertain. It is, however, well established that people with pre-existing respiratory or cardiac disorders are most risk of the acute effects from exposure to particles. Heart and breathing problems are worsened in sensitive groups, from days of restricted activity to premature mortality (DoE, 1996).

1.4.3 The potential affects of airborne particulate matter

Diesel engine emissions are a major contributor to the particulate load, particularly in urban air. In 1993, the QUARG described increasing evidence that an increase in mortality and morbidity may be associated with a rise concentration of particulate matter in urban air. They cited the work of Pope and colleagues (Pope *et al.*, 1992) who had found a linear positive relationship between the airborne concentration of PM10 and both daily mortality from all causes and respiratory morbidity. However, without a convincing biological mechanism, the causal relationship could not be fully demonstrated. More recent studies, including time series studies in which day to day changes in mortality and illness are shown to be related to concentrations of airborne particulate matter, have strengthened the epidemiological evidence for the adverse health effects of airborne particulates. Anderson

et al. (1995) found, in a detailed evaluation of the December 1991 pollution episode in London, that there was an increase of about 10 % in mortality during the week of the episode compared with the same period in earlier years. A large scale study based upon the American Cancer Society database of over half a million people has included data on fine particulate matter from some 50 urban areas as well as particulate sulphate data from 151 urban areas. After controlling for smoking and other risk factors, a clear relationship between cardiopulmonary and lung cancer mortality and concentrations of particulate air pollution was established (Pope *et al.*, 1995). The increased mortality was correlated with levels of pollution found commonly in US cities. Although clear associations with increases in mortality and short term pollution episodes were also shown, Pope is convinced that it is the long term chronic exposure that is most important in terms of real loss of health and loss of life (Pope *et al.*, 1995).

It has to be borne in mind that scepticism for the role of air pollution in mortality and morbidity still exists. Pope and co-workers themselves are concerned that some other factor might be causing the deaths – not least from the complex regression analysis method used to analyse data, or inadequate control of other factors such as weather variables or other pollutants. Moolgavkar reanalysed Pope's data and concluded that although there was an association between air pollution and mortality, it was impossible to isolate one component of air pollution as being responsible (Reichhardt, 1995).

As well as variations in morbidity and mortality (the most certain measurement), a variety of indicators of ill health have been followed in relation to acute effects of airborne particulate matter such as time off school or work, respiratory, cardiovascular or other symptoms requiring hospital emergency treatment or admission, exacerbation of asthma and changes in lung function. The reported health effects associated with particulate matter exposure were summarised by Reichhardt (1995) as:

- mortality
- increased hospital use: *admissions, emergency room visits*
- increased pneumonia and exacerbation of chronic obstructive pulmonary disease: *hospital admissions, emergency room visits*
- exacerbations of asthma: *attacks, bronchodilator use, emergency room visits, hospital admissions*
- increased respiratory symptoms: *cough, upper and lower respiratory tract problems*
decreased lung function

Airborne particles, in addition to promoting exacerbations of lung disease, have an additional effect on the coagulability of blood, increasing the susceptibility of individuals to acute episodes of cardiovascular disease. Several haematological factors are not only known to be predicative of cardiovascular disease, but also arise as a consequence of inflammatory reactions (Seaton *et al.*, 1995).

It has been hypothesised that the ultrafine component of PM10 is responsible for its adverse effects, with free radical activity on their surface increasing their surface area compromising epithelial integrity (Seaton *et al.*, 1995). The ultrafine component of PM10 is not insignificant, for example in London urban pollution, half by number of the particulates collected were less than 0.1 μm . Fine particulates can travel for hundreds of kilometres and may remain suspended for weeks, as opposed to the larger particulates which are readily removed from the air through coagulation and the effect of rain in a matter of hours. Until we know more about the specific human effects of particulates, it is difficult to say whether overloading of the lung from high atmospheric pollution is the main contributor. Repeated inhalation of genotoxic substances from airborne particulates could also exceed the body's ability to eliminate and detoxify (Repace, 1982) and therefore pose a health risk of intoxication and cancer development through a chronic exposure mechanism (Hornberg *et al.*, 1997).

Whilst a direct causal link between diesel pollution, in particular particulates, and daily mortality has not been established, the growing evidence of their adverse effects on health cannot be ignored. Current mutagenicity studies on the emissions from diesel engines are important in the search for a mechanism of action, which would aid in demonstration of the causal link.

1.5 Legislation for diesel emissions and related ambient air pollution

Worldwide regulation of diesel engines varies, with current emissions legislation largely being related to new vehicles. The pollutants of diesel engine exhaust that are generally legally controlled include carbon monoxide, hydrocarbons (includes the many different organic compounds emitted, some of which are not in fact hydrocarbons), oxides of nitrogen (most abundant is nitric oxide, NO), and particulates (QUARG, 1993b). Engines are generally regulated so that the maximum total permitted weight of particulate matter, generated and collected under defined conditions, is specified. In Europe, a number of EC Directives have been released which relate specifically to control of engine emissions, summarised in Table 3.

New, stage III limits for emissions from vehicles are under discussion and are planned for introduction by the EEC in the year 2000 (QUARG, 1996). To meet these requirements the UK National Air Quality Strategy was formed and a consultation draft document issued in 1996. Proposed targets for eight pollutants, to be met by 2005, were set and are summarised in Table 4. There have been criticisms for not considering a special standard for fine particles PM_{2.5} (Walker, 1996), especially as PM_{2.5} has shown a better association with increased mortality than PM₁₀ in one study (Reichhardt, 1995). Criticism was also levied for not setting specific targets for traffic, as the amount of traffic on the roads in the UK is predicted to almost double between 1994 and 2005 (DoE, 1996).

The Government has gone some way to meeting this criticism through the implementation of the Road Traffic Reduction Act 1997 (Croner, 1999), although the impetus is placed on local authorities.

EC Directive	description
91/441/EEC	(enforced 1992) limits overall traffic emissions – specifically CO, hydrocarbons and oxides of nitrogen, and particulate
93/12/EEC	limits the sulphur content of diesel fuel to 0.05% from 1996
91/542/EEC	emission limits for particulate matter mass from diesel vehicles in force 1995/1996 for HGVs
94/12/EEC	emission limits for particulate matter mass from diesel vehicles in force 1996 for new cars
93/59/EEC	emission limits for particulate matter mass from diesel vehicles in force 1997 for diesel vans

Table 3. Selected European Community Directives relating to the regulation of emissions from diesel vehicles

pollutant	standard		
	concentration	measured as	specific objective
benzene	5ppb	running annual mean	to be achieved by 2005
1,3-butadiene	1ppb	running annual mean	to be achieved by 2005
carbon monoxide	10ppm	running 8 hr mean	to be achieved by 2005
lead	0.5µg/m3	annual mean	to be achieved by 2005
nitrogen dioxide	104.6ppb (20ppb)	1 hr mean (annual mean)	measured as the 99.9 th centile, to be achieved by 2005*
ozone	50 ppb	running 8 hr mean	measured as the 97 th centile, to be achieved by 2005*
particles PM10	50 µg/ml	running 24 hr mean	measured as the 99 th centile, to be achieved by 2005*
sulphur dioxide	100 ppb	15 min mean	measured as the 99.9 th centile, to be achieved by 2005*

PM10 is gravimetric method for measuring particle size using a size selective inlet collecting 50% of 10µm particles, less than 5% of 20 µm particles and more than 95% of 5µm particles
 *these objectives are to be regarded as provisional

Table 4. Summary of specific objectives for eight pollutants proposed by the UK National Air Quality Strategy

PM10 levels are currently measured in 9 UK cities, and average values over a day are around 15-35 $\mu\text{g}/\text{m}^3$ with daily maxima up to 70 $\mu\text{g}/\text{m}^3$ (Seaton *et al.*, 1995). At present, therefore, the Government's proposed target would be exceeded on a daily basis. Through implementation of targets, primary national emissions of PM10 are predicted to fall by about one quarter between 1995 and 2010, based upon consistent sales of diesel cars (QUARG, 1996). The implementation of these stricter emission levels will be partially negated, however, if there is a continued shift in the pattern of fleet turnover in the UK to the levels in Europe (approaching 50 % of the fleet in some European countries are diesel).

The setting of air quality objectives is only of benefit if strict monitoring and enforcement follow. Monitoring can be expensive and inaccurate, with large differences in pollutant levels found over small spatial distances, for example due to local wind speed (Croxford *et al.*, 1996). One of the methods for assessment of diesel used is derived from sulphur to carbon ratios in road tunnel air used by De Fre and colleagues (1994). Their work highlighted another of the problems of monitoring, exposure limits set by ambient air quality standards are exceeded for drivers stuck in stagnant traffic (rush hour) or for frequent tunnel users. This is of concern as studies have shown statistical associations between airborne particulate matter and increased mortality and sickness, even at levels well within current national air quality standards (Reichhardt, 1995). In the UK, technology to measure exhaust emissions at the roadside has been developed and widely applied. Such technologies, along with good inspection (through MOT) and maintenance programmes, have been deemed key in identifying gross polluters which contribute a disproportionate amount of the emissions. Whilst legislation and regulation are important, it appears that the need to reduce traffic volumes in urban areas is fundamental. Much of the interest in emissions has focused on cars and light duty vans because there are the greatest number of these categories of vehicle (Westerholm and Edgeback, 1994). Heavy-

duty vehicles, however, make the greatest contribution to diesel emissions and the most significant benefits would come from improved control of their emissions.

The imposition of stricter limits has already impacted on emissions through new car development and the introduction of improved diesel fuels (for example low sulphur diesel fuel introduced in 1996). There is therefore a need to re-assess mutagenicity in the light of these advances.

1.6 Reduction in diesel engine emissions

As well as through legislation, reduction in the emissions from diesel engines has been sought through engine performance (1.6.1), post-combustion devices such as particulate traps (1.6.2), and through the use of alternative fuels such as rapeseed methyl esters (1.6.3).

1.6.1 Improvements in engine performance to reduce emissions

Whilst the main focus for engine developers is fuel consumption and driveability, improvements in engine performance have helped to reduce emissions. Once the drawbacks of diesel combustion were known, for example, detailed mapping of diesel engine operation was undertaken to define operating modes with low emissions. This led to improved engine control to maintain the engine in these low emission modes (Westerholm & Edgeback, 1994). The introduction of electronic control units to control fuel injection in the late 1980s was a major advance, as it had previously been controlled mechanically and was prone to drifting out of tune. Additionally, build up of carbonaceous deposits over the vehicle's lifespan gradually reduced the injection rate, which led to new injector designs and ashless detergents which can reduce emissions by up to 25 % compared to fouled injectors (Hammerle *et al.*, 1994). Further modification of the fuel injection process for Direct Injection engines enabled a better distribution of fuel which

could then be burned more completely, reducing the formation of PAC. Improvements in the mid 1990s include higher pressure fuel injection and individual control of each injector which are expected to again provide a further reduction in engine emissions. One of the most significant advances in emission reduction so far has been the introduction in 1996 of a low sulphur diesel fuel, which reduced particulate emissions by up to 13 % for HGV. In addition, the toxicological and chemical characterisation of engine exhausts in relation to the quality of fuels may play an important role, providing basic information useful for the development of fuels with a lower environmental and therefore health impact (Crebelli *et al.*, 1995).

1.6.2 Post-combustion treatment devices

At the post-combustion stage, there has been an introduction of exhaust treatment devices such as catalysts and particulate traps, which typically remove up to 50 % of organic emissions (Horiuchi *et al.*, 1990). The catalysts in use on diesel vehicles are less active than petrol catalysts, in part because the sulphur in commercial diesel fuel would be converted to particulate sulphate, negating any benefit. Particulate traps have been shown to be effective (Hammerle *et al.*, 1994), but commercial introduction has been slow because they are difficult to control. Build up of particulate matter on the trap results in increasing exhaust back pressure which leads to a reduction in fuel economy and performance. Burning of the collected particulate occurs at high speeds and loads, but is not frequent enough to clear the trap. The addition of fuel catalysts such as iron or copper would reduce the temperature at which the particulate matter will burn encouraging more frequent regeneration, but the release of metal particles has its own environmental significance.

Significant improvements have been made in diesel engine design, catalysts, particulate traps and fuel composition. The use of the full range of emission control

technology resulted in a 10 times reduction of particulate emissions and 30 times reduction in particulate associated organic emissions for new vehicles (Hammerle *et al.*, 1994).

1.6.3 Alternative fuels

A second strategy for reduction of the impact of diesel emissions upon urban air quality would be to switch to alternative fuels like natural gas or electric traction. With the latter, the impact of emissions from electricity generation would have to be taken into account (QUARG, 1993b). Another alternative fuel would be the use of plant oils, which Diesel tested as early as 1900 for his then newly developed self ignition engine. Since the energy crisis in 1973, the research in this field has greatly expanded. Whilst combustion of crude rapeseed oil causes severe damage to the common diesel engine, rapeseed methyl esters (RME) are an adequate substitute for fossil diesel fuel (Bunger *et al.*, 1998). Investigation of their emissions is continuing.

1.7 Assessing the mutagenicity of chemical species

The relevance of mutagenicity testing to the adverse health effects of diesel in humans is discussed. The definition of mutagenicity (section 1.7.1), is followed by a discussion of the action of (1.7.2) and significance of mutagenic processes and their impact on the human race with particular reference to effects in germline and somatic cells (1.7.3). An outline of mutagenicity testing (1.8) will then precede a discussion of the chromosome aberration assay (1.9), the major test utilised in this screen.

1.7.1 What is mutagenicity?

A mutation is a change in the genetic information (for example amount or chemical structure of DNA), which may result in a change in the characteristics of a cell as a result of alterations in, or non-production of, proteins (or RNAs) specified by the mutated DNA.

The changes in the genetic information are heritable and transmitted through mitotic and/or meiotic division. A mutagen, therefore, is an agent capable of disturbing the integrity of the hereditary mechanism of a cell or organism (Fahrig, 1984). Of course some DNA changes have no phenotypic effect, either because the change occurs in non-coding DNA, or does not alter the primary amino acid sequence of a polypeptide or because the resulting changes in the amino acid sequence occurs in a non-critical region of the polypeptide. Not all variant proteins, therefore, have clinical consequences. The potential mechanisms for altering genetic information are complex. Mutagens may act directly upon the DNA, such as point mutations, whereby the base sequence of a gene is altered. As well as direct interaction with DNA, a potential mutagen may affect the more peripheral cell division processes by interaction with DNA precursors, enzymes of DNA synthesis, structural non-DNA components of chromosomes, components of the spindle fibre apparatus (Zimmerman and Taylor-Mayor, 1985), or by interference with repair systems. Colchicine, for example, is a chemical mutagen which interacts with the tubulin of the spindle fibres to prevent proper function of the spindle fibre apparatus (Fahrig, 1984).

Muller first demonstrated the induction of mutations in 1927 using X-rays, although his findings were not readily accepted. The field of chemical mutagenesis was set underway in 1942 by the discovery of Charlotte Auerbach and J.M. Robson that nitrogen mustard, a component of military poison gas, caused mutations. Since that time, the numbers of proven chemical mutagens rose exponentially, until the eventual realisation that mutagens were widely distributed in the environment (Zimmerman and Taylor-Mayer, 1985).

Whether mutations are induced events, such as by chemical mutagens, or spontaneous, they are always random events – the nature of the mutation is a matter of chance. Mutagens therefore act only to increase the rate at which a mutation takes place,

not to direct which genes are mutated (Cummings, 1990). That being said, however, some recent studies have indicated that mutation may not always be a truly random event, with particular genes or regions of chromosomes being targeted, for example Slijepcevic and Natarajan (1994a; 1994b) found chromosome damage in X-irradiated Chinese hamster cells is more frequent in euchromatin than heterochromatin and mapped in G-light bands. Those mutagens that result in a structural alteration of eukaryotic chromosomes are termed clastogenic (Fahrig, 1984). The broader term of mutagenicity encompasses clastogens which, by definition, act to result in a change in the gross DNA chemical structure. The term genotoxic implies that a test chemical is capable of damaging DNA in a chemical sense, an effect usually monitored by the induction of point mutations or chromosome aberrations. One of the classic definitions of genotoxic was given by Druckrey:

‘any agent which, by virtue of its physical or chemical properties, can induce or produce heritable changes in those parts of the genetic apparatus that exercise homeostatic control over somatic cells, thereby determining their malignant transformation’

(Druckrey, 1973)

This definition was cited by Ashby in 1995, and he described it as as good as or better than subsequent definitions. A carcinogen is defined as a chemical capable of increasing the incidence of cancer in any species of mammal when administered by any route (Heddle, 1982).

1.7.2 Action of mutagens

As a mutagen, radiation has been shown to increase the frequency of chromosome aberrations (Lloyd and Edwards, 1983) and other mutational events at the molecular level such as DNA damage including strand breaks and base deletions (Cummings, 1990). Radiation penetrates directly from the environment to damage DNA.

Chemical mutagens, however, follow a more indirect route. The principal methods of exposure to chemicals are ingestion, inhalation, or absorption through the skin – the

chemicals must then be able to penetrate the nucleus and cause changes in DNA (Cummings, 1990). Chemicals act in a variety of ways, such as intercalating agents, as base analogues (substitute for bases during nucleotide synthesis), by deamination of bases, and less specifically cause DNA damage through strand breaks and crosslinking with or between strands, or may interfere with DNA repair mechanisms. Importantly, chemicals entering the body are often recognised and metabolically activated by cytochromes in an attempt to speed up their expulsion. This does not always have the desired effect, and can result in a previously unreactive chemical being modified to a mutagen (section 1.8.4). Mutagens normally induce more than one type of mutational change, the nature of the change being characteristic to that mutagen, and dependent upon the type of DNA alteration and the organism's secondary response to the DNA modification (Gatehouse *et al.*, 1990).

1.7.3 The significance of mutagens

Throughout history, spontaneous mutation has been an essential part of species development through natural selection, neutral drift and molecular drive. Mutations occur continuously during the cell replication process, at a seemingly high 'background' rate. The vast majority of these are corrected by one of several DNA repair mechanisms functioning in the cell, which as well as correcting errors made during replication, recognise damage to the DNA molecule. The importance of DNA repair has been highlighted by our knowledge of repair deficient human syndromes, such as xeroderma pigmentosum. This is an autosomal recessive disorder whereby individuals are deficient (have an 80 % reduction) in excision repair of thymidine dimers, a multigene process. Affected individuals are therefore extremely sensitive to sunlight (UV radiation), which causes thymidine dimers. A mutation in any one of the genes of this DNA repair leads to clinical symptoms, skin tumours, and ultimately death. Even for people whose DNA repair

systems are fully functional, overexposure to UV radiation can overload the repair system so that tumours result.

Mutagens in the environment therefore serve to increase the background mutation rate in cells. Mutations which are not repaired may have consequences to the individual. Both large and small changes in DNA sequences have been demonstrated to be relevant in altering the phenotype of organisms. This led DuBridge and Calos (1987) to describe the process of mutational change as a fundamental aspect of biology. More than 20 years ago, the mutation of DNA by chemical and physical agents was shown to often be mirrored by their capacity to elicit tumours in animals (McCann *et al.*, 1976). The genetic basis of many cancers is now widely accepted. For example through molecular and cytogenetic techniques showing that many tumour cells which carry somatically acquired genomic alterations, and evidence from aggregation of certain types of tumour within families (which hinted at the wider area of inherited predisposition to cancer). Thus in somatic cells, chemically and physically induced mutations primarily have potential carcinogenic significance, often through alterations in DNA which activate proto-oncogenes, or through loss or inactivation of tumour suppressor genes (Bryant, 1993). In the proposed multi step induction of many cancers (Fearon and Vogelstein, 1990), each mutation of DNA is a possible cancer induction step, underlining the significance of an awareness of increases in human mutations through mutagens. Other than cancer, it has been suggested mutations in somatic cells may also be responsible for other pathological conditions in man, and may play a role in the ageing process (Hartman, 1983).

As well as the effect of mutation on somatic cells and tissues, mutations have heritable mutagenic significance in germ cells (Hedde, 1982). Around 1 % of all liveborn infants are affected in some way by genetic disease which resulted from a mutation in germ cells (DuBridge and Calos, 1987). At 16 weeks gestation, around 30 % of

spontaneous abortions are chromosomally abnormal (Seller, 1982). Whilst some of these may be due simply to errors during replication, the effect of mutation exposure on the primordial germ cells is a possibility. Aneuploidy, having more or fewer than an exact multiple of the haploid number of chromosomes, has been shown to be induced by chemicals such as diazepam (Kirkland, 1998). Aneuploidy has a massive impact on human health, for example an additional chromosome 21, as in Down Syndrome, is the commonest identified cause of mental retardation in humans. Specific structural alterations of germ-line chromosomes also appear to predispose to development of particular tumours (Hanson & Cavenee, 1988). We therefore need to assess the risk to human health of all potential mutagens, including chemicals, in our environment.

1.8 The testing of compounds for their mutagenicity

The following quote succinctly explains development of mutagenicity testing:

‘we would like to know what the important sources of mutation are, in an effort possibly to limit exposure to them or to neutralise their activity’

DuBridge and Calos (1987)

The goal of mutagenicity testing is to identify chemicals that cause genetic damage in humans. There are presently over 6 million chemical compounds known, with almost 500,000 used in manufacturing processes (Cummings, 1990). New industrial chemicals are being introduced at a rate of 700 – 3,000 per year, of which only a small number have been fully tested for mutagenic effects.

1.8.1 Carcinogenicity and mutagenicity testing in vivo

The traditional test of choice for carcinogenicity testing in particular would be a long-term *in vivo* animal study, suitable for providing conclusive evidence of carcinogenicity for the chemical under assessment. Such studies are, however, limited due to their vast expense

and the time taken for each experiment, which can run into years. Justification for the use of live laboratory animals is increasingly called into question in the light of raised public awareness regarding animal welfare. It is therefore logistically impossible to test all new and highlighted existing compounds by classical toxicological methods in animals. This, along with scientific advances in genetics, carcinogenesis, and molecular biology has led to the expansion and acceptance of short term tests as predictors of mutagenesis.

1.8.2 Short term in vitro mutagenicity assays

Short term *in vitro* assays were therefore developed to address in part the drawbacks of long term *in vivo* assays, and in recent years scientific advances have led to a widespread validation and acceptance of such tests. More than one hundred short-term tests have been described in the literature, with a small proportion of these now in common use (Dunkel, 1983). The *in vitro* assay has many advantages, not least of which is the significantly reduced cost compared to full scale *in vivo* assessment. In addition, short-term *in vitro* assays require relatively small quantities of test sample, and provide relatively rapid results. The battery of tests commonly used include the chromosome aberration assay *in vitro*, bacterial mutation assays (the Ames test, Ames *et al.*, 1975), sister chromatid exchange measurement, genotoxicity studies using yeast cultures, DNA adducts, and gene mutation assays in cultured mammalian cells.

1.8.3 Mammalian cell assays

In his work on the effects of environmental agents on human populations, Chu (1983) highlighted the advantages of mutagenesis studies in mammalian cells. He described such systems as unquestionably more relevant to man than are bacterial, fungal, or insect systems, combined with the advantage that cultured cells offer the advantage of ease of handling, low cost, and rapidity of assay. Importantly, mammalian cell assays give a

measure of the intrinsic response of the mammalian genome to mutagens (Cole *et al.*, 1990). For many studies, the fact that short term assays require relatively small quantities of test sample is crucial. The main drawback of cultured mammalian cells is their inability to mimic whole organism response and sufficiently activate potential mutagens. This is overcome to a certain extent by the addition of an exogenous metabolic activation system, derived from treated rat livers. There are a range of mammalian assays that are based upon the detection of chromosome changes using microscopy, including the induction of structural chromosome aberrations, which was the assay chosen for use during this study.

1.8.4 Metabolic activation

Many chemicals, including many carcinogens and mutagens, are neither toxic nor naturally reactive to DNA (electrophilic) themselves (Hedde, 1982). The active forms (their metabolites) are generated within the organism during metabolism in certain tissues (primarily the liver in mammals). The biological system involved contributes to its own damage by providing the enzymes and cofactors necessary to generate these electrophilic, genotoxic metabolites. P-450 and P-448 mixed function oxidases catalyse activation, usually by oxidation.

One of the major disadvantages of most cultured mammalian cells is that they have little intrinsic metabolic activation capacity. CHO cells have a minimal level of cytochrome P450 activity and would therefore be incapable of activating some potential mutagens. This is overcome during mutation assays by the addition of an exogenous metabolic activation system. The post-mitochondrial supernatant (S9) from rat livers pre-treated with an enzyme inducer such as Aroclor 1254 is the most widely used (Kirkland, 1990). The S9 fraction is combined with co-factors glucose-6-phosphate and NADP, a composition which is suitable for converting most compounds to active and reactive forms (de Serres and Hollaender, 1980). Careful control of the S9 fraction, including the source

and age of the animal, and the inducer used, are crucial for quality control. There is limited evidence that factors such as the age of the animal may influence the mutagenicity of chemicals through a reduction in activating capacity (Raineri *et al.*, 1986; Brennon-Craddock *et al.*, 1987). The S9 mix is also toxic to cells, and therefore exposure to the test agent in the presence of S9 has to be limited to a maximum of 3 to 6 hours for monolayer cultures (Ishidate, 1990).

1.8.5 Assessment of cytotoxic effect of unknown compounds

Detectable levels of mutation, for example chromosome aberrations, are often found only at doses of the mutagen where some reduction in cell viability is exhibited (Scott *et al.*, 1990). Therefore the cytotoxicity of the test agent is assessed in a preliminary assay, the results of which aid in the selection of suitable screening doses. There are a range of methods for assessing cytotoxic effect, the most common being to determine the effect of the test agent on mitotic index at the time when the cells would be harvested in the mutation assay. Whilst this method is commonly utilised, the effect on mitotic rate is not strictly a reflection of the toxicity of a chemical, as a reduction in the number of mitotic cells may merely be evidence of a cell cycle delaying effect of the chemical. A more direct method of assessing the toxicity of a chemical is to measure its effect on cell viability in the cell system to be used for the chromosome aberration assay, for example by neutral red vital staining (Fiennes *et al.*, 1987). The uptake of neutral red by lysosomes and Golgi bodies was used by Fiennes and widely by other authors in cell culture assays (for example Wilson, 1992) to quantify viable cell numbers.

Under OECD (Organisation for Economic Co-operation and Development) and US EPA recommendations, the highest concentration of a test substance for aberration testing should suppress mitotic activity by 50 % (Lee *et al.*, 1994). The UKEMS (United Kingdom Environmental Mutagen Society) advise a wider 50 – 75 % reduction, with the

countenance that the reduction should not be so great that there are insufficient cells for analysis (Scott *et al.*, 1990). The importance of observing some reduction in mitotic activity is emphasised by the general consideration that negative results are valid only when a significant degree of cytotoxicity has been induced. Where no degree of cytotoxicity is exhibited, there is a recommended maximum testing dose 10 mM or 2–3 mg/ml (Kirkland, 1990). For tests higher than 10 mM, the osmolality of the culture is ascertained as a number of highly soluble, non-toxic, non-DNA reactive substances such as sodium chloride and sucrose have been found to be clastogenic at very high concentrations, probably due to changes in the osmolality of the culture medium (Ishidate *et al.*, 1984).

1.9 The assessment of mutagenicity through the chromosome aberration assay

1.9.1 Overview

In mutagenicity testing, the chromosome aberration assay is an established procedure for examining the adverse effects of chemical and physical agents on mammalian cells (Dean & Danford, 1984). The assay has been used widely since its development (Galloway *et al.*, 1985, 1987, 1997; Sofuni *et al.*, 1990), and the relevance of testing for the ability of a chemical to induce chromosome aberrations is now well established (Kirkland, 1998). The aim of the assay is to detect the induction of microscopically visible changes in chromosome structure. These changes are as a result of chromosome breakage (clastogenesis) and can range from a chromatid gap, which is a small discontinuity in the DNA, to triradial chromosomes as a result of complex interchanges. Recent large collaborative studies have brought together worldwide expertise in the field to resolve differences in methodologies (Galloway *et al.*, 1997).

The use of the chromosome aberration assay is part of the ‘tiered approach’ to chemical testing, the development of which has taken many years of experimentation and

discussion, reviewed by Kirkland (1998). Ishidate (1990) reported that the chromosome aberration assay had been incorporated into the genetic toxicology guidelines of many countries following the recommendations of the OECD, and the concerns of a study by IPCS (International Programme on Chemical Safety)/WHO (World Health Organisation) which indicated that a large number of genotoxic chemicals would be considered non-toxic if tested only by the Ames test. Carcinogens such as benzene, diethylstilbestrol (DES), and asbestos are usually negative in bacterial mutation assays, but are clastogenic and interfere with chromosome segregation during mitosis and result in aneuploidy. The OECD guidelines (1988) for genetic toxicology testing of chemicals emphasised that test systems should cover two genotoxic endpoints – gene mutation and chromosomal aberration.

1.9.2 The significance of chromosome aberrations

A DNA break or discontinuity caused by the test chemical is either rejoined or repaired to restore the original structure, left unrejoined, or rejoined inaccurately to produce a chromosome rearrangement (Bender *et al.*, 1974). In fact, Evans (1983), described the interaction between the test chemical and DNA as not resulting in a direct breakage of the phosphodiester backbone of the DNA or chromosome, but that such breakage or exchange followed as a consequence of misreplication at sites of damage in the DNA during the succeeding normal S phase of DNA replication. The unit of breakage and rearrangement with virtually all mutagens is therefore the single chromatid, with the exception of very densely ionizing particulate radiations. Thus, mutations that occur during (or after) chromosome replication are seen to involve single chromatids when observed at the subsequent mitosis, whereas breakages and rearrangements that involve unduplicated G₁ chromatids themselves become duplicated in S to give chromosome-type aberrations.

A positive result in the chromosome aberration assay demonstrates that the agent can induce gross structural changes *in vitro*. The presence of such chromosome aberrations are usually lethal to cells in the first few cycles after their induction, either because they cannot survive mitosis for mechanical reasons, or due to loss of vital genetic information (Dean & Danford, 1984). Their presence is, however, significant because they are taken as indicators of more subtle chromosome damage that is compatible with cell division, such as reciprocal translocation, inversion, or small deletions. As discussed in section 1.7.3, in somatic cells these may contribute to neoplastic changes, for example translocations at the sites of proto-oncogenes can alter their gene expression (Minden, 1987), and chromosome deletions, rearrangements and whole chromosome loss can lead to the elimination of tumour suppressor genes, resulting in malignancy (Phillips, 1987). Subtle chromosome damage in germ cells may lead to heritable genetic changes through dominant lethality, congenital malformations or indeed to perinatal mortality (Chandley, 1981). That some aberrations lead to stable chromosomal mutations was shown by Ishidate (1990), who recultured colonies of cells which survived MNNG treatment. When subsequently G-banded cells were analysed, around 50 % of the colonies showed karyotypes differing from the original cells – new stable cell populations.

On a more fundamental level, cytogenetic damage is indicative of the interaction of the test compound with DNA and consequently of its potential to induce other genotoxic damage such as gene mutations (Richold *et al.*, 1990). There is also the possibility that one of the indirect effects of mutagen exposure on chromosome structure is as a consequence of damage to nucleotides that could be later incorporated into the chromosome (Evans, 1983). The correlation between chromosome aberrations and carcinogenicity is important. Ishidate (1990) cites a recent review where 93 % of well-known carcinogens were clastogenic in the aberration assay with or without metabolic activation. A negative result in the chromosome aberration assay *in vitro* has been shown

to strongly indicate a lack of potential for *in vivo* clastogenesis, as almost all *in vivo* clastogens have given positive results *in vitro* when fully tested (Thompson, 1986; Ishidate *et al.*, 1988b).

Cytogenetic variation, in the absence of known mutagens, is a common feature of all mammalian development. The use of chromosomal changes as end points for detecting exposure to mutagens is appropriate since a significant proportion of inherited genetic diseases in man are directly attributable to chromosomal mutations involving changes in chromosome structure or number. For example, approximately 1 in 170 live newborn babies has a chromosomal mutation that may have an adverse effect on health and development of the child, to some extent. Chromosome damage is therefore a very appropriate endpoint to be utilised in test systems to detect chemical mutagens (Evans, 1983).

1.9.3 Mechanism of chromosome aberration induction

The majority of chemical mutagens and carcinogens interact with cellular DNA and induce chromosome damage in mammalian cells. Modes of action of mutagens include intercalation (between bases), adduct formation with DNA (e.g. alkylation, strand linking), base analogues incorporated into DNA, deamination of DNA (e.g. nitrous acid), strand scission (e.g. bleomycin), and interference with the mitotic apparatus (Rinkus and Legator, 1980). Two key concepts have been proposed regarding the production of chromosomal aberrations. The first was by Sax in 1940, who published his 'breakage first' hypothesis and went on to develop a one-hit or two-hit kinetics and the role of repair in radiation induced chromosome aberrations. An alternative, proposed by Revell in 1959, was the 'exchange' hypothesis for X-ray induced chromatid aberrations, where all chromosome aberrations are the consequence of an inter- or intra-chromosomal exchange, with incomplete exchanges resulting in deletions (Palitti, 1998). It has more recently been

shown that both models are correct, with a proportion of aberrations being formed by each mechanism (Savage and Harvey, 1991).

It has now been widely accepted that the primary step in the induction of aberrations is the interaction of the mutagen with DNA, forming a DNA lesion. This interaction is mediated by the chromosome dynamic structure and levels of organisation of chromatin. It has generally been observed that there is a non-random induction of chromosome aberrations by different clastogens. In X-irradiated Chinese hamster cells, Slijepcevic and Natarajan (1994) found damage to be more frequent in euchromatic regions than in heterochromatic. The role of DNA repair enzymes, and their use as a research tool, has led to more recent unveiling of aberration formation. The DNA lesion (strand break or damaged bases) is converted to a strand break either by DNA replication or by repair mechanisms. Clastogens whose mode of action falls into the DNA replication category (S-dependent agents), such as UV light and alkylating agents, produce aberrations by misreplication - chromosomal damage is formed once the DNA containing lesion has undergone a round of replication. For the latter category, S-independent agents (such as X-rays), aberrations are produced by misrepair of DNA lesions independent of DNA replication.

Amongst the most recent discoveries, reviewed by Palitti (1998), has been the demonstration that the DNA double strand break is the most important lesion which leads to chromosome aberrations in repair-competent cells (Natarajan *et al.*, 1990), and that processes leading to the formation of dicentrics and translocations are different (Natarajan *et al.*, 1994). Using FISH, Balajee was able to show that interstitial telomeric sequences may make the chromosome more prone to spontaneous breakage or breakage following treatment with clastogenic agents (Balajee *et al.*, 1994).

1.9.4 The chromosome aberration assay method

1.9.4.1 Introduction

For the assay of an unknown compound, an exponentially growing culture of cells are treated with the test agent for a set period (so that cells in all stages of the cell cycle are exposed to the test agent), with or without metabolic activation (Scott *et al.*, 1990). Cells are harvested at around 1.5 cycles post treatment, so that analysis takes place in the first full cell cycle after treatment, with an allowance for the unsynchronised nature of the cell culture and for any delaying effect the test agent has on the cell cycle. Observations made earlier than this, or after the second mitosis, tend to underestimate the frequency of aberrations, as many aberrant cells fail to survive the first mitosis (Dean & Danford, 1984). As well as cell death, underestimation may arise after several cell divisions because acentric fragments and other unstable structural rearrangements such as rings and dicentrics may be lost (Hollaender, 1971). Accumulation of cells in metaphase for microscopic analysis is essential and is achieved by addition of colcemid (a spindle inhibitor that is a synthetic derivative of colchicine), around two hours prior to harvest. The discovery that colchicine arrested eukaryotic cell in mitosis, by Blakeslee in 1937, was one of the two technical innovations that were crucial in the development of the methodology. The second, by Hsu in 1952, was that exposure of mammalian cells to hypotonic solution expands cells and distributes chromosomes evenly throughout the cell (Dean and Danford, 1984). After harvesting and solid staining, cells are examined for the presence of gross readily visible chromosome aberrations which are recorded.

1.9.4.2 Mammalian cell lines used to assay for chromosomal aberrations

The choice of cell system for detection of chromosomal aberrations is important. Firstly, the cell system used must have been sufficiently validated by showing reproducible sensitivity to known clastogens. Several cell types are in common use, including human lymphocytes, with the most popular in toxicological studies being continuous cell lines

derived from the Chinese hamster. Continuous cell lines have the advantage of providing an easily accessed source of clonal cells for repeated assays, they are easily grown and can be synchronised. With regard to the chromosomes themselves, cell types are favoured which have a relatively small number of large chromosomes to facilitate quick and accurate aberration scoring. An international expert working group in Australia in 1994 concluded that there was no one cell type preferable for testing (Galloway *et al.*, 1997).

The Chinese hamster cell lines as a group are well suited for chromosome aberration determinations because their short cell cycles ensure rapid proliferation in a simple culture medium. They also have a small number of relatively large chromosomes, and a DNA mass similar to that of the human cell therefore providing a comparable amount of DNA for exposure. Established cell lines are, however, sensitive to high spontaneous chromosome aberration frequencies, polyploidy and endoreduplications. These can be minimised by careful tissue culture techniques such as avoiding overdense growth and routine checking for mycoplasma infections (Scott *et al.*, 1990). One of the criticisms levelled against the use of continuous cell lines is that cells *in vitro* are genetically unstable and may show drift in sensitivity to mutagens (Fox, 1985). Karyotypic stability is essential and maintained by passaging for a maximum of 15 times before cells are discarded and frozen stocks resuscitated (Loveday *et al.*, 1989). The use of known mutagens as positive controls in each assay check for any drift in sensitivity of the cells.

The continuous mammalian cell line, CHO-K1, was selected for use in this study. CHO has been described as the most widely used cell line for the study of both induced chromosome aberrations and sister chromatid exchanges (Dean & Danford, 1984). Its main advantages over the use of human lymphocytes include its regulated clonal nature, whereas the source and therefore type of lymphocytes may vary from assay to assay. The

CHO-K1 cells also has less than half the number of chromosomes ($2n = 19-21$) of the human lymphocyte, but contain approximately the same amount of DNA making the chromosomes large and easily visible. CHO cells continue to feature prominently in the examination of the ability of chemicals to induce cytogenetic changes and thus identify potential mutagens or carcinogens (Loveday *et al.*, 1989; Galloway *et al.*, 1995, 1997). A CHO cell line has been used for *in vitro* cytogenetic studies on a variety of chemicals in the USA since 1980 under the National Toxicology Program (Sofuni *et al.*, 1990).

1.9.4.3 The CHO cell line

The Chinese hamster ovary cell line was first isolated in 1957 from an ovary culture of the Chinese hamster, *Cricetulus griseus*, (Puck *et al.*, 1958), and the CHO cells used today are clones or subclones of this isolate. A complete karyologic analysis of CHO was presented by Deavan & Peterson (1973), who found 13 altered chromosomes when compared to the parental Chinese hamster cell, and a modal chromosome number of 21. The modal number differs from the original $2n = 22$, the karyotype having undergone extensive rearrangement including inversions and translocations. Analysis of G-banding patterns has shown that all of the template-active genome has been retained (Deavan & Peterson, 1973).

The widely used CHO-K1 subclone was first described by Kao & Puck (1970), and found to differ from CHO cells in that one small telocentric chromosome was missing. This cell line therefore ordinarily has a chromosome number of 20, although chromosome number can often vary from cell to cell. Cells of the CHO line grow rapidly, dividing every 12-14 hours, and are fibroblastic in nature, although they do not elongate to any great extent. The long arm of the X chromosome in CHO cells has a secondary constriction, which has been shown to be a preferential breakpoint similar to the fragile sites observed in several human chromosomes (Loveday *et al.*, 1989). Galloway and co-workers (1997) highlighted the frequent breakage of a large metacentric chromosome in

CHO cells treated with clastogens, giving rise to an acrocentric chromosome and an acentric fragment. The common aberration can be suspected in karyotypes of 22 objects instead of the usual 21.

1.9.4.4 Aberration assay control

Usage of control cultures for all assays is a well established part of the procedure. Erratic control values invalidate experiments as they signal that some essential parameter is not under control. Constant monitoring of the background aberration rate is essential in continuous cell cultures, which are not restricted by the usual homeostatic regulations *in vivo* e.g. nervous and endocrine systems. Without strict *in vivo* regulation, continuous cells will tolerate environmental stresses and spontaneous mutations more readily and these may be reflected in their karyotype. Monitoring is therefore achieved by use of solvent or negative controls.

A positive control is included when testing a compound of unknown genetic activity, at concentrations which induce a relatively low frequency of aberrations to ensure sensitivity of the assay. Chemicals used as positive controls are selected from those that are well documented in the literature, and which are then shown to act reproducibly in the chosen test (Kirkland and Fox, 1993). Different controls are used in activation and non-activation parts of an *in vitro* test, and in this study were selected from Ishidate (1990).

1.9.4.5 Sampling time

A sampling time of 1.5 times the cell cycle from the beginning of treatment is generally recommended in the chromosome aberration assay. It is usual to harvest cells a full cycle after exposure to the test agent, ordinarily in the first metaphase after treatment, as the majority of chemical agents that induce chromosome damage require the cell to undergo an S-phase (DNA replication) before aberrations develop. The additional half cycle time

allows for a moderate cell cycle delay, as the cell cycle length can be altered by toxic agents as the cell may enter an extended G1 or even a short G0 in response to the unfavourable conditions. Ishidate (1988) found that a number of chemicals gave a negative response at 24 hours and positive at 48 hours, indicating a very extensive mitotic delay at clastogenetic doses. It has therefore been recommended that if negative or equivocal results are obtained with a single harvesting time at 1.5 normal cycle times, a repeat test should include an additional sampling time at approximately 24 hours later (Scott *et al.*, 1990).

1.9.4.6 Culture conditions and choice of concentrations

As extremes of pH can be clastogenic (Morita *et al.*, 1989), the effect of the material under test on the pH of the culture medium is required. High sample concentrations may result in changes in physiological conditions, such as pH or osmolality of the culture medium, which can indirectly stimulate the incidence of chromosome aberrations (Ishidate, 1990). Strict regulation of culture conditions is essential to eliminate aberrations which result from increased osmolality or low pH. These have been postulated as being responsible for the 50 % of chemicals that are clastogenic *in vitro* but which fail to induce chromosome aberrations *in vivo* (Thompson, 1986; Ishidate *et al.*, 1988). A minimum of three sample concentrations for testing are required for the production of a dose response curve. The range of sample concentrations is normally selected after an initial cytotoxicity assay has been performed. Doses are then selected which cause a significant reduction in mitotic index, give some degree of mitotic inhibition, and a lowest dose which is on the borderline of toxicity. Because many chemicals are clastogenic only at cytotoxic doses, it is imperative that there is an indication of the level of cytotoxicity in the final test, as repeatability of cytotoxicity levels is difficult to achieve.

1.9.4.7 Scoring of aberrations, statistical analysis and interpretation of results

Metaphase analysis of chromosome aberrations is carried out by an experienced observer who is familiar with the karyotype of the cell line used for the test, and with all the various types of structural changes that can be induced. Generally, the 'percentage of cells with aberrations' rather than the number of aberrations per cell is considered for analysis, so as not to distort results in cases where there were a high number of aberrations in any one cell (Sofuni *et al.*, 1990). Aberrations scored as chromosome or chromatid gaps have usually been excluded from aberration totals and therefore not included for statistical analysis, as their true nature is still not understood. Where chromosome aberrations yields were on the borderline of statistical significance above controls, further investigations are normally recommended if the inclusion of gaps makes the yields clearly significant. Where replicate cultures have been analysed, homogeneity is checked before combining results for evaluation (Richardson *et al.*, 1989). In earlier studies, a linear trend test was used to test for evidence of a dose response (Galloway *et al.*, 1985, 1987; Margolin *et al.*, 1986). After international collaboration, the use of the Fisher's exact test has been generally adopted to compare frequencies of aberrations in control cells and at each dose level (Richardson *et al.*, 1989; Galloway *et al.*, 1997). A Bonferroni or Dunnett type adjustment of the *P* value has been used to allow for multiple dose comparisons against a common control (Galloway *et al.*, 1997).

1.10 Mutagenicity of diesel emissions, PAH, and airborne particulates

The testing of diesel emissions is complicated by the complex nature of the organic output, of which only a fraction of the several hundred compounds present have been identified. The mutational analysis of complex mixtures is therefore discussed (1.10.1), followed by a description of the systems used to actually collect and extract the organic compounds present in diesel emissions for analysis (1.10.2). The remainder of the section describes

previous mutagenicity testing of diesel, from whole emission extracts, emission fractions and airborne particulate fractions, to testing of the PAC compounds present.

1.10.1 Mutagenicity testing of complex samples

Several different strategies have been described for the evaluation of the toxicological properties of complex mixtures: integrative (studying the mixture as a whole), dissective (dissecting a mixture to determine the causative constituents), and synthetic (studying interactions between agents in simple combinations) (Mauderly, 1993). Bioassay-directed fractionation is an example of the dissective approach, and has been used previously to identify mutagenic fractions of organic extracts of diesel exhaust particles (Schuetzle and Lewtas, 1986), and was the approach adopted in this study (Figure 2).

The process involves separation of solvent extracts of the adsorbant (gas-phase) or particulate matter into fractions of increasing polarity using open-column liquid chromatography or HPLC. Short-term bioassays are then used to determine which fractions are most mutagenic (Shuetzle and Daisey, 1990). Through repetition of the chemical fraction and biological testing, sub-fractions with high concentrations of mutagenic compounds can be isolated for the eventual determination of the constituents by chemical analysis. Separation may also unveil unidentified chemicals within a complex mixture, whose activity may be masked in the crude extract by the presence of other chemicals which are actively toxic to the test organisms (Zimmerman and Taylor-Mayer, 1985). Whilst characterisation of the mutagenicity and carcinogenicity of individual compounds within a complex mixture is important, it is also crucial to consider their interactions and the impact these may have on overall adverse potential – the synthetic approach. The synergistic and antagonistic action of individual aromatic hydrocarbons has been demonstrated on several occasions. Several mutagenic and non mutagenic PAH enhance the mutagenicity of B[a]P. However, the majority of mutagenic PAH (particularly

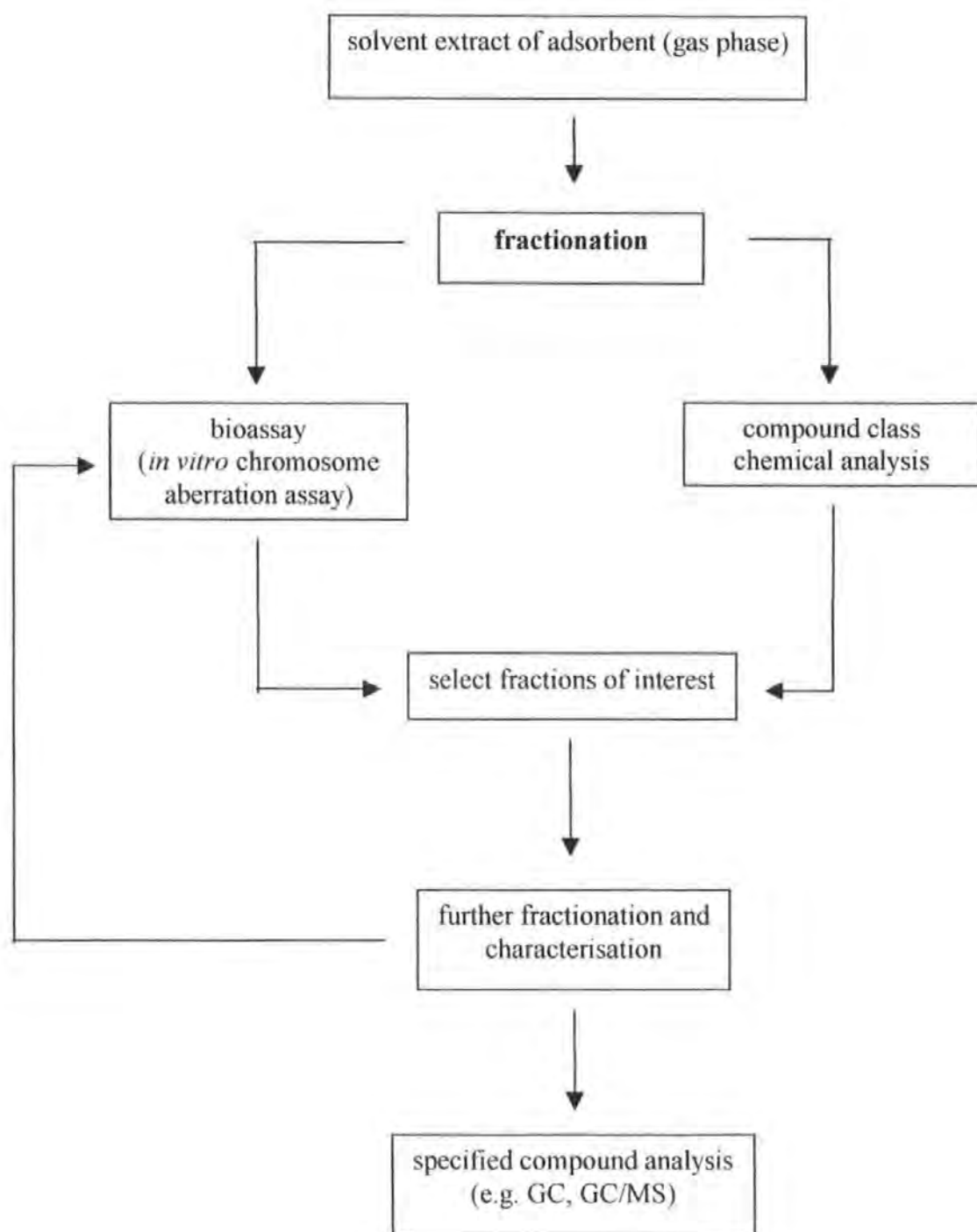


Figure 2. Bioassay directed chemical analysis scheme for identification of mutagenic agents in complex mixtures (adapted from Schuetzle and Daisey, 1990)

those with 5 or more rings) reduce or completely suppress the mutagenicity of B[a]P. The higher the number of rings present in a PAH, the less of the PAH is needed to inhibit or enhance mutagenicity of PAH (Hermann, 1981).

1.10.2 Mutagenicity testing of whole diesel emissions

The mutagenicity and carcinogenicity of complete organic extracts of diesel emissions has been assessed in a variety of test systems, which are discussed below. The mode of collection, and thus the exact chemical nature, of the diesel engine emissions varies between studies, and indeed is not always fully specified. Engines may have been operated under United States or European ‘driving test cycles’, where engine conditions are altered according to a set pattern in an attempt to mimic public traffic. For example the US Federal Test Procedure 75, which operates for 31.5 minutes over a range of speeds with an average at 34 km/h (Bunger *et al.*, 1998; Andersson *et al.*, 1998). Other researchers have used a defined diesel emission extract or standard reference material SRM 1650 (Ostby *et al.*, 1997; Ensell *et al.*, 1998). Table 5 lists the main variables in engine emission collection materials and methodology that have differed between studies. Through collection of diesel engine emissions at a range of set engine conditions of speed and load, as used during this study and previously (Kingston, 1994; Enya *et al.*, 1997), mutagenicity can be correlated with engine operating conditions which could guide future engine improvements and emission regulation.

The characterisation, and therefore control, of emissions from diesel engines is obviously dependent on an experimental sampling system capable of collecting all relevant compounds adequately. The US EPA dilution tunnel and filter sampling system was one of the first sampling systems developed, and has been widely adopted for PAC research use in many countries. The system was devised to mimic the natural dilution and cooling of the exhaust stream as it leaves the tailpipe, with particulate-associated PAC collected on

stage of collection	possible variations in equipment or methods
diesel engine	heavy duty or light duty engine capacity (litres) direct or indirect fuel injection
engine operating conditions	transient driving cycle idling engine set conditions of speed and load
engine sampling system	dilution tunnel collection of gaseous organics TESSA
fractionation	silica gel fractionation/ HPLC solvents and volumes used

Table 5. Major variations in materials and methodology affecting chemical make up of diesel engine emissions and emission fractions assessed for mutagenicity in different studies

filters which may then be extracted with solvents to provide a soluble organic fraction. Drawbacks of this system include inefficient sampling of hydrocarbons and PAC that have remained in the vapour phase (Petch *et al*, 1987), and the significant problem of artefact formation (in particular nitro-PAH) on the carbon particles as the diluted exhaust continues to pass through the filter (Lach & Winkler, 1998). As a significant mass of sample is essential for mutagenicity testing, the relatively prolonged exposure time of the filter accentuates the problem artefact formation.

To address the drawbacks of the dilution tunnel, a unique exhaust stream sampler - TESSA (Total Exhaust Solvent Scrubbing Apparatus) - was developed at Plymouth (Petch *et al.*, 1987). The TESSA is a stainless steel tower linked to a single combustion chamber of the engine. The exhaust passes through the tower against a counter-current of pressurised solvent spray, and is stripped of all hydrocarbons and PAC before they can adsorb onto carbon particles. Therefore gaseous organics are adequately sampled, and to

prevent artefact formation, the solvent is removed rapidly through an exit pipe into ultra pure water to quench further reactions.

1.10.2.1 Assay of whole diesel emission organic extracts in short term assays

The organic extracts of diesel emissions were shown to be mutagenic in bacterial assays some time ago (reviewed in Schuetzle & Daisey, 1990). Mutagenicity is largely dependent on the aromatic content of the fuel (Crebelli *et al.*, 1995), and to some extent the test cycle emissions are collected under (Bunger *et al.*, 1998). Supplementary metabolic activation in the form of rat liver S9 has been reported to reduce the mutagenic effect (Clark and Vigil, 1980; Wang *et al.*, 1981; Bunger *et al.*, 1998). Diesel exhaust organic extracts have also been shown to be mutagenic in a number of *in vitro* mammalian assays, including micronucleus induction *in vitro* (Gu *et al.*, 1992), DNA adducts (Gallagher *et al.*, 1993), and chromosome aberrations and sister chromatid exchanges (Hasegawa *et al.*, 1988; Kingston, 1994). Kingston (1994) found clastogenicity dependent on engine operation conditions of speed and load which the samples were collected under. In the cell transformation assay, diesel exhaust particulate extracts were positive in their ability to transform rat tracheal epithelial (RTE) cells into cells with neoplastic potential (Ensell *et al.*, 1998), and BALB/c-3T3 cells (Hasagawa *et al.*, 1988).

1.10.2.2 Assay of whole diesel emission extracts in vivo

Short-term assays of diesel engine emission extracts have been replicated *in vivo*, primarily in mice. Whilst they failed to induce micronuclei (Ong *et al.*, 1985; Morimoto *et al.*, 1986), Wong *et al.* (1996) was able to demonstrate the presence of adducts in the DNA of rats exposed to a diesel inhalation carcinogenicity regime, which established the *in vivo* genotoxicity of diesel emissions (Rosenkranz, 1986). More recently diesel exhaust particulates were shown to induce morphological transformation RTE cells expressed *in vivo* (Ensell *et al.*, 1998). Animal studies have shown that chronic heavy exposures to

diesel engine exhaust can cause lung pathology and associated physiological effects (Mauderly, 1994), and other types of cancer (Rosenkranz, 1987). Indeed diesel engine exhaust was classified as carcinogenic to experimental animals by the IARC (1989). In rats exposed chronically by inhalation, diesel has been shown to be a pulmonary carcinogen. The response is, however, questionable in mice and negative in Syrian hamsters (Mauderly, 1994). Whilst the usefulness of animal experiments in providing a warning of possible carcinogenicity is not disputed (Morgan *et al.*, 1997), methodology in trying to mimic the occupational environment can bring its own problems. In the case of rat inhalation chronic exposures, the short life of the animal necessitates exposure to extreme concentrations in order to induce a response. Such doses overwhelm the defence mechanisms of the animal, resulting in impaired lung clearance mechanisms so that particles gradually accumulate in the lungs, with a resultant particle or lung overload (HEI, 1995). This detracts from resembling the exposure in the workers occupational environment. There can also be the problem that many animal species have an increased incidence of certain malignancies not found in man (Morgan *et al.*, 1997).

There are, therefore, two mechanisms which may explain diesel exhaust particulate carcinogenicity (Mauderly, 1992). There is a possible genotoxic mechanism where tumour development results from the interaction of particle associated organics with pulmonary cell DNA. If tumours follow the overloading and retardation of lung clearance, however, the subsequent accumulation of particles, inflammation, and the interaction of inflammatory mediators with cell proliferative processes and DNA is suggestive of an epigenetic mechanism. Carcinogenesis could be the result of the parallel action of these two mechanisms - direct genotoxic damage and indirect damage mediated by the immune-response of the lung to the inhalation of large numbers of fine particles (Schlesinger, 1995). It may also be that diesel exhaust induces lung cancer by different mechanisms in different species (HEI, 1995).

1.10.3 Mutagenicity and carcinogenicity of fractionated diesel emissions

Schuetzle and co-workers were one of the first to fractionate diesel exhaust organic extracts (1980), into fraction groups of aliphatic compounds, moderately polar, and polar compounds. The aliphatic fraction includes mainly straight chain hydrocarbons and 2/3 ring PAH. The moderately polar, or aromatic fraction includes many substituted PAH, particularly oxy- and nitro-PAH. The polar fraction has been the most difficult section of emissions to classify and analyse, because polar compounds are generally non-volatile and therefore cannot be analysed by GC/MS without derivatization. Using an alternative method, the presence of di-functional compounds such as hydroxyvaleric acid, succinic acid, and polyols, plus di-substituted alkanes with hydroxy, aldehyde, carboxyl, nitrate, and nitrite esters were identified (Schuetzle and Daisey, 1990). A number of acetylating agents including alkylnitrates, which are known to react with DNA, have been shown to be at their highest concentration in the polar fraction (Schuetzle and Daisey, 1990).

In Ames assays, Schuetzle *et al.* (1980) ascribed more than 65 % of the direct acting mutagenicity to the moderately polar (aromatic) fractions, in which they detected mostly oxy- and nitro-PAH. They did not, however, assay the final polar fraction at that time. Other authors have concurred, attributing between 10 and 40 % of the direct acting mutagenicity of diesel to substituted PAH, in particular nitro-PAH (Pederson & Siak, 1981; Ohe, 1984). More recently, Hayakawa *et al.* (1997) found nearly 62 % of the direct acting mutagenicity in the moderately polar fraction, with strong mutagenicity (35 %) also present in the final polar fraction. Fractions of diesel exhaust containing non-aromatic (aliphatic compounds) did not provoke tumours in rats, whereas fractions containing PAHs with 4 or more rings were found to be potent tumour inducers (Grimmer *et al.*, 1987). Fractionated diesel emissions have also been injected into the adult brain of rats, to elucidate the possible adverse effects of motor vehicle exhausts on the central nervous

system. The latter fractions, containing nitro-PAH and polar group compounds, caused major lesions and some disappearance of immunoreactivity (Andersson *et al.*, 1998).

1.10.4 Mutagenicity of fractions of airborne particulates

As discussed, emissions from diesel-powered vehicles are a significant contributor to levels of particulate matter in ambient air. In contrast to diesel emissions, assays of the organic extracts of ambient particulate matter have found nitro-PAHs to account for only 10-20 % of total mutagenic activity (Arey *et al.*, 1988; Tokiwa *et al.*, 1983). Higher levels of direct acting mutagenicity were found in the polar fractions, suggesting the presence of other so far unidentified mutagenic species (Kamens *et al.*, 1985; Schuetzle and Lewtas, 1986; Nisioka *et al.*, 1988).

1.10.5 Mutagenicity and carcinogenicity of polycyclic aromatic compounds

1.10.5.1 Introduction

As well as testing the whole and fractionated diesel exhaust extracts, research has also focused on mutagenicity testing of some of the several hundred PAC identified in diesel emissions. It was initially thought that PAH were primarily responsible for the mutagenic activity of diesel exhaust emissions. It has since been shown, however, that most of the mutagenic activity in diesel particulate extracts is concentrated in fractions other than the PAH fraction. Components of the aromatic fraction, shown to exhibit strong direct acting mutagenicity, have received the widest attention, in particular nitro-PAC compounds.

1.10.5.2 Mutagenicity of polycyclic aromatic hydrocarbons

It has been proposed that the structural configuration of PAH and their active metabolites may be central to their mutagenic and carcinogenic potential, according to the 'bay region' hypothesis. The bay region relates to a concave area of the periphery of aromatic hydrocarbons, which exhibits distinctive NMR properties (Dipple, 1985). In a detailed

study, Pahlman and Pelkonen, (1987) found PAHs without a bay region (including anthracene, fluorene, naphthene, and pyrene) were not mutagenic. Most of the bay region PAHs they tested (including B[a]P, benz[a]anthracene, triphenylene) were mutagenic, and although three were not (phenanthrene, benzo[e]pyrene, and perylene) they did not dismiss the bay region structure as being important in mutagenic potential.

The most abundant group of PAH occurring in diesel fuels are generally naphthalene and alkylnaphthalenes (Pemberton *et al.*, 1997). Although negative in bacterial assays, the mutagenicity of naphthalene was confirmed *in vivo* in the mouse micronucleus assay, the *Vicia faba* chromosome aberration assay, and the wing SMART (somatic mutation and recombination test) in *Drosophila melanogaster* (Delgado-Rodriguez *et al.*, 1995). In humans, naphthalene produces toxic effects by inhalation, ingestion or adsorption through the skin causing e.g. nausea, vomiting, headaches, fever, anaemia, liver necrosis, convulsions and even coma. It is also toxic for various animal species (Delgado-Rodriguez *et al.*, 1995).

Benzo[a]pyrene has been the most studied PAH, and has shown carcinogenicity after oral administration, intraperitoneal injection, subcutaneous injection, inhalation or after direct application into the lungs or onto the skin of experimental animals (IARC, 1983). For the unsubstituted PAHs in general, a minimum of 4 benzene rings is required for, but does not guarantee, carcinogenic activity (Dipple, 1985). Many other individual PAHs have been shown to have mutagenic potential (Pahlmann and Palkonen, 1987), including several members of the alkyl-PAH group of compounds in bacterial assays. 2-methylanthracene, 9-methylanthracene, 2-methylphenanthrene are direct acting mutagens in Ames bacterial strains. The di and tri-methylfluorenes are indirect acting mutagens, requiring the addition of metabolic activation in the form of rat liver S9 to exhibit a positive response (Scheepers and Boss, 1992). There has been the suggestion from several

investigators that after nitro-PAH, the unresolved mutagenic activity of diesel emissions may be due to oxy-PAHs. One oxy-PAH found abundantly in diesel exhaust, 9-fluorenone, was however not mutagenic in the Ames assay (Schuetzle *et al.*, 1980).

1.10.5.3 *Mutagenicity of nitro-PAH species*

The contribution of diesel engine emissions to nitro-PAH levels in the environment is thought to be significant. The majority of nitro-PAH are potent direct acting mutagens in the Ames test (McCann *et al.*, 1975; Nachtman and Wolff, 1982), although the small amount of testing of this group in mammalian systems has been less conclusive. 1-Nitropyrene (1-NP) and its isomers were preliminarily identified as the major mutagenic species in diesel exhaust in Ames assays (Schuetzle, 1983; Tokiwa *et al.*, 1987). The genotoxicity of 1-nitropyrene has however been described as weak, even in some bacterial systems (Ensell *et al.*, 1998). In mammalian assays, reports of 1-NP are mixed. It induced chromosome aberrations in a Chinese hamster lung cell line with S9 (Matsuoka *et al.*, 1991), and increased SCEs in CHO cells with S9. 1-NP induces cell transformation in some cell lines (BALB/3T3 cells) but not others (RTE cells) (Ensell *et al.*, 1998). Without S9, 1-NP was negative in the HGPRT assay in CHO cells (Heflich *et al.*, 1985), and only weakly positive for the induction of DNA strand breaks in CHL fibroblasts (Edwards *et al.*, 1986). The addition of S9 did not promote activation of 1-NP. The carcinogenicity of 1-NP is still questionable. It has been found to be tumourigenic and non-tumourigenic, although in one study the positive assessment was later changed when a contamination of the sample of 0.2 – 0.3 % with highly mutagenic dinitropyrenes was discovered (Tokiwa *et al.*, 1987).

The detection of nitro-PAH with the highest recorded direct acting activity in the Ames assay overturned earlier conclusions about 1-NP. The dinitropyrenes (DNPs) have been attributed with up to 43 % of the direct acting mutagenicity of diesel emissions

(Nakagawa *et al.*, 1983; Schuetzle and Daisey, 1990). 1,6-dinitropyrene and to a slightly lesser extent 1,8-dinitropyrene are powerful bacterial mutagens, and although they account for only a small amount of the nitro-PAHs in diesel exhaust, they make a significant contribution to the mutagenicity associated with diesel particles because of their potency. DNPs induce chromosome aberrations in CHL cells without metabolic activation (Matsuoka *et al.*, 1991), and are tumourigenic in rats, inducing a range of tumours (Imaida, 1988).

Another nitro-PAH, 3-nitrobenzanthrone, was recently isolated from the organic extracts of both diesel exhaust and airborne particulates and was identified as a new class of powerful mutagen. Mutagenicity in Ames assay was very high, equivalent to that of previously highest recorded levels for 1,8-dinitropyrene, and micronuclei were induced *in vivo*, suggesting its potential genotoxicity to mammals (Enya *et al.*, 1997). Concentrations of 3-nitrobenzanthrone were highest at high load, warning of the potential dangers of engine overloading, and suggesting a need for stronger regulation over the load limit of diesel trucks (Pearce, 1997).

A number of other nitro-PAH have been identified in diesel emissions, including 1- and 2-nitronaphthalene. 1-nitronaphthalene was mutagenic in some mammalian cell culture assays (Shelby and Stasiewicz, 1984; Boyes *et al.*, 1991), but not carcinogenic (Shelby and Stasiewicz, 1984). In contrast, 2-nitronaphthalene induces bladder tumours in monkeys (Beland *et al.*, 1985). This highlights the difference in carcinogenicity and mutagenicity that may be observed between different isomers, for example 6-nitro-benzo[a]pyrene shows greater mutagenic activity in the presence of S9, whilst 1- and 3- nitro-benzo[a]pyrene are potent direct acting mutagens (Beland *et al.*, 1985).

Although they are direct acting mutagens, it is important to note that nitro-PAH must be metabolised to bind covalently to DNA. *Salmonella typhimurium*, the bacterial strain predominantly used in Ames testing, contains a family of nitroreductases capable of reducing nitro-PAHs to their reactive metabolites. Strains deficient in nitroreductase enzymes, and importantly mammalian systems, generally show decreased sensitivity towards nitro-PAH induced mutations (Beland *et al.*, 1985). It is possible that in animals, intestinal bacteria may play a critical role in the metabolic activation of certain nitroaromatic compounds (Beland *et al.*, 1985). As discussed in section 1.10.2, the nitro-PAH are particularly susceptible to formation as artefacts of prolonged engine emission sampling, and their contribution to mutagenicity may therefore be overestimated. For example in studies using the TESSA sampling system, designed to reduce artefact contributions, concentrations of 1-nitropyrene were considerably lower than some reported in the literature (Collier, 1995).

1.11 Aims of the investigation

Continuous alterations in Government regulations relating to diesel emissions in response to increased awareness of their adverse health effects mean that newer engines, emission control devices, and fuels are released each year. Mutagenicity testing conducted in the early 1980's, almost twenty years ago, cannot therefore be relied upon to accurately reflect the potential mutagenic effects of emissions currently emitted from diesel powered vehicles. The need for continued assessment in line with current technology is crucial. Testing of diesel emissions in mammalian system assays has lagged behind the main focus of work in bacterial systems, despite a recommendation from the IARC in 1989 that such testing was required. Although there has now been more than 20 years work, knowledge of the compounds within diesel emissions responsible for their mutagenic effect is limited.

Only a handful of studies to address this using biologically directed fractionation of diesel emissions have taken place, and again a full study in mammalian systems is rare.

The aims of the study were therefore to address some of the above mentioned areas through collection and preparation diesel engine emission samples from a modern light-duty diesel engine using a low-sulphur fuel. The collection of samples over a range of engine conditions of speed and load, was to be followed by fractionation and assay for their mutagenic effect using the chromosome aberration assay in CHO cells. This information was then to be used to guide further emission sample collection and sample fractionation, in a bioassay-directed manner. The objective was to isolate the most mutagenic fractions, and compare the effect of engine speed and load on mutagenicity, and the contribution of measured engine outputs of NO_x, hydrocarbons, and smoke. The inclusion of the diesel fuel in fractionation and mutation assays was to facilitate a comparison of pre- and post-combustion effects.

2. MATERIALS AND METHODS

2.1 Collection and preparation of diesel samples

2.1.1 Diesel engine set up and fuel description

The test engine for this research was a Perkins Prima 2 litre four cylinder light-duty direct injection diesel engine (of the type used commercially in small vans) on a standard test bed set up (Figure 3). The engine exhaust manifold had previously been modified to allow sampling from one cylinder (Rhead *et al.*, 1992). To apply load to the engine (torque, Nm), the test bed included a Borghi and Saveri FA100 eddy-current dynamometer, controlled by a Test Automation Series Compact Controller which also displayed the speed (rpm). The engine throttle was controlled manually by a threaded control rod with adjusting screw.

A stock of fuel was selected and set aside in 50 gallon drums. This reliable stock of low sulphur No.2 DERV fuel (Table 6) was then used throughout the research to supply the engine and for all testing of the fuel. The engine was supplied with fuel from a 10 litre header tank. The lubricating oil used was Shell Heavy Duty Rimula X, grade 15/30W.

Properties	Value
Specific gravity at 15°C	0.8570 kg/l
Aromatic content (%wt.)	37.4
mono-aromatics	30.7
di-aromatics	5.7
tri-aromatics	1.0
Carbon (%wt.)	87.2
Hydrogen (%wt.)	13.0
Sulphur	350 ppm
Boiling range	211 – 370.5 °C
Viscosity at 40°C	4.051 cSt

Table 6. Properties of the low sulphur No.2 DERV diesel fuel used throughout this research work (figures provided by the fuel refiner)

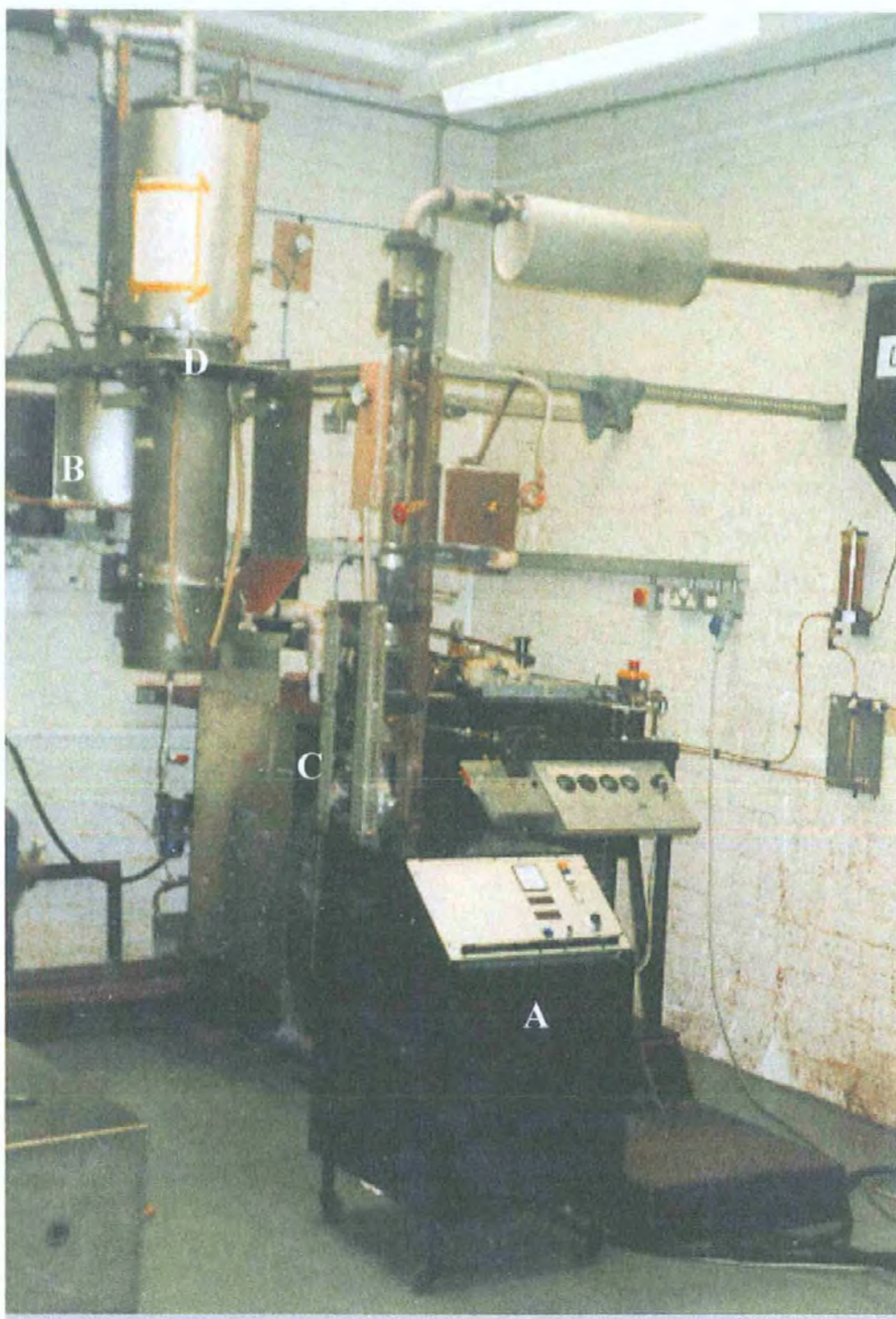


Figure 3. The diesel engine test bed set up at Plymouth. The photograph shows the Test Automation Series Compact Controller (A) which controls the dynamometer and displays engine speed. The solvent reservoir (B) and the dynamometer are located at the rear of the engine (C). The TESSA sampling tower is shown on the left hand side (D)

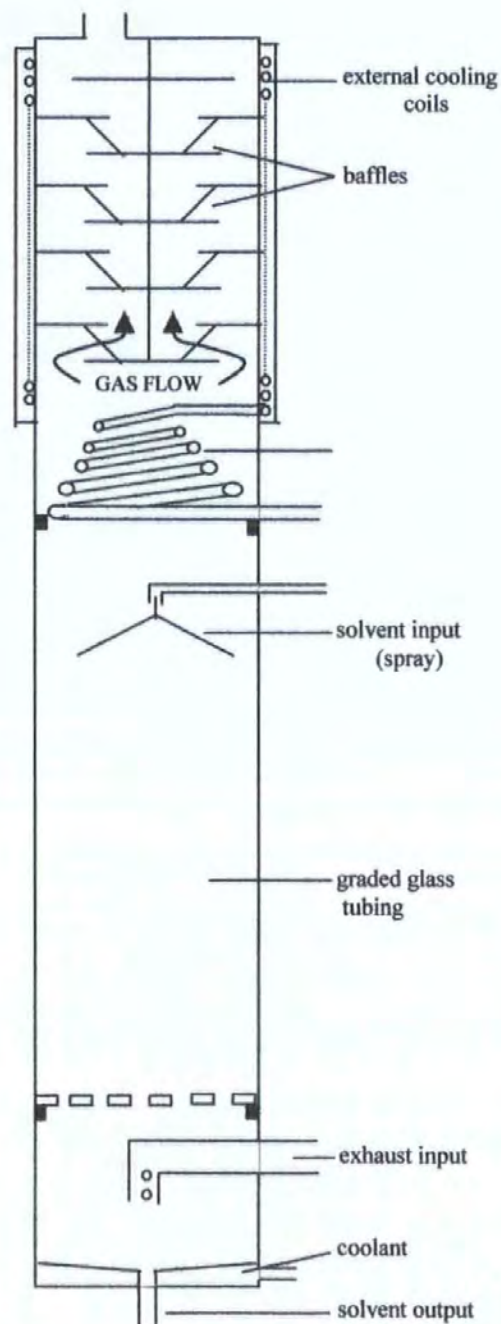
2.1.2 *The Total Exhaust Solvent Stripping Apparatus (TESSA)*

The exhaust gas sampling system used throughout this research, the TESSA, was developed to sample the exhaust close to the combustion chamber (Petch *et al.*, 1987), the advantages of which are discussed in section 1.10.2. The TESSA comprises a stainless steel tower in three sections (Figure 4). The cooled bottom section contains the exhaust entry point, which is fed directly from one combustion chamber of the engine by a slideable plate mechanism, and an exit pipe at the base via which samples are collected. The middle section incorporates the main solvent entry point where the solvent is sprayed under pressure down the tower as the exhaust gasses pass upwards. This area is also filled with short sections of glass tubes which provide a large surface area for interaction between solvent and organics in the exhaust stream. The top of the tower contains a water and baffle cooling section and also has a solvent entry point so that the tower can be washed from the top with solvent.

2.1.3 *Collection of emission samples*

Before sampling, the engine was conditioned by running at a high speed (4000 rpm) and load (80 Nm) for one hour. To ensure proper cooling of the engine and TESSA during operation, the water reservoir was filled with a mixture of ice and water and the cooling system switched on. The speed and load was then set to that desired and the engine run for a further 15 minutes to equilibrate. When ready to sample, a solvent-clean Winchester flask was placed under the outflow pipe to collect the emission sample. The solvent reservoir was filled with solvent [1:1 dichloromethane (DCM): methanol], typically 1200 ml of each solvent for a 2 minute engine sample, and the pressure controlling solvent flow increased to 1 bar. The taps were opened so that the solvent was sprayed under pressure into TESSA for 5 seconds to wet the tower, and then the exhaust flow switched into the base of the tower enabling the exhaust stream to be sampled for a total of 2 minutes. The exhaust flow was then switched back away from the tower, and collection of

(a) diagram of TESSA



(b) photograph of TESSA



Figure 4. The Total Exhaust Solvent Scrubbing Apparatus (TESSA) for engine emission sampling

the sample continued until the solvent reservoir empty. To quench further reactions, 500 ml of de-ionised water was added to each Winchester bottle, which were then stored in the dark at -4°C until work-up. The collection procedure was then repeated up to six times at the set speed and load to give replicate emission samples from sequential runs of TESSA, each sample being collected into a separate Winchester flask. If samples were required from different speed and load conditions, the engine settings were altered and the engine run at the new speed and load for 15 minutes to equilibrate before collection recommenced.

For each speed and load, fuel consumption was measured. The fuel was fed to the engine via a fuel/water separator before entering a 400 ml fuel burette (with measurement increments of 100 ml, 200 ml, and 400 ml), which was normally bypassed during sampling. For fuel consumption measurements, fuel supply was switched to the fuel burette and the consumption of a set volume of fuel timed for that particular speed and load, giving a fuel consumption measurement in litres/minute.

2.1.4 Engine runs performed and emission samples collected

Samples were collected over a range of speeds (1000 – 3500 rpm) and loads (5 – 75 Nm) within the engine's range, during eight engine sampling sessions. A complete list of all engine runs performed, fuel consumption, and sample masses obtained are given below in Table 7.

engine conditions speed (rpm) load (Nm)		date of sampling session	emission sample	fuel consumption (l/min)	mass of sample (mg)
3500	75	25.01.96	ES 3	0.146	107.6
			ES 4		71.4
			ES 5		71.2
			ES 6		65.9
			ES 7		65.0
1000	55	25.06.96	ES17	0.034	17.3 ^b
			ES18		49.5
			ES19		43.6
			ES20		39.0
			ES21		44.8
			ES22		54.2
3000	5	27.06.96	ES23	0.044	184.5
			ES24		101.5 ^b
			ES25		129.0
			ES26		121.5
			ES27		132.8
			ES28		20.1 ^b
			ES29		709.7 ^a
1000	5	02.07.96	ES30	0.011	36.7
			ES31		27.1
			ES32		33.4
			ES33		31.1
			ES34		18.4
			ES35		17.2 ^b
1000	55	02.07.96	ES36	0.034	224.7 ^a
2000	30	16.01.97	ES70	0.043	52.9
			ES71		87.8
			ES72		86.5
			ES73		86.3
			ES74		63.6
2000	55	17.01.97	ES75	0.034	79.2
			ES76		82.8
			ES77		59.3
			ES78		86.8
			ES79		91.9
3000	30	20.01.97	ES80	0.068	84.2
			ES81		123.2
			ES82		145.1
			ES83		129.2
			ES84		116.8
3000	55	22.01.97	ES85	0.096	166.5
			ES86		132.5
			ES87		132.9
			ES88		139.9
			ES89		128.5
			ES90		132.3
1000	55	22.01.97	ES91	0.034	291.8 ^a

^a sampling time of 5 minutes instead of usual 2 minutes

^b part of emission sample lost during work up procedure

Table 7. Diesel engine runs performed, fuel consumption, and sample masses achieved from each consecutive 2 minute sampling session

2.1.5 Sample preparation

To prepare samples for testing and obtain an accurate sample mass, carbonaceous particulate matter and all traces of extraction solvent were removed. All procedures were performed under subdued lighting, and equipment surrounded in aluminium foil, to minimise photo-degradation of light sensitive species. Winchester flasks were removed from cold storage and the contents filtered through glass micro-fibre filters (Whatman GF-F, previously Soxhlet extracted overnight in DCM) under pressure to remove particulates from the sample. By washing with solvent, all emission sample compounds were removed from the solid matter. Filters were changed several times for each sample. The methanol was then removed from the sample by liquid-liquid partition. The filtered sample was then poured into a 5 l separating funnel, to which 0.5 l of de-ionised water was added, the contents carefully mixed and allowed to settle into two distinct phases. The lower phase, which contained the emission sample in DCM only, was then drained into a 500 ml round bottomed flask. The aqueous phase was re-extracted with two aliquots of 50 ml of DCM, again collected in the flask. To remove DCM, the sample was rotary evaporated to a volume of approximately 20 ml. At this stage the sample was examined for the presence of water which settled onto the surface, and if present the liquid-liquid partition was repeated on a smaller scale. The sample was transferred to a 25 ml round bottomed flask and rotary evaporation continued until a volume of less than 1 ml obtained. The sample was transferred to a pre-weighed vial and blown down to a constant weight under a gentle stream of nitrogen. Labelled samples were then stored at -20°C until required.

2.2 Fuel and engine emission sample fractionation

An overview of the fractionation of samples performed in this study is shown in Figure 5. The separation of the emission and fuel samples into aliphatic, aromatic and polar compounds was performed because the complex diesel fuel and emission samples gave

conflicting results when tested as a whole (Kingston, 1994). Separation enabled testing to be concentrated on those fractions which were thought to be the most mutagenic from bacterial tests, or suggested by the chemical make-up of particular fractions. Fractionation also enabled further testing of those emission samples that were cytotoxic at low concentrations (Kingston, 1994), and thus to investigate whether cytotoxicity was masking mutagenicity within the complex chemical mixture of such samples.

2.2.1 Silica gel column fractionation of fuel and whole emission samples

Engine emission and fuel samples were separated by silica gel column fractionation into three groups of compounds – aliphatic, aromatic and polar. The aliphatic fraction, eluted using hexane (Rathburns, HPLC grade), is comprised of straight chain hydrocarbons and PAH. The aromatic fraction, eluted with DCM (Rathburns, HPLC glass distilled grade), contains organic compounds with a de-localised electron ring. The final elution with methanol (Rathburns, HPLC grade) removes all remaining chemicals from the column and makes up the polar fraction.

Prior to fractionation, all glassware was washed in 1-2% Decon (BDH), rinsed in tap water, distilled water and finally deionized water and left to dry completely. Silica gel (Aldrich, 60-100 mesh) and acid washed sand (BDH) were soxlet extracted in DCM for 24 hours, dried, and stored in a hot air oven. The silica gel was activated by oven drying for 24 hours at 185°C before use. To carry out the separation, a glass fretted chromatography column (SGL Ltd, 30 cm x 1 cm) was carefully rinsed with DCM, then hexane, and then refilled with hexane. Hexane was then added to 8 g of pre-weighed silica and stirred for a few seconds until no further gasses evolved, the column tap was opened, and the silica in hexane slurry rapidly added to the column. To ensure even distribution of the silica, the column was tapped with a rubber tube until the silica settled and the hexane drained until level with the top of the silica. The silica was kept wet at all times until the final elution to

prevent cracking of the column. A plug of approximately 0.5 cm depth of acid washed sand was then added to the column to avoid disturbing the silica when samples added.

A sample of mass 50 to 100 mg was weighed and then added to a few drops of hexane. The sample was added to the column using a long-form Pasteur pipette, and the tap opened to allow the sample to enter the silica. Fractions, in solvent, were collected into a 50 ml round bottomed flask. The sample vial was rinsed twice again with hexane, and the rinsings added to the column each time. This helps to ensure a tight band of the sample on the column facilitating a cleaner separation. Approximately 3 ml of hexane was then added to the column, the tap opened and allowed to run down, this was repeated and then the remainder of 20 ml of hexane added to the column and the tap opened to slowly elute the aliphatic fraction. This procedure was then repeated with 20 ml of DCM, including the rinsing of the vial, to elute the aromatic fraction. Finally, the polar fraction was eluted in the same manner using 20 ml methanol. The addition of methanol to the column causes the silica to crack. Each fraction is then rotary evaporated to a volume of approximately 0.5 ml, transferred to a pre-weighed vial, and dried to a constant weight under a gentle stream of nitrogen. A small aliquot each sample was retained separately for chemical analysis by gas chromatography (GC). The first fractionated samples, and randomly chosen subsequent fractions, were analysed by GC to check that the separation into fractions was successful and as expected.

A total of twenty one emission samples, two or more from each set of engine conditions, and two diesel fuel samples were fractionated in this manner. Selection of emission samples for fractionation was based upon similarity of mass, and where possible, samples which were collected consecutively from the engine. The first two minute sample from each sampling session was not used as the mass was frequently inconsistent with the masses of subsequent samples, which may be a reflection of the tower not being

completely washed prior to commencement of the sampling session. Where samples were combined before fractionation to give adequate sample mass, consecutive emission samples were always selected, for example ES 18 (1000 rpm/55 Nm, mass 49.5 mg) was combined with ES 19 (1000 rpm/55 Nm, mass 43.6 mg). The details of samples fractionated together with fraction masses obtained are given in section 3.2.1.

2.2.2 *Fractionation of the aromatic group of compounds by HPLC*

Further separation of the aromatic fraction of the fuel and of two engine emission samples (ES 29, 3000 rpm/ 5 Nm; ES 36 and ES 91, 1000 rpm/ 55 Nm) into 1-ring, 2-ring, and 3+ - rings was performed using HPLC. The engine emission samples were specially collected for further separation by sampling for 5 minutes instead of the usual two minutes to provide a greater sample mass. The separation by HPLC was carried out by a Dr Robin Pemberton from the Environmental Sciences department at the University with my assistance. Samples were fractionated by normal phase semi-preparative HPLC. The solvent programme used was hexane 3ml/min for 50 minutes, DCM 3ml/min for 50 – 100 minutes, and hexane 3ml/min until column equalised, with a column pressure for pure hexane at 146 bar. Retention times were calculated from fractionation of a small sample, mass 30 mg, and were as follows:

aliphatic	15 – 24 minutes
mono-aromatic	24 – 33 minutes
di-aromatic	33 – 46 minutes
tri- + aromatic	46 – 68 minutes

To assess the success of the fractionation, samples were analysed and assessed by Dr Pemberton by gas chromatography /mass spectrometry (GC/MS). Results indicated a good separation with low contamination of the fractions. The mono-aromatic fuel fraction (93.3 mg), for example, was contaminated with 3.31 mg of di- and tri-aromatics (3.54 %), the di-aromatic fraction (24.5 mg) was contaminated with 1.34 mg (5.47 %), and the tri-aromatic fraction (7.1 mg) was contaminated with 0.08 mg (1.23 %).

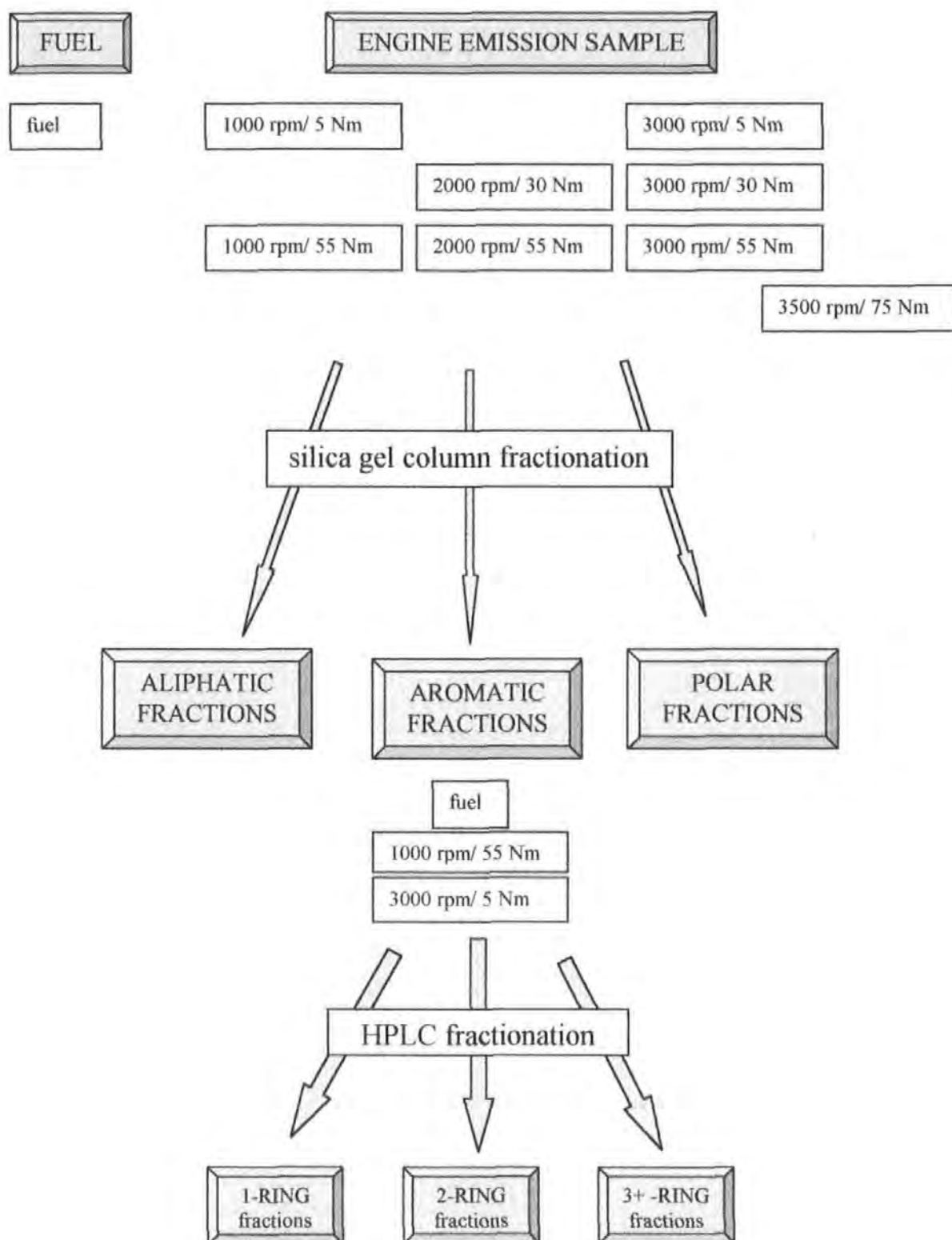


Figure 5. Scheme of fractionation for diesel fuel and engine emission samples collected over a range of engine speeds (1000 – 3000 rpm) and loads (5 to 75 Nm)

2.3 Mammalian cell line characterisation

2.3.1 CHO-K1 cell line details

The continuous cell line derived from the Chinese hamster, CHO-K1, was used for all testing during the study. The benefits of this cell line are described in section 1.9.4.3. All cell manipulations were performed in a horizontal laminar flow hood, and all chemicals used were sterile and of cell culture quality. Chinese hamster ovary cells (CHO-K1) were obtained from the European collection of animal cell cultures (ECACC, number 85051005) as a growing culture, which was expanded to provide sufficient cells for freezing to conserve this particular stock. Upon receipt, the 25 cm² flask of growing cells was incubated at 37°C for 2 days, with a change of culture medium after 24 hours. The flask was then sub-cultured (section 2.4.1) into 75 cm² flasks at a concentration of 5×10^4 cells/ml and incubated at 37°C. When semi-confluent, the cells within these flasks were combined and frozen at -70°C and in liquid nitrogen (section 2.4.2) to establish the first stock. Cells were routinely sub-cultured for a maximum of fifteen times during the study in order to maintain karyotypic stability (Galloway *et al.*, 1985), and resuscitated from frozen stocks when required.

2.3.2 Cytogenetic characterisation of the cell line

The karyotype and chromosome number of the CHO-K1 cell line were established at the start of the study. The level of polyploidy and endoreduplication, together with the spontaneous aberration rate, were then also checked. To assess the normal chromosome complement of the CHO-K1 cell line after sub-culture at Plymouth, two thousand well spread metaphases from untreated cultures were identified and their chromosome number recorded. The number of polyploid (tetraploid) and endoreduplicated cells was also noted. Photographs were taken of several cells with undamaged chromosomes, and one was selected from which a karyotype was prepared. Chromosomes were cut from the original photograph and placed in descending order of size, and then re-photographed to give the

karyotype presented in the Results section. An initial assessment of the level of spontaneous chromosome aberrations was also performed (as in section 2.6.4) in a similar manner from examination of untreated preparations, and was repeated by scoring of control cultures during experimentation.

2.4 Cell line handling and maintenance

2.4.1 Routine sub-culture

Cells were cultured in medium consisting of nutrient mixture Ham's F12 with L-glutamine (at 146 mg/ml) (Gibco) supplemented with 10 % foetal calf serum (Gibco, reserved batch number 30A0760A). Routine sub-culture of cells took place at confluency, typically every 3-5 days. The culture medium was gently poured away and the monolayer washed twice with 2 x 5ml of Dulbecco's phosphate buffered saline (PBS) (Gibco), before 1ml of trypsin (Gibco, 0.25%, 1:250) was added and washed over the cells. The excess trypsin was poured away and the flask placed at 37°C until cells detached from the surface of the flask and rounded up, checked by microscopic examination. Trypsin action was halted by gently resuspending the cells in 10 ml of culture medium. The resuspended cells were counted using a haemocytometer and set in 25cm² and 75cm² disposable flasks (Falcon) at a concentration of 5×10^4 cells/ml, and incubated at 37°C.

2.4.2 Freezing and resuscitation of cells

Semi-confluent flasks of cells were selected and the cells detached from the flask with trypsin as described above. Detached cells were resuspended in culture medium and transferred in 5ml batches into sterile centrifuge tubes, with a little being removed for counting. Cells were centrifuged at 850 rpm for 10 minutes, and then gently resuspended in freezing medium A or B (Table 8) at a concentration of 4 to 6×10^6 cells/ml. Freezing medium A, consisting of 91 % foetal calf serum, was recommended by the ECACC for

maximal cell survival upon resuscitation. Freezing medium B, 20 % foetal calf serum, was the medium routinely used for freezing cells in the laboratory. Both were used to enable a direct comparison. Cells resuspended in freezing medium were then transferred in 1ml aliquots into cryovials (Nunc, BDH Ltd) and placed in an insulated box at -70°C for 24 hours to facilitate a slow reduction in temperature (1°C per minute) to maintain cell integrity. After 24 hours, half of the vials were transferred to liquid nitrogen for longer term storage, and half were stored at -70°C as a backup against the potential problem of failure of liquid nitrogen.

	Freezing Medium A ¹	Freezing Medium B ²
nutrient mixture Ham's F12 with L-glutamine		6 ml
glycerol cryoprotectant (Sigma)	0.9 ml	2 ml
foetal calf serum	9.1 ml	2 ml
total	10 ml	10 ml

¹As recommended by ECACC for maximum cell survival

²As used routinely in the laboratory

Table 8. Constituents of alternative freezing media used to store Chinese hamster ovary CHO-K1 cells at -70°C and in liquid nitrogen (-196°C)

To resuscitate frozen cells, a vial was removed from liquid nitrogen or -70°C freezer, and thawed quickly by running the base of the vial under a warm tap. Once thawed, cells were gently pipetted into a 25 cm^2 flask containing 7 ml of pre-warmed culture medium. To allow maximum initial cell attachment, the flask was left in the laminar flow hood for 1 hour, and then transferred to an incubator at 37°C . After 24 hours, the initial medium was replaced with 7 ml of fresh culture medium. Once confluent, cells were sub-cultured in the normal manner.

2.4.3 *Sterility checking of media and cell cultures*

All cultures and medium were routinely checked for bacterial and yeast infections. Aliquots of 0.5 ml of media and cells in suspension were added to 5 ml of nutrient broth and to 5 ml of thioglycollate broth and incubated at 33°C and 37°C for 1 week, checking daily for the presence of infection. Tryptone Soy Agar (TSA) and yeast extract spread plates were also prepared, incubated at 33°C and 37°C, and checked daily for the growth of colonies.

Growing cultures were checked for mycoplasma using the Hoechst 33258 method (Freshney, 1993). Cover slips were washed in phosphate-free soap (7X, Gibco), rinsed in distilled water and then sterilised in a hot air oven. Cells were seeded onto coverslips (in sterile 35 mm petri-dishes) at 5×10^4 cells/ml, gassed with 50 ml of CO₂ and incubated at 37°C in 1 litre airtight boxes until they reached 20-50% confluence. The monolayer was rinsed firstly with PBS, and then with a 1:1 mix of PBS and cold fixative (3:1 methanol:glacial acetic acid), and finally with pure fixative. Fresh fixative was then added at about 0.5 ml/cm² and left for 10 minutes. The fixative was poured away and the monolayer rinsed with deionized water. A freshly prepared 50 ng/ml solution of Hoechst 33258 (Sigma) in PBS was added and left for 5 minutes at room temperature. The stain was decanted and the coverslips again rinsed with water. The coverslip was mounted cell side down onto a slide containing one drop of mountant (50% glycerine in 0.44M citrate, 0.11M phosphate buffer, pH 5.5). Pre-fixed positively and negatively infected Human Vero cell preparations (ECACC) were stained and mounted in the same way as described above. Cells were examined under UV fluorescence at x100 magnification for the presence of fluorescing cocci or filaments.

2.5 *Cytogenetic techniques*

Metaphase preparations of CHO-K1 cells were made by suspension harvest of the cells in culture (section 2.5.1). Fixed cells were then dropped onto slides, stained and mounted, and then examined under the microscope (section 2.5.4).

2.5.1 *Cell harvesting*

Cells to be harvested were incubated with colcemid (Sigma, 2.5 µg/ml final concentration), a spindle inhibitor, present for the final two hours. The medium was then carefully poured away and the cell monolayer washed twice with 5 ml of PBS. Trypsin (1 ml) was added to each flask, washed over the cells, and the excess poured away. Flasks were incubated for about 5 minutes at 37°C until cells starting to detach from the base of the flask, checked by examination under the inverted microscope. Rounded up cells were then gently resuspended in 5 ml of fresh culture medium, and the cell suspension transferred to centrifuge tubes and spun at low speed (600 rpm) for 5 minutes. The supernatant was carefully removed, and the cell pellet resuspended in 5 ml of freshly prepared KCl (BDH Ltd, 0.56%) using a short form siliconised glass pasteur pipette. After 10 minutes at room temperature, the tubes were again centrifuged for 5 minutes at 600 rpm, and then the supernatant removed. Ice-cold freshly prepared fixative (3:1 methanol:glacial acetic acid) was added drop-wise to each tube to resuspend the cells in the first fix. Cells were then centrifuged at a higher speed (1000 rpm) for 5 minutes, the supernatant poured away, and the pellet resuspended in fresh fixative for the second fix. The centrifugation and resuspension were repeated to give the third fix, in which the cells were left for at least 30 minutes. After this time, tubes were centrifuged at 1000 rpm for 5 minutes, the supernatant poured away, and the cells resuspended in several drops of fresh ice-cold fixative to give an opaque cell suspension.

2.5.2 Slide preparation and staining

Metaphase spread preparations were made using the dropping technique. Clean grease-free twin-frosted microscope slides (Chance Proper, BDH) were soaked in ice cold distilled water. Slides were removed from the water just prior to use and blotted on clean paper towels to leave a thin film of water over the surface. The freshly resuspended cells were then dropped from a long-form siliconised pasteur pipette onto the cold wet slides from a height of approximately 9 inches. Four or five drops along the surface of the slide was usually sufficient to produce a suitable cell preparation for examination. Slides were placed on a hot plate at 36°C and allowed to dry. To stain, slides were placed in staining trays and immersed in a 5% solution of Gurr Giemsa's stain (improved R66 solution, BDH) in buffer pH 6.8 (Gurr, BDH) for 20 minutes. The stain was washed away from the dish, the slides rinsed and allowed to dry at room temperature.

Each slide was then permanently mounted with a 22 x 50 mm coverslip. Because of the nature of the mounting materials, all mounting was carried out in a fume cupboard. Xylene (BDH) was washed over the slide using a pasteur pipette, and then a drop of Gurr DePeX mounting medium (BDH) added to the centre of the slide. A coverslip was placed over the mountant and gently pushed down using a mounting needle to remove any bubbles. Slides were then placed on a high temperature hot plate for several hours to encourage an even spread of mountant, then left to cool and harden. Stained, mounted slides were then ready for examination under the microscope.

2.5.3 Giemsa banding

For Giemsa G-banding, actively growing cells were harvested in the normal manner (section 2.5.1) and dropped onto clean slides. Once dry, slides were stored for 3-5 days at room temperature to age the preparation. To commence banding, slides were placed in pre-heated 2 x SSC (standard saline citrate buffer – 0.3 M NaCl with 0.03 M trisodium

citrate) in coplin jars in a 60 °C waterbath for 1 hour. Trypsin (0.25%), diluted 1 in 50 with PBS, was washed over the slide for 20 seconds, and then rinsed off with distilled water. Slides were stained with 5% Giemsa for 20 minutes, mounted with DePeX and examined under the microscope.

2.5.4 Microscopy and photomicrography

Cell preparations were examined on a Reichert-Jung Polyvar microscope equipped with x40 and x100 planapochromat objectives, with the green filter in position. Cells of interest were photographed with a Konica 35mm camera with automatic exposure control on the Polyvar microscope, which incorporated a x2 supplemental lens. Black and white photographs were taken using Ilford Delta 400 film. For fluorescence work, the U1 incident light fluorescence module was used with ultra-violet (BP330-380) exciter filter, dichroic mirror (DS420), and barrier filter (LP418).

2.6 Mutagenicity Testing

All samples for testing were firstly assessed for cytotoxic effect on CHO-K1 cells using neutral red vital staining (2.6.1), to indicate the range of concentrations to be tested. Samples were then tested in the chromosome aberration assay both with (2.7.6) and without metabolic activation (2.6.2). The criteria for aberration identification is also described here (2.6.4).

2.6.1 Cytotoxicity testing

It is recommended (OECD and US EPA, Lee *et al.*, 1994) that suspected clastogens are tested to a maximum concentration of 50 % toxicity (section 1.8.5). Initial cytotoxicity assays were therefore performed on all samples to establish doses which would reduce cell viability by about 50%, thus selecting the highest concentration for testing in subsequent

chromosome aberration assays. The method followed was that of dye uptake by viable cells after Fiennes *et al.* (1987). An aqueous stock solution of neutral red (BDH) at 0.1% w/v was prepared, autoclaved, then acidified with 2 drops of glacial acetic acid per 100 ml, and stored in the dark at 4°C. A 24 well multi-well plate (Falcon) was seeded at 4×10^4 cell/ml, placed in a 1 litre sealed plastic container, and incubated for 24 hours at 37°C. Two wells were included with medium only as background controls for the neutral red dye uptake. A set of concentrations of the sample to be tested, usually increasing by ten-fold, was prepared and 10 µl of each concentration added to wells in duplicate. Control wells with no treatment were included. The cells were then incubated for a further 14-18 hours, after which the medium was removed. Neutral red stock solution was diluted 1:9 with pre-warmed PBS and 1 ml added to the wells. The cells were incubated for a further 2 hours to allow neutral red dye uptake. The residual neutral red dye was then discarded and each well rapidly washed with PBS, ensuring careful aspiration of the second wash. Cold extraction buffer (1:1 absolute ethanol: 0.1M citrate buffer pH 4.2) was added to each well in aliquots of 1 ml to release intracellular dye. After 20 minutes, dye uptake was detected spectrophotometrically against an extraction buffer blank at 540 nm in a spectrophotometer. Cytotoxic effects of exposure to samples were then assessed by comparison of absorbance readings of treated wells to controls.

2.6.2 Chromosome aberration testing

All chromosome aberration tests were carried out following the basic method of Galloway *et al.* (1985, 1987). Stock solutions of fuel and engine emission samples for testing were prepared in dimethyl sulphoxide (DMSO, BDH). 25cm² flasks were seeded with CHO cells at 5×10^4 cell/ml and incubated overnight at 37°C to allow cell attachment and division. Replicate cultures were set so that two flasks were set per concentration to be tested, as well as two control flasks containing solvent only, and two positive control flasks. The following day, all flasks were removed from the incubator and the test sample

added in volumes of no more than 40µl. This meant that the solvent, DMSO, was kept at a concentration of no more than 0.05 % as per guidelines (Kirkland, 1990). At the same time, 40 µl of DMSO was added to the control flasks, and 80 µl of freshly prepared N-methyl-N'-nitro-N-nitrosoguanidine (MNNG) added to each of the positive control flasks to give a final concentration of 0.15 µg/ml. The flasks were returned to the incubator for a further 16-18 hours, with colcemid present for the final two hours. Cells were then harvested and slides prepared as described in 2.5.1 and 2.5.2. A summary of all fuel and emission samples assayed for chromosome aberrations is given in section 2.8.

2.6.3 *Assessment of mitotic rate*

The mitotic indices of control and treated cultures were assessed at each dose level. One thousand cells were randomly counted across each slide using the x10 objective, and the number of these cells in mitosis was recorded. This provided a mitotic rate, MR, per 1000 cells.

2.6.4 *Scoring metaphase preparations for chromosome aberrations*

One hundred metaphase cells per dose level, where possible, were selected for scoring on the basis of good morphology and with a chromosome number of modal number ± 2 (Galloway *et al.*, 1985). Where it was not possible to score 100 cells from one slide, consecutive slides from that dose level were recorded until this figure was reached or until all slides had been examined. Each slide was scanned under x10 magnification, and selected metaphase cells examined under x100 oil immersion for the presence of aberrations. The chromosome number of each cell examined was recorded on a data sheet to ensure that the correct number of cells had been examined. Where aberrations were found, the vernier reading and type(s) of aberration were also recorded. The identification of the type of aberration followed the recommendations of Scott *et al.* (1983), whereby aberrations were firstly divided into two main groups; chromosome - where both

chromatids affected; and chromatid - where only one chromatid affected (Table 8). Within each group, aberrations were identified and recorded individually and then classified after Galloway *et al.* (1985). The separation into classes was to provide information about types of aberration, and are listed in Table 9.

Gaps, defined here as a discontinuity of the chromatid smaller than its width, or greater than the width with connecting strands of DNA or protein visible, and endoreduplications were recorded but not included in totals for aberrations. A continuous assessment of polyploidy was also undertaken, with polyploid cells defined as those with one or more extra haploid sets of chromosomes, expressed as number of polyploid cells/100 cells examined. Results were expressed as total number of aberrations per dose, and as percentages of cells with aberrations. The latter was used as the base unit for the assessment of damage, as once one aberration has occurred in a cell the usual consequence is that the cell will die and thus additional aberrations have little or no further biological relevance (Richardson *et al.*, 1989).

group	class	type of aberration
chromosome type	simple	breaks
	complex	exchanges, including dicentric with fragment, centric ring and fragment, and acentric rings (double minutes)
	other	pulverised cells, heavily damaged chromosomes
chromatid type	simple	break or deletion, isochromatid break or deletion
	complex	exchanges, including inter- (e.g. quadradial) and intrachange, chromatid exchange (e.g. triradial)

Table 9. Classification of structural chromosome aberrations

2.6.5 *Chromosome aberration assay of a known mutagen in the CHO-K1 cell line*

To check the potential of the CHO-K1 cell line for identifying mutagens, and to select a positive control compound, the cells were assayed with the known direct-acting mutagen, MNNG (Sigma). The standard aberration assay method was followed (2.6.2). Briefly, ten flasks of CHO-K1 cells were set at 5×10^4 cells/ml and incubated for approximately 24 hours. A stock solution of MNNG was prepared in sterile water, and then added to flasks to give replicate cultures with final concentrations of 0.075, 0.15, 0.30, and 0.60 $\mu\text{g/ml}$. This range of concentrations includes doses with published effects (Galloway *et al.*, 1985; Ishidate, 1988). The final two flasks were left untreated (control cultures). Cells were incubated in the presence of the mutagen for 18 hours, and then harvested with colcemid present for the final two hours. Slides were prepared and examined for chromosome aberrations, and a dose response curve produced (Kirkland and Fox, 1993) which is presented in section 3.4.4. Aberrations were compared to published data to ensure a suitable level of activity within the cell line.

2.7 *Metabolic activation*

2.7.1 *Introduction*

Most chemical carcinogens and mutagens are biologically inactive until they are converted enzymatically into electrophilic, genotoxic metabolites. The key reaction for most chemical classes is oxidation, catalysed by microsomal NADPH-dependent cytochrome P448/P450 mixed-function oxidases (Dean & Danford, 1984). CHO cells in culture lack the ability to metabolically activate chemicals at a significant rate because of low mixed function oxidase activity, and therefore enzyme-rich fractions of mammalian tissue homogenates are added to the cell culture system to represent human activation. In this case, the enzyme-rich fractions are in the form of Aroclor-1254-induced rat liver S9.

2.7.2 Preparation of rat liver S9 fraction

The method followed was basically that of Venitt *et al.* (1984), and the procedure was carried out under Home Office Project Licence PPL 30/1139. Male Wistar rats of 6-8 weeks old (approximately 200g) were injected intraperitoneally with 0.1 ml of a 200 mg/ml solution of Aroclor 1254 in peanut oil by a licensed technician. The Aroclor 1254, a mixture of polychlorinated biphenyls, serves as a pre-treatment for the liver increasing enzyme activity. Five full days after treatment the rats were killed and their livers removed. To ensure sterility of the S9, all work was carried out aseptically with sterile equipment and chemicals. Each liver is placed immediately into a covered beaker of ice-cold saline on ice, and when all have been removed they were transferred to a sieve and washed with 750 ml ice-cold saline. Excess fluid was removed by shaking and blotting with gauze. The livers were weighed and 3 volumes of 0.15M KCl reserved and kept on ice. The livers were chopped finely using scissors and then homogenised with a Potter hand-homogeniser, a little at a time, with some of the reserved KCl. Once all the liver was homogenised, the remaining KCl was added and shaken well until the contents uniform. The homogenate was then centrifuged at 9000g for 20 minutes in cooled centrifuge tubes at 2°C. When centrifugation was complete, the supernatant was carefully poured into a fresh flask, shaken to uniformity, and then dispensed into cryovials standing in a dry-ice/alcohol freezing mixture. The vials were then transferred to liquid nitrogen.

2.7.3 Sterility checking of S9 mix

To ensure the preparation procedure had not resulted in any contamination of the S9 mix, 2 ml was reserved from each batch for sterility checking. For bacterial contamination, 200µl was spread onto two nutrient agar plates, and for yeast contamination, 200 µl onto two yeast extract plates. The plates were incubated and checked daily for 7 days for any sign of contaminant growth.

2.7.4 Determination of cytochrome P450

To give an indication of the activity of each S9 preparation, the total cytochrome P450 content (the sum of all the various isoenzymes) was determined spectrophotometrically (Lake, 1987). When the reduced P450 enzymes combine with carbon monoxide, a characteristic absorption spectrum with a maximum at 450 nm is given. The method used was as follows. First, the microsomal fraction was diluted 1:2 with 0.2M phosphate buffer, pH 7.4, and placed on ice. A small quantity of sodium dithionite was added and mixed gently. The sample poured into a cuvette and scanned to give a baseline reading between 400 and 500 nm. The contents of the cuvette are then bubbled gently with carbon monoxide for 1 minute, and the difference spectrum recorded. A prominent absorption maximum at around 450 nm was seen. To calculate the cytochrome P450 concentration, the difference between absorption maximum at around 450 nm and at 490 nm (corrected for absorption difference between wavelengths prior to bubbling with CO) is determined [ΔA (450-490)nm]. The cytochrome P450 concentration of the sample is given by the following formula:

cytochrome P450 concentration (nmol P450/ ml S9 fraction)

$$= \frac{\Delta A(450-490)\text{nm}}{1} \times \frac{1000}{91^a} \times \frac{\text{vol. S9 sample (ml)} + \text{vol. phosphate buffer}}{\text{vol. of S9 sample}}$$

^a molar extinction coefficient of cytochrome P450 has been determined to be 91 cm²/nmol (Omura & Sato, 1964)

2.7.5 Composition of S9 mix

The S9 metabolic activation system is NADPH dependent, and hence requires the addition of cofactors before incorporation into the cultures. The S9, cofactors, and any buffer are collectively known as the S9 mix. A wide variety of varying S9 mixes have been described (Galloway *et al.*, 1985; Sofuni *et al.*, 1990; Dean & Danford, 1984). One of the

simplest is that described by Benford and Hubbard (1987), which was adopted for use in this investigation. For assays that proved negative with the normal concentration S9 mix, selected tests were repeated with twice the volume of S9 in the mix, 2 x S9, as recommended (Kirkland, 1990). The constituents and volumes of the S9 mixed used are shown below in Table 10.

Component	S9 mix (1 x S9)	S9 mix (2 x S9)
Serum free Ham's F12 media	43.05 ml	41.55 ml
S9 fraction	1.5 ml	3.0 ml
NADP solution (80 mM)	0.225 ml	0.225 ml
Glucose-6-phosphate solution (100mM)	0.225 ml	0.225 ml
Total	45.0 ml	45.0 ml

Table 10. Composition of S9 mixes used in cytotoxicity and chromosome aberration assays requiring metabolic activation

2.7.6 Characterisation of S9 activity in chromosome aberration assays

To gauge the suitability of the activity of the S9 for use in the chromosome aberration assay, aberration assays were carried out with a known indirect-acting mutagen cyclophosphamide (CP) over a range of concentrations. The results were scored and compared to data given by Galloway *et al.* (1985) for S9 used regularly in their laboratory. The outline method used in all aberration assays was that of Galloway *et al.* (1985, 1987), and for assaying S9 activity was as follows. Twelve 25 cm² tissue culture flasks were set with CHO cells at a concentration of 5×10^4 cells/ml, and incubated overnight at 37°C. The following day, solutions of the cofactors NADP (80mM) and G-6-P (100mM) were prepared and frozen. A solution of the mutagen cyclophosphamide was also prepared at room temperature. Vials of S9 were removed from liquid nitrogen and were left to thaw at room temperature with the cofactors, and were then stored on ice. The S9 mix was

prepared on ice in the laminar flow hood. The medium was poured off the cells, the monolayer washed with PBS, and then 8 ml of S9 mix added. The relevant volume of CP was measured and added to each flask. Flasks were incubated for 2 hours in the presence of S9 mix and CP at 37°C, after which time the flasks were removed and the monolayer washed twice with PBS. Fresh complete culture medium was then added to each flask in volumes of 8 ml, and the flasks returned to the incubator for a further 12-14 hours, with colcemid (0.1 ml of a 200µg/ml solution) present for the final two hours. The cells were then harvested and slides prepared as described in sections 2.5.4 and 2.5.5. After preparation of a dose response curve, aberrations were scored and compared to published data (Galloway *et al.*, 1995) for similar experiments to ensure an adequate level of S9 activity (section 3.6.3). The experiment was repeated for the second batch of S9 prepared.

2.7.7 Cytotoxicity testing with metabolic activation

The cytotoxicity assay was repeated for fuel and emission samples in the presence of metabolic activation, following the method described in 2.6.1. A 24 well multi-well plate was seeded at 4×10^4 cell/ml, placed in a 1 litre sealed plastic container, and incubated for 24 hours at 37°C. Two wells were included with medium only as background controls for the neutral red dye uptake. The following day, S9 mix was prepared as described previously (2.7.6), together with a set of concentrations of the sample to be tested, usually increasing by ten-fold. The existing medium was removed from each well (by pipette), and the wells rinsed with PBS. One ml of S9 mix and then the sample were added to each well, and the cells incubated at 37°C. After 2 hours, the S9 mix and sample were removed, the cell monolayer washed twice with PBS, and then replaced with fresh culture medium. The cells were then returned to the incubator for a further 12-16 hours, after which the medium was removed and diluted neutral red dye added. The procedure was then identical to that used for assay without S9 (section 2.6.1). Finally, dye uptake was detected

spectrophotometrically against an extraction buffer blank at 540 nm. Cytotoxic effects of exposure to samples were then assessed by comparison of absorbance readings of treated wells to controls.

2.7.8 Chromosome aberration assay with metabolic activation

For testing for chromosome aberrations with metabolic activation, the method of Galloway *et al.* (1985, 1987) was again followed where cells were exposed to the test chemical in S9 mix (Table 10) for 2 hours, the medium replaced, and cells harvested 14-16 hours later. The method used was as follows - flasks were set and incubated overnight as described in previous sections. The next day, solutions of the cofactors NADP (80mM) and G-6-P (100mM) were prepared and frozen. A solution of the indirect-acting mutagen, cyclophosphamide (CP), was also prepared at room temperature. Vials of S9 were removed from liquid nitrogen and were left to thaw at room temperature with the cofactors, and were then stored on ice. The S9 mix was prepared on ice in the laminar flow hood. The medium was poured off the cells, the monolayer washed with PBS, and then 8 ml of S9 mix added. The relevant volume of each test chemical was measured and added to each flask, with S9 mix and DMSO only added to control flasks, and 50 μ l of CP (to give a final concentration of 25 μ g/ml) added to positive control flasks. Flasks were incubated for 2 hours at 37°C, after which time the flasks were removed and the monolayer washed twice with PBS. Fresh complete culture medium was then added to each flask in volumes of 8 ml, and the flasks returned to the incubator for a further 12-14 hours, with colcemid present for the final two hours. The cells were then harvested and slides prepared as described in sections 2.5.1 and 2.5.2.

2.8 Summary of cytotoxicity and chromosome aberration assays performed

A summary of all fuel and emission samples assayed for their effect cytotoxic and clastogenic effect are given below in Table 11.

sample	sample fraction					
	aliphatic	aromatic	polar	1-ring aromatic	2-ring aromatic	3+ -ring aromatic
fuel	✓ [†]	✓		✓	✓	✓
1000 rpm/ 5 Nm	✓ [†]	✓	✓			
1000 rpm/ 55 Nm	✓ [†]	✓	✓	✓	✓	
2000 rpm/ 30 Nm			✓*			
2000 rpm/ 55 Nm			✓*			
3000 rpm/ 5 Nm	✓	✓	✓	✓	✓	✓
3000 rpm/ 30 Nm			✓*			
3000 rpm/ 55 Nm			✓*			

* samples assayed without S9 only

[†] samples assayed for cytotoxicity only

Table 11. Summary of all fuel and emission samples assayed for their cytotoxic effect in the neutral red dye assay in CHO-K1 cells, and subsequently for their clastogenicity in the chromosome aberration assay in CHO-K1 cells. Assays were performed both with and without metabolic activation (rat liver S9 fraction) except those marked *

2.9 Statistical analyses

For analysis of the statistical significance of increases in chromosome aberrations, the cell was taken as the base unit for assessment, as opposed to the chromosome or chromatid (i.e. aberrations per cell). This is the practice adopted by Galloway *et al.* (1985) and other authors (Richardson *et al.*, 1989). Therefore, although the total number of chromosome aberrations at each dose was recorded, analysis was based on the percentage of cells with chromosome aberrations so that once one aberration has occurred in a cell further aberrations were not included, and this also solves the potential problem of cells with multiple aberrations. The statistical tests were adopted following guidelines of the UKEMS (Richardson *et al.*, 1989) and the latest recommendations of a US and Japanese

collaboration described in Galloway *et al.* (1997). Variation between replicate cultures was assessed using appropriate dispersion statistics (2.9.1), and significance of absolute increase in aberrations over the solvent control at each dose assessed with Fisher's exact test (2.9.2).

2.9.1 Variation between replicate cultures in percentage of cells with aberrations

Where replicate cultures were scored, a test for homogeneity was performed to assess the validity of combining data for further analysis. The binomial dispersion test, as described by Richardson *et al.* (1989), was used. The test statistic, X^2 , was calculated from the following formula:

$$X^2 = \sum_{i=0}^t \sum_{j=1}^{m_i} \frac{(r_{ij} - n_{ij}p_i)^2}{n_{ij}p_i(1 - p_i)}$$

The treatments are numbered from 0 to t, where t0 is the solvent control. In the i th treatment ($i = 0$ to t), the number of replicate cultures is m_i (in this case 2). From the j th replicate ($j = 1$ to m_i), n_{ij} cells are sampled of which r_{ij} are found to contain aberrations.

The proportion of aberrant cells in the i th treatment is $p_i = r_i / n_i$. The X^2 test statistic, with

$$\sum_{i=0}^t (m_i - 1) \quad \text{degrees of freedom}$$

was then compared to the upper percentage points of the X^2 distribution with to assess the heterogeneity between replicate cultures ($X^2 < \text{critical value at upper 5 \% point indicating no evidence of heterogeneity}$). If there was no significant difference between replicate cultures, data from the replicate cultures were then pooled for analysis of chromosome aberrations.

2.9.2 Chromosome aberration data

The proportion of aberrant cells at each concentration was compared to the proportion of aberrant cells in the solvent control using Fisher's exact test (Galloway *et al.*, 1997; Richardson *et al.*, 1989). The Fisher's exact test was developed for use with small samples, and therefore a test such as chi-squared may appear more appropriate. However, the assessment of chromosome aberration data is special in that whilst a high number of cells are normal, a low number of cells are damaged. Thus examination of a small change in the number of damaged cells is required, for which Fisher's exact test is now generally used. Calculations were performed using a statistical program (Langsrud, 1999), which was validated using the published figures of Richardson *et al.* (1989). The criteria for classifying test compounds as positive, weak positive, and negative clastogens follows that of Galloway *et al.* (1997). This brought together features of both the National Toxicology Program (USA) studies (Galloway *et al.*, 1987) and the criteria used in Japan (Sofuni *et al.*, 1990), and is summarised below in Table 12.

To compensate for the multiplicity of data comparisons against a common control, a Bonferroni correction was applied (Lovell, 1990). Data were tested at the 5 % significance level in all cases, and therefore to assess probability that the number of aberrant cells was increased sufficiently over the control level to be clastogenic the significance level was divided by the number of comparisons made (the number of doses, for example $0.05 / 4 \text{ doses} = 0.0125$). As the exact significance varies between samples depending upon the number of concentrations assayed, the significance actually tested against is quoted in Tables in the results section for each sample. In the general text, probabilities are referred to as significant ($P < 0.05$) or not significant ($P > 0.05$) to avoid confusion.

criteria	decision
2 doses significant ($P \leq 0.05$) or 1 dose significant and $\geq 10\%$ cells with aberrations	POSITIVE
1 dose significant ($P \leq 0.05$) but $< 10\%$ cells with aberrations	WEAK POSITIVE
no significant increases	NEGATIVE

Table 12. Criteria for classification of results of statistical analyses of data produced from chromosome aberration assays (based on Galloway *et al.*, 1997).

3. RESULTS

3.1 Engine runs performed and emission samples collected

Three sets of diesel emission samples were collected over a range of speed and load conditions (Table 7, section 2.1.4). Initial samples collected in January 1996 were based on predictions of aromatic content from maps of the engine performance supplied by the engine manufacturers (Appendix D). The second set of engine conditions were chosen for direct comparison with earlier work on the total emission samples (Kingston, 1994), and were collected in June and July 1996. The final set of samples were collected in January 1997, the conditions for which were chosen to ensure a more complete picture of emissions over the engine range of speed and load. Six repeats of each two minute sample were collected immediately after one another to ensure consistency of collection conditions. For further HPLC fractionation into aromatic ring compounds, greater masses of emission sample were required. To ensure a greater mass of sample without overheating the engine, non-standard collection was performed over 5 minutes with emissions passing through the tower on a one minute on, one minute off basis (three minutes on in total). Two sets of conditions of speed and load were selected, 3000 rpm/5 Nm, and 1000 rpm/55 Nm. For the 1000 rpm/55 Nm load sample (ES 36), a sample mass of 224.7 mg was collected, which was felt to be too small for further studies. A repeat sample was therefore collected 6 months later in January 1997 (ES 91, 291.8 mg). Because these samples were collected 6 months apart, they were fractionated separately and analysed by GC/MS (section 3.2.2) before being combined for testing.

3.1.1 Mass of total engine emission samples collected

Individual masses for each total emission sample collected are presented in Materials and Methods, section 2.1.4. The average mass of a 2 minute sample (from the six samples collected consecutively) is plotted against its speed and load below in Figure 6. A clear relationship between increasing engine speed and increasing total emission sample mass can be seen, with the exception of the samples collected at 3500 rpm and 75 Nm. The

emission sample mass also increases with increasing engine load, although to a lesser extent. The figure highlights the wide difference in sample masses obtained during each 2 minute sampling session, from an average 27.3 mg at 1000 rpm speed and 5 Nm load to 138.8 mg at 3000 rpm speed and 55 Nm load. Such differences emphasise the fact that for certain speeds and load conditions, it was necessary to combine samples before and after fractionation to obtain sufficient sample masses for testing (section 3.2.1).

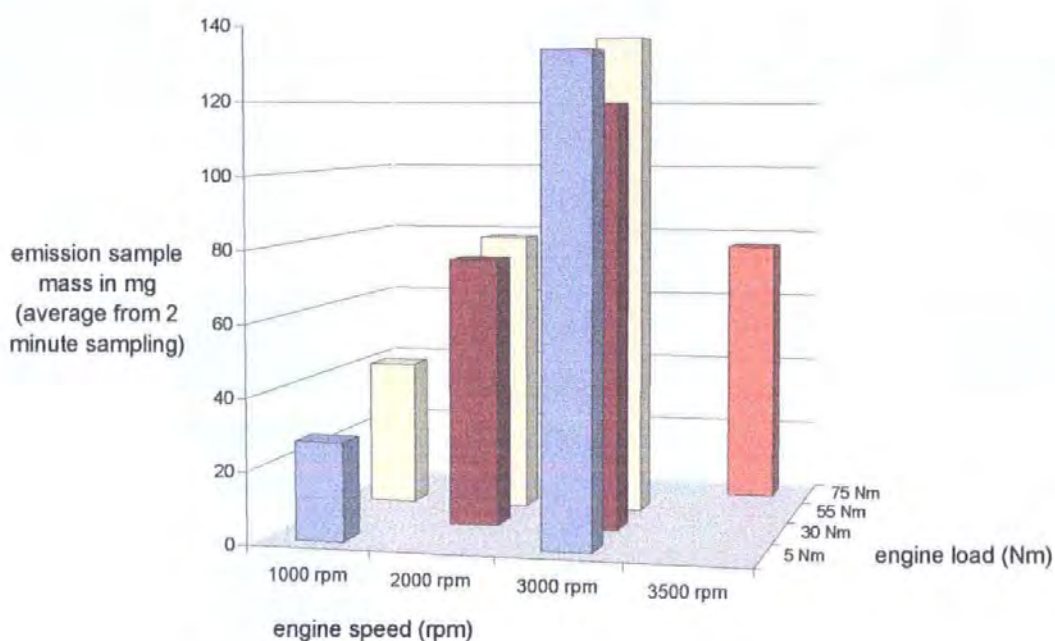


Figure 6. Average mass of total emission sample obtained from six consecutive 2 minute engine emission sampling sessions at each set of engine speed and load conditions

3.1.2 Fuel consumption of the test engine during sample collection

For each condition of speed and load that samples were collected under, the fuel consumption was measured as described in section 2.1.3, the results of which are presented here in Table 13. Although not a quantitative measure, fuel consumption gives an indication of the engine's operating efficiency during sample collection for each set of conditions. Fuel consumption was lowest during sampling at 1000 rpm and 5 Nm

(consumption 0.011 l/min), conditions of low speed and load where the burden on the engine was small. At the opposite extreme, a high fuel consumption of 0.146 l/min was recorded during engine conditions of high speed (3500 rpm) and high load (75 Nm), when the burden on the engine was at its greatest. Intermediate engine conditions exhibited intermediary levels of fuel consumption, with both the engine speed and load applied to the engine being contributory to fuel expenditure. For example, the fuel consumption was higher at 2000 rpm speed with 55 Nm load (0.061 l/min) than with a higher speed of 3000 rpm and lower load of 5 Nm (0.046 l/min). Fuel expenditure was closely matched when high speed, low load conditions (3000 rpm/5 Nm) are compared to mid speed and mid load (2000 rpm/30 Nm).

Under the same engine parameters of speed and load, fuel consumption was almost identical when measured on different dates. This suggests, therefore, that the condition of the engine did not deteriorate or alter significantly between collections.

Engine speed (rpm)	Engine load (Nm)	Sampling date	Fuel consumption (l/min)
3500	75	25/01/96	0.146
3000	55	22/01/97	0.096
3000	30	20/01/97	0.068
2000	55	17/01/97	0.061
3000	5	27/06/96	0.044
2000	30	16/01/97	0.043
1000	55	25/06/96	0.034
1000	55	02/07/96	0.034
1000	55	22/01/97	0.034
1000	5	02/07/96	0.011

Table 13. Engine diesel fuel consumption (litres/min) recorded during sample collection for each set of engine conditions of speed and load

3.2 Fuel and emission sample fractionation

3.2.1 Silica gel column fractionation of fuel and whole emission samples

Selected fuel and engine emission samples collected were fractionated into aliphatic, aromatic and polar groups of compounds by silica gel column fractionation (section 2.2.1) for testing in the chromosome aberration assay. Emission samples were combined both prior to and post-fractionation to provide a sufficient mass of sample to complete all assays where possible. Samples combined were always those collected successively on the same day under the same conditions to ensure consistency. In addition, samples of similar mass were chosen to be combined and tested. This usually excluded the first sample taken under each set of conditions, which was frequently of dissimilar mass to the rest of the set. Such a difference may have arisen where the tower was not 'washed' in between sampling sessions, and ignoring this sample ensured that cross contamination of organic species from different sampling conditions did not occur. In all cases where samples were combined, this took place prior to testing to ensure all assays were performed with a uniform, consistent sample.

The mass of emission sample obtained after each 2 minute engine sampling was dependent upon the engine conditions of speed and load (Table 7, section 2.1.4), in a similar way to fuel consumption. Higher engine speeds correlated to larger sample masses, and to a lesser extent increased engine load was also correlated with larger sample masses. For example the average sample mass of the six emissions samples collected at 1000 rpm and 5 Nm was 27.3 mg, which was increased to an average 75.4 mg at 2000 rpm and 30 Nm, and to a high average mass of 138.8 mg at engine conditions 3000 rpm speed and 55 Nm load. The emission and fuel samples chosen for fractionation are given in Table 14, together with the masses of each fraction recovered. Post fractionation recovery was high with an average 90.7 % (83 – 99 %) of the original fraction recovered when individual fraction masses are combined. A minimum of approximately 25 mg of sample was

required to conduct a full range of testing for cytotoxicity and then in the chromosome aberration assay both with and without metabolic activation, with the actual mass required dependent on the range of concentrations to be tested. For less cytotoxic samples, each assay required a range of larger sample concentrations.

Several of the fractions were selected for chemical analysis by gas chromatography (GC, section 2.2.1) to confirm the success of the fractionation. The GC operation and subsequent analysis of traces was performed by Dr Pemberton from the Environmental Sciences department at the University. The chemical make up of all fractions tested was as expected, validating the fractionation technique.

For the fuel fractionation, the initial sample was limited only by the maximum mass that could be applied to each glass column at one time (approximately 100 mg). Two large initial samples were therefore separated at one time to give sufficient fraction masses for testing throughout. The aliphatic sample masses (123 and 110 mg) and aromatic masses (80.9 and 56.6 mg) were sufficient for all assays. As the fuel contains minimal polar group compounds, the small masses of this fraction achieved after separation were attributed to the probable presence of detergents in the fuel. For the emission samples, the mass available for fractionation was limited in the first place by the mass achieved during each 2 minute engine sampling. In the case of two of the emission samples (1000 rpm/55 Nm and 1000 rpm/5 Nm), total emission samples were combined prior to fractionation to ensure a sufficient mass of sample for consistent silica gel column separation. This was particularly important for engine samples collected at 1000 rpm speed and 5 Nm load, where the average TES was a low 27.3 mg. Combination of ES 30 and ES 31 gave a mass of 63.8 mg for fractionation, and ES 32 plus ES 33 were combined to a mass of 64.5 mg for fractionation.

emission sample (ES)	engine conditions (rpm/ Nm)	sample mass (mg)	aliphatic fraction mass (mg)	aromatic fraction mass (mg)	polar fraction mass (mg)	total fraction mass (mg) (recovery %)
FUEL		233.7	123 F 7	80.9 F 8	7.7 F 9	211.6 (91)
FUEL		187.9	110 F 10	56.6 F 11	1.9 F 12	168.5 (90)
4	3500/75	71.4	18	14.6	33.9	66.5 (93)
5		71.2	11.7	13.0	34.2	58.9 (83)
6		65.9	9.8	11.6	*	
18+19	1000/55	93.1	35.5 ES 43	28.2 ES 44	19.2 ES 45	82.9 (89)
21+22		99	37.2 ES 46	33.7 ES 47	22.5 ES 48	93.4 (94)
26	3000/5	121.5	50.4 ES 37	36.0 ES 38	27.4 ES 39	113.8 (94)
27		132.8	47.8 ES 40	34.9 ES 41	28.9 ES 42	111.6 (84)
30+31	1000/5	63.8	20.8 ES 49	18.9 ES 50	23.3 ES 51	63.0 (99)
32+33		64.5	18.2 ES 52	18.9 ES 53	20.5 ES 54	57.6 (89)
71	2000/30	87.8	*	*	31.0 ES 107	
72		86.5	*	*	30.5 ES 110	
78	2000/55	86.8	*	*	31.1 ES 113	
79		91.9	*	*	31.8 ES 116	
83	3000/30	129.2	*	*	37.9 ES 119	
84		116.8	*	*	36.2 ES 122	
86	3000/55	132.5	*	*	49.0 ES 125	
87		132.9	*	*	51.9 ES 128	

* fractions were not evaporated to dryness therefore no sample mass is available

Table 14. Summary of the silica column fractionation of fuel and diesel engine emission samples collected during 2 minute sampling over a range of engine conditions of speed and load, the fraction masses achieved, and percentage recovery of the original sample. Sample numbers (F/ES) are given in blue for those samples used in subsequent testing

The relative mass of each fraction obtained was not consistent for samples collected under different engine conditions (Figure 7). For this reason it was not possible to predict accurately how much of each fraction would be achieved and therefore be available for

testing. This was another reason for combining samples to ensure that there were sufficient fraction masses for each assay. For the fuel for example, the aliphatic fraction made up the majority 61.5 % of the original sample, with aromatic compounds forming an average 36 %, and polar a minimal 2.5 %. At conditions of low speed and low load (1000 rpm/5 Nm), the polar fraction predominated being 36 % of the total fraction, with almost equal percentages of aliphatic and aromatic compounds at approximately 32 %. The aliphatic fraction was the greatest by sample mass for both emission samples collected at 3000 rpm/5 Nm and 1000/55 Nm. These two samples also had very similar polar fractions, at 24 and 25 % of the total sample mass. The aromatic compound contribution to the 1000 rpm/55 Nm sample was greater at 35 % compared to the 3000 rpm/5 Nm sample (31 %). The aromatic fraction, for all three of the emission samples where percentage contribution was calculated, was similar and within a 3 % range (32 – 35 %).

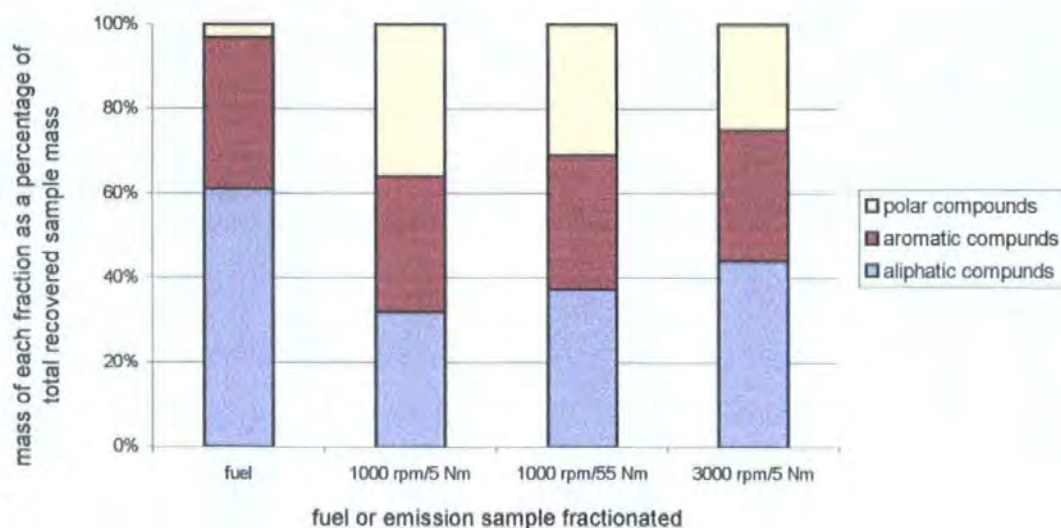


Figure 7. The average mass of aliphatic, aromatic and polar group compounds, expressed as a percentage of the total mass recovered, from silica column separation of combined samples of diesel fuel and engine emission samples collected at 3000 rpm/5 Nm, 1000 rpm/55 Nm and 1000 rpm/5 Nm

3.2.2 Fractionation of the aromatic group of compounds by HPLC

Three high mass engine samples (ES 29, ES 36, and ES 91) were obtained by altering the emission sample collection timing as discussed in section 3.1. These samples, together with fuel, were fractionated by HPLC into 1-ring, 2-ring and 3+ aromatic ring fractions (section 2.2.2). Sample masses achieved are given in Table 15. The fractionation of the high mass 5 minute engine samples was performed completely by HPLC, and therefore the mass of aromatic compounds prior to separation is not known. The contribution of 3-ring and larger ring compounds to the aromatic fraction as a whole can be seen to be small for all four of the separations performed. Contamination of each fraction with other compounds was assessed by gas chromatography/mass spectrometry (GC/MS) by Dr Pemberton, the results of which showed that there was less than 6 % contamination of each fraction (section 2.2.2). GC/MS chromatography traces were provided for the 3+ -ring fractions (fuel and emission sample collected at 3000 rpm and 5 Nm), and are shown in Appendix C. The relative abundance of selected compounds with significant peaks are given in Figure 123, Appendix C.

Sample	Engine conditions (rpm/ Nm)	Total mass (mg)	Fraction mass (mg)						Total fraction mass (mg)
			1 -ring		2 -ring		3+ -rings		
FUEL			186	R 40	103.7	R 26	13.1	R 27	302.8
ES 29	3000 / 5	709.7	44	R 41	91.5	R 32	17.6	R 33	153.1
ES 36	1000 / 55	224.7	38.6	R 28	17.6	R 29	2.6	R 30	58.8
ES 91	1000 / 55	291.8	41	R 37	14.3	R 38	3.7	R 39	59

Table 15. Fuel and diesel engine emission samples collected during 5 minute sampling at three different engine conditions of speed and load, their total mass and the masses of aromatic ring fractions obtained after separation by HPLC. Sample numbers (R) are given in blue for those samples used in subsequent testing

At 11 % of the total fraction recovered, the 3+ -ring fraction of the emission sample collected at 3000 rpm and 5 Nm (ES 29) is, however, more than twice the 3+ -ring fraction of the fuel or the second emission sample (Figure 8). The contribution of the 1-ring and 2-ring compounds to each of the total fraction masses differs widely. The 1-ring fraction comprises 62 % of the fuel aromatic sample, a much lower 29 % of ES 29 (3000 rpm/5 Nm), and a majority 68 % of ES 36 and ES 91 (1000 rpm/5 Nm emission samples combined). The 2-ring fraction forms a majority 60% of the mass of the aromatic fraction of ES 29 (3000 rpm/5 Nm), and much lowers percentages of the fuel (34 %) or of the emission samples collected at 1000 rpm and 5 Nm (ES 36 and ES91) at 27 %.

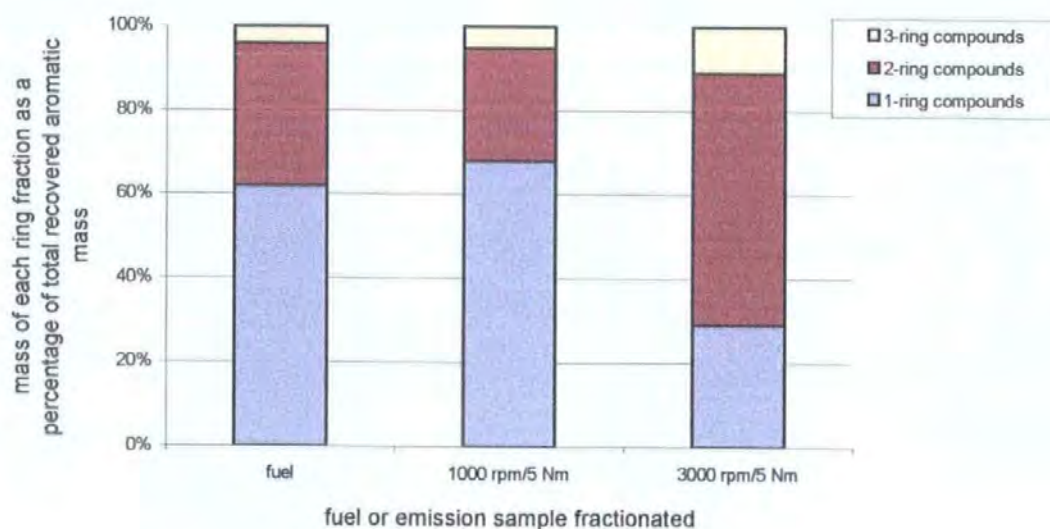


Figure 8. The average mass of 1-ring, 2-ring, and 3+ -ring compounds, expressed as a percentage of the total aromatic mass recovered, from HPLC separation of samples of diesel fuel and engine emission samples collected at 3000 rpm/5 Nm, and combined emission samples collected at 1000 rpm/5 Nm

3.3 Chinese hamster ovary cell line characterisation

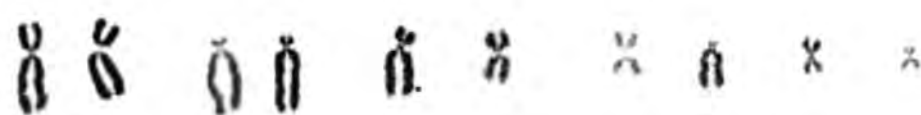
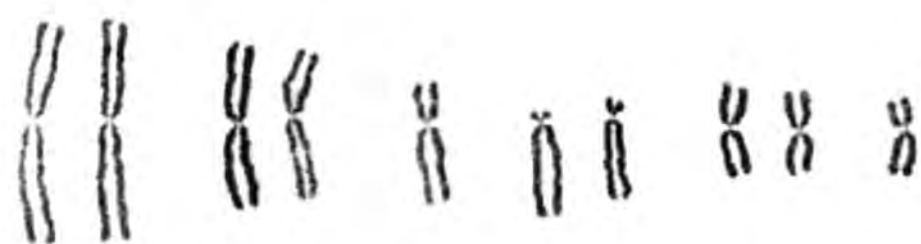
The cell line purchased for dedicated use in these experiments is detailed in section 2.3.1. Upon receipt, the cell line was allowed to settle and then sub-cultured to enable frozen stocks to be established. The cells were then checked for sterility and mycoplasma infection (section 2.3.4). Actively growing cells, including cells resuscitated from frozen stocks, were harvested, stained and mounted over several months to provide a stock of slides for assessment and analysis.

3.3.1 Karyotype of CHO-K1 cell line after sub-culture at Plymouth

During initial assessment of the suitability of the cell line for aberration assays, slides of untreated cells were examined for well spread metaphases with few or no crossovers of chromosomes, which were photographed. From these photographs, karyotypes were prepared (section 2.3.2) and a 'representative' karyotype was selected (Figure 9, Plate 1). The cell selected has 20 chromosomes, including 2 pairs of large metacentrics, a pair of large acrocentric chromosomes, and several medium sized meta- and submetacentrics. The remaining smaller chromosomes are made up of a range from telocentric to metacentric. Under continuous culture, there has been a well documented deviation of the CHO cell line from the chromosomes of the diploid tissue from which it was derived which has a chromosome number $2n = 22$ (Deavan and Peterson, 1973). In the solid stained karyotype prepared, twelve of the chromosomes can be paired (i.e. 6 pairs of homologous chromosomes, or chromosomes with large regions of homology), with the remainder being significantly different from each other as to be unmatched. In their detailed examination of the CHO cell line in 1973, Deaven and Petersen concluded that with only minor exceptions, one haploid set of chromosomes had remained intact in the CHO cell, and that all of the template active genome had been retained (CHO differs from CHO-K1 in having one extra small telocentric chromosome). This appears to be true in general for the CHO-K1 cell line used during this study. G-banding of one chromosome 1 from CHO-K1 cells

Figure 9. Karyotype of a Chinese hamster ovary CHO-K1 cell and the metaphase spread preparation from which it was derived. The chromosomes were solid stained with Giemsa

CHO-K1 KARYOTYPE



10 μ m



maintained at Plymouth shows that the banding pattern is largely unchanged from the ideogram of the Chinese hamster chromosome 1 published in 1976 by Ray and Mohandas (Figure 10).

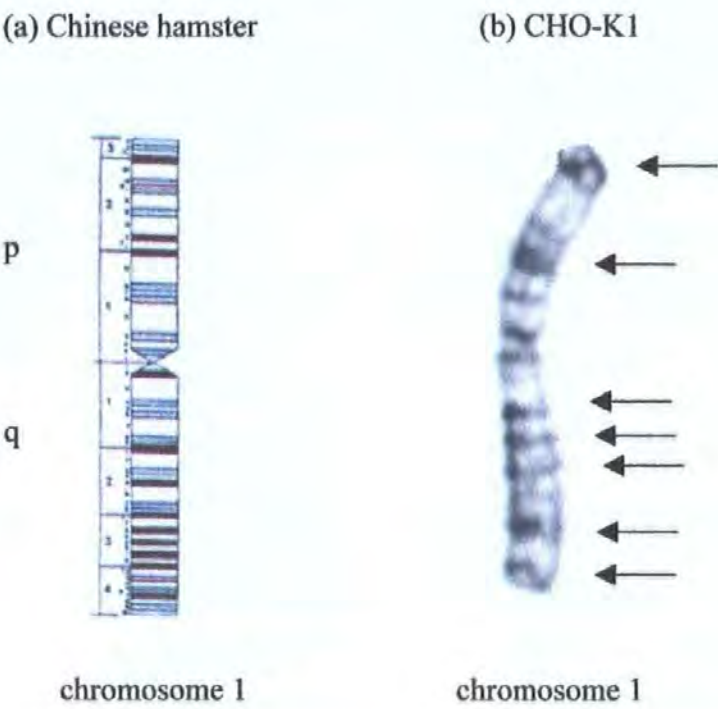


Figure 10. Ideogram of chromosome 1 from the Chinese hamster *Cricetulus griseus* (a) and photograph of a G-banded chromosome 1 from the Chinese hamster ovary cell line CHO-K1 (b). Arrows indicate the presence of corresponding dark bands present on both chromosomes.

For other chromosomes there have, however, been major rearrangements from the original Chinese hamster cell. Using chromosome specific DNA libraries and FISH, Balajee and colleagues (1995) analysed some of the spontaneous rearrangements of chromosome material in cell lines including CHO-K1. They highlighted rearrangement of certain chromosomes, for example DNA from chromosome 3 of the Chinese hamster exhibited signals from 5 separate chromosomes in the CHO-K1 cells line, indicating at least 3 major rearrangements. G-banding of the CHO-K1 cell line used shows that whilst the q arm and centric regions of chromosome 3 are largely unchanged, the upper portion of 3p differs from that of the Chinese hamster ideogram presented (Figure 11). This concurs

with the rearrangement described by Balajee *et al.* (1995) for chromosome 3. For other chromosomes, for example chromosome 4, rearrangement has been so extensive that tracking changes would be almost impossible without high resolution G-banding or FISH molecular studies (Figure 12).

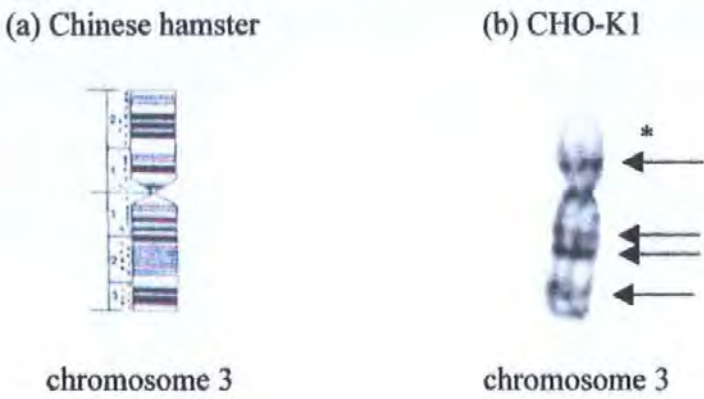


Figure 11. Ideogram of chromosome 3 from the Chinese hamster *Cricetulus griseus* (a) and photograph of a G-banded chromosome 3 from the Chinese hamster ovary cell line CHO-K1 (b). Arrows indicate the presence of corresponding dark bands present on both chromosomes, and * indicates dissimilar region

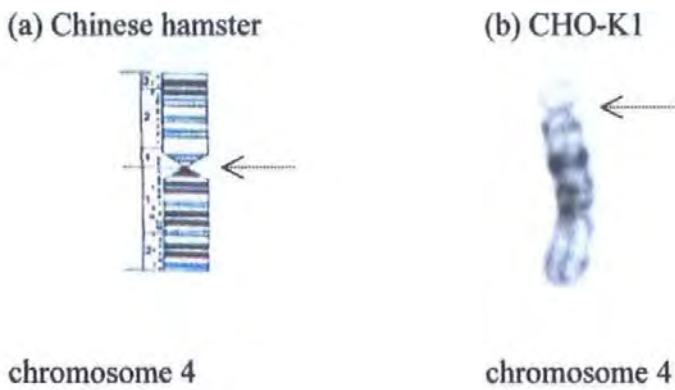


Figure 12. Ideogram of chromosome 4 from the Chinese hamster *Cricetulus griseus* (a) and photograph of a G-banded chromosome 4 from the Chinese hamster ovary cell line CHO-K1 (b). The arrow indicates centromeric position

The X chromosome in the CHO cell line has a secondary constriction on its long arm (Slijepcevic and Natarajan, 1995), which was identifiable in many of the metaphase spreads examined. The area of the secondary constriction, when observed, was a paler staining region compared to the rest of the chromosome. In some cells there was a definite chromosome gap formed at this junction, however these were not included in scoring of aberrations because of their suspected nature as a preferential breakpoint (Galloway *et al.*, 1997).



Figure 13. Giemsa-banded metaphase preparation of a Chinese hamster ovary CHO-K1 cell (from which the chromosomes in Figures 10 - 12 are derived)

3.1.1 Assessment of chromosome number and polyploidy of CHO-K1 cell line after sub-culture at Plymouth

From untreated cells, metaphase preparations were examined for polyploidy and to assess the normal chromosome complement in the CHO-K1 line sub-cultured at Plymouth

(section 2.3.2). Two thousand well spread metaphases were identified and their chromosome number counted. The most frequent chromosome complement (modal number) was 19 chromosomes, with 40.4 % of the cells examined having this chromosome number (Figure 14). The number of cells with a chromosome complement of 20 was just slightly less at 36.5 % of the two thousand metaphases examined. Therefore, most of the cells scored had a chromosome number of 19 or 20 chromosomes (76.5 % of all metaphases in total). In all subsequent assays, cells for aberration analysis were selected not only on the basis of good morphology under low power, but also those with a chromosome number in the range 17 to 21 i.e. the modal number 19 ± 2 , following the recommendations of Dean & Danford (1984). Polyploidy, in the form of tetraploidy ($4n$), was observed at a level of approximately 6 % within the cell line during this initial assessment. The level of polyploidy was reduced to 2-3% by careful culture techniques, and thereafter assessed regularly throughout the study.

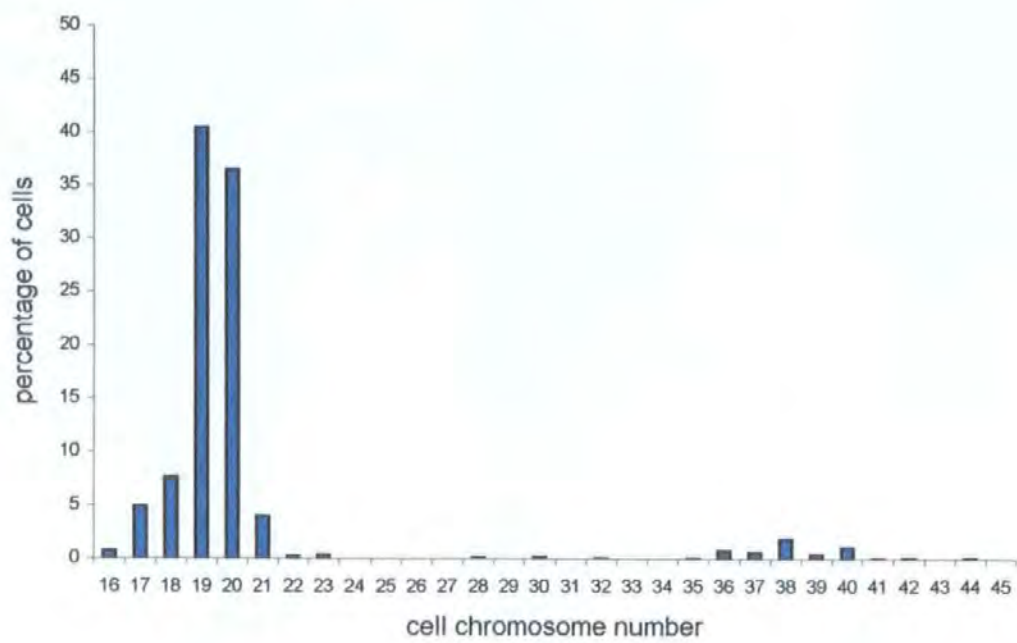


Figure 14. Chromosome number in 2,000 metaphases of the Chinese hamster ovary CHO-K1 cell line following subculture at Plymouth

3.3.3 *Assessment of basal chromosome aberration rate of untreated CHO-K1 cells*

The CHO-K1 cell line was assessed for its suitability for use in chromosome aberration assays by measurement of the chromosome aberration rate in untreated cells, both with and without rat liver S9 metabolic activation. Cells resuscitated after freezing in liquid nitrogen and at -80°C were also evaluated. The background rate was initially assessed at 3 to 5 %. The cell line was therefore deemed suitable for use in mutagenicity testing as the levels of spontaneous aberrations were within UKEMS guidelines of 5 % maximum (Scott *et al.*, 1990). Subsequently, the spontaneous aberration frequency was checked regularly from analysis of untreated control cultures. During the three years of experimentation, the spontaneous aberration rate remained at 5 % or below.

3.3.4 *Chromosome aberration assay of known mutagens in the CHO-K1 cell line*

The initial assessment of the cell line included assaying CHO-K1 cells with the known direct-acting mutagen, N-methyl-N'-nitro-N-nitrosoguanidine (MNNG) to check their potential for identifying mutagens and assess MNNG as a positive control. MNNG was tested at 0.075, 0.15, 0.30, and 0.60 µg/ml, a range that included concentrations previously assessed in other studies (Galloway *et al.*, 1985; Ishidate, 1988). Aberrations observed ranged from 8 to 35 %, which were consistent with those of Galloway *et al.* (1985). A dose response curve showed that the number of aberrations increased with increasing MNNG concentration (Figure 15). From these assay results, the 0.15 µg/ml dose was selected for use as the direct-acting positive control in all future aberration assays. At this concentration the number of aberrations observed ranged from 10-12 %, making MNNG sufficiently sensitive to detect low levels of clastogenicity.

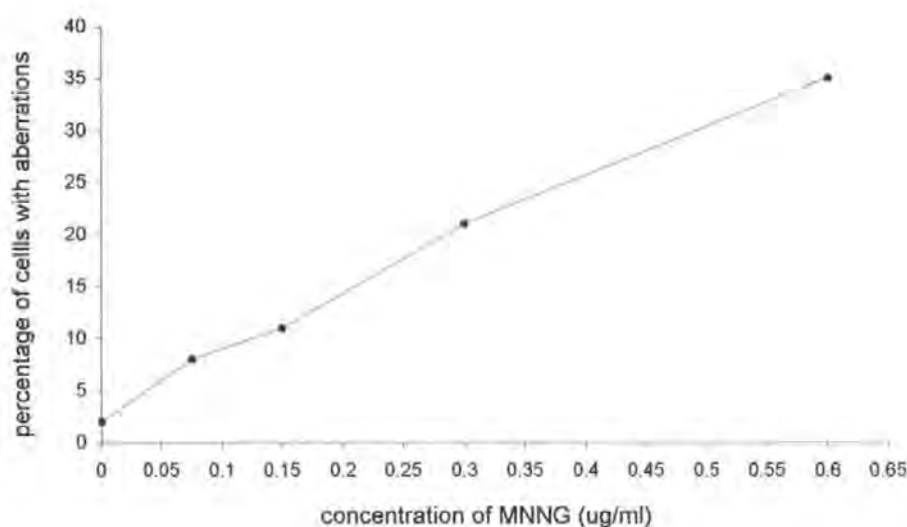


Figure 15. Dose response curve for the direct acting mutagen MNNG showing the number of chromosome aberrations induced in Chinese hamster ovary CHO-K1 cells

3.4 Types of chromosome aberration observed in CHO-K1 cells

Chromosome aberrations in metaphase preparations of the CHO-K1 cell line were identified and recorded following the classification given by Dean and Danford (1984, section 2.6.4.). A range of aberration types were observed in control and treated cultures, with the more complex exchange-type more prevalent in positive control and emission fraction treated cells.

3.4.1 Polyploidy and endoreduplication

Polyloid (tetraploid, $4n$) and endoreduplicated cells (Figure 16) were observed in all cultures within acceptable background rates of 5 % and 2-3 % respectively. The rates of these two were not significantly raised in any of the treated cultures.

3.4.2 Chromosome gaps and 'simple' aberrations

Chromosome gaps were recorded when a discontinuity in the DNA was less than the width of the chromatid arm, or when 'connecting' strands of DNA or proteins were visible in the gap region (Figure 17). Larger discontinuities in the DNA, or where the chromatid arm was displaced, were recorded as chromatid or chromosome breaks.

3.4.3 Complex chromosome aberrations

Unresolved interchange between chromatid arms resulted in the formation of several complex-type chromosome structures such as dicentric (Figure 18a) and ring (Figure 18b) chromosomes, dicentric tri-radials (Figure 19a), and tricentric chromosome structures (Figure 19b). Under more extreme clastogenic exposure, single CHO cells were observed containing multiple aberrations (Figure 20a and b).



Figure 16. Example of a Giemsa stained metaphase preparation of a Chinese hamster ovary CHO-K1 cell in which endoreduplication has occurred



Figure 17. Example of a chromatid gap type of aberration observed in Giemsa stained metaphase preparations of Chinese hamster ovary CHO-K1 cells during the study (aberrant chromosome indicated by arrow)

(a) dicentric chromosome



(b) ring chromosome



Figure 18. Examples of chromosome type aberrations observed in Giemsa stained metaphase preparations of Chinese hamster CHO-K1 cells during the study (aberrant chromosome indicated by arrow)

(a) dicentric triradial



(b) tricentric structure



Figure 19. Examples of complex exchange aberrations observed in Giemsa stained metaphase preparations of Chinese hamster CHO-K1 cells during the study (aberrant chromosome indicated by arrow)

(a) multiple aberrations



(b) multiple aberrations



Figure 20. Examples of Giemsa stained metaphase preparations of Chinese hamster CHO-K1 cells observed containing multiple aberrations (selected aberrant chromosome indicated by arrow)

3.5 Metabolic activation

Metabolic activation for chromosome aberration assays was provided in the form of rat liver S9 fraction, prepared under Home Office licence from male Wistar rats as described in section 2.4.1.

3.5.1 Fractions of S9 collected

The collection of S9 for testing was performed twice. The second collection was necessary to provide a greater volume of S9 for subsequent use. In addition, the activity of S9 is gradually lost when stored for greater than a year (Venitt *et al.*, 1984). In January 1995, the pre-treated livers from two male Wistar rats of weight 240 g each (combined liver weight 27.1 g) were homogenised and the S9 fraction prepared (section 2.4.1), which gave a total S9 volume of 58 ml. Aliquots of the S9 were used to check sterility, the results of which were negative confirming that the S9 fraction was sterile. The remainder was frozen in volumes of 1 and 2 ml and stored at - 80°C. Any S9 thawed and not used on the same day during testing was discarded and not refrozen on the advice of Venitt *et al.* (1984). The second collection of S9 was during July 1996 from the livers of seven male Wistar rats, weight approximately 190 g each. From the rats' total liver weight of 74.83 g, 200 ml of S9 volume was produced. Again sterility checks were negative confirming that the S9 fraction prepared was not contaminated, and samples were stored in volumes of 2 ml at -80 °C.

3.5.2 Cytochrome P450 in preparations of S9 collected

When complexed with CO, reduced cytochrome P450 gives a characteristic absorption spectrum with a maximum at 450 nm. The total cytochrome P450 (all various isoenzymes) of each batch of S9 was therefore determined spectrophotometrically as described in section 2.4.3, with the resulting absorbance spectra shown below in Figure 21. The absorbance spectra for each of the two batches showed a similar pattern, with a prominent

absorption maximum at 450 nm in both cases. From the difference between this absorbance at 450 nm and the absorbance at wavelength 490 nm, the concentration of cytochrome P450 was calculated.

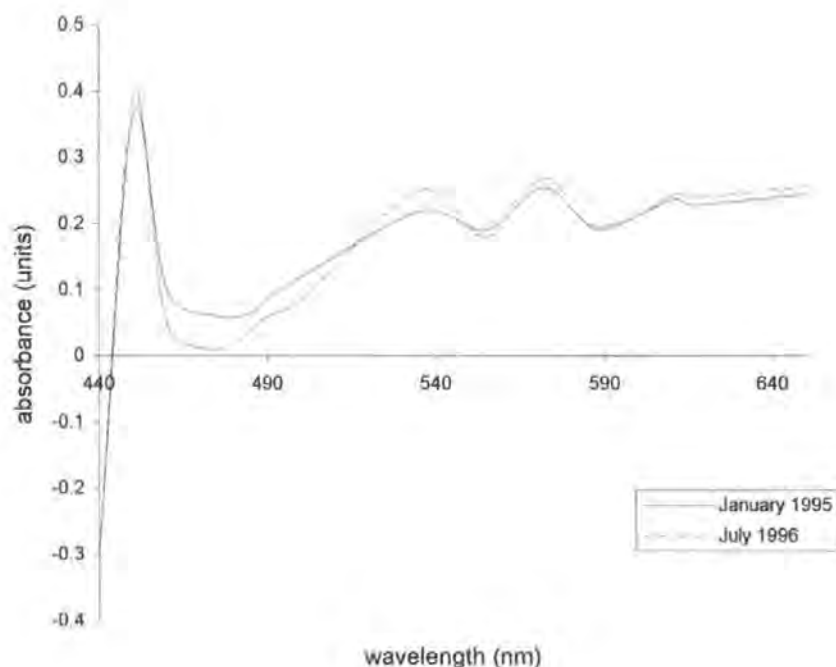


Figure 21. Absorbance spectra of reduced cytochrome P450 in two batches (prepared in January 1995 and July 1996) of the S9 fraction of rat livers from male Wistar rats, pre-treated with Aroclor 1254

For the first batch of S9 (January 1995), the cytochrome P450 concentration was calculated as 9.198 nmol / ml of S9. The second batch of S9 had slightly improved activity at 11.01 nmol cytochrome P450 /ml of S9. The increased activity of the second batch may have been due to the younger age of the rats used with a contribution from greater competency in techniques. The P450 concentration was deemed sufficient provided the activity was confirmed by testing in the chromosome aberration assay itself.

3.5.3 Characterisation of S9 activity with a known indirect acting mutagen, cyclophosphamide

To assess the activity and suitability of the S9 produced for use in the chromosome aberration assay, assays were performed in the presence of the known indirect-acting mutagen cyclophosphamide (CP). CP was assayed with the standard S9 mix (1x, section 2.7.5) at concentrations of 12.5, 25, 50, and 100 $\mu\text{g/ml}$ for both batches of S9. A dose-related increase in the number of aberrations was observed (Figure 22). The aberrations produced when using the two different batches of S9 were consistent with each other. The concentration 25 $\mu\text{g/ml}$, which produced aberrations in the range 14–17 % aberrant cells, was selected for use in future testing. This is the dose used by Galloway *et al.* (1985), and the number of aberrations seen in this study were consistent with their published figures.

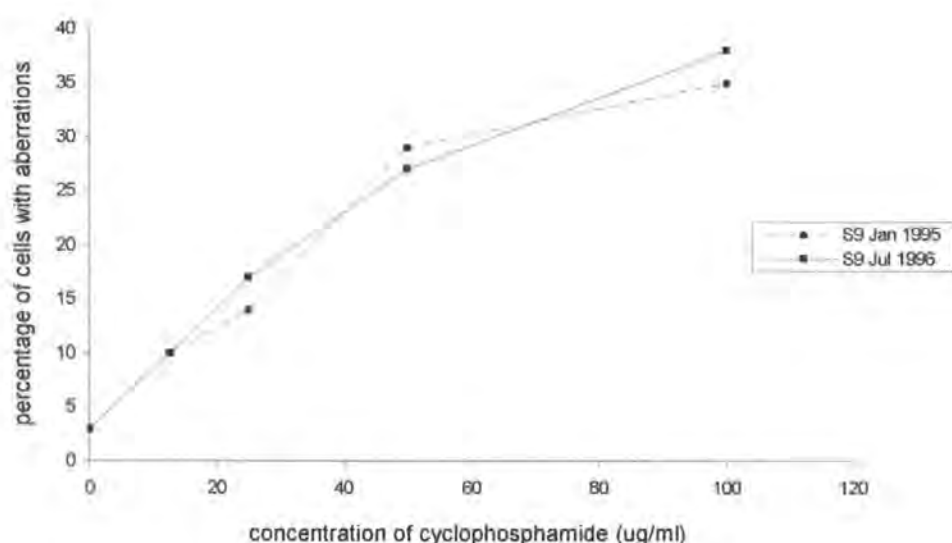


Figure 22. Dose response curves for the indirect-acting mutagen cyclophosphamide with two batches of S9 showing the number of chromosome aberrations induced in Chinese hamster ovary CHO-K1 cells

3.6 Cytotoxicity testing

Under guidelines (UKEMS, 1990; US EPA, OECD), it is recommended that known and unknown samples are tested to a maximum of 50 % toxicity. At more than 50 % toxicity, evidence of mutation induction should be interpreted with great caution as sampling error at high levels of kill may lead to spurious results. There is also a need to assess cytotoxicity because in many cases, a detectable level of chromosome aberrations is only found at doses of clastogens which induce some evidence of cytotoxicity (Scott *et al.*, 1990). All fuel and emission samples were therefore assayed for their cytotoxicity prior to testing in the chromosome aberration assay. Under the method selected (Fiennes *et al.*, 1987), cells are incubated with the test chemical (with or without metabolic activation) and then with neutral red dye, which is taken up by the remaining live cells. The length of exposure to the test chemical was the same as used in the aberration assays. For assays without metabolic activation, cells were exposed to the test sample for 16 –18 hours continuously. With metabolic activation cells were exposed to each sample for 2 hours only, followed by a 16 hour recovery in the presence of fresh medium. The dye uptake is measured spectrophotometrically, with cytotoxic effects assessed by comparison of treated samples to controls. Lowered absorbance readings therefore corresponded to low dye uptake and therefore low cell viability. During chromosome aberration assays, the cytotoxicity was re-measured by calculation of the mitotic index at each concentration to ensure that cytotoxic levels were achieved in the assays itself. A fall in mitotic rate is an indicator of increased cytotoxicity, although the fall may also reflect other cellular effects such as cell cycle delay.

The concentrations chosen for cytotoxicity assays were over a wide range (ten-fold increases in doses) to ensure any toxicity present was detected. Most assays were performed in duplicate at concentrations of 2, 20, and 200 µg/ml , with an additional dose at 50 µg/ml in selected cases. Replicate solvent control wells (DMSO) and untreated

control wells were included in all assays. To assess background neutral red not removed during washing, wells were incubated with CHO medium only. These wells gave an average absorbance reading of 0.05 units. Thus when the absorbance falls to this level, there can be assumed to be total cell killing.

3.6.1 Cytotoxicity of aliphatic fractions of diesel engine emission samples

As the aliphatic fraction of diesel fuel and engine emissions is generally regarded as containing only unreactive straight chain hydrocarbons, it was not expected to be mutagenic, but was tested for completeness. The aliphatic fractions of the engine run set collected in June 1996 together with the fuel were assessed for cytotoxicity, both with and without metabolic activation. The aliphatic fraction of one emission sample, that collected at 3000 rpm speed and 5 Nm load (ES 37+40) was selected for the full range of testing in the cytotoxicity and chromosome aberration assays both with and without metabolic activation.

3.6.1.1 Cytotoxicity of the aliphatic fraction of diesel fuel

When fractionated, 223.7 mg of fuel produced an aliphatic fraction of 123 mg (F7), which made up 58 % of the total fractionated mass. Sample F7 was tested for its cytotoxicity at concentrations from 2 µg/ml to 200 µg/ml, with and without metabolic activation. The results are presented graphically in Figure 81 (Appendix A). The mean of the replicate cultures assayed is shown, with the solvent control taken as the value at concentration zero. Without metabolic activation, there was a slight reduction in neutral red dye uptake with increasing concentration of aliphatic fuel fraction F7. Even at the highest concentration tested of 200 µg/ ml, however, the absorbance recorded did not fall below the lower levels of absorbance observed in the control wells.

The absorbance for the solvent controls was in fact slightly lower than the absorbance of treated wells, but this can be accounted for in the variability of the technique. There was therefore no toxicity exhibited by the fuel aliphatic fraction without metabolic activation. With metabolic activation (Figure 82, Appendix A), there a small reduction in absorbance at the lowest concentration of 2 µg/ml compared to controls, which levelled out between 2 µg/ml and 200 µg/ml. The difference between cell viability for controls and the fuel aliphatic fraction at 200 µg/ml was small and therefore not significant in view of the variability in absorbance levels recorded.

The aliphatic fraction of the diesel fuel used during these experiments was therefore not cytotoxic without metabolic activation up to concentrations of 200 µg/ml. In the presence of S9, the fuel aliphatic fraction showed some evidence of a toxic effect at 2 µg/ml. At higher concentrations of the aliphatic fraction of fuel there was a small dose related reduction in neutral red absorbance, with a reduction in cell viability to 64 % of control levels at 200 µg/ml. Cell viability was not reduced to the 50 % level at any concentration tested. The difference in baseline levels between assays with and without metabolic activation is again due to the variability of the technique – the assays were performed at different times with different batches of neutral red, disposable plastics and cuvettes. In all cases for the cytotoxicity assay, the main comparison is between the solvent control and concentrations tested within that assay.

3.6.1.2 Cytotoxicity of aliphatic fraction of the diesel emission sample collected at 3000 rpm speed and 5 Nm load

Diesel engine emission sample ES 26 (mass 121.5 mg) collected at 3000 rpm speed and 5 Nm load was fractionated and produced an aliphatic fraction of mass 50.4 mg (ES 37), which was 44 % of the total fractions recovered. In the same way, ES 27 (mass 132.8 mg) was fractionated to produce an aliphatic fraction of 47.8 mg (ES 40), 43 % of the total

fractions recovered. The two aliphatic fractions from these engine emission samples collected at 3000 rpm and 5 Nm, ES 37 and ES 40, were then combined and used for all subsequent testing.

Without metabolic activation, there was no notable reduction in neutral red dye uptake in the wells treated with aliphatic fraction ES 37+40 when compared to control wells (Figure 83, Appendix A). The absorbance for the solvent controls was in fact slightly lower than the absorbance in all treated wells. There was therefore no toxicity exhibited by this aliphatic fraction without metabolic activation. With metabolic activation in the form of rat liver S9, there was again no reduction in absorbance for the treated wells at any concentration tested compared to controls (Figure 84, Appendix A). The results show that at the concentrations tested (up to a maximum of 200 µg/ml), the aliphatic fraction of diesel engine emissions collected at 3000 rpm speed and 5 Nm load had no effect on CHO cell viability, and was therefore not cytotoxic.

3.6.1.3 Cytotoxicity of aliphatic fraction of the diesel emission sample collected at 1000 rpm speed and 55 Nm load

The mass of total emission samples at this speed and load was relatively low, and therefore TES from successive engine runs were combined prior to fractionation (ES 18 with ES 19, and ES 21 with ES 22). Fractionation of ES 18+19 (combined mass 93.1 mg) gave an aliphatic fraction of mass 35.5 mg (ES 43, 38 % of the total fractionated mass). Fractionation of ES 21+22 (combined mass 99 mg) gave an aliphatic fraction of 37.2 mg (ES 46, again 38 % of the total fractionated mass). The two aliphatic fractions ES 43+46 were then combined and used for all subsequent testing (an aliphatic fraction of 72.7 mg from total 8 minutes engine sampling). When assayed both with and without metabolic activation (Figures 85 and 86, Appendix A), there was a slight variation in the neutral red absorbance and therefore cell viability over the range of concentrations tested (2 to

200 µg/ml). There was, however, no overall reduction in cell viability compared to controls. The aliphatic fraction ES 43+46, collected at 1000 rpm and 55 Nm, was therefore not cytotoxic to CHO cells.

3.6.1.4 Cytotoxicity of aliphatic fraction of the diesel emission sample collected at 1000 rpm speed and 5 Nm load

As with the previous sample, the masses of the 2 minute total emission samples produced at this speed and load were low (average mass 27 mg for 2 minute emission sampling). The TES from two successive engine runs were combined prior to fractionation (ES 30 with ES 31, and ES 32 with ES 33). Fractionation of ES 30+31 (combined mass 63.8 mg) gave an aliphatic fraction of mass 20.8 mg (ES 49, 33 % of the total fractionated mass). Fractionation of ES 32+33 (combined mass 64.5 mg) again gave an aliphatic fraction of 18.2 mg (ES 52, 28 % of the total fractionated mass). The two aliphatic fractions ES 49+52 were then combined and used for all subsequent testing (an aliphatic mass of 39 mg from a total of 8 minutes engine sampling).

The level of absorbance recorded when ES 49+52 was tested for cytotoxicity showed a slight variation, but this was not a dose related decrease. The absorbance and therefore cell viability at the highest concentration of 200 µg/ml was higher than controls, in both assays with and without metabolic activation (Figures 87 and 88, Appendix A). The aliphatic fraction ES 49+52, collected at 1000 rpm and 5 Nm, is not cytotoxic to CHO cells with or without metabolic activation up to a concentration of 200 µg/ml.

3.6.2 Cytotoxicity of the aromatic fractions of diesel fuel and engine emissions

The aromatic fractions of the diesel fuel and of the three engine emission samples collected during June 1996 were assayed to assess their cytotoxicity.

3.6.2.1 Cytotoxicity of the aromatic fraction of diesel fuel

Diesel fuel fractionated in September 1996 produced an aliphatic fraction of mass 80.9 mg (F8), which was 38 % of the total fractions recovered. Without metabolic activation, the aromatic fraction of the fuel exhibited a marked cytotoxic effect on the CHO cell monolayer at a concentration of 50 $\mu\text{g/ml}$, with absorbance falling from a control level of 0.321 units to 0.084 units. At the highest concentration tested of 200 $\mu\text{g/ml}$ there was a near complete cell killing (Figure 89, Appendix A). Within the confines of the assay, this equates to a near total cell killing because of the background level of neutral red dye not completely washed away during the harvesting procedure. From the graph, the critical 50 % reduction in cell viability was estimated to take place at a concentration of 30 $\mu\text{g/ml}$. The aromatic fuel was therefore tested up to a concentration of 40 $\mu\text{g/ml}$ in the chromosome aberration assay without metabolic activation.

In the presence of S9 there was a less marked reduction in cell viability for the aromatic fuel fraction compared to non-metabolically activated cells (Figure 90, Appendix A). The direct comparison is, of course, not strictly relevant because of the difference in exposure times of the two assays. At the highest concentration tested of 200 $\mu\text{g/ml}$ there was a slightly less than 50 % reduction in cell viability. Absorbance levels fell sharply between aromatic concentrations of 2 and 50 $\mu\text{g/ml}$, with a more gentle slope of reduction then from 50 to 200 $\mu\text{g/ml}$. When an initial chromosome aberration assay was performed, however, the fuel aromatic fraction had a marked effect on mitotic index. At concentrations of 100 and 200 $\mu\text{g/ml}$ there were insufficient metaphases to enable scoring. A re-test was therefore performed with concentrations up to 40 $\mu\text{g/ml}$. The aromatic fraction of diesel fuel therefore has a toxic effect on CHO cells, with the most severe outcome seen without metabolic activation.

3.6.2.2 *Cytotoxicity of aromatic fraction of the diesel emission sample collected at 3000 rpm speed and 5 Nm load*

Engine emission sample ES 26 and 27 were fractionated separately and the resulting aromatic fractions combined to give a sample mass of 70.9 mg (ES 38+41), the aromatic being 31 % of the total fractions recovered. This fraction, ES 38+41, was used for all subsequent testing (aromatic fraction mass of 70.9 mg from a total of 4 minutes engine sampling).

The aromatic fraction ES 38+41 exhibited marked cytotoxicity on CHO cells at a concentration of 50 µg/ml when compared to control wells. The toxic effect of this fraction was dose dependent with the most marked effect between doses of 20 and 50 µg/ml, when cell viability fell from approximately 80% to 15%. The 50 % cytotoxic level was estimated from the graph (Figure 91, Appendix A) to be at a concentration of around 30 µg/ml. When the aromatic fraction was metabolically activated with S9, the cytotoxic effect was less marked although a dose related decrease in cell viability was evident (Figure 92, Appendix A). There was a significant variation between the replicate cultures at the critical dose of 50 µg/ml, where what may be an erroneous point skewed the overall response. The cytotoxic effect was however clear with a 72 % reduction in cell viability at the highest concentration of 200 µg/ml. 50 % cytotoxicity was estimated to take place at a concentration of approximately 100 µg/ml. The aromatic fraction of the diesel engine emissions collected at 3000 rpm speed and 5 Nm load were therefore cytotoxic to CHO cells at concentrations between 50 and 200 µg/ml, both with and without metabolic activation.

3.6.2.3 Cytotoxicity of aromatic fraction of the diesel emission sample collected at 1000

rpm speed and 55 Nm load

The masses of the 2 minute total emission samples produced at this speed and load were reduced in comparison to other samples, and therefore samples from two successive engine runs were combined prior to fractionation (ES 18 with ES 19, and ES 21 with ES 22). Fractionation of ES 18+19 (combined mass 93.1 mg) gave an aromatic fraction of mass 28.2 mg (ES 44, 30 % of the total fractionated mass). Fractionation of ES 21+22 (combined mass 99 mg) gave an aromatic fraction of 33.7 mg (ES 47, 34 % of the total fractionated mass). The two aromatic fractions ES 44+47 were then combined and used for all subsequent testing (an aromatic fraction of 61.9 mg from total 8 minutes engine sampling).

When not metabolically activated, the aromatic fraction ES 44+47 exhibited a strong cytotoxic effect, reducing cell viability to near minimal at a concentration of 50 $\mu\text{g/ml}$ (Figure 93, Appendix A). The toxic effect increased with increasing aromatic fraction concentration from little or no effect at 2 $\mu\text{g/ml}$ to maximal effect at 50 $\mu\text{g/ml}$ – almost complete toxicity induced over a fairly narrow range of concentrations. A level of 50 % cell killing was achieved at a concentration of less than 30 $\mu\text{g/ml}$. In the presence of metabolic activation, the aromatic fraction ES 44+47 again had a toxic effect on the CHO cells (Figure 94, Appendix A). At a concentration of 50 $\mu\text{g/ml}$ there was a large difference between the absorbance level in replicate cultures making interpretation difficult as either it was could not be assumed that either value was correct. The average was therefore taken for the purposes of assessing an approximate 50 % cytotoxicity, which gave a concentration of 80 $\mu\text{g/ml}$.

3.6.2.4 Cytotoxicity of aromatic fraction of the diesel emission sample collected at 1000 rpm speed and 5 Nm load

The masses of the 2 minute total emission samples produced at this speed and load were low (average mass 27 mg for 2 minute emission sampling). The TES from two successive engine runs were combined prior to fractionation (ES 30 with ES 31, and ES 32 with ES 33). Fractionation of ES 30+31 (combined mass 63.8 mg) gave an aromatic fraction of mass 18.9 mg (ES 50, 30 % of the total fractionated mass). Fractionation of ES 32+33 (combined mass 64.5 mg) again gave an aromatic fraction of 18.9 mg (ES 53, 29 % of the total fractionated mass). The two aromatic fractions ES 50+53 were then combined and used for all subsequent testing (an aromatic mass of 37.8 mg from a total of 8 minutes engine sampling).

Like the other aromatic fractions, the fraction ES 50+53 collected at 1000 rpm speed and 5 Nm load exhibited a marked cytotoxic effect in the neutral red dye assay without metabolic activation (Figure 95, Appendix A). There was no effect on cell viability at the lowest concentration tested, 2 µg/ml. Between the next two concentrations of 20 µg/ml and 50 µg/ml, cell viability was reduced to a minimal 16 %. The aromatic fraction ES 50+53 is therefore highly toxic to CHO cells, with a 50 % cell killing at a concentration of less than 30 µg/ml. When assayed with S9, the aromatic fraction ES 50+53 was cytotoxic, but to a lesser extent than without S9 (Figure 96, Appendix A). The replicate cultures were not closely matched, especially at 50 µg/ml, exhibiting an approximate 30 % difference in neutral red absorbance. For this reason the mean absorbance was used to estimate 50 % viability. Approximately 50 % of cells were destroyed at a concentration of just less than 50 µg/ml.

3.6.3 Cytotoxicity of the 1-ring aromatic fractions of diesel fuel and engine emission samples

The aromatic fraction of diesel fuel and of emission samples collected at 3000 rpm and 5 Nm, and 1000 rpm and 55 Nm were further fractionated by HPLC into 1- ring, 2- ring and 3+ -rings (Section 2.2.2). The ring fractions were then assessed for their cytotoxicity in the neutral red dye assay prior to being assayed for chromosome aberrations.

3.6.3.1 Cytotoxicity of the diesel fuel 1-ring aromatic fraction

Diesel fuel was fractionated by HPLC to produce 186 mg of 1-ring group compounds (R 40), which was 61 % of the totalled fractions recovered. The 1-ring aromatic fraction of fuel had a severe toxic effect on CHO cells, reducing cell viability almost completely at the highest concentration tested of 200 µg/ml. There was no effect at 2 µg/ml, then an acute reduction in absorbance at 20 µg/ml which levelled off at 50 µg/ml before sharply decreasing again to a minimal level at 200 µg/ml. The levelling off between 20 and 50 µg/ml was identical in both replicates, and made evaluation of 50 % cytotoxicity more difficult. From the graph (Figure 97, Appendix A), the concentration which resulted in an approximate 50 % cell death was estimated as 60 µg/ml. With metabolic activation, there was a slight reduction in cell viability at 20 µg/ml, but this reduction was not sustained at higher concentrations (Figure 98, Appendix A). At the highest concentration of 200 µg/ml the number of cells surviving was only slightly less than controls, a viability of 80 %. Therefore, the 1-ring aromatic fraction of diesel fuel exhibits cytotoxicity at 20 µg/ml only. When assayed in the presence of S9, the 1-ring diesel fuel is not cytotoxic up to the maximum concentration tested of 200 µg/ml.

3.6.3.2 Cytotoxicity of the 1-ring aromatic fraction of the diesel emission sample collected at 3000 rpm speed and 5 Nm load

An aromatic fraction of 210.7 mg from a TES (709.7 mg) collected at 3000 rpm and 5 Nm (5 minute sampling) was fractionated by HPLC to produce 44 mg of 1-ring group compounds (R 41), which was 29 % of the totalled fractions recovered. Without metabolic activation, the 1 –ring aromatic fraction R41 exhibited a marked cytotoxic effect on CHO cells (Figure 99, Appendix A). The toxic effect could be seen as early as at 2 µg/ml, where there was an approximate 20 % reduction in cell viability from control levels. The reduction in cell viability was approximately dose related, with complete toxicity at the highest concentration of 200 µg/ml. The level of 50 % toxicity was estimated at 80 µg/ml. When assayed with S9, the action on cell viability was very different (Figure 100, Appendix A). The absorbance levels showed a small reduction at 2 and 20 µg/ml, but returned to controls levels at 50 µg/ml. At the highest concentration of 200 µg/ml, there was a small but significant reduction in cell viability compared to control levels. Therefore, the 1 –ring aromatic fraction collected at 3000 rpm and 5 Nm is cytotoxic at low concentrations without metabolic activation, and exhibits a weak toxic effect at high concentrations when assayed with metabolic activation.

3.6.3.3 Cytotoxicity of the 1-ring aromatic fraction of the diesel emission sample collected at 1000 rpm speed and 55 Nm load

TES of mass 291.8 mg and 224.7 mg collected at 1000 rpm and 55 Nm (5 minute sampling) were fractionated by HPLC to produce 38.6 mg (R 28) and 41 mg (R 37) of 1-ring group compounds, which were combined for testing. The 1 –ring aromatic fraction R 28+37 showed a conclusive dose related reduction in cell viability when assayed in the neutral red vital staining assay. There was a 50 % reduction in cell survival by a concentration of less than 20 µg/ml, with complete cell killing at the highest concentration tested of 200 µg/ml (Figure 101, Appendix A). In the presence of S9, the toxic effect at

lower concentrations was less obvious, with a marginal increase in absorbance at 50 µg/ml. At 200 µg/ml, however, the toxic effect was conclusive, with a reduction to approximately 20 % cell survival. 50 % toxicity was estimated from the graph (Figure 102, Appendix A) to be at a concentration of 150 µg/ml.

3.6.4 Cytotoxicity of the 2-ring aromatic fractions of diesel fuel and engine emission samples

The HPLC separated 2- ring fraction of diesel fuel, and of engine emission samples collected at 3000 rpm and 5 Nm, and 1000 rpm and 55 Nm were assessed for their cytotoxicity in the neutral red dye assay in CHO-K1 cells.

3.6.4.1 Cytotoxicity of the diesel fuel 2-ring aromatic fraction

Diesel fuel was fractionated by HPLC to produce 103.7 mg of 2-ring group compounds (R 26), which was 34 % of the totalled fractions recovered. The 2-ring fraction of diesel fuel had a severe effect on cell viability without metabolic activation (Figure 103, Appendix A). There was a sharp dose related fall in the absorbance level from the DMSO solvent control at 2-ring fraction concentrations of 2 and 20 µg/ml, the latter causing a 86 % reduction in cell viability. The level of cell viability continued to decrease, with a less acute effect, up to the highest concentration tested of 200 µg/ml where there was minimal cell survival. The dose which resulted in an approximate 50 % cell killing was estimated at less than 15 µg/ml. In the chromosome aberration assay, the 2-ring fraction of the fuel was assayed up to 40 µg/ml to allow for overestimation of the cytotoxic effect at such low mass of fraction, with concentrations clustered at the lower doses.

When tested with metabolic activation in the form of rat liver S9, the 2-ring fraction of diesel fuel had a less severe effect than when tested without. Whilst there was

again a near total cell killing at the highest concentration of 200 µg/ml, the effect at lower concentration was not dose related and therefore unclear (Figure 104, Appendix A). There was a reduction in cell viability of 33 % at 20 µg/ml in both replicate wells, however at 50 µg/ml the cell viability was returned to control levels (again for both replicates). As replicate cultures showed almost identical values of neutral red, it was not possible to exclude any single points as possibly erroneous. A dose level for a 50 % reduction in cell survival was difficult to estimate because of the inconclusive results obtained from the cytotoxicity assay, and therefore testing in the aberration assay with S9 was performed over a wider range of concentrations, up to a maximum of 200 µg/ml.

3.6.4.2 Cytotoxicity of the 2-ring aromatic fraction of the diesel emission sample collected at 3000 rpm speed and 5 Nm load

An aromatic fraction of 210.7 mg from a TES (709.7 mg) collected at 3000 rpm and 5 Nm (5 minute sampling) was fractionated by HPLC, and produced 91.5 mg of 2-ring group compounds (R 32). For this engine emission sample, the 2-ring fraction formed the majority 60 % of the total of fractions recovered. Without metabolic activation, the 2-ring aromatic fraction R32 exhibited a marked cytotoxic effect on CHO cells (Figure 105, Appendix A). There was an acute reduction in cell viability at concentrations of 2 and 20 µg/ml of the 2-ring fraction (to 26 % of control levels at 20 µg/ml), and at 200 µg/ml the cell survival was minimal. The dose which produced an approximate 50 % reduction in cell viability was estimated at 15 µg/ml. In the chromosome aberration assay, the 2-ring fraction R32 was assayed up to 40 µg/ml, with concentrations clustered at the lower doses.

The 2-ring fraction of the emission sample collected at 3000 rpm and 5 Nm was assayed for its cytotoxic effect in the presence of metabolic activation. An overall reduction in cell viability was observed, with minimal cell survival at the highest concentration tested of 200 µg/ml (Figure 106, Appendix A). As with the 2-ring fuel

aromatic fraction, the cytotoxic effect did not follow a clear dose response pattern. There was a 30 % reduction absorbance levels at 20 µg/ml, but this was returned to control levels at 50 µg/ml. Again, this made estimation of 50 % absorbance levels impossible, and therefore the 2-ring fraction R 32 was assayed over a wider range of concentrations up to a maximum 200 µg/ml in the chromosome aberration assay with S9.

3.6.4.3 Cytotoxicity of the 2-ring aromatic fraction of the diesel emission sample collected at 1000 rpm speed and 55 Nm load

TES of mass 291.8 mg and 224.7 mg collected at 1000 rpm and 55 Nm (5 minute sampling) were fractionated by HPLC to produce 17.6 mg (R 29) and 14.3 mg (R 38) of 2-ring group compounds, which were combined for testing. The 2-ring aromatic fraction R 29+38 showed a conclusive dose related reduction in cell viability when assayed in the neutral red dye vital staining assay (Figure 107, Appendix A). A 50 % reduction in cell viability was achieved at a concentration of less than 20 µg/ml, with complete cell killing at the highest concentration tested of 200 µg/ml. The 2-ring fraction of the engine emission sample collected at 1000 rpm and 55 Nm (R 29+38) was therefore assayed up to 40 µg/ml in the chromosome aberration assay, with concentrations clustered at the lower doses.

When the cytotoxicity assay of 2-ring fraction R29+38 was repeated in the presence of rat liver S9, the effect on CHO cell survival was less severe. The response was not strictly dose-related, as the absorbance levels fell up to 20 µg/ml, and then rose slightly at 50 µg/ml, although the solvent control level of absorbance was not attained at this dose (Figure 108, Appendix A). Cell viability was minimal at the highest concentration of the 2-ring fraction (200 µg/ml). The absence of a clear dose response made estimation of 50 % cytotoxicity more difficult, although the overall cytotoxic effect of this fraction was

more severe than the 2-ring fuel or R 32 (3000 rpm/ 5 Nm) samples when assayed with S9 (summary graph, Figure 26b). The 2-ring fraction R29+38 was therefore assayed over a wider range of concentrations up to a maximum of 100 µg/ml in the chromosome aberration assay.

3.6.5 Cytotoxicity of the 3+ -ring aromatic fractions of diesel fuel and engine emission samples

The HPLC separated 3+ -ring fraction of diesel fuel and of the engine emission sample collected at 3000 rpm and 5 Nm were assessed for their cytotoxicity in the neutral red dye assay in CHO-K1 cells. As the combined mass of the 3+ -ring fraction of the engine emission sample collected at 1000 rpm and 55 Nm was only 6.3 mg, there was insufficient to perform both cytotoxicity and chromosome aberration assays. This sample was therefore reserved for testing in the chromosome aberration assay only.

3.6.5.1 Cytotoxicity of the diesel fuel 3+ -ring aromatic fraction

Diesel fuel was fractionated by HPLC to produce 13.1 mg of 3-ring group compounds (R 27), which was 4 % of the totalled fractions recovered. The 3-ring fraction of diesel fuel caused a clear dose related fall in cell viability from 2 to 50 µg/ml, at which point CHO cell survival was minimal (Figure 109, Appendix A). By a concentration of 20 µg/ml, the 3-ring fraction R 27 had reduced cell viability to 27 % of solvent control levels. R 27 was assayed in the chromosome aberration up to a maximum of 40 µg/ml.

When assayed in the presence of metabolic activation, the cytotoxic effect of the 3+ -ring fraction of diesel fuel was less clear at lower concentrations. Cell viability was reduced from solvent control levels at concentrations of 2 and 20 µg/ml, but then rose to unaffected levels at 50 µg/ml (Figure 110, Appendix A). At 200 µg/ml, there was an 85 %

reduction in CHO cell viability. Thus a dose related pattern of cytotoxicity was not observed. From the graph, 50 % cell killing was estimated at a concentration of just under 150 µg/ml of the 3+ -ring fuel sample. This sample was therefore assessed in the chromosome aberration assay with rat liver S9 at concentrations up to 200 µg/ml.

3.6.5.2 Cytotoxicity of the 3+ -ring aromatic fraction of the diesel emission sample collected at 3000 rpm speed and 5 Nm load

An aromatic fraction of 210.7 mg from a TES (709.7 mg) collected at 3000 rpm and 5 Nm (5 minute sampling) was fractionated by HPLC, and produced 17.6 mg of 3+ -ring group compounds (R 33). The 3+ -ring fraction formed 11 % of the total of fractions recovered. The engine emission 3+ -ring aromatic fraction R33 had a severe, dose related effect on the viability of CHO cells in the neutral red assay without metabolic activation (Figure 111, Appendix A). Cell survival was reduced to 67 % at 2 µg/ml, 18 % at 20 µg/ml, and at 50 µg/ml the 3+ -ring sample resulted in almost total cell killing. A 50 % reduction in cell viability was estimated at a dose of 10 µg/ml. In the chromosome aberration assay, the 3+ -ring fraction R 33 was assayed up to 40 µg/ml, with doses concentrated in the lower range.

The cytotoxicity assay was repeated in the presence of S9 metabolic activation. A dose related fall in the neutral red absorbance and therefore CHO cell viability was observed, with a less acute effect than without S9 (Figure 112, Appendix A). At 20 µg/ml cell viability was reduced to 74 % of solvent control levels, and the metabolically activated 3+ -ring emission sample fraction caused a complete cell killing at 200 µg/ml. The dose which resulted in a 50 % reduction in cell survival was estimated at 15 µg/ml. The fraction R 33 was, however, assayed up to 200 µg/ml in the chromosome aberration assay with S9 for direct comparison with the fuel 3+-ring sample.

3.6.6 Cytotoxicity of the polar fractions of diesel engine emission samples collected during June 1996

The polar fractions of the three engine emission samples collected during June 1996 (3000 rpm/5 Nm, 1000 rpm/55 Nm, and 1000 rpm/5 Nm) were assayed to assess their cytotoxicity both with and without metabolic activation in the neutral red vital staining assay in CHO cells. Each fraction was assayed at concentrations of 0.2, 2, 20, and 200 µg/ml without metabolic activation, with an additional dose of 50 µg/ml included in assays with S9. A further four polar group fractions from engine runs performed during January 1997 (2000 rpm/30 Nm, 2000 rpm/55 Nm, 3000 rpm/30 Nm, and 3000 rpm/55 Nm) were assayed for their cytotoxicity without metabolic activation. These later polar fractions were not assayed with metabolic activation in view of the fact that the first polar samples displayed direct-acting cytotoxicity. The range of concentrations was also altered to 2, 20, 50, and 200 µg/ml, the 0.2 µg/ml dose omitted and a dose of 50 µg/ml included to provide more detailed information over the range of doses shown to be cytotoxic for the original polar fractions. The fuel has negligible polar group compounds within it (from manufacturers data), and therefore the low mass polar fraction obtained from silica gel column separation of the fuel was not assayed.

3.6.6.1 Cytotoxicity of polar fraction of diesel emission sample collected at 3000 rpm and 5 Nm

Engine emission sample ES 26 and 27 were fractionated separately, and the resulting polar fractions combined to give a sample mass of 56.3 mg (ES 39+42). The polar fraction was 25 % of the total fractions recovered. This fraction, ES 39+42, was used for all subsequent testing (polar fraction mass of 56.3 mg from a total of 4 minutes engine sampling).

There was a sharp fall in cell viability for the polar fraction ES 39+42 from the solvent control to 20 µg/ml, where approximately 50 % cytotoxicity was exhibited by the

sample (Figure 113, Appendix A). The cytotoxic effect continued to a less acute extent up to the maximum concentration of 200 µg/ml, which resulted in almost complete cell killing. A clear dose response was evidenced. The polar fraction of the emission sample collected at 3000 rpm and 5 Nm was therefore tested up to a maximum 30 µg/ml in the chromosome aberration assay without metabolic activation. In the presence of rat liver S9, the polar fraction ES 39+42 exhibited a less severe cytotoxic effect on the CHO cells (Figure 114, Appendix A). No reduction in cell viability was induced at any of the first three (0.2, 2, and 20 µg/ml) concentrations tested, indeed cell viability was higher than that for the solvent control. At 200 µg/ml, cell survival was reduced to a level of 36 %, although the variation between replicate cultures at this concentration was high (mean absorbance 0.107 units, s.d. 0.103). 50 % cytotoxicity was estimated at a polar fraction dose of 150 µg/ml, which was selected as the maximum dose for chromosome aberration assay testing with S9.

3.6.6.2 Cytotoxicity of the polar fraction of the diesel emission collected at 1000 rpm speed and 55 Nm load

The masses of the 2 minute total emission samples produced at this speed and load were reduced in comparison to other samples, and therefore samples from two successive engine runs were combined prior to fractionation (ES 18 with ES 19, and ES 21 with ES 22). Fractionation of ES 18+19 (combined mass 93.1 mg) gave a polar fraction of mass 19.2 mg (ES 45, 23 % of the total fractionated mass). Fractionation of ES 21+22 (combined mass 99 mg) gave a polar fraction of 22.5 mg (ES 48, 24 % of the total fractionated mass). The two polar fractions ES 45+48 were then combined and used for all subsequent testing (a polar fraction of 41.7 mg from total 8 minutes engine sampling).

After an initial increase, the polar fraction ES 45+48 caused a dose related reduction in the viability of CHO cells as seen by neutral red absorbance (Figure 115,

Appendix A). Absorbance fell to 53 % at 20 µg/ml and 18 % at the maximum concentration of 200 µg/ml. The lower concentrations of the polar fraction, 0.2 and 2 µg/ml, did not correspond with a cytotoxic effect. The polar fraction of this engine emission sample was assayed at concentrations up to 30 µg/ml in the chromosome aberration test. Metabolic activation of the polar fraction ES 45+48 did not increase its cytotoxic effect on CHO cells. In the presence of S9, the absorbance levels rose marginally up to 20 µg/ml, and then fell to 83 % of the control at 50 µg/ml followed by a dramatic reduction to 12 % at 200 µg/ml (Figure 116, Appendix A). The dose which resulted in a 50 % reduction in cell viability was estimated to be 120 µg/ml. The polar fraction of the emission sample collected at engine conditions of 1000 rpm and 55 Nm was tested up to a concentration of 150 µg/ml in the chromosome aberration assay.

3.6.6.3 Cytotoxicity of the polar fraction of the diesel emission sample collected at 1000 rpm speed and 5 Nm load

The masses of the 2 minute total emission samples produced at this speed and load were low (average mass 27 mg for 2 minute emission sampling), and it was therefore necessary to combine fractions to provide sufficient mass of sample for testing. The TES from two successive engine runs were combined prior to fractionation (ES 30 with ES 31, and ES 32 with ES 33). Fractionation of ES 30+31 (combined mass 63.8 mg) gave a polar fraction of mass 23.3 mg (ES 51, 37 % of the total fractionated mass). Fractionation of ES 32+33 (combined mass 64.5 mg) gave a polar fraction of 20.5 mg (ES 54, 36 % of the total fractionated mass). The two polar fractions ES 51+54 were then combined and used for all subsequent testing (a polar mass of 43.8 mg from a total of 8 minutes engine sampling). In contrast with other engine emission samples, the polar fractions from engine runs at 1000 rpm and 5 Nm were the majority fraction by mass.

The pattern of cytotoxicity exhibited by polar fraction ES 51+54 was consistent with the polar fractions of emission samples previously tested. The viability of CHO cells fell with increasing polar fraction concentration, so that cell viability was reduced by 38 % at 20 µg/ml, and 81 % at 200 µg/ml (Figure 117, Appendix A). The level of 50 % cytotoxicity was estimated at a concentration of less than 50 µg/ml. This sample was assayed up to a concentration of 30 µg/ml in the chromosome aberration assay without metabolic activation, in line with the other polar fractions. When sample ES 51+54 was metabolically activated, a reduction in cell viability to 13 % of the solvent control level was observed at the highest dose tested of 200 µg/ml (Figure 118, Appendix A). The response at lower concentrations was less clear, with a reduction in cell viability of 32 % at 0.2 µg/ml, although the difference between replicate cultures was wide (mean absorbance 0.202 units, s.d. 0.082). This was followed by a return to near control levels at 2 and 20 µg/ml, and a marginal cytotoxic effect exhibited at 50 µg/ml (11 % reduction in cell viability). The absence of a clear dose response effect made estimation of 50 % cytotoxicity difficult. The polar fraction ES 51+54 was finally tested in the chromosome aberration assay with S9 to a maximum concentration of 100 µg/ml, which was dictated by the small mass of sample available for testing.

3.6.7 Cytotoxicity of the polar fractions of diesel engine emissions collected in January 1997

Fractionation of the total emission samples from engine runs performed during January 1997 (at speed and load 2000 rpm/30 Nm, 2000 rpm/55 Nm, 3000 rpm/30 Nm, and 3000 rpm/55 Nm), provided a further four polar group fractions for analysis. The four samples; ES 125 (3000 rpm/55 Nm), ES 119 (3000 rpm/30 Nm), ES 116 (2000 rpm/55 Nm), and ES 107 (2000 rpm/ 30 Nm) were assayed for their cytotoxicity in the neutral red dye assay in CHO cells without metabolic activation. These later polar fractions were not assayed with

metabolic activation in view of the fact that the first polar samples tested displayed direct-acting cytotoxicity. The range of concentrations was also altered to 2, 20, 50, and 200 $\mu\text{g/ml}$, the 0.2 $\mu\text{g/ml}$ dose omitted and a dose of 50 $\mu\text{g/ml}$ included to provide more detailed information over the range of doses shown to be cytotoxic for the original polar fractions.

The dose related reduction in cell viability produced by all four of these polar fractions was almost identical, and they are therefore discussed together here. Graphs of the response exhibited by individual samples are given in Appendix A – Figure 119 (ES 107), Figure 120 (ES 116), Figure 121 (ES 119), and Figure 122 (ES 125). An average 54 % reduction in CHO cell survival was exhibited at 20 $\mu\text{g/ml}$, followed by a further fall to almost total cell killing at 50 $\mu\text{g/ml}$. The level of 50 % cytotoxicity was estimated at just under 20 $\mu\text{g/ml}$, and therefore all four of the polar fraction samples were tested up to a maximum dose of 30 $\mu\text{g/ml}$ in the chromosome aberration assay without S9.

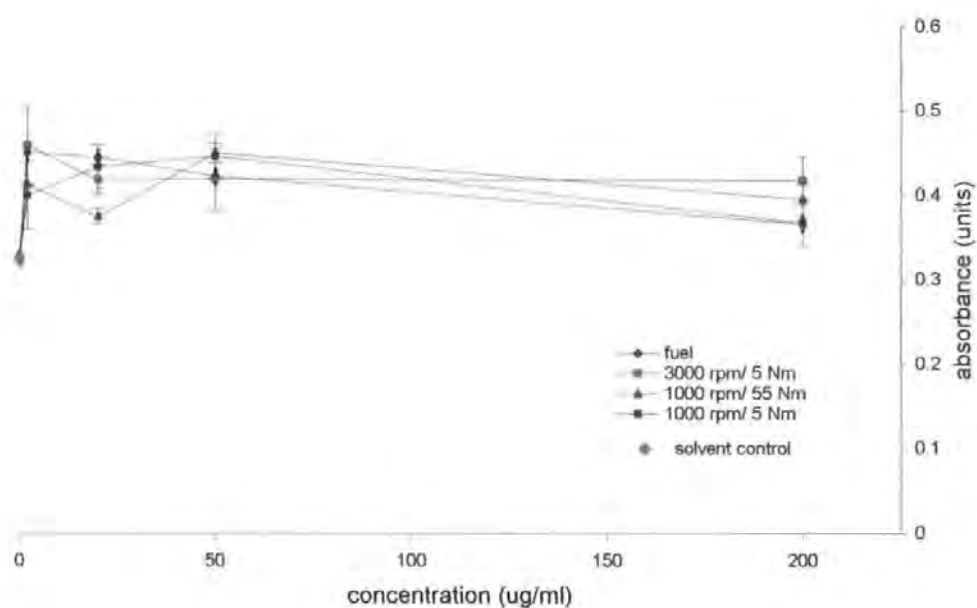
3.7 Overview of the cytotoxicity of diesel engine emission sample fractions

3.7.1 Cytotoxicity of the aliphatic fractions

The results for the cytotoxicity testing of the four aliphatic fractions assayed without S9 are shown together in Figure 23(a) overleaf. The absorbance recorded was restricted to a small range in all cases, with no significant reduction in cell viability for any of the samples assayed.

The cytotoxic effect of the four aliphatic fractions assayed with S9 is shown in Figure 23(b). In this case, the aliphatic fractions of the three engine emission samples show matching results, with no overall reduction in cell viability. In contrast, however, the minor cytotoxic effect of the fuel aliphatic fraction with S9 can be clearly seen.

(a) without metabolic activation



(b) with metabolic activation (rat liver S9 fraction)

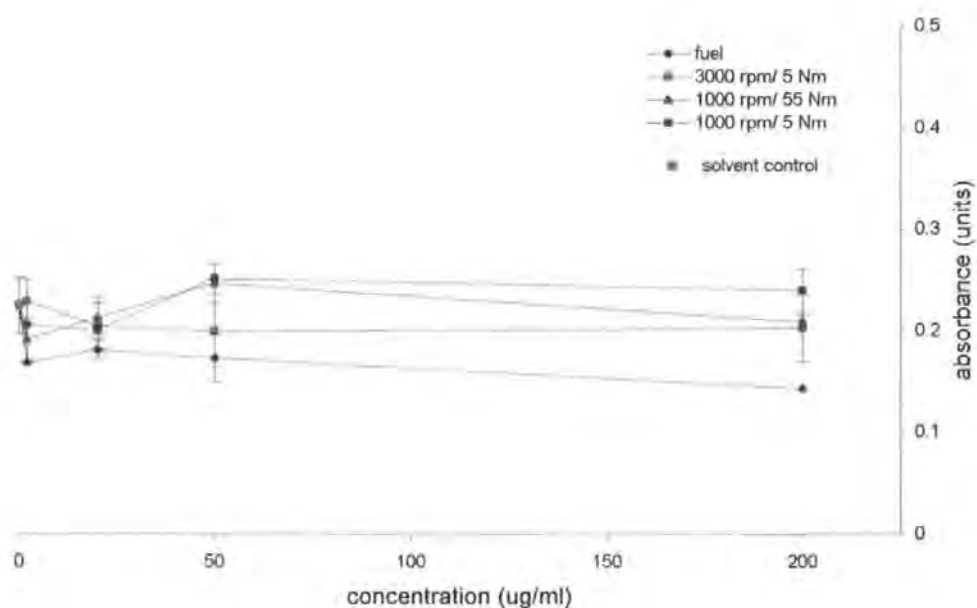


Figure 23. Cytotoxicity of the aliphatic fractions of diesel fuel and of emission samples collected at 3000 rpm/5 Nm, 1000 rpm/55 Nm and 1000 rpm/5 Nm in the neutral red dye assay in Chinese hamster CHO-K1 cells

3.7.2 *Cytotoxicity of the aromatic fractions*

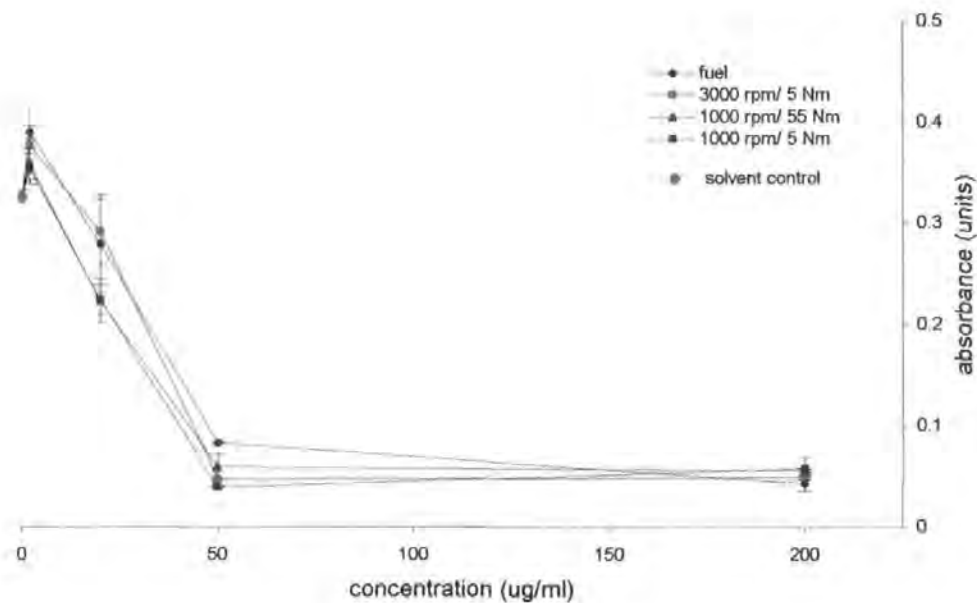
A graph of all four aromatic fractions, assayed for cytotoxic effect without metabolic activation, is shown in Figure 24(a). Without metabolic activation, the marked reduction in cell viability is almost identical in the four different samples, with the aromatic fractions having a very similar cytotoxic effect on the CHO cells.

When assayed with metabolic activation (Figure 24b), all three aromatic diesel engine emission samples exhibited a similar pattern of cytotoxic effect. The diesel fuel aromatic fraction exhibited a less marked affect, especially at the highest concentration assayed of 200 µg/ml.

3.7.3 *Cytotoxicity of the 1-ring aromatic fractions*

The results of the three cytotoxicity assays of the fuel, emission samples collected at 3000 rpm/5 Nm and 1000 rpm/55 Nm are shown graphically in Figure 25a (without S9), and Figure 25b (with S9). Without metabolic activation, the curves for all three samples show a similar pattern. There are, however, small but significant differences in their cytotoxicity, with R 28+37 (1000 rpm /55 Nm) showing the greatest toxic effect on CHO cells. At 200 µg/ml, all three samples were, however, clearly completely toxic to the cells. With S9, the results were variable but comparable for all three samples at the lower concentrations tested. At the highest concentration, the fuel and R 41 (3000 rpm/5 Nm) show similar non-cytotoxic effects. The sample collected at 1000 rpm and 55 Nm again exhibits a greater toxicity, with a significant decrease in cell viability at the 200 µg/ml.

(a) without metabolic activation



(b) with metabolic activation (rat liver S9 fraction)

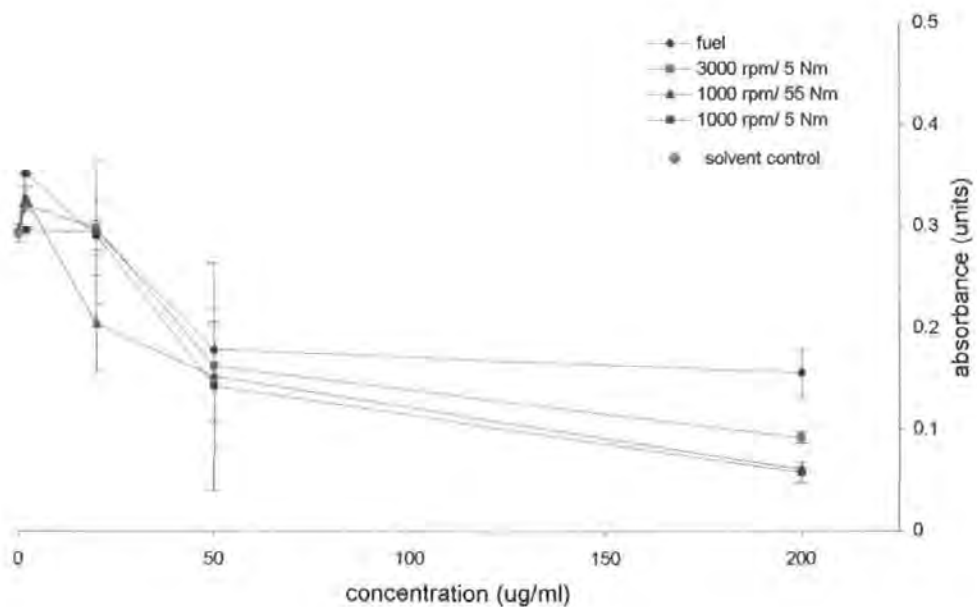
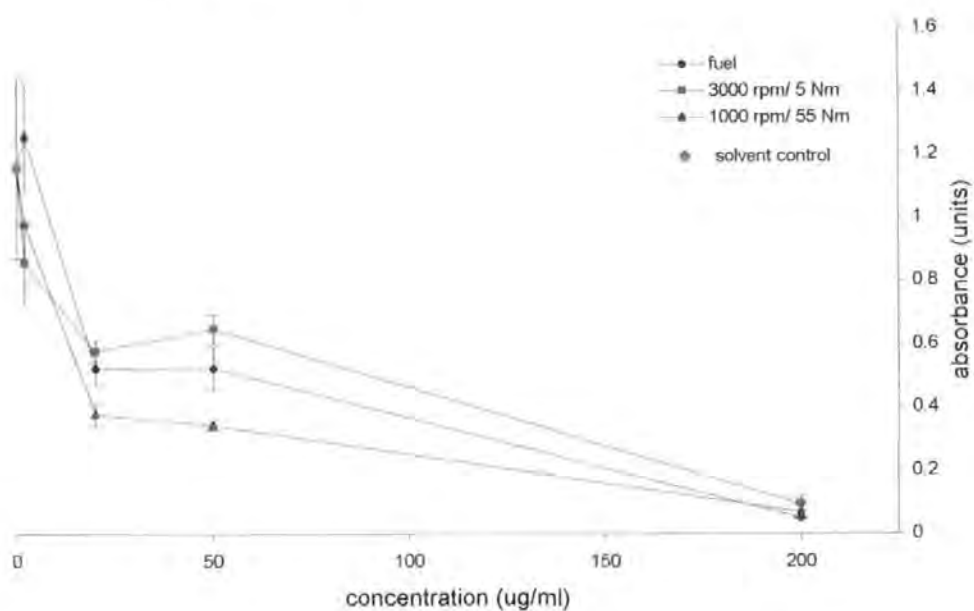


Figure 24. Cytotoxicity of the aromatic fractions of diesel fuel and of emission samples collected at 3000 rpm/5 Nm, 1000 rpm/55 Nm and 1000 rpm/5 Nm in the neutral red dye assay in Chinese hamster CHO-K1 cells

(a) without metabolic activation



(b) with metabolic activation (rat liver S9 fraction)

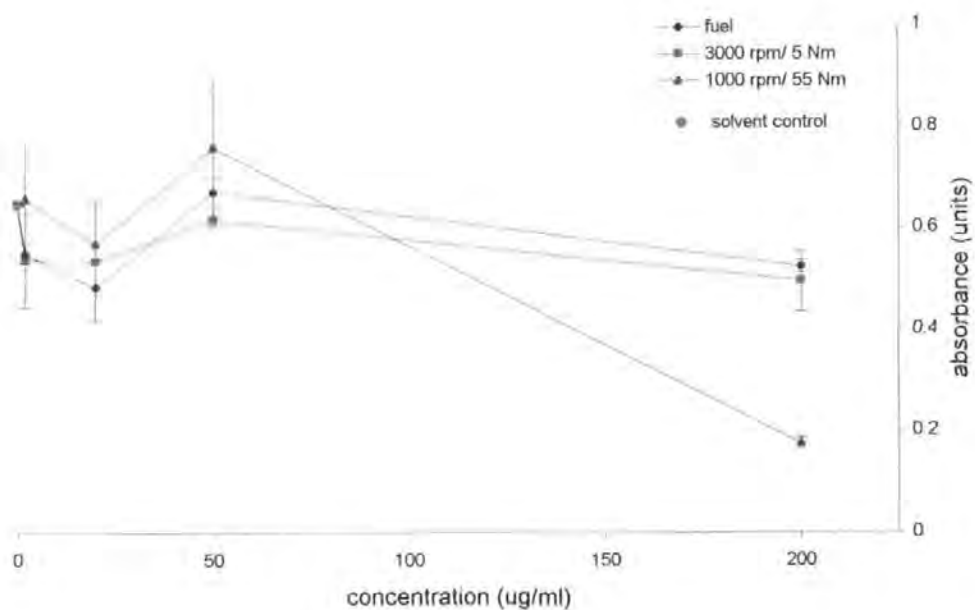


Figure 25. Cytotoxicity of the 1-ring aromatic fractions of diesel fuel and of emission samples collected at 3000 rpm/5 Nm and 1000 rpm/55 Nm in the neutral red dye assay in Chinese hamster CHO-K1 cells

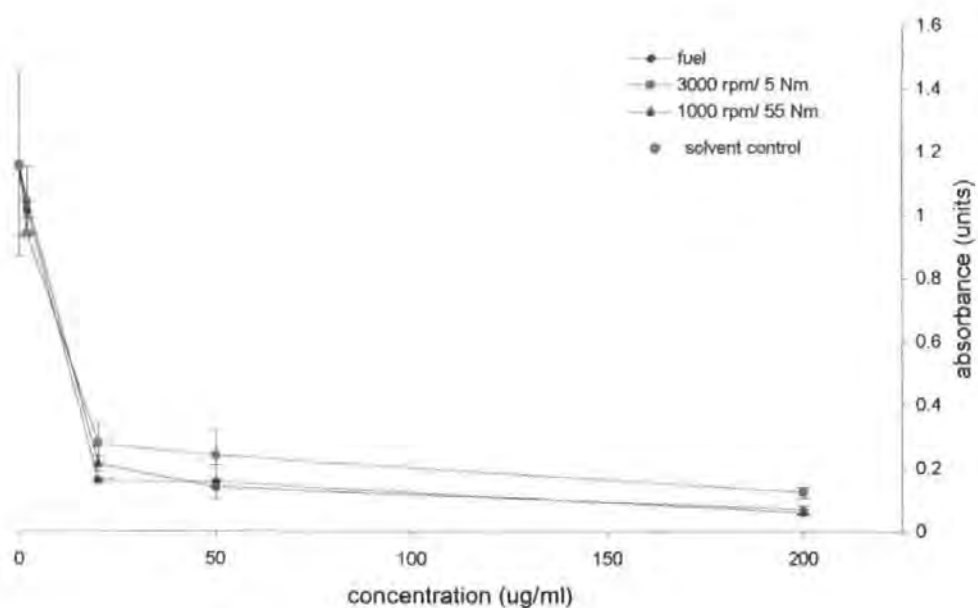
3.7.4 Cytotoxicity of the 2-ring aromatic fractions

The 2-ring aromatic fractions of the fuel and engine emission samples collected at 3000 rpm/5 Nm and 1000 rpm/55 Nm exhibited similar patterns of cytotoxic effect on CHO cells when assayed without metabolic activation (Figure 26a). All three fractions had reduced cell viability to less than 50 % by 20 µg/ml. The 2-ring fraction R 32 (3000 rpm/ 5 Nm) had slightly reduced toxicity in comparison to the other two samples. The cytotoxic effect of the three samples assayed with S9 was less clear, although cell viability was reduced to a minimal level at 200 µg/ml in each case. The summary graph (Figure 26b) shows that while each of the three curves followed a similar pattern, it is evident that the 2-ring fraction of emission sample collected at 1000 rpm and 55 Nm has a greater cytotoxic effect on the CHO cells at all concentrations assayed. The cytotoxic effect at 50 µg/ml was less in all three cases than the effect at 20 µg/ml, despite it being a higher concentration of sample.

3.7.5 Cytotoxicity of the 3+ -ring aromatic fractions

Only two of the samples separated by HPLC produced sufficient mass of 3+ -ring aromatic fraction for cytotoxicity testing. When assayed, both the fuel and fraction R 33 (3000 rpm/5 Nm) both exhibited a similar, severe direct-acting effect on the viability of the CHO cells (Figure 27a). Absorbance levels fell steeply, so that less than 25 % of cells survived at 20 µg/ml. The cytotoxicity of the emission sample fraction was slightly greater than the fuel 3-ring fraction up to 50 µg/ml. In contrast, in the presence of metabolic activation, the cytotoxic effect of the 3+ -ring samples assayed were not matched. The fuel sample exhibited a less severe cytotoxic effect than that of the emission sample fraction R 33. The graph shows the difference between the two curves is large, until the maximum concentration of 200 µg/ml is reached (Figure 27b). At this point the level of cell killing is more than 85 % for both samples.

(a) without metabolic activation



(b) with metabolic activation (rat liver S9 fraction)

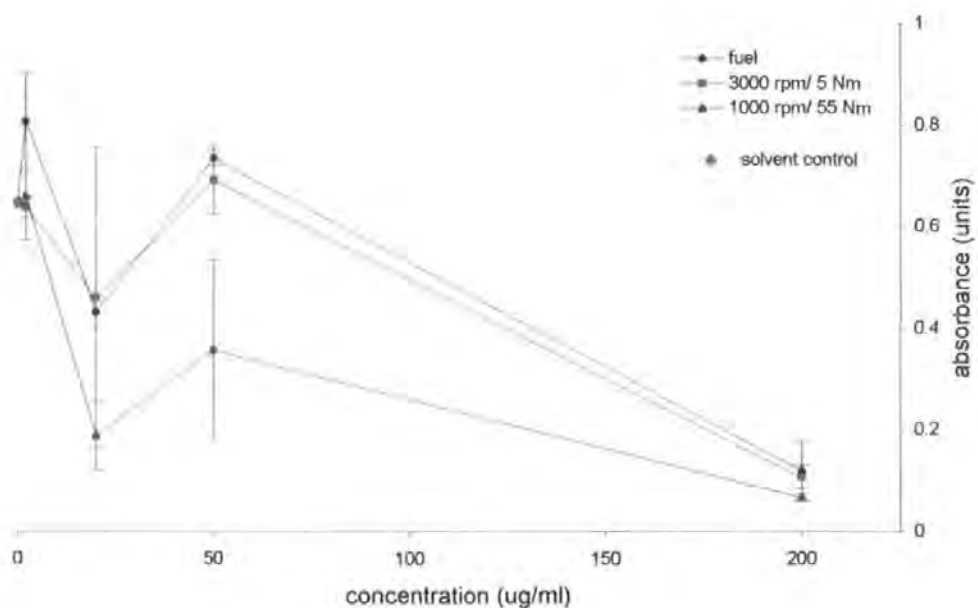
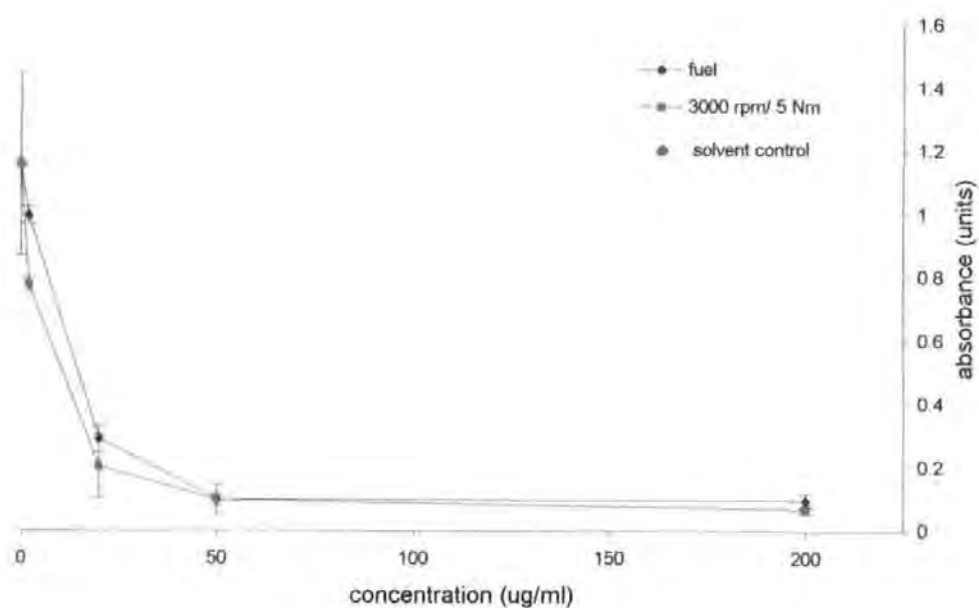


Figure 26. Cytotoxicity of the 2-ring aromatic fractions of diesel fuel and of emission samples collected at 3000 rpm/5 Nm and 1000 rpm/55 Nm in the neutral red dye assay in Chinese hamster CHO-K1 cells

(a) without metabolic activation



(b) with metabolic activation (rat liver S9 fraction)

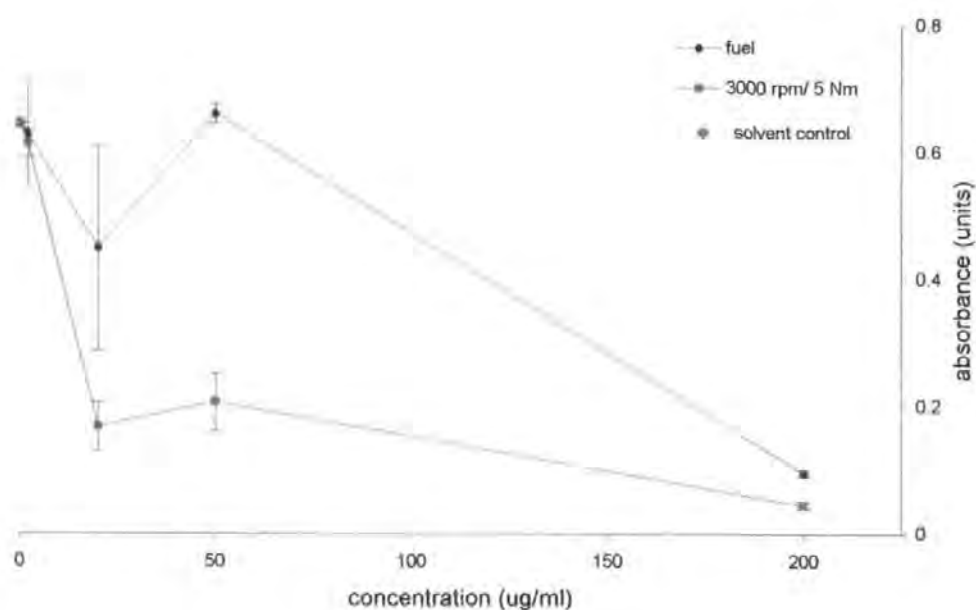


Figure 27. Cytotoxicity of the 3+ -ring aromatic fractions of diesel fuel and of the emission sample collected at 3000 rpm/5 Nm in the neutral red dye assay in Chinese hamster ovary CHO-K1 cells

3.7.6 Cytotoxicity of the polar fractions collected in June 1996

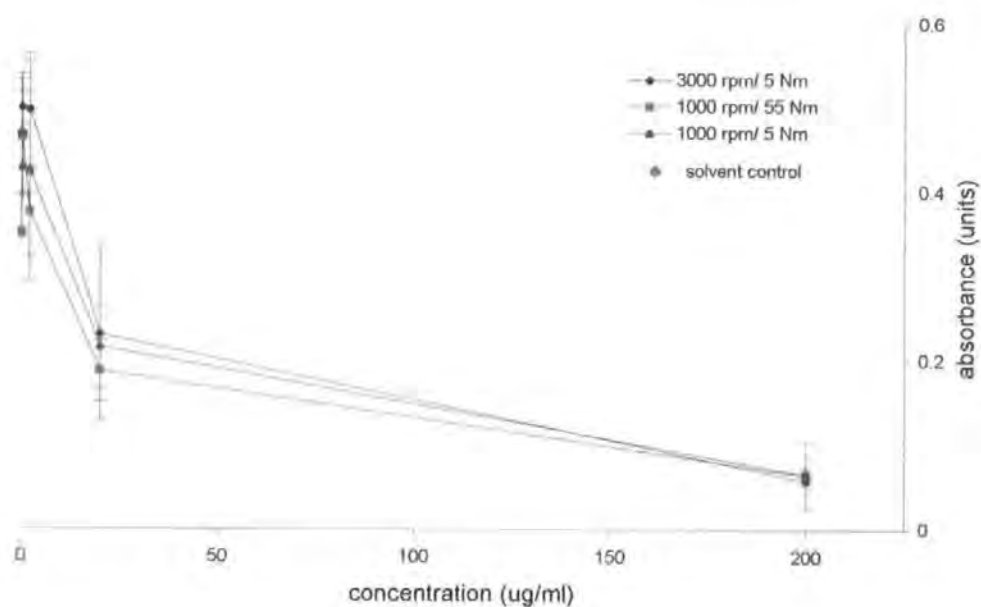
The three polar fractions exhibited a similar dose-related fall in the viability of CHO cells when assayed without metabolic activation (Figure 28a). There were small differences in the cytotoxic effect for each fraction, but these were not larger than the variation between replicates (as indicated by the error bars).

When metabolically activated, the three polar fractions ES 51+54, ES 45+48, and ES 39+42 all exhibited a toxic effect on cells at 200 µg/ml (Figure 28b). The fraction ES 39+42 (3000 rpm/5 Nm) was approximately 20 % less cytotoxic than the other two polar fractions at each concentration assayed.

3.7.7 Summary of the cytotoxicity of the polar fractions collected in January 1997

The second set of polar fractions were collected at the new engine conditions of 2000 rpm/30 Nm, 2000 rpm/55 Nm, 3000 rpm/30 Nm, and 3000 Nm/55 Nm. All four of the polar fractions caused a matched, acute dose dependant decrease in CHO cell viability (Figure 29). At 200 µg/ml there was minimal cell survival for each sample, as evidenced by neutral red absorbance.

(a) without metabolic activation



(b) with metabolic activation (rat liver S9 fraction)

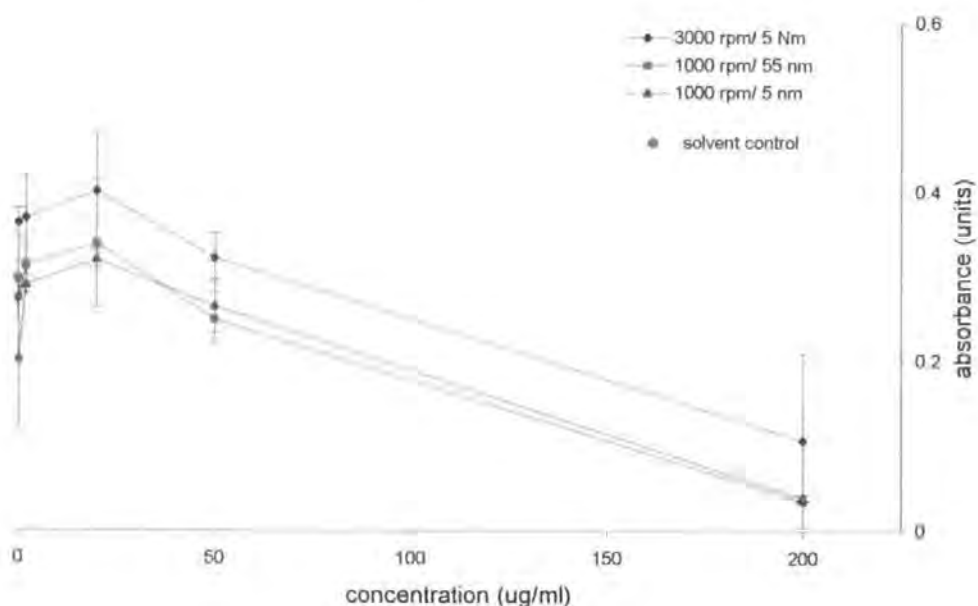


Figure 28. Cytotoxicity of the polar fractions of the emission samples collected at 3000 rpm/5 Nm, 1000 rpm/55 Nm, and 1000 rpm/5 Nm in the neutral red dye assay in Chinese hamster ovary CHO-K1 cells

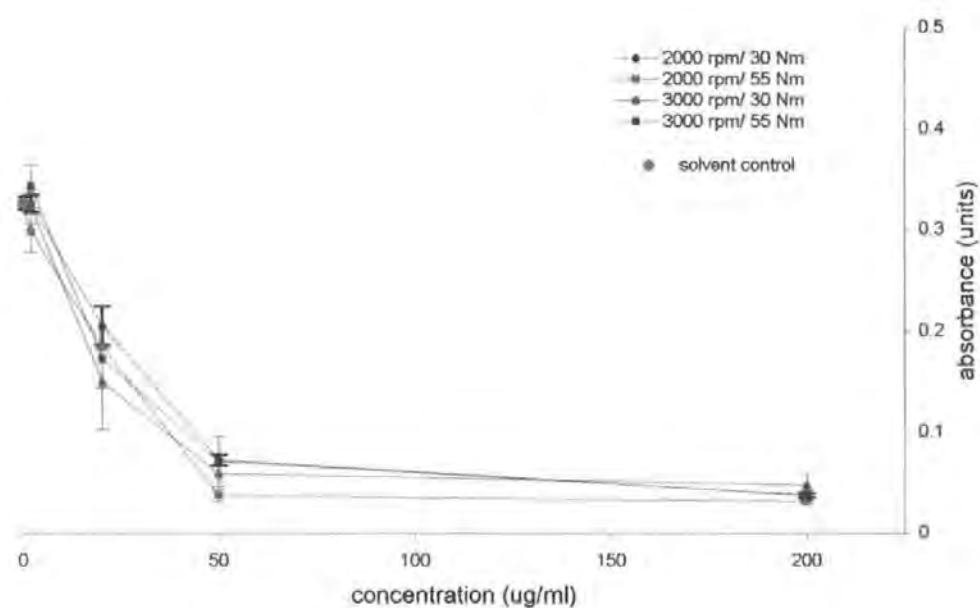


Figure 29. Cytotoxicity of the polar fractions of the four emission samples collected at 2000 rpm/30 Nm, 2000 rpm/55 Nm, 3000 rpm/30 Nm, and 3000 rpm/55 Nm in the neutral red dye assay in Chinese hamster ovary CHO-K1 cells, without metabolic activation

3.7.8 *Summary of cytotoxic assays performed without metabolic activation*

Summaries of cytotoxicity assays on the aliphatic, aromatic, aromatic ring, and polar fractions which were derived from the fuel and each total emission sample are shown in Table 16. The aliphatic fractions show no evidence of cytotoxicity up to the maximum concentration assayed of 200 µg/ml. From the whole aromatic fraction through increasing aromatic ring fractions a progressively more severe dose related increase in cytotoxic effect can be seen. For example for the fuel fractions, the aromatic fraction exhibits a 50-80 % reduction in cell viability (++) at 50 µg/ml, the 1-ring fraction achieves the same '++' reduction at a lower concentration of 20 µg/ml, and the 2-ring fraction exhibits a maximal 80 – 100 % reduction (+++) at 20 µg/ml. The pattern is not clear cut, however, as the 3+ -ring fuel fraction is slightly less cytotoxic (50 – 80 % reduction in cell viability) than the 2-ring fraction (maximal 80 – 100 % reduction) at 20 µg/ml. The general increase in dose related cytotoxicity with increasing ring size is repeated with each of the engine emission sample fractions. The most toxic fraction appears to be the 3-ring fraction of the engine emission collected at 3000 rpm and 5 Nm, which shows a small cytotoxic effect (25 – 50 % reduction in cell viability) at 2 µg/ml, and then maximal cytotoxic effect (80 – 100 % reduction) at remaining concentrations assayed of 20 – 200 µg/ml. All seven polar fractions exhibit increasing cytotoxicity with increased concentration. There is also a correlation with increased cytotoxicity at low dose (20 µg/ml) for the polar fractions of engine emission samples collected at high speed (3000 rpm). Overall, the ring fractions of the fuel and emission samples assayed exhibit the greatest cytotoxic effect without metabolic activation, closely followed by the polar fractions of several samples, in particular those collected at high speeds of 3000 rpm.

fuel or emission sample		sample concentration (µg/ml)				
		0.2	2	20	50	200
fuel	aliphatic		-	-	-	-
	aromatic		-	-	++	+++
	aromatic 1-ring		-	++	++	+++
	2-ring		-	+++	+++	+++
	3-ring		-	++	+++	+++
1000 rpm/5 Nm	aliphatic		-	-	-	-
	aromatic		-	+	+++	+++
	polar	-	-	+		+++
1000 rpm/55 Nm	aliphatic		-	-	-	-
	aromatic		-	+	+++	+++
	aromatic 1-ring		-	++	++	+++
	2-ring		-	+++	+++	+++
	polar	-	-	+		+++
3000 rpm/5 Nm	aliphatic		-	-	-	-
	aromatic		-	-	+++	+++
	aromatic 1-ring		+	++	+	+++
	2-ring		-	++	++	+++
	3-ring		+	+++	+++	+++
	polar	-	-	++		+++
2000 rpm/30 Nm	polar		-	+	++	+++
2000 rpm/55 Nm	polar		-	+	+++	+++
3000 rpm/30 Nm	polar		-	++	+++	+++
3000 rpm/55 Nm	polar		-	++	++	+++

- nil or minimal cytotoxic effect (< 25 % reduction in cell viability)
+ small cytotoxic effect (25 – 50 % reduction in cell viability)
++ large cytotoxic effect (50 – 80 % reduction in cell viability)
+++ maximal cytotoxic effect (80 – 100 % reduction in cell viability)
blank cells indicate sample not assayed at that concentration

Table 16. Cytotoxic effect of diesel fuel and engine emission sample fractions, collected over a range of engine speed and load, on the viability of Chinese hamster ovary CHO-K1 cells measured in the neutral red dye assay

3.7.9 *Summary of cytotoxic assays performed with metabolic activation (rat liver S9)*

Summaries of cytotoxicity assays repeated in the presence of metabolic activation, for aliphatic, aromatic, aromatic ring, and polar fractions of fuel and emission samples are shown in Table 17. Initial examination shows that with S9, over the same range of concentrations as previously assayed, each of the samples is generally less cytotoxic. Although the time between initial exposure and harvest is the same in both assays with and without S9, the S9 mix and sample are washed off after 2 hours and replaced with fresh medium so that direct exposure was for 2 hours only. In tests without S9, the sample is left in contact with the cell monolayer for the full 17 hours until harvest, and direct comparison is therefore not applicable. There is slight evidence of a fall in cell viability for one of the aliphatic fractions (the fuel aliphatic), which exhibited no direct acting cytotoxicity. There is a dose related increase in cytotoxicity at higher concentrations of aromatic fractions, and overall the 2- and 3+ -ring aromatic fractions are the most effective at reducing cell numbers. The polar fractions exhibit a cytotoxic effect at the highest concentration only of 200 µg/ml.

fuel or emission sample		sample concentration (µg/ml)				
		0.2	2	20	50	200
fuel	aliphatic		+	-	-	+
	aromatic		-	-	+	+
	aromatic 1-ring		-	+	-	-
	2-ring		-	+	-	+++
	3-ring		-	+	-	+++
1000 rpm/5 Nm	aliphatic		-	-	-	-
	aromatic		-	-	++	+++
	polar	+	-	-	-	+++
1000 rpm/55 Nm	aliphatic		-	-	-	-
	aromatic		-	+	+	++
	aromatic 1-ring		-	-	-	+++
	2-ring		-	++	+	+++
	polar	-	-	-	-	+++
3000 rpm/5 Nm	aliphatic		-	-	-	-
	aromatic		-	-	+	++
	aromatic 1-ring		-	-	-	-
	2-ring		-	+	-	+++
	3-ring		+	++	++	+++
	polar	-	-	-	-	++

- nil or minimal cytotoxic effect (< 25 % reduction in cell viability)

+ small cytotoxic effect (25 – 50 % reduction in cell viability)

++ large cytotoxic effect (50 – 80 % reduction in cell viability)

+++ maximal cytotoxic effect (80 – 100 % reduction in cell viability)

blank cells indicate sample not assayed at that concentration

Table 17. Cytotoxic effect of diesel fuel and engine emission sample fractions, collected over a range of engine speed and load, on the viability of Chinese hamster ovary CHO-K1 cells measured in the neutral red dye assay with metabolic activation (rat liver S9 fraction)

3.8 *Chromosome aberration assay results*

3.8.1 *The aliphatic fraction*

The aliphatic fraction from the total emission sample collected at 3000 rpm and 5 Nm was assayed for its clastogenicity in the chromosome aberration assay, both with and without metabolic activation, as described in section 2.6.2. The full data are given in Tables 54 and 55, Appendix B. During the cytotoxicity assay there was no reduction in cell viability up to the highest concentration tested of 200 µg/ml (Figures 83 and 84, Appendix A). The aliphatic fraction was therefore tested in the chromosome aberration assay to a maximum concentration of 600 µg/ml. This was the maximum final concentration that could be achieved from the pre-prepared stock solution, and very close to the limit of solubility in DMSO.

3.8.1.1 *The aliphatic fraction without metabolic activation*

In cultures treated with the aliphatic fraction ES 37+40, there was a dose related decrease in mitotic rate from 104 /1000 in the solvent control, to 80/1000 at 300 µg /ml and 59 /1000 at 600 µg/ml (Figure 30). Overall a near 50 % reduction in mitotic rate was achieved at the highest concentration. There was no corresponding increase in chromosome aberrations over this range of concentrations tested, with the number of aberrations remaining below the 5 % background level. None of the doses assayed produced a statistically significant increase in aberrations ($P > 0.05$, Fisher's exact test) over the solvent control (Table 18).

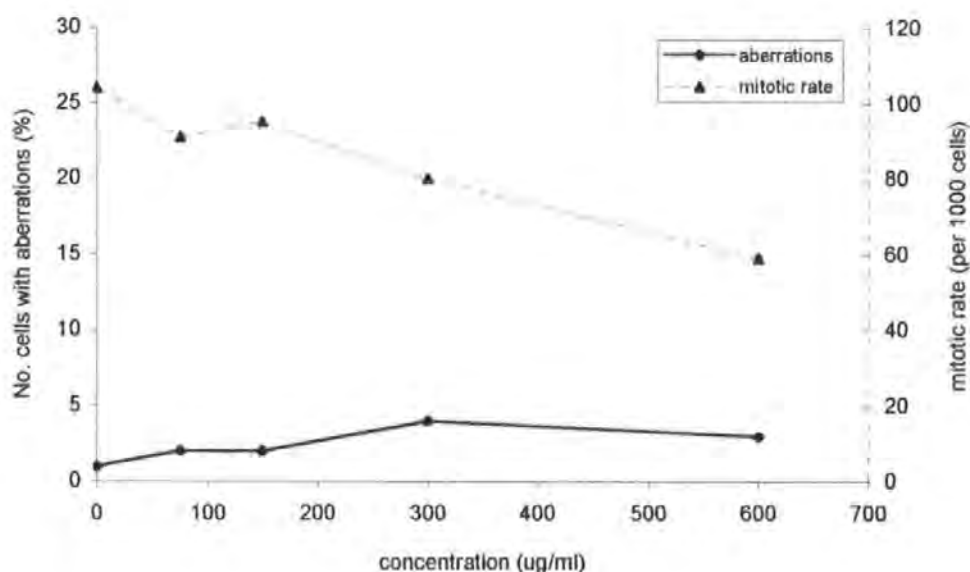


Figure 30. Mitotic rate and number of chromosome aberrations induced in Chinese hamster ovary CHO-K1 cells after exposure without metabolic activation to the aliphatic fraction of the diesel engine emission sample collected at 3000 rpm and 5 Nm (ES 37+40)

concentration (µg/ml)	no. cells with total aberrations /cells scored	probability P^1	number of doses significant ($P \leq 0.0125$) ²	clastogenicity of sample ³
0	1/ 100			
75	2/ 100	0.311		
150	2/ 100	0.311		
300	4/ 100	0.107		
600	3/ 100	0.186		
			0	negative

¹ Fisher's exact test (Richardson *et al.*, 1990), comparison to DMSO control (concentration zero above)

² probability testing at 5 % significance level with Bonferroni correction for multiple dose comparisons (0.05/4 doses)

³ criteria based on Galloway *et al.* (1997), section 2.9.2

Table 18. Chromosome aberrations induced in Chinese hamster ovary CHO-K1 cells exposed without metabolic activation to the aliphatic fraction of the diesel engine emission sample collected at 3000 rpm and 5 Nm (ES 37+40)

3.8.1.2 *The aliphatic fraction with metabolic activation*

In the presence of metabolic activation, the aliphatic fraction was again tested up to a concentration of 600 µg/ml. The mitotic rate remained relatively constant, at around 25 metaphases per 1,000 cells, from solvent control through the concentrations assayed (Figure 31). Whilst not giving a 50 % reduction in cell viability, testing was restricted to 600 µg /ml because it was the highest soluble dose and the greatest concentration that could be achieved while keeping the maximum CHO exposure to DMSO to 0.5 %. There was no significant increase ($P > 0.05$) in the number of chromosome aberrations over control levels at any concentration assayed (Table 19).

The aliphatic fraction of ES 37+40 (3000 rpm/5 Nm), when tested either with or without metabolic activation, resulted in no significant increase in chromosome aberrations in CHO-K1 cells at any dose tested, and was therefore not clastogenic.

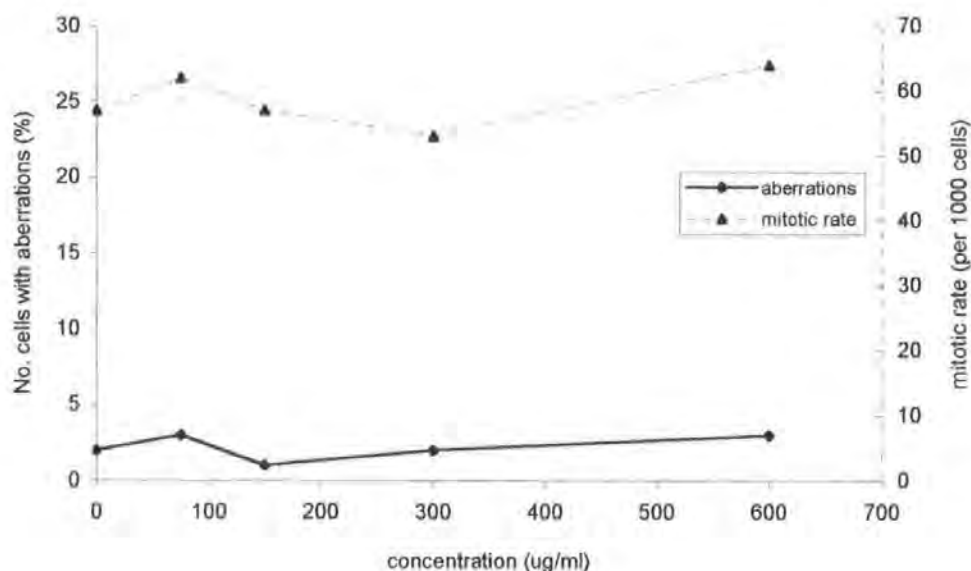


Figure 31. Mitotic rate and number of chromosome aberrations induced in Chinese hamster ovary CHO-K1 cells after exposure with metabolic activation (rat liver S9 fraction) to the aliphatic fraction of the diesel engine emission sample collected at 3000 rpm and 5 Nm (ES 37+40)

concentration (µg/ml)	no. cells with total aberrations /cells scored	probability P^1	number of doses significant ($P \leq 0.0125$) ²	clastogenicity of sample ³
0	2/ 100			
75	3/ 100	0.342		
150	1/ 100	0.688		
300	2/ 100	0.500		
600	3/ 100	0.342		
			0	negative

¹ Fisher's exact test (Richardson *et al.*, 1990), comparison to DMSO control (concentration zero above)

² probability testing at 5 % significance level with Bonferroni correction for multiple dose comparisons (0.05/4 doses)²

³ criteria based on Galloway *et al.* (1997), section 2.9.2

Table 19. Chromosome aberrations induced in Chinese hamster ovary CHO-K1 cells exposed with metabolic activation (rat liver S9 fraction) to the aliphatic fraction of the diesel engine emission sample collected at 3000 rpm and 5 Nm (ES 37+40)

3.8.2 *The aromatic fractions*

The aromatic fraction of the fuel (F8) and three engine emission samples ES 38+41 (3000 rpm/5 Nm), ES 44+47 (1000 rpm/55 Nm) and ES 50+53 (1000 rpm/5 Nm) were tested for their mutagenicity in the chromosome aberration assay, both with and without metabolic activation (Tables 56 to 64, Appendix B).

3.8.2.1 *The aromatic fractions without metabolic activation*

When assayed without metabolic activation, the aromatic fraction of the fuel (Figure 32) and the three engine emission samples assayed (Figures 33 to 35) showed a reduction in mitotic rate with increasing aromatic concentration. At 30 µg/ml, a decrease in cell viability of at least 50 % was observed in all cases. The maximum concentration tested was 40 µg/ml, when mitotic rate fell to around 15 % of the control rate. Aberrations were scored at this concentration with awareness that any positive response would be questionable at such high levels of toxicity. There was no increase in the rate of total chromosome aberrations over control and spontaneous values for either the fuel or the two emission samples collected at engine speed 1000 rpm (Tables 20, 22 and 23).

When assayed, the number of aberrations observed in response to the aromatic fraction ES 38+41 (3000 rpm/5 Nm) were elevated over normal background levels of $\leq 5\%$ (Figure 33). The percentage of cells in the control with aberrations was 5 %, and at concentrations of 10, 30, and 40 µg/ml this was raised to 7 %. Although not statistically significant ($P > 0.05$, Table 21), this was the first observation of an increase in chromosome aberrations over the 5 % level.

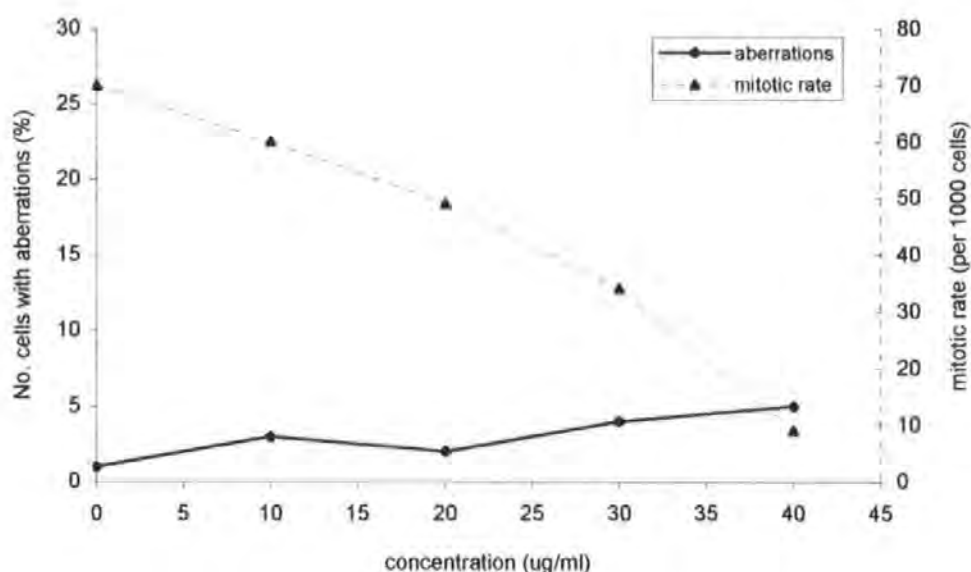


Figure 32. Mitotic rate and number of chromosome aberrations induced in Chinese hamster ovary CHO-K1 cells after exposure without metabolic activation to the aromatic fraction of diesel fuel (F 8)

concentration (µg/ml)	no. cells with total aberrations /cells scored	probability P^1	number of doses significant ($P \leq 0.0125$) ²	clastogenicity of sample ³
0	1/ 100			
10	3/ 100	0.186		
20	2/ 100	0.311		
30	4/ 100	0.107		
40	5/ 100	0.060		
			0	negative

¹ Fisher's exact test (Richardson *et al.*, 1990), comparison to DMSO control

² probability testing at 5 % significance level with Bonferroni correction for multiple dose comparisons (0.05/4 doses)

³ criteria based on Galloway *et al.* (1997), section 2.9.2

Table 20. Chromosome aberrations induced in Chinese hamster ovary CHO-K1 cells exposed without metabolic activation to the aromatic fraction of the diesel fuel (F 8)

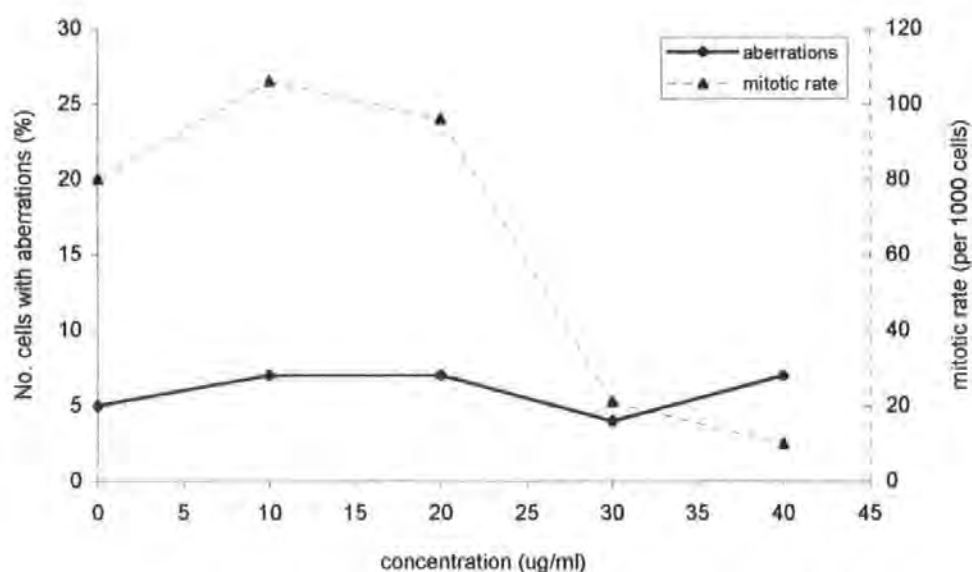


Figure 33. Mitotic rate and number of chromosome aberrations induced in Chinese hamster ovary CHO-K1 cells after exposure without metabolic activation to the aromatic fraction of the diesel engine emission sample collected at 3000 rpm and 5 Nm (ES 38+41)

concentration (µg/ml)	no. cells with total aberrations /cells scored	probability P^1	number of doses significant ($P \leq 0.0125$) ²	clastogenicity of sample ³
0	5/ 100			
10	7/ 100	0.285		
20	7/ 100	0.285		
30	4/ 100	0.625		
40	7/ 100	0.285		
			0	negative

¹ Fisher's exact test (Richardson *et al.*, 1990), comparison to DMSO control (concentration zero above)

² probability testing at 5 % significance level with Bonferroni correction for multiple dose comparisons (0.05/4 doses)²

³ criteria based on Galloway *et al.* (1997), section 2.9.2

Table 21. Chromosome aberrations induced in Chinese hamster ovary CHO-K1 cells exposed without metabolic activation to the aromatic fraction of the diesel engine emission sample collected at 3000 rpm and 5 Nm (ES 38+41)

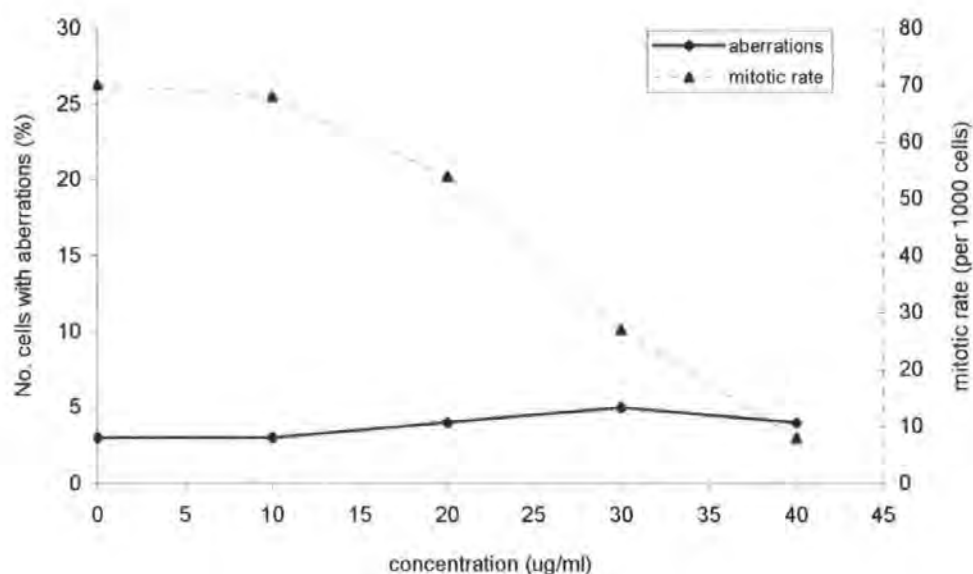


Figure 34. Mitotic rate and number of chromosome aberrations induced in Chinese hamster ovary CHO-K1 cells after exposure without metabolic activation to the aromatic fraction of the diesel engine emission sample collected at 1000 rpm and 55 Nm (ES 44+47)

concentration (µg/ml)	no. cells with total aberrations /cells scored	probability P^1	number of doses significant ($P \leq 0.0125$) ²	clastogenicity of sample ³
0	3/ 100			
10	3/ 100	0.500		
20	4/ 100	0.361		
30	5/ 100	0.250		
40	4/ 100	0.361		
			0	negative

¹ Fisher's exact test (Richardson *et al.*, 1990), comparison to DMSO control (concentration zero above)

² probability testing at 5 % significance level with Bonferroni correction for multiple dose comparisons (0.05/4 doses)

³ criteria based on Galloway *et al.* (1997), section 2.9.2

Table 22. Chromosome aberrations induced in Chinese hamster ovary CHO-K1 cells exposed without metabolic activation to the aromatic fraction of the diesel engine emission sample collected at 1000 rpm and 55 Nm (ES 44+47)

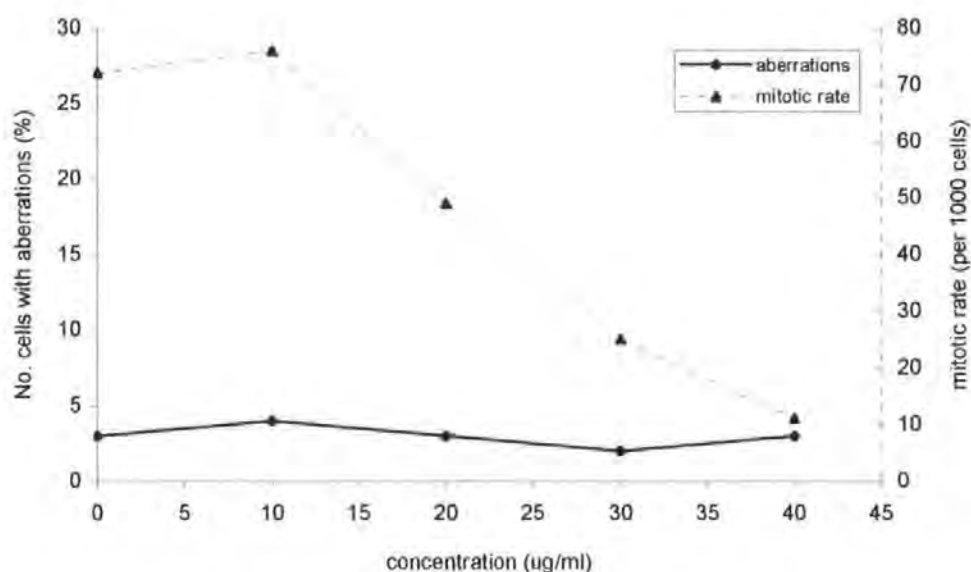


Figure 35. Mitotic rate and number of chromosome aberrations induced in Chinese hamster ovary CHO-K1 cells after exposure without metabolic activation to the aromatic fraction of the diesel engine emission sample collected at 1000 rpm and 5 Nm (ES 50+53)

concentration (µg/ml)	no. cells with total aberrations /cells scored	probability P^1	number of doses significant ($P \leq 0.0125$) ²	clastogenicity of sample ³
0	3/ 100			
10	4/ 100	0.361		
20	3/ 100	0.500		
30	2/ 100	0.658		
40	3/ 100	0.500		
			0	negative

¹ Fisher's exact test (Richardson *et al.*, 1990), comparison to DMSO control (concentration zero above)

² probability testing at 5 % significance level with Bonferroni correction for multiple dose comparisons (0.05/4 doses)

³ criteria based on Galloway *et al.* (1997), section 2.9.2

Table 23. Chromosome aberrations induced in Chinese hamster ovary CHO-K1 cells exposed without metabolic activation to the aromatic fraction of the engine emission sample collected at 1000 rpm and 5 Nm (ES 50+53)

The aromatic fraction of fuel and the three emission samples assayed resulted in a dose dependent reduction in mitotic rate to levels below 50 % cytotoxicity at the highest concentration tested of 40 $\mu\text{g/ml}$. The aromatic fraction of neither the diesel fuel nor either of the 1000 rpm emission samples caused an increase in chromosome aberrations over background levels. The third aromatic emission sample assayed (from total emission samples collected at 3000 rpm and 5 Nm) showed slightly elevated levels of chromosome aberrations, but these were not statistically significant nor dose related. Therefore the aromatic fractions from diesel fuel and emissions collected under speed and load conditions described show no evidence of clastogenicity in the chromosome aberration assay *in vitro* without metabolic activation (Figure 36).

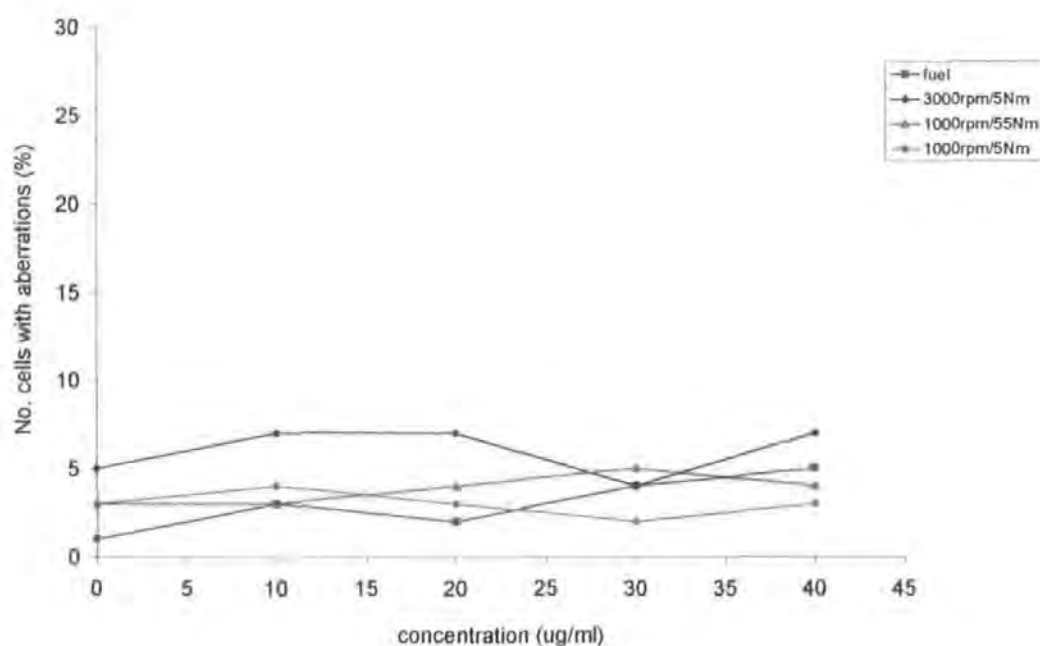


Figure 36. Summary of the percentage of cells with total aberrations induced in Chinese hamster ovary CHO-K1 cells after exposure without metabolic activation to aromatic fractions of diesel fuel and emission samples ES 38+41 (3000 rpm/5 Nm), ES 44+47 (1000 rpm/55 Nm) and ES 50+53 (1000 rpm/5 Nm)

3.8.2.2 *The aromatic fractions assayed with metabolic activation*

The assessment of the mutagenic potential of the four aromatic fractions (3.8.2) was repeated in the presence of metabolic activation at concentrations 0, 10, 20, 30 and 40 µg/ml. Results are given in Tables 57, 59, 60, 62 and 64 (Appendix B).

For two of the samples, the fuel aromatic fraction F8 and ES 50+53 (1000 rpm and 5 Nm), there was a fall in mitotic rate with increasing concentration, resulting in an overall reduction in mitotic rate of greater than 50 % at 40 µg/ml (Figures 37 and 40). The mitotic rate of the aromatic fraction ES 44+47 (1000 rpm/55 Nm) also fell with increasing sample concentration, but only as far as 59 % of control levels (Figure 39). For the remaining aromatic fraction, ES 38+41 (3000 rpm/5 Nm), there was no reduction in mitotic rate from control levels at any concentration tested (Figure 38). The assay was then repeated with an additional concentration of 100 µg/ml with 2x S9 mix (Table 60, Appendix B), which contains a double concentration of S9 within the mix (section 2.7.5). A reduction in mitotic rate was observed, but the reduction was still less than the 50 % recommended for maximum dosage levels. 100 µg/ml was, however, the maximum concentration that could be tested within the limits of the stock solution prepared.

When scored for aberrations, the aromatic fractions of the fuel (F8), and emission samples ES 38+41 (3000 rpm/5 Nm) and ES 44+47 (1000 rpm/55 Nm) caused no significant increase in either the number or type of chromosome aberrations over normal spontaneous levels (Tables 24 to 26). The maximum number of aberrations observed was 5 % of cells with aberrations. In the third emission sample, ES 50+53 (1000 rpm/5 Nm, Figure 40), a total of 7 % of cells were aberrant at a dose of 10 µg/ml. This was above normal background rates, and was statistically significant ($P < 0.05$, Table 27) when compared to the DMSO solvent control. Under the decision criteria adopted (after Galloway *et al.*, 1997), this aromatic fraction ES 50+53 was therefore classified as a

'weakly positive' clastogen. However, this positive result was not repeated at any of the three higher concentrations tested which all fell within the spontaneous range. In addition, the rate of aberrations in the solvent control was particularly low in this case (0 aberrations /100 cell scored), which has an effect on the statistical significance.

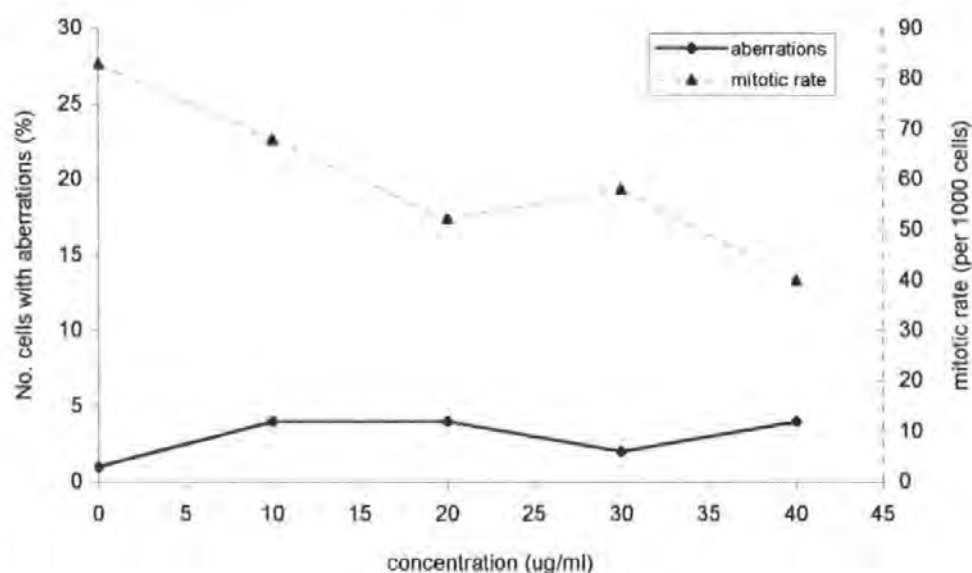


Figure 37. Mitotic rate and number of chromosome aberrations induced in Chinese hamster ovary CHO-K1 cells after exposure in the presence of metabolic activation (rat liver S9 fraction) to the aromatic fraction of the diesel fuel (F 8)

concentration (µg/ml)	no. cells with total aberrations /cells scored	probability P^1	number of doses significant ($P \leq 0.0125$) ²	clastogenicity of sample ³
0	1/ 100			
10	4/ 100	0.107		
20	4/ 100	0.107		
30	2/ 100	0.311		
40	4/ 100	0.107		
			0	negative

¹ Fisher's exact test (Richardson *et al.*, 1990), comparison to DMSO control (concentration zero above)

² probability testing at 5 % significance level with Bonferroni correction for multiple dose comparisons (0.05/4 doses)

³ criteria based on Galloway *et al.* (1997), section 2.9.2

Table 24. Chromosome aberrations induced in Chinese hamster ovary CHO-K1 cells exposed in the presence of metabolic activation (rat liver S9 fraction) to the aromatic fraction of diesel fuel sample F 8

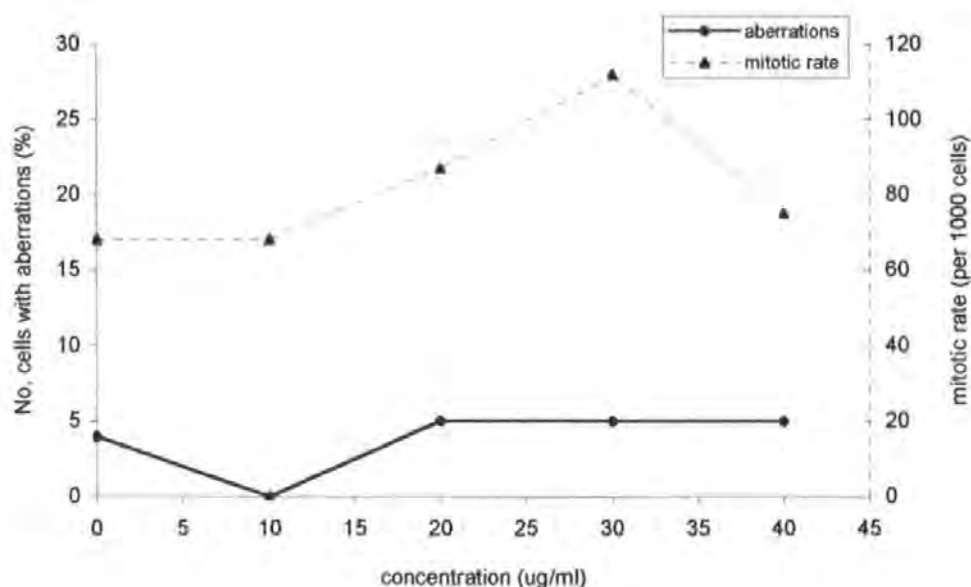


Figure 38. Mitotic rate and number of chromosome aberrations induced in Chinese hamster ovary CHO-K1 cells after exposure with metabolic activation (rat liver S9 fraction) to the aromatic fraction of the diesel engine emission sample collected at 3000 rpm and 5 Nm (ES 38+41)

concentration (µg/ml)	no. cells with total aberrations /cells scored	probability P^1	number of doses significant ($P \leq 0.01$) ²	clastogenicity of sample ³
0	4/ 100			
10	0/ 100	0.970		
20	5/ 100	0.374		
30	5/ 100	0.374		
40	5/ 100	0.374		
100 ⁴	5/ 100	0.500		
			0	negative

¹ Fisher's exact test (Richardson *et al.*, 1990), comparison to DMSO control (concentration zero above)

² probability testing at 5 % significance level with Bonferroni correction for multiple dose comparisons (0.05/4 doses)

³ criteria based on Galloway *et al.* (1997), section 2.9.2

⁴ assayed with 2 x S9 mix, with statistical comparison to a different DMSO solvent control (5/100 aberrant cells)

Table 25. Chromosome aberrations induced in Chinese hamster ovary CHO-K1 cells exposed with metabolic activation (rat liver S9 fraction) to the aromatic fraction of the diesel engine emission sample collected at 3000 rpm and 5 Nm (ES 38+41)

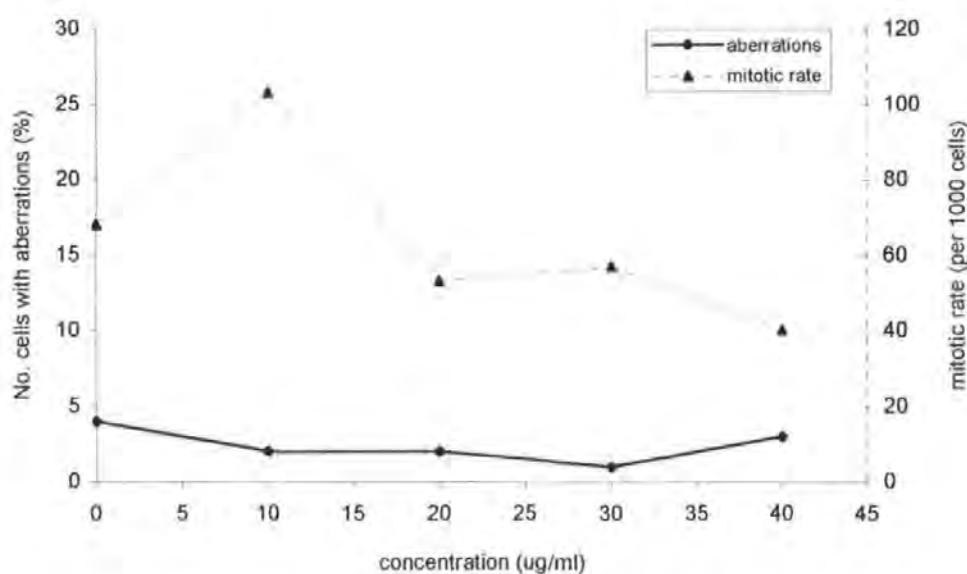


Figure 39. Mitotic rate and number of chromosome aberrations induced in Chinese hamster ovary CHO-K1 cells after exposure with metabolic activation (rat liver S9 fraction) to the aromatic fraction of the diesel engine emission sample collected at 1000 rpm and 55 Nm (ES 44+47)

concentration (µg/ml)	no. cells with total aberrations /cells scored	probability P^1	number of doses significant ($P \leq 0.0125$) ²	clastogenicity of sample ³
0	3/ 100			
10	2/ 100	0.777		
20	2/ 100	0.777		
30	1/ 100	0.893		
40	3/ 100	0.639		
			0	negative

¹ Fisher's exact test (Richardson *et al.*, 1990), comparison to DMSO control (concentration zero above)

² probability testing at 5 % significance level with Bonferroni correction for multiple dose comparisons (0.05/4 doses)

³ criteria based on Galloway *et al.* (1997), section 2.9.2

Table 26. Chromosome aberrations induced in Chinese hamster ovary CHO-K1 cells exposed with metabolic activation (rat liver S9 fraction) to the aromatic fraction of the diesel engine emission sample collected at 1000 rpm and 55 Nm (ES 44+47)

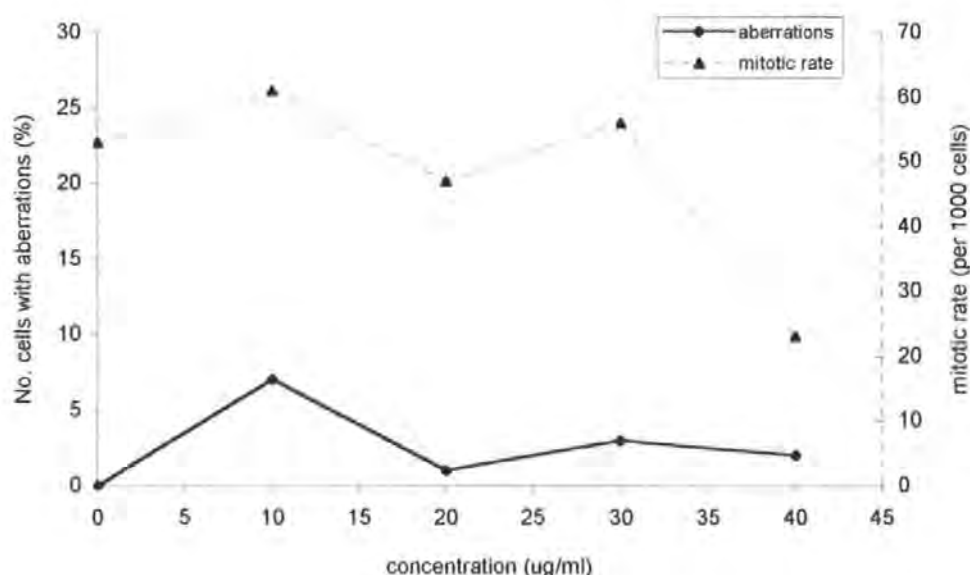


Figure 40. Mitotic rate and number of chromosome aberrations induced in Chinese hamster ovary CHO-K1 cells after exposure with metabolic activation (rat liver S9 fraction) to the aromatic fraction of the diesel engine emission sample collected at 1000 rpm and 5 Nm (ES 50+53)

concentration (µg/ml)	no. cells with total aberrations /cells scored	probability P^1	number of doses significant ($P \leq 0.0125$) ²	clastogenicity of sample ³
0	0/ 100			
10	7/ 100	5.12×10^{-3}		
20	1/ 100	0.373		
30	3/ 100	0.0912		
40	2/ 100	0.185		
			1	weak positive

¹ Fisher's exact test (Richardson *et al.*, 1990), comparison to DMSO control (concentration zero above)

² probability testing at 5 % significance level with Bonferroni correction for multiple dose comparisons (0.05/4 doses)

³ criteria based on Galloway *et al.* (1997), section 2.9.2

Table 27. Chromosome aberrations induced in Chinese hamster ovary CHO-K1 cells exposed with metabolic activation (rat liver S9 fraction) to the aromatic fraction of the diesel engine emission sample collected at 1000 rpm and 5 Nm (ES 50+53)

In summary, the aromatic fractions of the fuel and both emission samples collected at 1000 rpm effected a dose dependant fall in mitotic rate when assayed with metabolic activation. Over the same range of concentrations, the aromatic fraction of ES 38+41 (3000 rpm /5 Nm) had no adverse effect on the mitotic rate in CHO cells. The aromatic fraction of the diesel fuel (F 8) and of emission samples collected at 3000 rpm/5 Nm (ES 38+41) and 1000 rpm /55 Nm (ES 44+47) did not exhibit clastogenicity in CHO-K1 cells when assayed with metabolic activation (Figure 41 below). The aromatic fraction from the total emission sample collected at 1000 rpm/5 Nm (ES 50+53) was identified as a weak clastogen as exposure of CHO-K1 cells to this fraction caused a statistically significant increase in aberrations at one dose only.

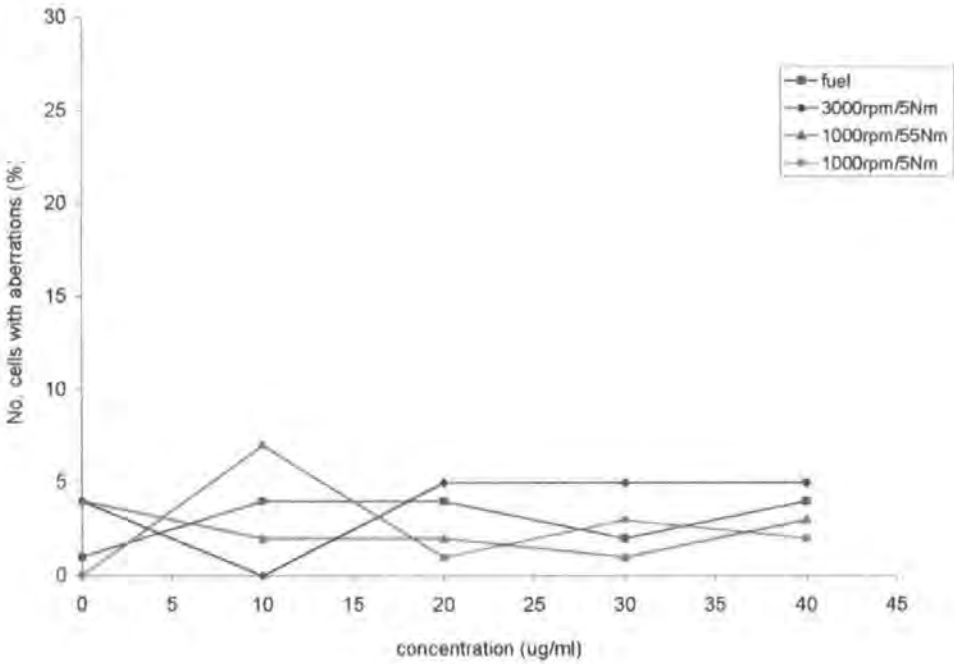


Figure 41. Summary of the percentage of cells with total aberrations induced in Chinese hamster ovary CHO-K1 cells after exposure to aromatic fractions of diesel fuel and emission samples ES 38+41 (3000 rpm/5 Nm), ES 44+47 (1000 rpm/55 Nm) and ES 50+53 (1000 rpm/5 Nm), assayed with metabolic activation (rat liver S9 fraction)

3.8.3 *The 1-ring aromatic fractions*

The diesel fuel and two emission samples were fractionated by HPLC to separate ring fractions from each other (section 2.2.2). The 1-ring fraction, containing a group of 1-ring aromatic compounds, was then assayed for its mutagenicity in the chromosome aberration assay both with and without metabolic activation, the results of which are shown in Tables 65 to 70, Appendix B.

3.8.3.1 *Clastogenicity of the 1-ring aromatic fractions without S9*

In the cytotoxicity assays, the 1-ring fuel fraction R 40 and 1-ring emission sample fraction R 41 (3000 rpm/5 Nm) exhibited a similar effect on cell viability and were therefore both tested at 0, 12.5, 25, 50 and 75 µg/ml in the chromosome aberration assay without S9 (Figures 42 and 43). There was a reduction in mitotic rate with increasing ring fraction concentration, with the fuel fraction exhibiting a more marked decrease (to 34 % of control at 50 µg/ml whereas R 41 fell to only 54% of control level at the same concentration). The mitotic rate at 75 µg/ml in both cases was less than 10 % of controls and therefore aberrations were not this assessed at this concentration. There was no significant increase in the percentage of cells with total chromosome aberrations over background levels for either the fuel (R 40) or emission sample R 41 at any concentration tested up to the maximum of 50 µg/ml (Tables 28 and 29).

The third 1-ring fraction tested, R 28+37 (1000 rpm/55 Nm), had a more marked effect on cell viability in the initial cytotoxicity assay. This sample was therefore tested for its effect on chromosome aberrations at reduced concentrations of 0, 10, 15, 20, and 50 µg/ml (Figure 44). A dose dependant decrease in mitotic rate was seen over the range of concentrations tested, so that at 20 µg/ml the mitotic rate had fallen to 55 % of untreated levels. At the highest concentration of 50 µg/ml the mitotic rate was only 4 % of control

level, and therefore aberrations were not scored. With the fall in mitotic rate there was no corresponding increase in the total number of chromosome aberrations for the 1-ring fraction of the emission collected at 1000 rpm speed and 5 Nm load. The level of aberrations were not significantly different from background levels at any concentration tested (Table 30).

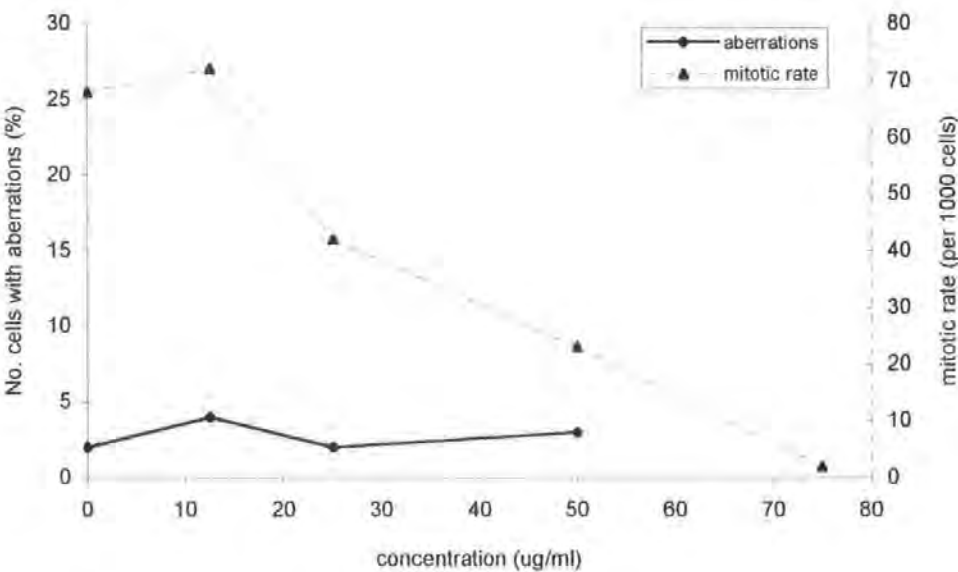


Figure 42. Mitotic rate and number of chromosome aberrations induced in Chinese hamster ovary CHO-K1 cells after exposure without metabolic activation to the 1-ring aromatic fraction of the diesel fuel (R 40)

concentration (µg/ml)	no. cells with total aberrations /cells scored	probability <i>P</i> ¹	number of doses significant (<i>P</i> ≤ 0.0167) ²	Clastogenicity of sample ³
0	2/ 100			
12.5	4/ 100	0.224		
25	2/ 100	0.500		
50	3/ 100	0.342		
			0	negative

¹ Fisher's exact test (Richardson *et al.*, 1990), comparison to DMSO control (concentration zero above)
² probability testing at 5 % significance level with Bonferroni correction for multiple dose comparisons (0.05/3 doses)
³ criteria based on Galloway *et al.* (1997), section 2.9.2

Table 28. Chromosome aberrations induced in Chinese hamster ovary CHO-K1 cells exposed without metabolic activation to the 1-ring aromatic fraction of the diesel fuel (R 40)

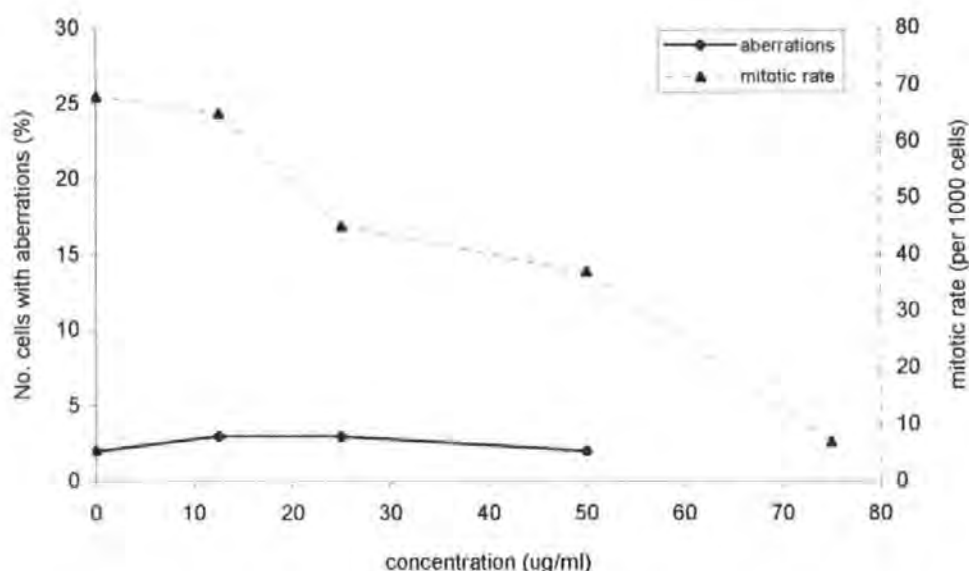


Figure 43. Mitotic rate and number of chromosome aberrations induced in Chinese hamster ovary CHO-K1 cells after exposure without metabolic activation to the 1-ring aromatic fraction of the diesel engine emission sample collected at 3000 rpm and 5 Nm (R 41)

concentration ($\mu\text{g/ml}$)	no. cells with total aberrations /cells scored	probability P^1	number of doses significant ($P \leq 0.0167$) ²	clastogenicity of sample ³
0	2/ 100			
12.5	3/ 100	0.342		
25	3/ 100	0.342		
50	2/ 100	0.500		
			0	negative

¹ Fisher's exact test (Richardson *et al.*, 1990), comparison to DMSO control (concentration zero above)

² probability testing at 5 % significance level with Bonferroni correction for multiple dose comparisons (0.05/3 doses)

³ criteria based on Galloway *et al.* (1997), section 2.9.2

Table 29. Chromosome aberrations induced in Chinese hamster ovary CHO-K1 cells exposed without metabolic activation to the 1-ring aromatic fraction of the diesel engine emission sample collected at 3000 rpm and 5 Nm (R 41)

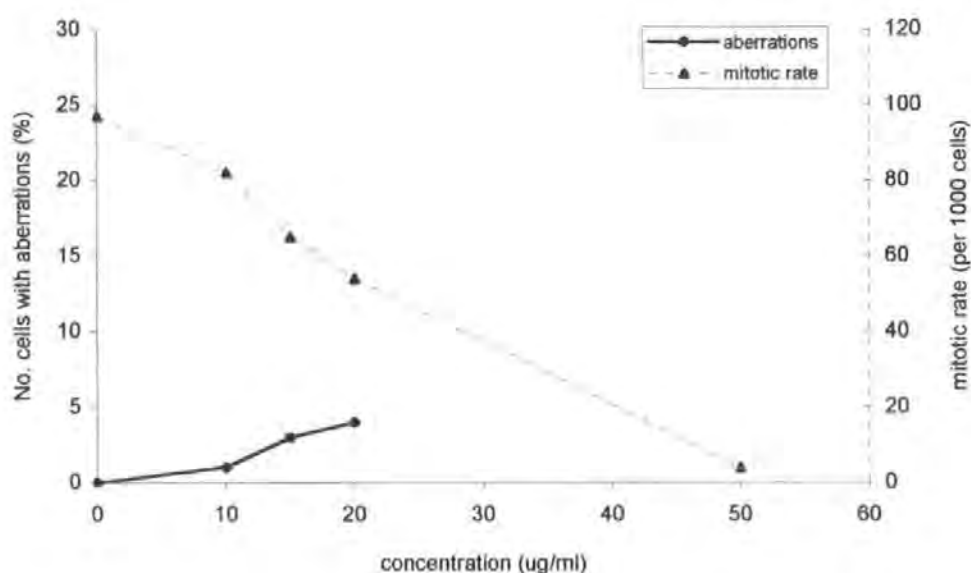


Figure 44. Mitotic rate and number of chromosome aberrations induced in Chinese hamster ovary CHO-K1 cells after exposure without metabolic activation to the 1-ring aromatic fraction of the diesel engine emission sample collected at 1000 rpm and 55 Nm (R 37)

concentration ($\mu\text{g/ml}$)	no. cells with total aberrations /cells scored	probability P^1	number of doses significant ($P \leq 0.0167$) ²	clastogenicity of sample ³
0	0/ 100		0	negative
10	1/ 100	0.373		
15	3/ 100	0.091		
20	4/ 100	0.045		

¹ Fisher's exact test (Richardson *et al.*, 1990), comparison to DMSO control (concentration zero above)

² probability testing at 5 % significance level with Bonferroni correction for multiple dose comparisons (0.05/3 doses)

³ criteria based on Galloway *et al.* (1997), section 2.9.2

Table 30. Chromosome aberrations induced in Chinese hamster ovary CHO-K1 cells exposed without metabolic activation to the 1-ring aromatic fraction of the engine emission sample collected at 1000 rpm and 55 Nm (R 28+37)

To summarise, the 1-ring fractions of the diesel fuel and emission samples R 41 (3000 rpm/ 5 Nm) and R 37 (1000 rpm/ 55 Nm) caused a dose related reduction in the mitotic rate of CHO-K1 cells over a range of concentrations. When scored for chromosome aberrations to a maximal dose that effected a 50 % reduction in mitotic rate, there was no significant increase ($P \leq 0.05$) in the total number of cells with aberrations over solvent control levels (Figure 45).

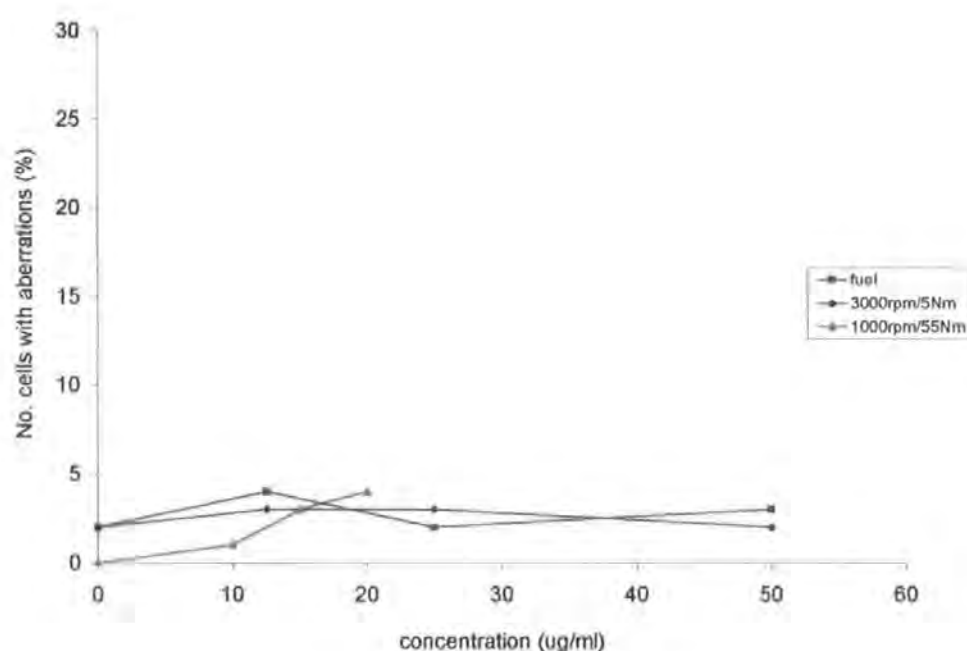


Figure 45. Summary of the percentage of cells with total aberrations induced in Chinese hamster ovary CHO-K1 cells after exposure without metabolic activation to 1-ring aromatic fractions of diesel fuel R 40 and emission samples R 41 (3000 rpm/ 5 Nm), and R 28+37 (1000 rpm/55 Nm).

3.8.3.2 *Clastogenicity of the 1-ring aromatic fraction with metabolic activation*

The 1-ring aromatic fractions of diesel fuel and two emission samples (R 41 and R 37) were assessed for their clastogenicity in the presence of metabolic activation in CHO cells. From information gained from cytotoxicity assays, all three samples were tested at 0, 25, 50, 100, and 200 µg/ml. Fraction R 28+37 (1000 rpm/55 Nm) was tested additionally at 150 µg/ml. Full data are given in Tables 66, 68, and 70, Appendix B.

The assessment of the effect of the 1-ring fractions on mitotic rate was inhibited by a low mitotic rate in the control (42/1000) which was increased at the low concentrations of some of the samples assayed (maximum 61/1000). However, for all three fractions there was a clear decrease in mitotic index with increasing fraction concentration (Figures 46 to 48). The effect on mitotic rate was greatest for fraction R 28+37 (which fell by approximately two thirds at 200 µg/ml), then the fuel R 40 (to 66 % of controls at 200 µg/ml), with the least overall effect on mitotic rate effected by fraction R 41 (a fall of approximately 25 % at the highest concentration tested of 200 µg/ml). This was a similar pattern as seen for each fraction when assayed without S9 (section 3.8.3.1). The number and type of chromosome aberrations was scored up to 200 µg/ml for all three samples. For all three of the 1-ring fractions assayed with S9, the number of aberrations observed remained at 5 % or below, and therefore not raised above normal background levels. There was no statistically significant increase ($P > 0.05$) in chromosome aberrations for metabolically activated 1-ring aromatic fractions (Tables 31 to 33).

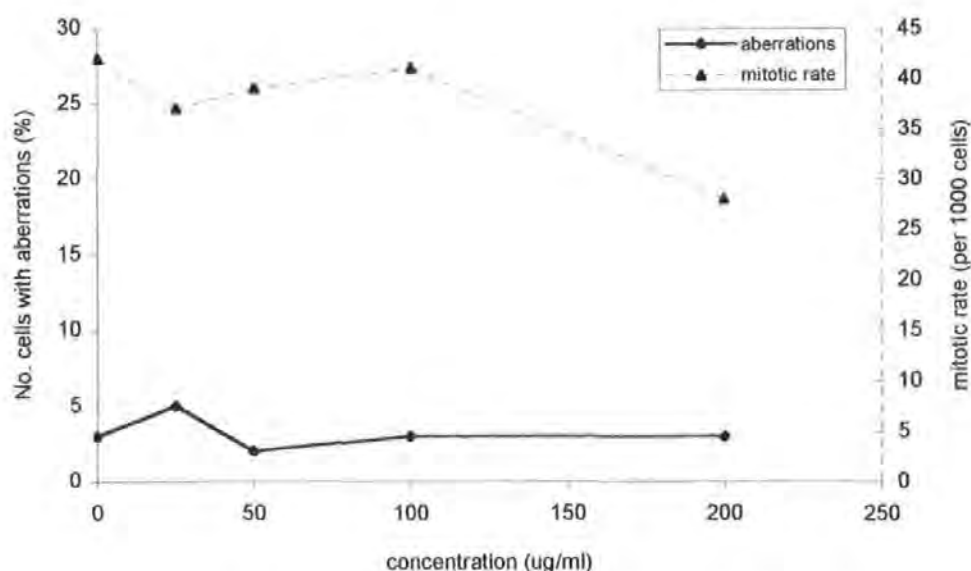


Figure 46. Mitotic rate and number of chromosome aberrations induced in Chinese hamster ovary CHO-K1 cells after exposure with metabolic activation (rat liver S9 fraction) to the 1-ring aromatic fraction of diesel fuel (R 40)

concentration (µg/ml)	no. cells with total aberrations /cells scored	probability P^1	number of doses significant ($P \leq 0.0125$) ²	clastogenicity of sample ³
0	3/ 100			
25	5/ 100	0.250		
50	2/ 100	0.658		
100	3/ 100	0.500		
200	3/ 100	0.500	0	negative

¹ Fisher's exact test (Richardson *et al.*, 1990), comparison to DMSO control (concentration zero above)

² probability testing at 5 % significance level with Bonferroni correction for multiple dose comparisons (0.05/4 doses)

³ criteria based on Galloway *et al.* (1997), section 2.9.2

Table 31. Chromosome aberrations induced in Chinese hamster ovary CHO-K1 cells exposed with metabolic activation (rat liver S9 fraction) to the 1-ring aromatic fraction of the diesel fuel (R 40)

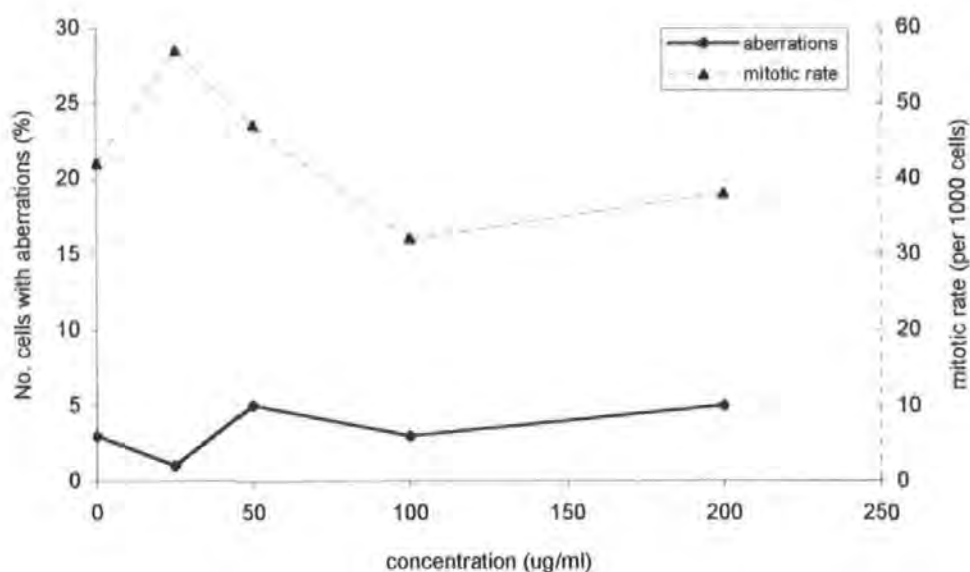


Figure 47. Mitotic rate and number of chromosome aberrations induced in Chinese hamster ovary CHO-K1 cells after exposure with metabolic activation (rat liver S9 fraction) to the 1-ring aromatic fraction of the diesel engine emission sample collected at 3000 rpm and 5 Nm (R 41)

concentration (µg/ml)	no. cells with total aberrations /cells scored	probability P^1	number of doses significant ($P \leq 0.0125$) ²	clastogenicity of sample ³
0	3/ 100			
25	1/ 100	0.814		
50	5/ 100	0.250		
100	3/ 100	0.500		
200	5/ 100	0.250		
			0	negative

¹ Fisher's exact test (Richardson *et al.*, 1990), comparison to DMSO control (concentration zero above)

² probability testing at 5 % significance level with Bonferroni correction for multiple dose comparisons (0.05/4 doses)

³ criteria based on Galloway *et al.* (1997), section 2.9.2

Table 32. Chromosome aberrations induced in Chinese hamster ovary CHO-K1 cells exposed with metabolic activation (rat liver S9 fraction) to the 1-ring aromatic fraction of the diesel engine emission sample collected at 3000 rpm and 5 Nm (R 41)

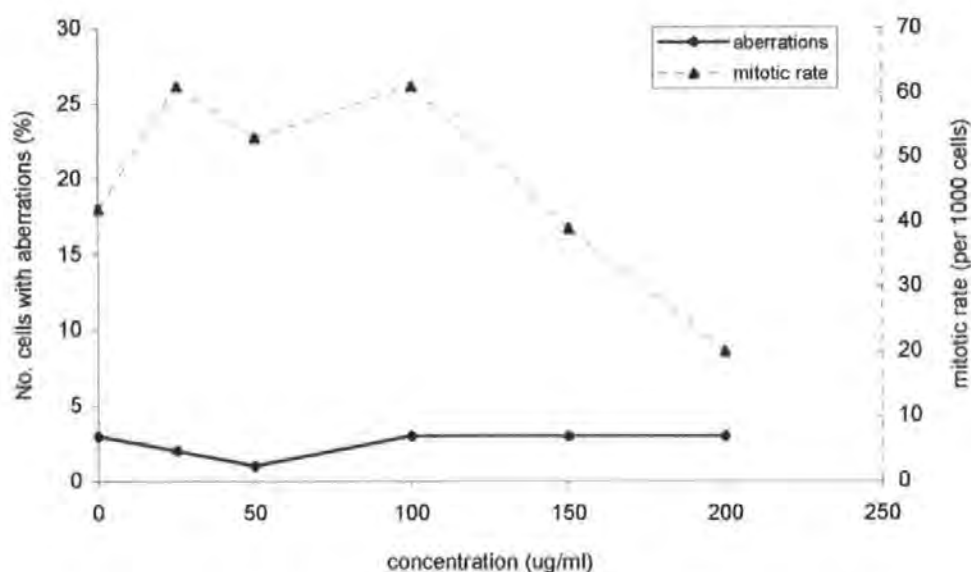


Figure 48. Mitotic rate and number of chromosome aberrations induced in Chinese hamster ovary CHO-K1 cells after exposure with metabolic activation (rat liver S9 fraction) to the 1-ring aromatic fraction of the diesel engine emission sample collected at 1000 rpm and 55 Nm (R 28+37)

concentration (µg/ml)	no. cells with total aberrations /cells scored	probability P^1	number of doses significant ($P \leq 0.01$) ²	clastogenicity of sample ³
0	3/ 100		0	negative
25	2/ 100	0.658		
50	1/ 100	0.814		
100	3/ 100	0.500		
150	3/ 100	0.500		
200	3/ 100	0.500		

¹ Fisher's exact test (Richardson *et al.*, 1990), comparison to DMSO control (concentration zero above)

² probability testing at 5 % significance level with Bonferroni correction for multiple dose comparisons (0.05/5 doses)

³ criteria based on Galloway *et al.* (1997), section 2.9.2

Table 33. Chromosome aberrations induced in Chinese hamster ovary CHO-K1 cells exposed with metabolic activation (rat liver S9 fraction) to the 1-ring aromatic fraction of the diesel engine emission sample collected at 1000 rpm and 55 Nm (R 28+37)

The 1-ring aromatic fractions of diesel fuel R40 and two engine emission samples R 41 and R 37 (3000 rpm/5 Nm and 1000 rpm/55 Nm) were assayed for their clastogenicity in the presence of metabolic activation. In all three samples a dose-related fall in mitotic rate was exhibited, although the extent of the reduction in mitotic rate varied between samples. Non of the three samples caused an increase in the number of chromosome aberrations at any concentration over spontaneous rates previously seen (Figure 49), and all three were therefore classed as not clastogenic.

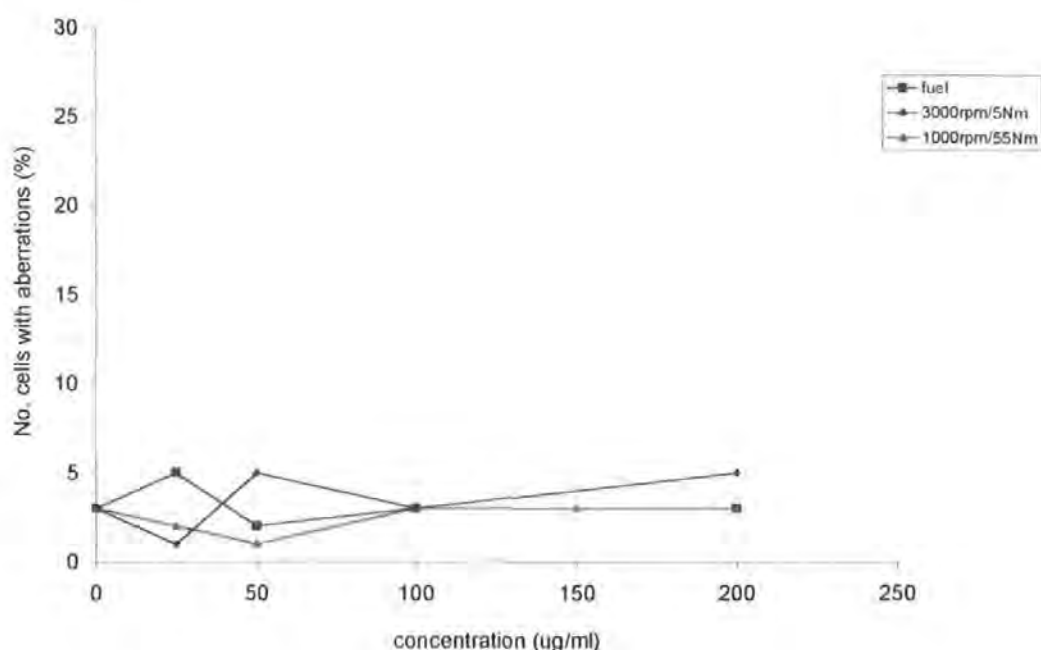


Figure 49. Summary of the percentage of cells with total aberrations induced in Chinese hamster ovary CHO-K1 cells after exposure with metabolic activation (rat liver S9 fraction) to I-ring aromatic fractions of diesel fuel R 40 and emission samples R 41 (3000 rpm/5 Nm), and R 28+37 (1000 rpm/55 Nm)

3.8.4 *The 2-ring aromatic fractions*

As stated, the diesel fuel and two emission samples (3000 rpm/5 Nm and 1000 rpm/55 Nm) were fractionated by HPLC to separate into different ring group fractions. The 2-ring fraction, containing a group of 2-ring aromatic compounds, was then assayed for its mutagenicity in the chromosome aberration assay both with and without metabolic activation. Full results are given in Tables 71 to 76, Appendix B.

3.8.4.1 *The 2-ring aromatic fractions assayed without metabolic activation*

Following the results of the effect of the 2-ring group compounds in cytotoxicity tests, all three 2-ring fractions were tested in the chromosome aberration assay at concentrations of 0, 5, 10, 15, 20, and 40 µg/ml. For all three fractions, a dose related reduction in mitotic rate was seen (Figures 50 to 52). With the fuel 2-ring fraction (R 26), mitotic rate remained fairly stable up to 15 µg/ml, then fell sharply to 39 % of controls at 20 µg/ml, with no mitotic cells visible at the highest concentration of 40 µg/ml (Figure 50). The 2-ring fractions of the two emission samples (R 32 and R 29+38) exhibited a more severe effect on the number of cells in mitosis. In both cases, the mitotic index fell to around 39 % of control levels at 15 µg/ml and less than 30 % at 20 µg/ml (therefore these were not scored for aberrations).

The adverse effect of the diesel fuel R26 and emission sample R 32 (3000 rpm/5 Nm) 2-ring fractions on mitotic rate did not correspond to a significant increase in the number of chromosome aberrations (Tables 34 and 35). The total number of chromosome aberrations found in CHO cells after exposure to R 26 and R 32 without metabolic activation did not increase above 5 % at any concentration tested. For the third 2-ring sample assayed without metabolic activation R 29+38 (1000 rpm/55 Nm), the number of aberrations rose to 6 % of cells with total aberrations at the highest concentration scored of 15 µg/ml (Figure 52). This very slight rise above the normal background rate was not

statistically significant ($P > 0.05$, Table 36), and has to be assessed with a note of caution as the mitotic index at this concentration was reduced to 37 % of control levels. That being said, however, it may be an early indication of the clastogenicity of compounds within this group which is masked by cytotoxicity.

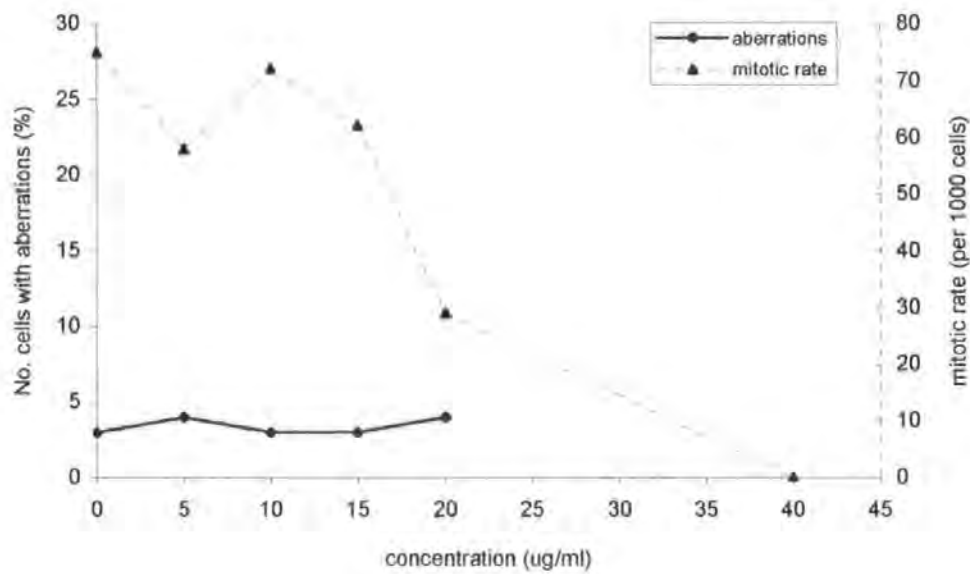


Figure 50. Mitotic rate and number of chromosome aberrations induced in Chinese hamster ovary CHO-K1 cells after exposure without metabolic activation to the 2-ring aromatic fraction of diesel fuel (R 26)

concentration (µg/ml)	no. cells with total aberrations /cells scored	probability <i>P</i> ¹	number of doses significant (<i>P</i> ≤ 0.0125) ²	clastogenicity of sample ³
0	3/ 100			
5	4/ 100	0.361		
10	3/ 100	0.500		
15	3/ 100	0.500		
20	4/ 100	0.361		
			0	negative

¹ Fisher's exact test (Richardson *et al.*, 1990), comparison to DMSO control (concentration zero above)
² probability testing at 5 % significance level using Bonferroni correction for multiple dose comparisons (0.05/4 doses)
³ criteria based on Galloway *et al.* (1997), section 2.9.2

Table 34. Chromosome aberrations induced in Chinese hamster ovary CHO-K1 cells exposed without metabolic activation to the 2-ring aromatic fraction of diesel fuel (R 26)

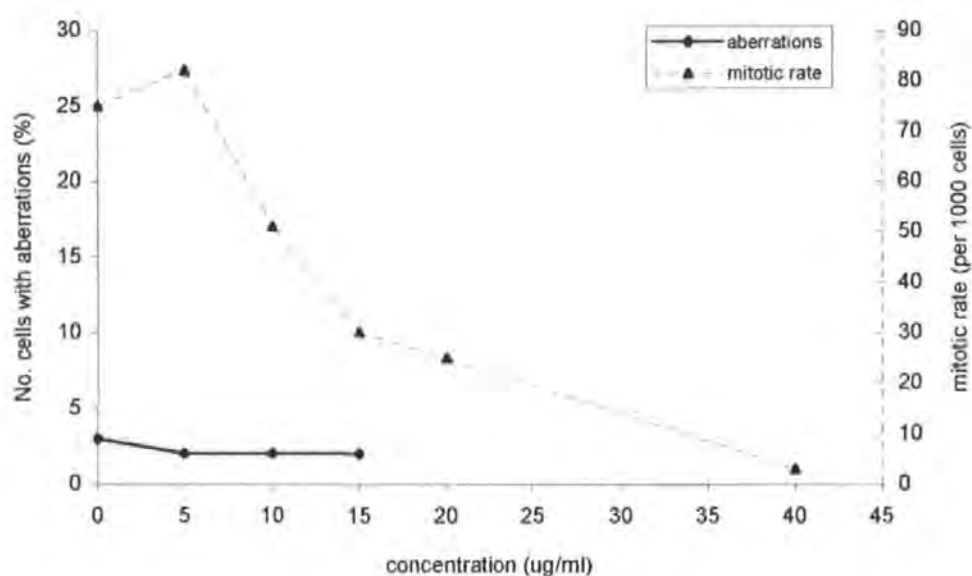


Figure 51. Mitotic rate and number of chromosome aberrations induced in Chinese hamster ovary CHO-K1 cells after exposure without metabolic activation to the 2-ring aromatic fraction of diesel engine emission sample collected at 3000 rpm and 5 Nm (R 32)

concentration ($\mu\text{g/ml}$)	no. cells with total aberrations /cells scored	probability P^1	number of doses significant ($P \leq 0.0167$) ²	clastogenicity of sample ³
0	3/ 100		0	negative
5	2/ 100	0.658		
10	2/ 100	0.658		
15	2/ 100	0.658		

¹ Fisher's exact test (Richardson *et al.*, 1990), comparison to DMSO control (concentration zero above)

² probability testing at 5 % significance level using Bonferroni correction for multiple dose comparisons (0.05/3 doses)

³ criteria based on Galloway *et al.* (1997), section 2.9.2

Table 35. Chromosome aberrations induced in Chinese hamster ovary CHO-K1 cells exposed without metabolic activation to the 2-ring aromatic fraction of the diesel engine emission sample collected at 3000 rpm and 5 Nm (R 32)

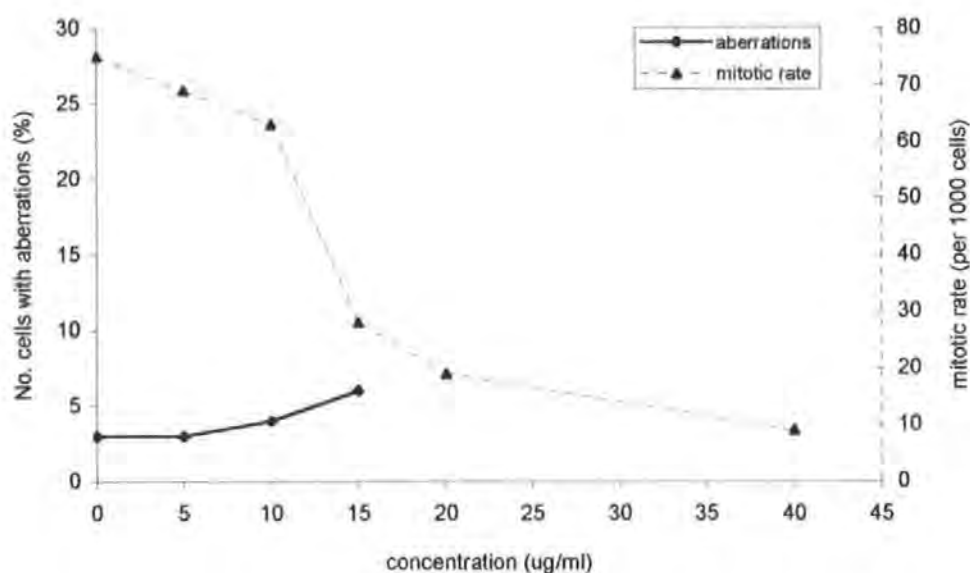


Figure 52. Mitotic rate and number of chromosome aberrations induced in Chinese hamster ovary CHO-K1 cells after exposure without metabolic activation to the 2-ring aromatic fraction of diesel engine emission sample collected at 1000 rpm and 55 Nm (R 29+38)

concentration ($\mu\text{g/ml}$)	no. cells with total aberrations /cells scored	probability P^1	number of doses significant ($P \leq 0.0167$) ²	clastogenicity of sample ³
0	3/ 100			
5	3/ 100	0.500		
10	4/ 100	0.361		
15	6/ 100	0.167		
			0	negative

¹ Fisher's exact test (Richardson *et al.*, 1990), comparison to DMSO control (concentration zero above)

² probability testing at 5 % significance level using Bonferroni correction for multiple dose comparisons (0.05/3 doses)

³ criteria based on Galloway *et al.* (1997), section 2.9.2

Table 36. Chromosome aberrations induced in Chinese hamster ovary CHO-K1 cells exposed without metabolic activation to the 2-ring aromatic fraction of the diesel engine emission sample collected at 1000 rpm and 55 Nm (R 29+38)

Therefore, the 2-ring aromatic fractions of the fuel and two emission samples (3000 rpm/5 Nm, 1000 rpm/55 Nm), when tested in the CHO cell chromosome aberration system without S9, caused a dose related reduction in mitotic rate over a range of relatively low concentrations. There was, however, no corresponding statistically significant increase in the total number of aberrations for any of the three samples (Figure 53). The 2-ring aromatic fractions of diesel fuel and emission samples were therefore not clastogenic without metabolic activation at any of the concentrations assayed.

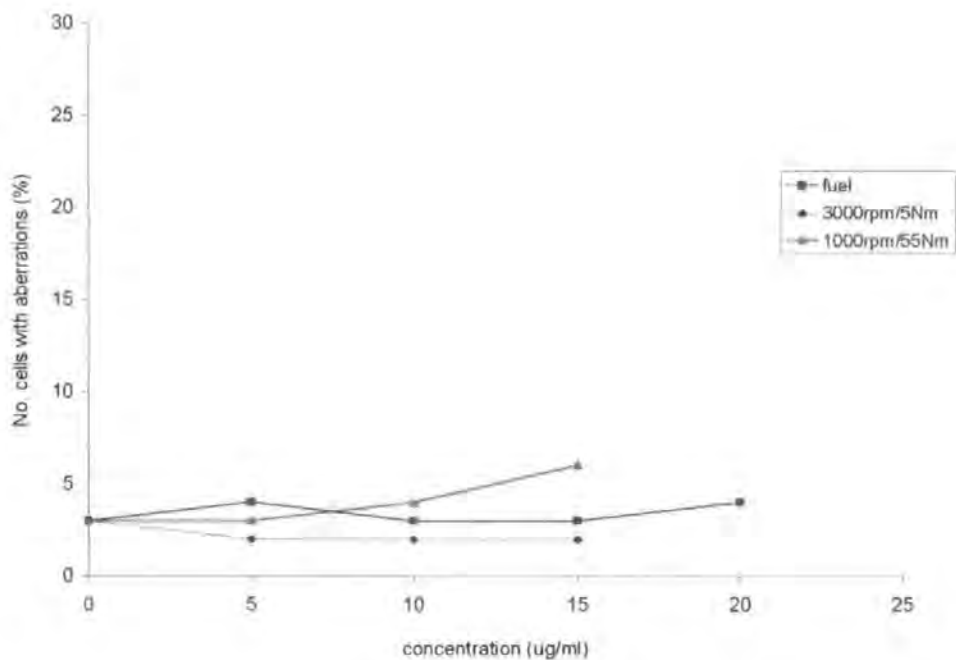


Figure 53. Summary of the percentage of cells with total aberrations induced in Chinese hamster ovary CHO-K1 cells after exposure without metabolic activation to 2-ring aromatic fractions of diesel fuel R 26 and diesel emission samples R 32 (3000 rpm/5 Nm), and R 38 (1000 rpm/55 Nm)

3.8.4.2 *The 2-ring aromatic fractions assayed with metabolic activation*

A dose related cytotoxic effect over the full range of concentrations assayed was not observed for any of the three 2-ring aromatic fraction samples when assayed with S9, although almost complete cell killing was achieved in each case at the highest concentration tested of 200 µg/ml. This made the effect of these fractions on cell viability more difficult to interpret and therefore the selection of doses for aberration testing less straightforward. The 2-ring fractions of the fuel (R26) and emission sample R 32 (3000 rpm/5 Nm) were tested in the chromosome aberration assay over a wider range at concentrations of 0, 25, 50, 100, 150, and 200 µg/ml. The reduction in cell viability for the second emission sample, R 29+38 (1000 rpm/55 Nm), was more marked and this sample was therefore tested at 0, 10, 20, 40, and 100 µg/ml. Full aberration and mitotic rate scores are given in Tables 72, 74, and 76, Appendix B.

A reduction in the mitotic index of the CHO cells with increasing concentration was observed for all three 2-ring samples with S9. The effect was slightly obscured by a low mitotic rate in the controls of 45/1000. For the fuel ring fraction there was an approximate 50 % reduction in mitotic rate at the highest concentration scored for aberrations (200 µg/ml, Figure 54). At this concentration, the mitotic rate for emission sample R 32 had fallen more sharply to 27 % of the control rate (Figure 55). For emission fraction R 29+38, the mitotic index was reduced to 59 % at 40 µg/ml, and to 17 % at 100 µg/ml (Figure 56).

For the first time, exposure of cells to emission sample fractions from different sources resulted in differing effects on the number of aberrations, and therefore clastogenicity. The number of chromosome aberrations in CHO-K1 cells exposed to the 2-ring fraction of diesel fuel increased with increasing fraction concentration when metabolic

activation was present (Figure 54). Aberrations rose from 2 % of cells in the solvent control, to 11 % at 25 µg/ml and finally to 14 % at 200 µg/ml. The increase in the number of aberrations from control levels was statistically significant ($P < 0.05$) at 25 and 50 µg/ml, and highly significant ($P < 0.01$) at 100 and 200 µg/ml (Table 37). As the 2-ring aromatic fraction of the fuel showed a statistically significant increase in aberrations at more than two concentrations when assayed with S9, this fraction met the criteria described in section 2.9.2 and was classified as clastogenic.

The amount and type of aberrations were recorded after exposure of emission fraction R 32 to CHO cells, to a maximum concentration of 150 µg/ml (Figure 55). The significant cytotoxic effect exhibited at 200 µg/ml precluded the scoring of this concentration for aberrations. The total percentage of cells with aberrations remained within the 5 % background rate at all concentrations, and there was thus no significant increase ($P > 0.05$) in the total number of cells with aberrations (Table 38). Therefore the 2-ring aromatic fraction of the emission sample collected at 3000 rpm and 5 Nm was not clastogenic when assayed with metabolic activation.

For the 2-ring fraction R 29+38 (1000 rpm/5 Nm) the mitotic rate at the highest concentration tested of 100 µg/ml was too low (7/1000) to make the scoring of aberrations informative. Chromosome aberrations were therefore scored at concentrations of 0, 10, 20, and 40 µg/ml. As can be seen in Figure 56, the number of aberrations rose above the 5 % background rate at each of the three concentrations tested, to 8, 11, and 9 % of cells with total aberrations. Although the increase in the number of aberrations was statistically significant ($P < 0.05$) at only one of the doses assayed, 20 µg/ml (Table 39), the fraction was classified as clastogenic as the percentage of cells with aberrations was increased above 10 % at this dose (Galloway *et al.*, 1997).

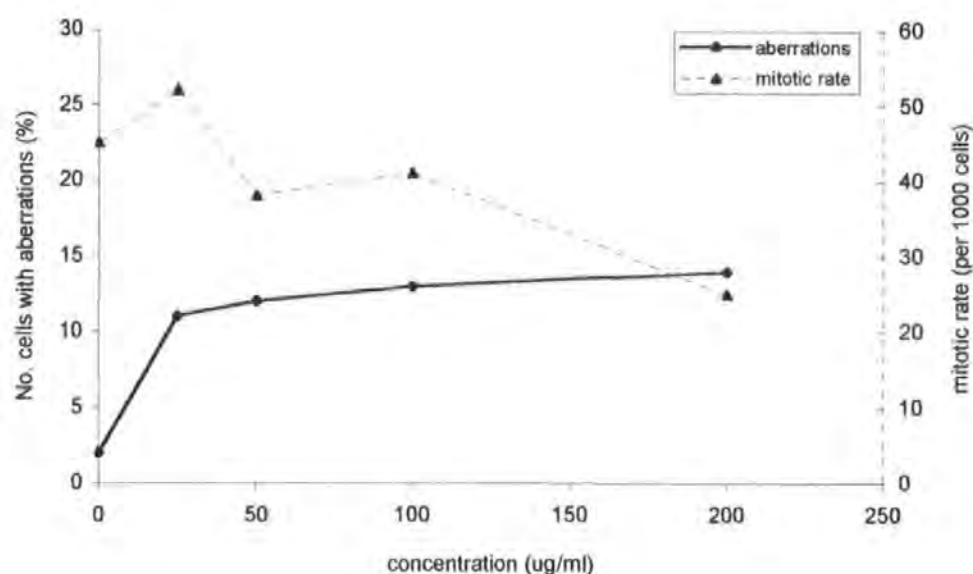


Figure 54. Mitotic rate and number of chromosome aberrations induced in Chinese hamster ovary CHO-K1 cells after exposure with metabolic activation (rat liver S9 fraction) to the 2-ring aromatic fraction of the diesel fuel (R 26)

concentration (µg/ml)	no. cells with total aberrations /cells scored	probability P^1	number of doses significant ($P \leq 0.0125$) ²	clastogenicity of sample ³
0	2/ 100			
25	11/ 100	5.240×10^{-3}		
50	12/ 100	2.845×10^{-3}		
100	13/ 100	1.525×10^{-3}		
200	14/ 100	8.404×10^{-4}		
			4	positive

¹ Fisher's exact test (Richardson *et al.*, 1990), comparison to DMSO control (concentration zero above)

² probability testing at 5 % significance level using Bonferroni correction for multiple dose comparisons (0.05/4 doses)

³ criteria based on Galloway *et al.* (1997), section 2.9.2

Table 37. Chromosome aberrations induced in Chinese hamster ovary CHO-K1 cells exposed with metabolic activation (rat liver S9 fraction) to the 2-ring aromatic fraction of the diesel fuel (R 26)

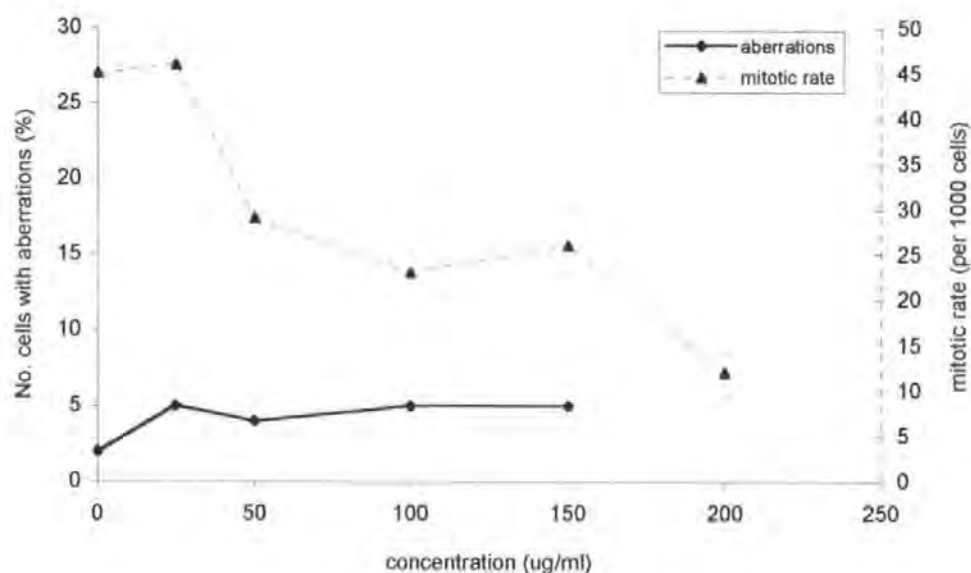


Figure 55. Mitotic rate and number of chromosome aberrations induced in Chinese hamster ovary CHO-K1 cells after exposure with metabolic activation (rat liver S9 fraction) to the 2-ring aromatic fraction of the diesel engine emission sample collected at 3000 rpm and 5 Nm (R 32)

concentration (µg/ml)	no. cells with total aberrations /cells scored	probability P^1	number of doses significant ($P \leq 0.0125$) ²	clastogenicity of sample ³
0	2/ 100			
25	5/ 100	0.141		
50	4/ 100	0.224		
100	5/ 100	0.141		
200	5/ 100	0.141		
			0	negative

¹ Fisher's exact test (Richardson *et al.*, 1990), comparison to DMSO control (concentration zero above)

² probability testing at 5 % significance level using Bonferroni correction for multiple dose comparisons (0.05/4 doses)

³ criteria based on Galloway *et al.* (1997), section 2.9.2

Table 38. Chromosome aberrations induced in Chinese hamster ovary CHO-K1 cells exposed with metabolic activation (rat liver S9 fraction) to the 2-ring aromatic fraction of the diesel engine emission collected at 3000 rpm and 5 Nm (R 32)

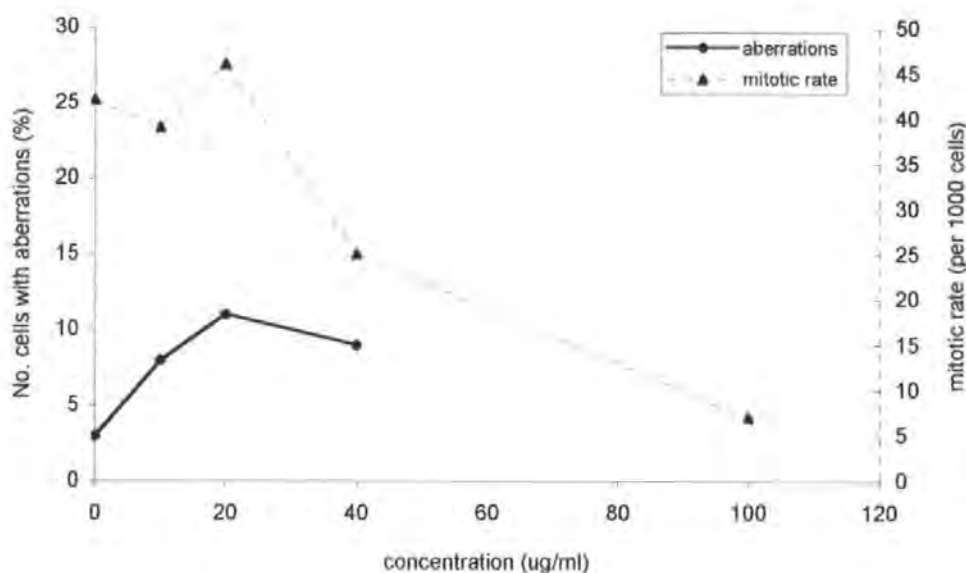


Figure 56. Mitotic rate and number of chromosome aberrations induced in Chinese hamster ovary CHO-K1 cells after exposure with metabolic activation (rat liver S9 fraction) to the 2-ring aromatic fraction of the diesel engine emission sample collected at 1000 rpm and 55 Nm (R 29+38)

concentration ($\mu\text{g/ml}$)	no. cells with total aberrations /cells scored	probability P^1	number of doses significant ($P \leq 0.0167$) ²	clastogenicity of sample ³
0	3/ 100			
10	8/ 100	0.0681		
20	11/ 100	0.0148		
40	9/ 100	0.0417		
				1 positive

¹ Fisher's exact test (Richardson *et al.*, 1990), comparison to DMSO control (concentration zero above)

² probability testing at 5 % significance level using Bonferroni correction for multiple dose comparisons (0.05/3 doses)

³ criteria based on Galloway *et al.* (1997), section 2.9.2

Table 39. Chromosome aberrations induced in Chinese hamster ovary CHO-K1 cells exposed with metabolic activation (rat liver S9 fraction) to the 2-ring aromatic fraction of the diesel engine emission collected at 1000 rpm and 55 Nm (R 29+38)

In the chromosome aberration assay with S9, the 2-ring aromatic fractions exhibited differing effects on the percentage of CHO cells with aberrations. Exposure to all three samples caused a dose-related fall in mitotic index, although the concentrations over which this decrease was exhibited varied between samples. The 2-ring aromatic fraction R 32 (3000 rpm/5 Nm) did not result in an increase of chromosome aberrations over normal spontaneous rates when assayed with S9. The second engine emission sample, R 29+38 (1000 rpm/55 Nm), was more cytotoxic and was therefore tested for effect on aberrations at lower concentrations. The total number of cells with aberrations was increased to a maximum of 11 %, which was statistically significant when compared to the solvent control. The 2-ring aromatic fraction of the diesel fuel (R 26), when exposed to the CHO cell system with S9, resulted in a statistically significant increase in the number of aberrations over controls at all concentrations tested (Figure 54). The 2-ring fraction of the diesel fuel and emission sample R 29+38 (1000 rpm/55 Nm) were therefore clastogenic in CHO-K1 cells in the presence of metabolic activation.

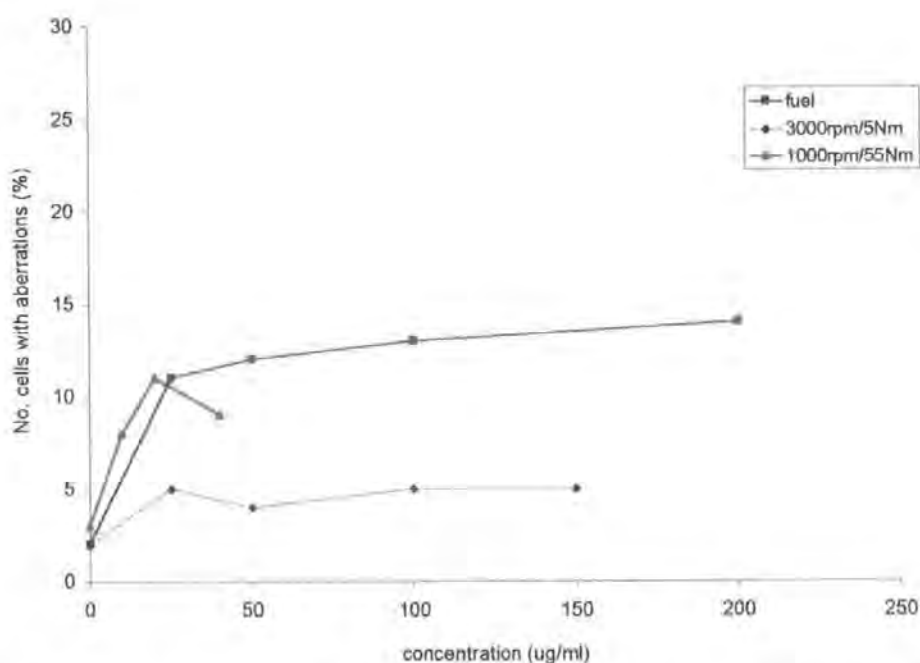


Figure 57. Summary of the percentage of cells with total aberrations induced in Chinese hamster ovary CHO-K1 cells after exposure with metabolic activation (rat liver S9 fraction) to the 2-ring aromatic fractions of diesel fuel R 26 and the diesel emission samples R 32 (3000 rpm/5 Nm) and R 29+38 (1000 rpm/55 Nm)

3.8.5 *The 3+ -ring aromatic fractions*

The diesel fuel and two emission samples (collected at 3000 rpm/5 Nm and 1000 rpm/55 Nm) were fractionated by HPLC to separate into different ring group fractions. The 3+ -ring fraction, containing a group of 3-ring and greater aromatic compounds, was then assayed for its mutagenicity in the chromosome aberration assay both with and without metabolic activation (results shown in Tables 77 to 80, Appendix B). The fractionation of the emission sample collected at 1000 rpm/55 Nm produced a very small sample of 3+ -ring group compounds. A second engine collection and fractionation produced more sample to give combined total mass of 3.2 mg. This was still insufficient to perform the full range of testing, and was reserved until the results of the other 3-ring assays were known. The sample was then exposed to CHO cells in the chromosome aberration assay with S9 at concentrations of 0, 25, 50, and 100 µg/ml. Assay of this fraction however produced poor chromosome preparations which were unfortunately unsuitable for aberration scoring, and there was insufficient sample for a repeat test to be performed. There are therefore no results presented for the 3+ -ring fraction of the engine emission sample collected at 1000 rpm and 55 Nm.

3.8.5.1 *The 3-ring aromatic fractions assayed without metabolic activation*

After initial cytotoxicity testing, the 3+ -ring fraction of the fuel R 27 and emission sample fraction R 33 (3000 rpm/5 Nm) were tested in the chromosome aberration assay without S9 at concentrations of 0, 5, 10, 20, and 40 µg/ml. The emission sample fraction R 33 was assayed additionally at 2.5 µg/ml. The mitotic index fell with increasing sample concentration for both 3+ -ring fractions (Figures 58 and 59). The reduction followed a similar pattern in both samples, with a mitotic index of around 39 % of controls at 20 µg/ml (the highest concentration scored for aberrations), and to less than 5 % at 40 µg/ml.

The fall in mitotic rate with increasing diesel fuel 3+ -ring fraction concentration is shown in Figure 58. Along with the reduction in mitotic rate, an increase in the number of aberrations can be seen. The total percentage of cells with chromosome aberrations was raised above the 5 % background rate (to 8 %) at the highest concentration scored of 20 µg/ml. This increase was not statistically significant ($P > 0.05$, Table 40), and occurred at a concentration which effected a greater than 50 % reduction in mitotic rate. Further separation of this fraction would be needed to fully assess clastogenicity, which may be masked here by cytotoxicity.

Exposure of the 3+ -ring fraction of emission sample R 33 (3000 rpm/5 Nm) to CHO cells resulted in a reduction in mitotic rate with increasing concentration, shown in Figure 59. Corresponding with this fall in mitotic index was an increase in the number of chromosome aberrations with increasing ring fraction concentration. The total percentage of cells with aberrations was raised above the spontaneous 5 % level at all concentrations scored for aberrations, to a maximum of 9 % of cells with aberrations. The increase in aberrations was not statistically significant at any dose when probabilities were corrected for multiple dose comparison ($P > 0.05$, Table 41). Prior to correction, however, the increase in aberrations to 9/100 at the highest dose of 20 µg/ml was significant ($P = 0.0417$). In addition, at the two lower doses assayed, the increase in aberrations gave a probability of close to 5 % ($P = 0.0681$ for both samples). The borderline increases in aberrations observed here for the 3+ -ring aromatic fraction of the diesel emission collected at 3000 rpm and 5 Nm indicates that further investigation into the clastogenicity of this sample is warranted.

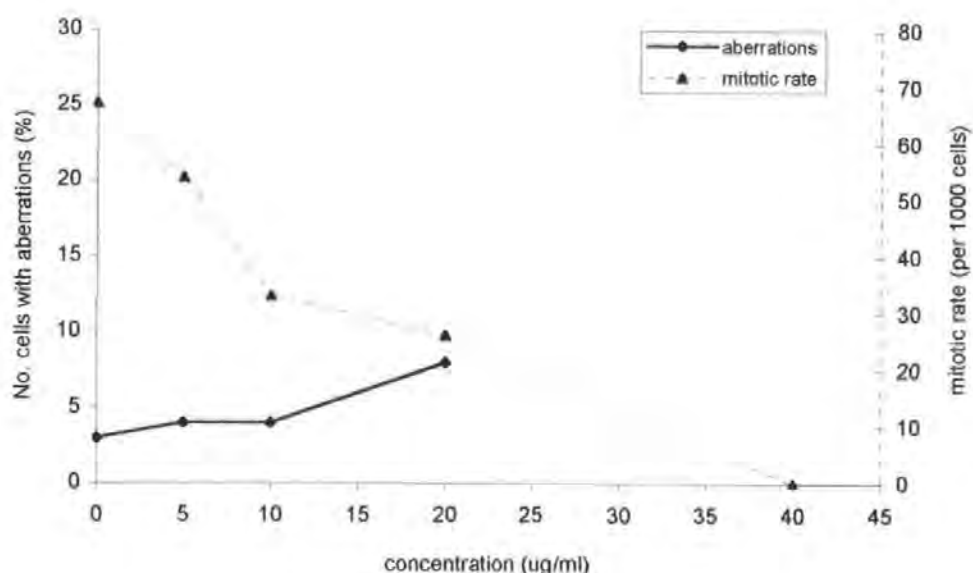


Figure 58. Mitotic rate and number of chromosome aberrations induced in Chinese hamster ovary CHO-K1 cells after exposure without metabolic activation to the 3+ -ring aromatic fraction of diesel fuel (R 27)

concentration ($\mu\text{g/ml}$)	no. cells with total aberrations /cells scored	probability P^1	number of doses significant ($P \leq 0.0167$) ²	clastogenicity of sample ³
0	3/ 100			
5	4/ 100	0,3610		
10	4/ 100	0.3610		
20	8/ 100	0.0681		
			0	negative

¹ Fisher's exact test (Richardson *et al.*, 1990), comparison to DMSO control (concentration zero above)

² probability testing at 5 % significance level using Bonferroni correction for multiple dose comparisons (0.05/3 doses)

³ criteria based on Galloway *et al.* (1997), section 2.9.2

Table 40. Chromosome aberrations induced in Chinese hamster ovary CHO-K1 cells exposed without metabolic activation to the 3+ -ring aromatic fraction of diesel fuel (R 27)

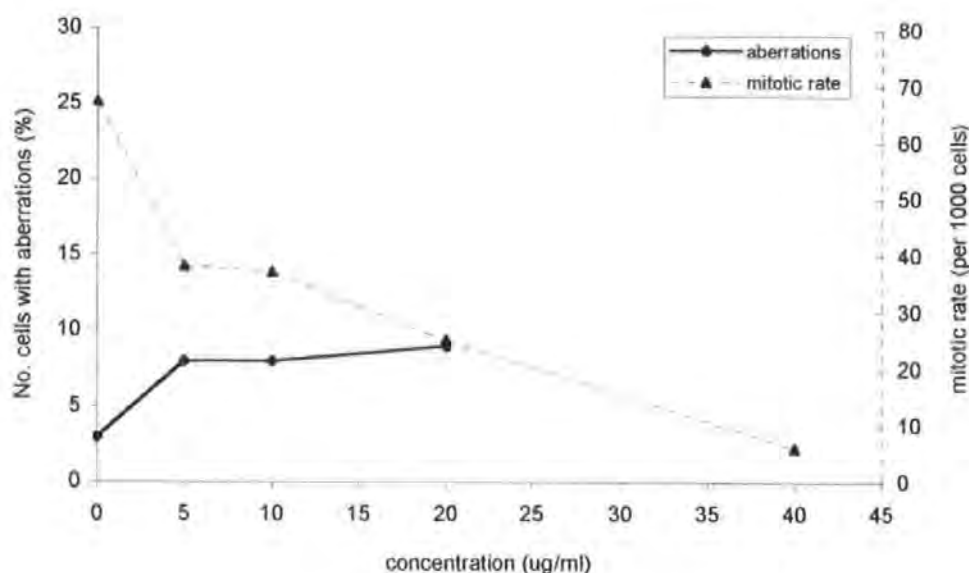


Figure 59. Mitotic rate and number of chromosome aberrations induced in Chinese hamster ovary CHO-K1 cells after exposure without metabolic activation to the 3+ -ring aromatic fraction of diesel engine emission sample collected at 3000 rpm and 5 Nm (R 33)

concentration ($\mu\text{g/ml}$)	no. cells with total aberrations /cells scored	probability P^1	number of doses significant ($P \leq 0.0167$) ²	clastogenicity of sample ³
0	3/ 100			
5	8/ 100	0.0681		
10	8/ 100	0.0681		
20	9/ 100	0.0417		
			0	negative

¹ Fisher's exact test (Richardson *et al.*, 1990), comparison to DMSO control (concentration zero above)

² probability testing at 5 % significance level using Bonferroni correction for multiple dose comparisons (0.05/3 doses)

³ criteria based on Galloway *et al.* (1997), section 2.9.2.

Table 41. Chromosome aberrations induced in Chinese hamster ovary CHO-K1 cells exposed without metabolic activation to the 3+ -ring aromatic fraction of the diesel engine emission sample collected at 3000 rpm and 5 Nm (R 33)

3.8.5.2 *The 3-ring aromatic fractions assayed with metabolic activation*

Initial cytotoxicity testing in the presence of metabolic activation for the 3+ -ring fraction of the fuel R 27 gave inconclusive results in the critical concentration range. The cytotoxicity results for emission sample fraction R 33 (3000 rpm/5 Nm) were less irregular, but to ensure aberration testing included concentrations that effected a 50 % reduction in cell viability, a wider range of concentrations was selected. The 3+ -ring fractions were therefore tested at concentrations of 0, 25, 50, 100, and 200 µg/ml in the presence of metabolic activation. The emission sample fraction was assayed additionally at 150 µg/ml.

Both the fuel and the emission sample 3+ -ring fractions effected a dose related reduction in mitotic index (Figures 60 and 61), although the low control mitotic rate made the effect less clear. For the fuel fraction R 27, the mitotic rate was reduced to 67 % of controls at 100 µg/ml, with no mitoses at all detectable at 200 µg/ml. The effect of the emission fraction on mitotic rate was more marked. The number of mitoses fell to 51 % at 100 µg/ml, with no detectable mitotic cells at either 150 or 200 µg/ml. Both samples were therefore scored for aberrations up to a concentration of 100 µg/ml.

With the fall in mitotic rate, a corresponding increase in the percentage of cells with aberrations was seen for the 3+ -ring fraction of the fuel with S9 (Figure 60). The total number of aberrations rose from 13 % of cells at 25 µg/ml, to 16 % at 50 µg/ml, and 21 % at 100 µg/ml. The increase to 13 % of cells with aberrations at 25 µg/ml was statistically significant when compared to the solvent control ($P < 0.05$, Table 42). At the highest concentrations assayed of 50 and 100 µg/ml, the rise in the number of aberrations over the solvent control was highly significant ($P < 0.01$). As there was a significant increase in the percentage of cells with aberrations at more than two doses, the 3+ -ring

fraction of the diesel fuel was classified as clastogenic in the presence of metabolic activation.

In a similar response to the fuel 3+ -ring fraction, the percentage of cells with aberrations after exposure to emission fraction R 33 (3000 rpm/5 Nm) with S9 was increased over control levels (Figure 61). The increase in the number of aberrations was dose related, from 9 % of cells with aberrations at 25 µg/ml to 20 % of cells with aberrations at 100 µg/ml. At the two higher concentrations assessed, 50 and 100 µg/ml, the increase in the number of aberrations over the solvent control was highly statistically significant ($P < 0.01$). As the 3+ -ring fraction R 33, when exposed to CHO cells in the presence of metabolic activation, resulted in a significant increase in the number of aberrations at two dose levels, this also was classified as an indirect-acting clastogen (Table 43).

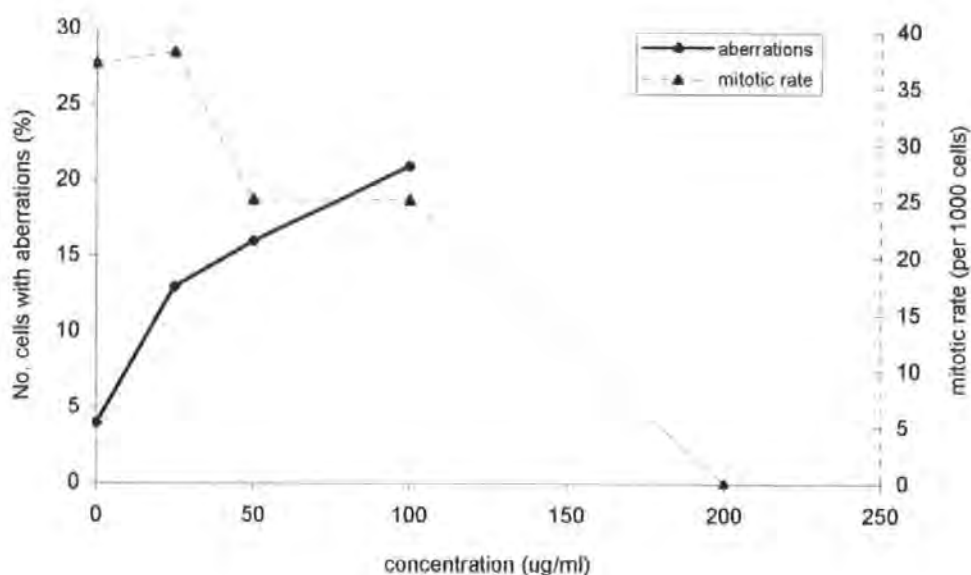


Figure 60. Mitotic rate and number of chromosome aberrations induced in Chinese hamster ovary CHO-K1 cells after exposure with metabolic activation (rat liver S9 fraction) to the 3+ -ring aromatic fraction of diesel fuel (R 27)

concentration (µg/ml)	no. cells with total aberrations /cells scored	probability P^1	number of doses significant ($P \leq 0.0167$) ²	clastogenicity of sample ³
0	4/ 100			
25	13/ 100	0.0123		
50	16/ 100	2.405×10^{-3}		
100	21/ 100	1.176×10^{-3}	3	positive

¹ Fisher's exact test (Richardson *et al.*, 1990), comparison to DMSO control (concentration zero above)

² probability testing at 5 % significance level using Bonferroni correction for multiple dose comparisons (0.05/3 doses)

³ criteria based on Galloway *et al.* (1997), section 2.9.2

Table 42. Chromosome aberrations induced in Chinese hamster ovary CHO-K1 cells exposed with metabolic activation (rat liver S9 fraction) to the 3+ -ring aromatic fraction of diesel fuel (R 27)

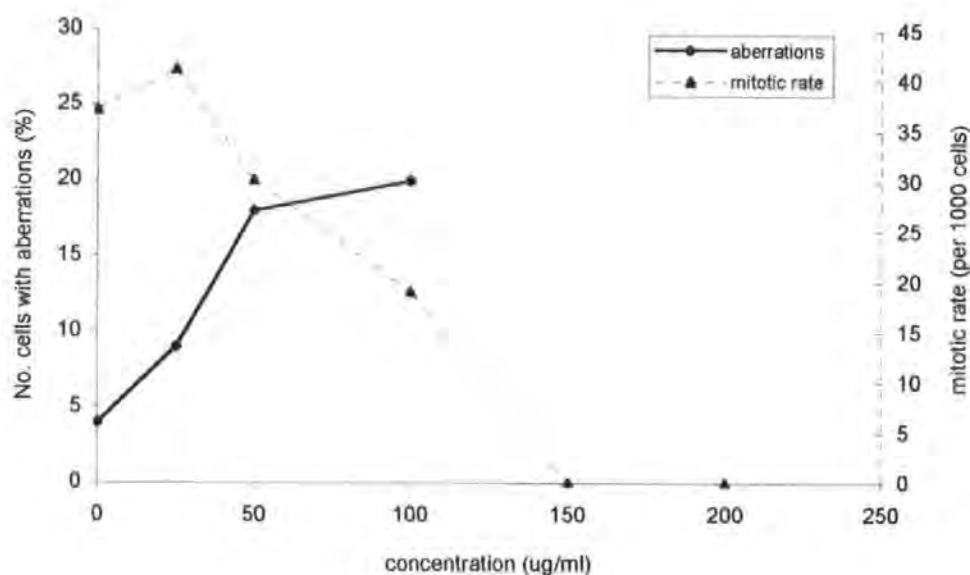


Figure 61. Mitotic rate and number of chromosome aberrations induced in Chinese hamster ovary CHO-K1 cells after exposure with metabolic activation (rat liver S9 fraction) to the 3+ -ring aromatic fraction of diesel engine emission sample collected at 3000 rpm and 5 Nm (R 33)

concentration ($\mu\text{g/ml}$)	no. cells with total aberrations /cells scored	probability P^1	number of doses significant ($P \leq 0.0167$)	clastogenicity of sample ³
0	4/ 100			
25	9/ 100	0.0830		
50	18/ 100	7.480×10^{-4}		
100	20/ 100	2.213×10^{-4}		
			2	positive

¹ Fisher's exact test (Richardson *et al.*, 1990), comparison to DMSO control

² probability testing at 5 % significance level using Bonferroni correction for multiple dose comparisons ($0.05/3$ doses)

³ criteria based on Galloway *et al.* (1997), section 2.9.2

Table 43. Chromosome aberrations induced in Chinese hamster ovary CHO-K1 cells exposed with metabolic activation (rat liver S9 fraction) to the 3+ -ring aromatic fraction of engine emission sample collected at 3000 rpm and 5 Nm (R 33)

3.8.5.3 Summary of the 3+ -ring fractions

Without metabolic activation, exposure of CHO cells to the 3+ -ring fractions of the fuel and R 33 (3000 rpm/5 Nm) did not result in a statistically significant increase in aberration levels over the solvent control. The percentage of cells with aberrations was raised above the background rate for one concentration of the fuel 3+ -ring fraction (20 µg/ml), and for all three concentrations scored for the emission sample 3+ -ring fraction. The high level of toxicity of these two fractions may be masking a mutagenic effect. When the 3+ -ring fractions of the fuel and the emission sample collected at 3000 rpm/5 Nm were assayed in the presence of S9, they resulted in a highly significant increase in the total number of aberrations at 2 or more doses. Both of these 3+ -ring fractions are therefore clastogenic in CHO-K1 cells with metabolic activation. The aberration results are summarised in Figure 62, below.

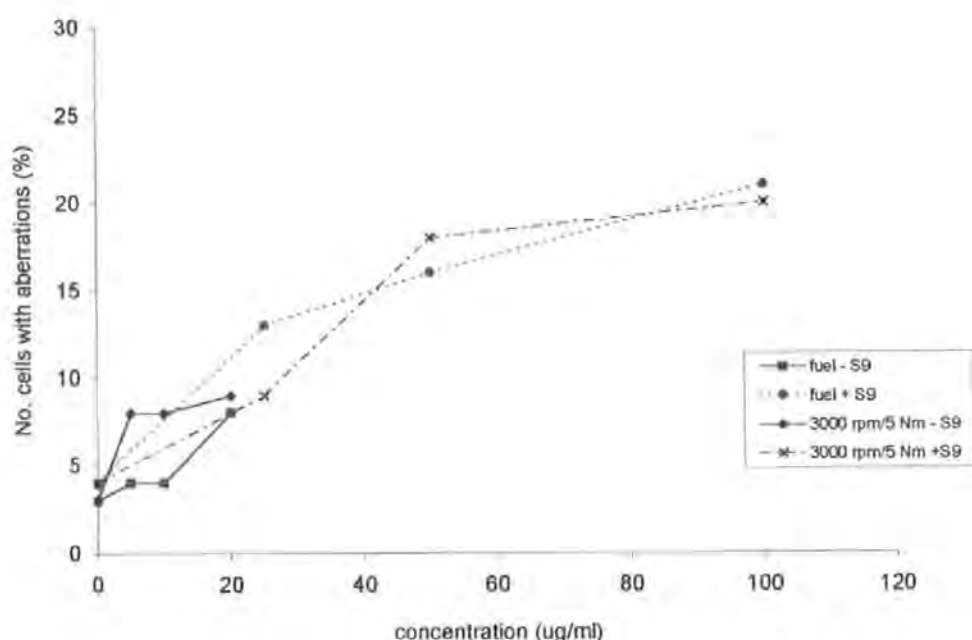


Figure 62. Summary of the chromosome aberrations induced in Chinese hamster ovary CHO-K1 cells after exposure without, and with, metabolic activation (rat liver S9 fraction) to the 3+ -ring fractions of diesel fuel (R27) and the engine emission sample collected at 3000 rpm and 5 Nm (R 33)

3.8.6 *The polar fractions*

The polar fractions of seven emission samples were assayed for their mutagenicity in the chromosome aberrations assay. Fractionation of the fuel did not produce a polar fraction of any significance, which corresponded with the composition data provided by the fuel suppliers. The polar fractions of the first three engine emission samples, ES 39+42 (3000 rpm /5 Nm), ES 45+48 (1000 rpm/55 Nm) and ES 51+54 (1000 rpm/5 Nm) were assayed both with and without metabolic activation (results shown in Tables 81 to 92, Appendix B).

Following the method of Galloway *et al.* (1987), one hundred metaphase cells from each dose were normally scored for the presence of aberrations during this study. To confirm the positive results exhibited, and to assess the conformity between replicate cultures, one hundred cells were scored from each of two replicate cultures for the three polar emission fractions described above. Homogeneity between replicate cultures was tested using the binomial dispersion test (section 2.9.1, Richardson *et al.*, 1990). No evidence of heterogeneity was found (results shown in Tables 82, 84, 86, 88, 90, and 92, Appendix B) and therefore the aberration data from replicates were combined prior to significance testing using Fisher's exact test. From the final series of engine runs, the polar fractions of four emission samples collected at 2000 rpm/30 Nm (ES 107), 2000 rpm /55 Nm (ES 116), 3000 rpm/30 Nm (ES 119) and 3000 rpm/ 55 Nm (ES 125) were assayed for their effect on chromosome aberrations in the absence of metabolic activation only (Tables 93 to 96, Appendix B).

3.8.6.1 The polar fractions collected during June 1996, assayed without metabolic activation

Polar emission fractions from a total of seven different engine emission samples were assayed for their mutagenicity in the chromosome aberration assay without S9. During cytotoxicity assays (section 3.7.6), almost matched effects on cell viability were exhibited by each of the polar fractions. Therefore all of the fractions were assayed for aberrations at concentrations of 5, 10, 20, and 30 µg/ml. An additional concentration of 1 µg/ml was included in the first series of testing, and was analysed for one sample only (ES 51+54, 1000 rpm/5 Nm).

When tested in the CHO cell chromosome aberration assay, the polar fraction ES 39+42 (3000 rpm/5 Nm) exhibited a concentration dependant reduction in mitotic rate (Figure 63). The number of mitoses fell from average 53.5/1000 in the solvent controls to 23.5/1000 at 30 µg/ml polar fraction concentration, the highest dose tested (a decrease in mitotic rate of approximately 44 %). At 5 and 10 µg/ml, there was no increase in the percentage of cells with aberrations over the expected background rate of 5 %. At 20 µg/ml fraction concentration, there was a sharp increase in the number of aberrations to 19 %, with a further increase at 30 µg/ml to mean 25 %. At both these concentrations, the increase in the number of aberrations over control levels was highly significant ($P < 0.01$, Table 44). With two positive doses, the polar fraction of the engine emission collected at 3000 rpm and 5 Nm was classified as clastogenic without S9, and therefore as a direct acting clastogen.

Over the range of concentrations tested, the polar fraction ES 45+48 (1000 rpm/55 Nm) effected a dose dependant reduction in mitotic index, to around 32 % of the control level at 30 µg/ml (Figure 64). The number of chromosome aberrations found in cells after

exposure to this polar fraction remained below 5 % at doses of 5 and 10 µg/ml, and thus they were not different statistically from the solvent control. Once the concentration was increased to 20 µg/ml, the number of aberrations rose significantly to 26/ 200, with a further increase at 30 µg/ml to 43/ 200 - a dose related increase in the number of aberrations. At both the higher doses, the increase in the number of aberrations over control levels was highly significant ($P < 0.01$, Table 45). The polar fraction of the diesel engine emission collected at 1000 rpm and 55 Nm was therefore clastogenic in the *in vitro* chromosome aberration assay without metabolic activation.

The mitotic index of the CHO cells fell with increasing polar fraction concentration, after exposure of ES 51+54 (1000 rpm/5 Nm). Whilst a similar response to polar fractions ES 39+42 and ES 45+48, the reduction in the number of mitoses in this case was more marked. The mitotic rate at 20 µg/ml was reduced to 34 % of the control rates, and to only 15 % at 30 µg/ml (Figure 65). A dose related increase in the percentage of cells with chromosome aberrations was exhibited over the full range of concentrations tested with ES 51. At concentrations of 1, 5, and 10 µg/ml, the number of aberrations was increased above the 5 % expected spontaneous rate, to a maximum of 8.5 % of cells with aberrations. These increases were not, however, statistically significant when compared to the solvent controls ($P > 0.05$, Table 46). Increases in the percentage of cells with aberrations were higher at 20 µg/ml (to 19 % of cells) and at 30 µg/ml (to mean 26.5 % of cells). At these higher concentrations the increase in the numbers of aberrations was highly significant ($P < 0.01$) in both cases compared to controls. The polar fraction of the engine emission sample collected at 1000 rpm and 5 Nm was therefore clastogenic to CHO-K1 cells without metabolic activation.

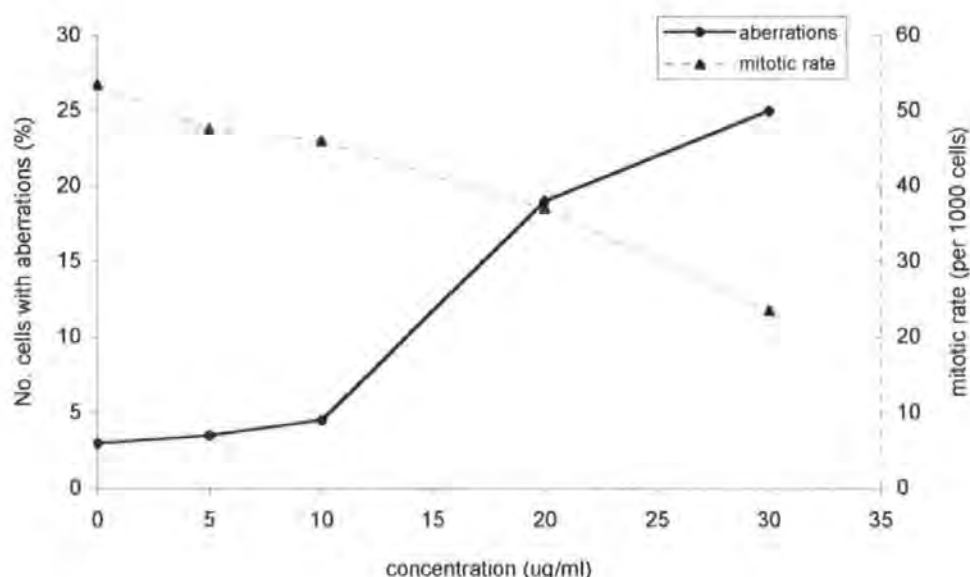


Figure 63. Mitotic rate and number of chromosome aberrations induced in Chinese hamster ovary CHO-K1 cells after exposure without metabolic activation to the polar fraction of the diesel engine emission sample collected at 3000 rpm and 5 Nm (ES 39+42)

concentration ($\mu\text{g/ml}$)	no. cells with total aberrations /cells scored	probability P^1	number of doses significant ($P \leq 0.0125$) ²	clastogenicity of sample ³
0	6/ 200			
5	7/ 200	0.394		
10	9/ 200	0.223		
20	38/ 200	6.495×10^{-8}		
30	50/ 200	1.742×10^{-11}		
			2	positive

¹ Fisher's exact test (Richardson *et al.*, 1990), comparison to DMSO control (concentration zero above)

² probability testing at 5 % significance level using Bonferroni correction for multiple dose comparisons (0.05/4 doses)

³ criteria based on Galloway *et al.* (1997), section 2.9.2

Table 44. Chromosome aberrations induced in Chinese hamster ovary CHO-K1 cells exposed without metabolic activation to the polar fraction of diesel engine emission sample collected at 3000 rpm and 5 Nm (ES 39+42)

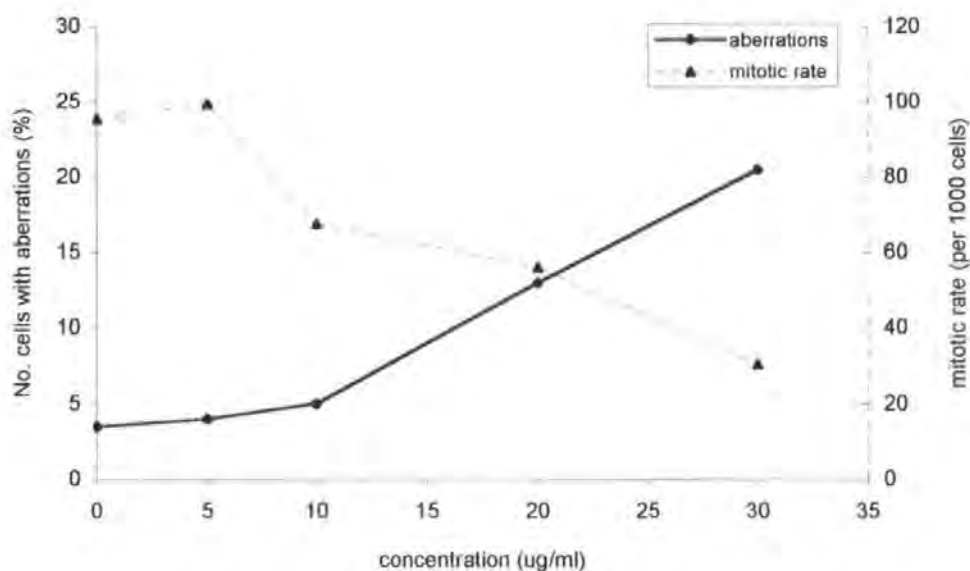


Figure 64. Mitotic rate and number of chromosome aberrations induced in Chinese hamster ovary CHO-K1 cells after exposure without metabolic activation to the polar fraction of the diesel engine emission sample collected at 1000 rpm and 55 Nm (ES 45+48)

concentration ($\mu\text{g/ml}$)	no. cells with total aberrations /cells scored	probability P^1	number of doses significant ($P \leq 0.0125$) ²	clastogenicity of sample ³
0	7/ 200			
5	8/ 200	0.400		
10	10/ 200	0.236		
20	26/ 200	2.493×10^{-4}		
30	41/ 200	3.535×10^{-7}		
			2	positive

¹ Fisher's exact test (Richardson *et al.*, 1990), comparison to DMSO control (concentration zero above)

² probability testing at 5 % significance level using Bonferroni correction for multiple dose comparisons (0.05/4 doses)

³ criteria based on Galloway *et al.* (1997), section 2.9.2

Table 45. Chromosome aberrations induced in Chinese hamster ovary CHO-K1 cells exposed without metabolic activation to the polar fraction of diesel engine emission sample collected at 1000 rpm and 55 Nm (ES 45+48)

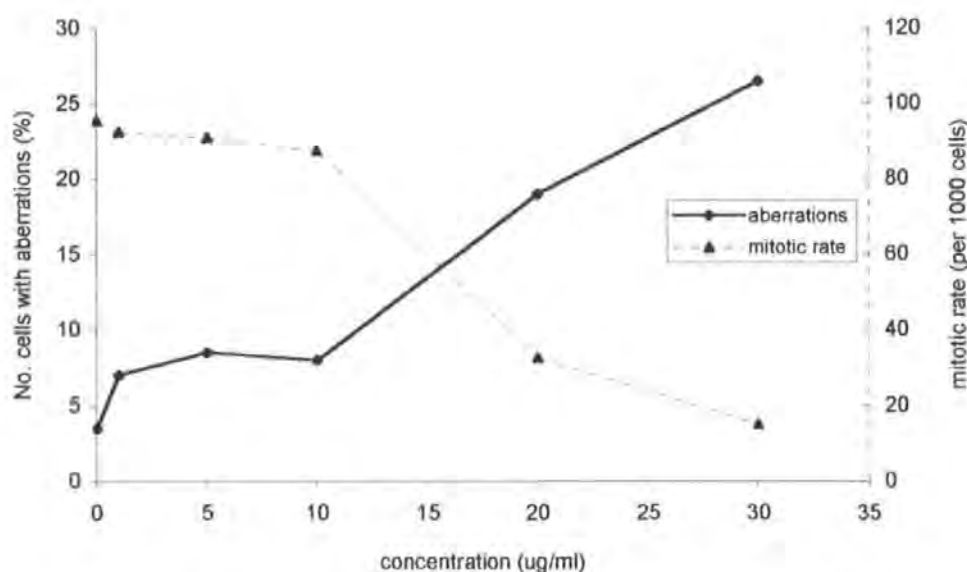


Figure 65. Mitotic rate and number of chromosome aberrations induced in Chinese hamster ovary CHO-K1 cells after exposure without metabolic activation to the polar fraction of the diesel engine emission sample collected at 1000 rpm and 5 Nm (ES 51+54)

concentration ($\mu\text{g/ml}$)	no. cells with total aberrations /cells scored	probability P^1	number of doses significant ($P \leq 0.01$) ²	clastogenicity of sample ³
0	7/ 200			
1	14/ 200	0.062		
5	17/ 200	0.019		
10	16/ 200	0.028		
20	38/ 200	2.376×10^{-7}		
30	53/ 200	9.814×10^{-12}		
			2	positive

¹ Fisher's exact test (Richardson *et al.*, 1990), comparison to DMSO control (concentration zero above)

² probability testing at 5 % significance level using Bonferroni correction for multiple dose comparisons (0.05/4 doses)

³ criteria based on Galloway *et al.* (1997), section 2.9.2

Table 46. Chromosome aberrations induced in Chinese hamster ovary CHO-K1 cells exposed without metabolic activation to the polar fraction of engine emission sample collected at 1000 rpm and 5 Nm (ES 51+54)

3.8.6.2 *The polar fractions collected during January 1997, assayed without metabolic activation*

After exposure to the polar fraction ES 107 (2000 rpm/30 Nm), the mitotic rate of cells was unchanged at the lower concentrations (Figure 66). A reduction in mitotic rate was evidenced at the higher concentrations of 20 and 30 µg/ml (to approximately 50 % of the control rate). The percentage of cells with total chromosome aberrations rose steadily with increasing polar fraction concentration, from total 1 aberration at 5 µg/ml, to a significant 8 aberrations at 10 µg/ml ($P < 0.05$), 20 aberrations at 20 µg/ml, and finally 24 aberrations at 30 µg/ml (both highly significant, $P < 0.01$, Table 47). With three positive doses, the polar fraction ES 107 (2000 rpm/30 Nm) was clearly clastogenic without metabolic activation.

The effect of the polar sample ES 116 (2000 rpm/55 Nm) on mitotic rate was similar to the previous polar sample, ES 107, with a near control rate until 10 µg/ml and then a dose related fall at subsequent concentrations. The reduction at the highest concentration was, however, less marked, being 69 % of the control mitotic index. The number of chromosome aberrations increased steadily with increasing fraction concentration (Figure 67). At 5 and 10 µg/ml, the percentage of cells with aberrations was not significantly increased from the background level. At the higher concentrations, the polar fraction has a clear mutagenic effect, with the percentage of cells with total aberrations increased to 18 at 20 µg/ml and 21 at 30 µg/ml. The increase in the number of aberrations at both of these doses was highly significant ($P < 0.01$) when compared to controls (Table 48). With two significant doses, the polar fraction ES 116 (2000 rpm/55 Nm) was classified as clastogenic in CHO-K1 cells without metabolic activation.

After exposure to the polar fraction ES 119 (from emission sample collected at 3000 rpm and 30 Nm), the mitotic rate in CHO cells was largely unaffected at 5 and 10

$\mu\text{g/ml}$ (Figure 68). At higher concentrations, the mitotic index was reduced by the polar fraction in a dose dependant manner. At the highest concentration assayed, the mitotic rate was 41 % of that recorded in the control. The percentage of cells with chromosome aberrations rose steadily from within spontaneous rates at 5 $\mu\text{g/ml}$, to 10 % of cells with aberrations at 10 $\mu\text{g/ml}$ (not statistically significant, $P > 0.05$). At 20 $\mu\text{g/ml}$ and 30 $\mu\text{g/ml}$ the percentage of cells with aberrations was 17 and 24 % respectively, both of which were highly significant ($P < 0.01$) compared to the control (Table 49). The polar fraction of the engine emission collected at 3000 rpm and 30 Nm, when assayed without S9, was therefore clastogenic.

In the polar fraction of the engine emission collected at 3000 rpm and 55 Nm (the most extreme polar fraction assayed in terms of engine conditions) the effect on cultured CHO cells in terms of mitotic rate was more clearly dose dependant than for other polar fractions, with a fall in mitotic index from the lowest concentration tested (Figure 69). In similarity with other polar fractions, the effect on dividing cells was more severe at the higher concentrations tested, leading to a mitotic rate that was 44 % of the control rate at 30 $\mu\text{g/ml}$. The effect of polar fraction ES 125 exposure on chromosome aberrations was comparable to previous polar fractions. No effect could be detected at 5 $\mu\text{g/ml}$, a slight but non-significant effect at 10 $\mu\text{g/ml}$, and then highly significant increases ($P < 0.01$) in the percentage of cells with chromosome aberrations at 20 and 30 $\mu\text{g/ml}$ (Table 50). The total number of aberrations detected at the highest concentration was 29, which were found in 23 % of cells overall. The polar fraction ES 125 was therefore clastogenic without metabolic activation.

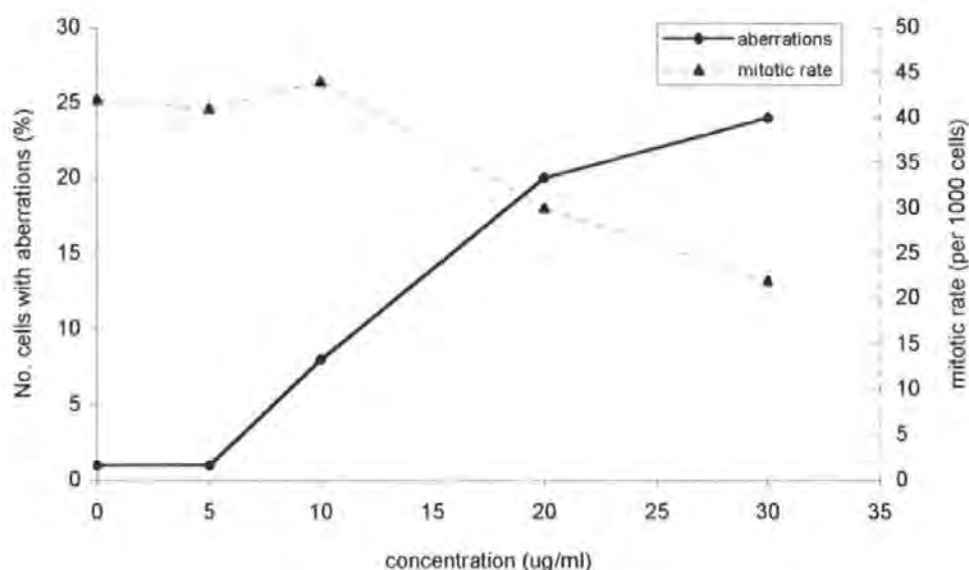


Figure 66. Mitotic rate and number of chromosome aberrations induced in Chinese hamster ovary CHO-K1 cells after exposure without metabolic activation to the polar fraction of the diesel engine emission sample collected at 2000 rpm and 30 Nm (ES 107)

concentration ($\mu\text{g/ml}$)	no. cells with total aberrations /cells scored	probability P^1	number of doses significant ($P \leq 0.0125$) ²	Clastogenicity of sample ³
0	1/ 100			
5	1/ 100	0.501		
10	8/ 100	9.510×10^{-3}		
20	20/ 100	2.085×10^{-6}		
30	24/ 100	9.358×10^{-8}		
			3	positive

¹ Fisher's exact test (Richardson *et al.*, 1990), comparison to DMSO control (concentration zero above)

² probability testing at 5 % significance level using Bonferroni correction for multiple dose comparisons (0.05/4 doses)

³ criteria based on Galloway *et al.* (1997), section 2.9.2

Table 47. Chromosome aberrations induced in Chinese hamster ovary CHO-K1 cells exposed without metabolic activation to the polar fraction of the diesel engine emission sample collected at 2000 rpm and 30 Nm (ES 107)

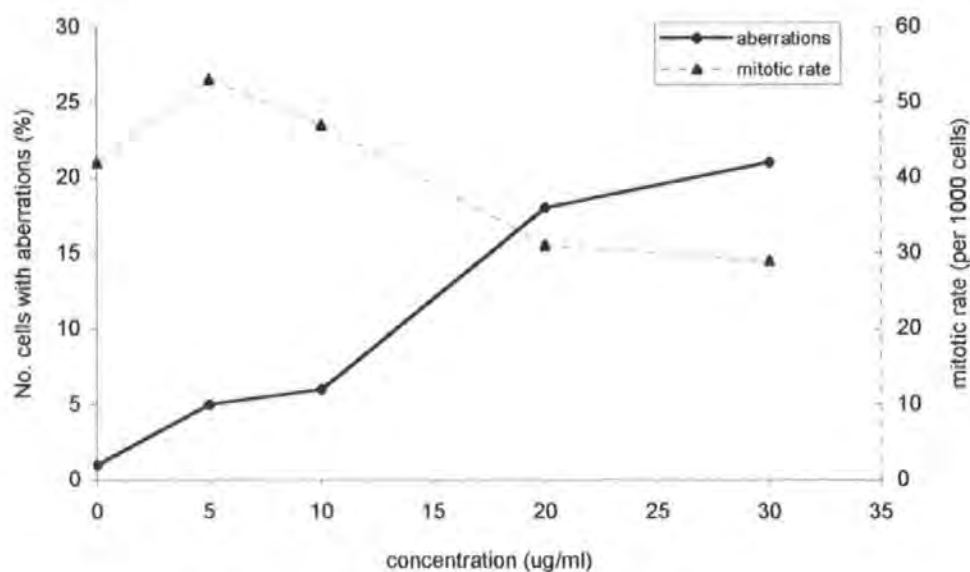


Figure 67. Mitotic rate and number of chromosome aberrations induced in Chinese hamster ovary CHO-K1 cells after exposure without metabolic activation to the polar fraction of the diesel engine emission sample collected at 2000 rpm and 55 Nm (ES 116)

concentration (µg/ml)	no. cells with total aberrations /cells scored	probability P^1	number of doses significant ($P \leq 0.0125$) ²	clastogenicity of sample ³
0	1/ 100			
5	5/ 100	0.061		
10	6/ 100	0.033		
20	18/ 100	9.341×10^{-6}		
30	21/ 100	9.726×10^{-7}		
			2	positive

¹ Fisher's exact test (Richardson *et al.*, 1990), comparison to DMSO control (concentration zero above)

² probability testing at 5 % significance level using Bonferroni correction for multiple dose comparisons (0.05/4 doses)

³ criteria based on Galloway *et al.* (1997), section 2.9.2

Table 48. Chromosome aberrations induced in Chinese hamster ovary CHO-K1 cells exposed without metabolic activation to the polar fraction of the diesel engine emission sample collected at 2000 rpm and 55 Nm (ES 116)

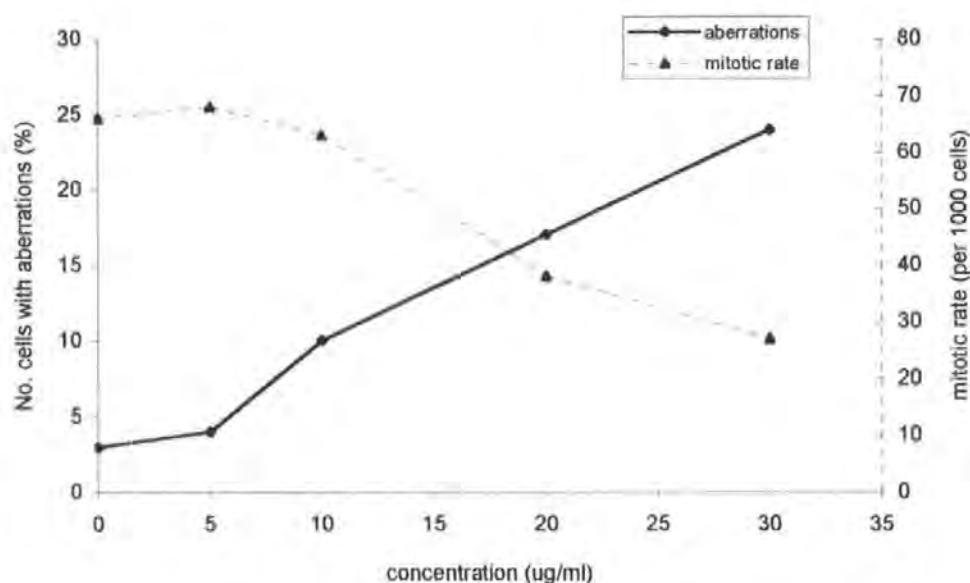


Figure 68. Mitotic rate and number of chromosome aberrations induced in Chinese hamster ovary CHO-K1 cells after exposure without metabolic activation to the polar fraction of the diesel engine emission sample collected at 3000 rpm and 30 Nm (ES 119)

concentration ($\mu\text{g/ml}$)	no. cells with total aberrations /cells scored	probability P^1	number of doses significant ($P \leq 0.0125$) ²	clastogenicity of sample ³
0	3/ 100			
5	4/ 100	0.361		
10	10/ 100	0.025		
20	17/ 100	4.358×10^{-4}		
30	24/ 100	3.937×10^{-6}	2	positive

¹ Fisher's exact test (Richardson *et al.*, 1990), comparison to DMSO control (concentration zero above)

² probability testing at 5 % significance level using Bonferroni correction for multiple dose comparisons (0.05/4 doses)

³ criteria based on Galloway *et al.* (1997), section 2.9.2

Table 49. Chromosome aberrations induced in Chinese hamster ovary CHO-K1 cells exposed without metabolic activation to the polar fraction of the diesel engine emission sample collected at 3000 rpm and 30 Nm (ES 119)

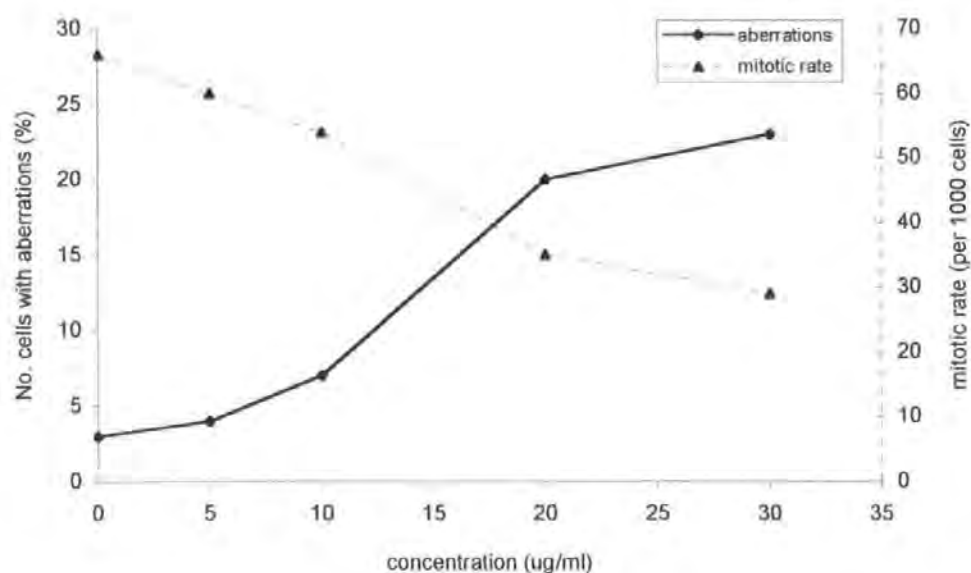


Figure 69. Mitotic rate and number of chromosome aberrations induced in Chinese hamster ovary CHO-K1 cells after exposure without metabolic activation to the polar fraction of the engine emission sample collected at 3000 rpm and 55 Nm (ES 125)

concentration ($\mu\text{g/ml}$)	no. cells with total aberrations /cells scored	probability p^1	number of doses significant ($P \leq 0.0125$) ²	clastogenicity of sample ³
0	3/ 100			
5	4/ 100	0.361		
10	7/ 100	0.108		
20	20/ 100	6.224×10^{-5}		
30	23/ 100	7.990×10^{-6}		
			2	positive

¹ Fisher's exact test (Richardson *et al.*, 1990), comparison to DMSO control (concentration zero above)

² probability testing at 5 % significance level using Bonferroni correction for multiple dose comparisons (0.05/4 doses)

³ criteria based on Galloway *et al.* (1997), section 2.9.2

Table 50. Chromosome aberrations induced in Chinese hamster ovary CHO-K1 cells exposed without metabolic activation to the polar fraction of the diesel engine emission sample collected at 3000 rpm and 55 Nm (ES 125)

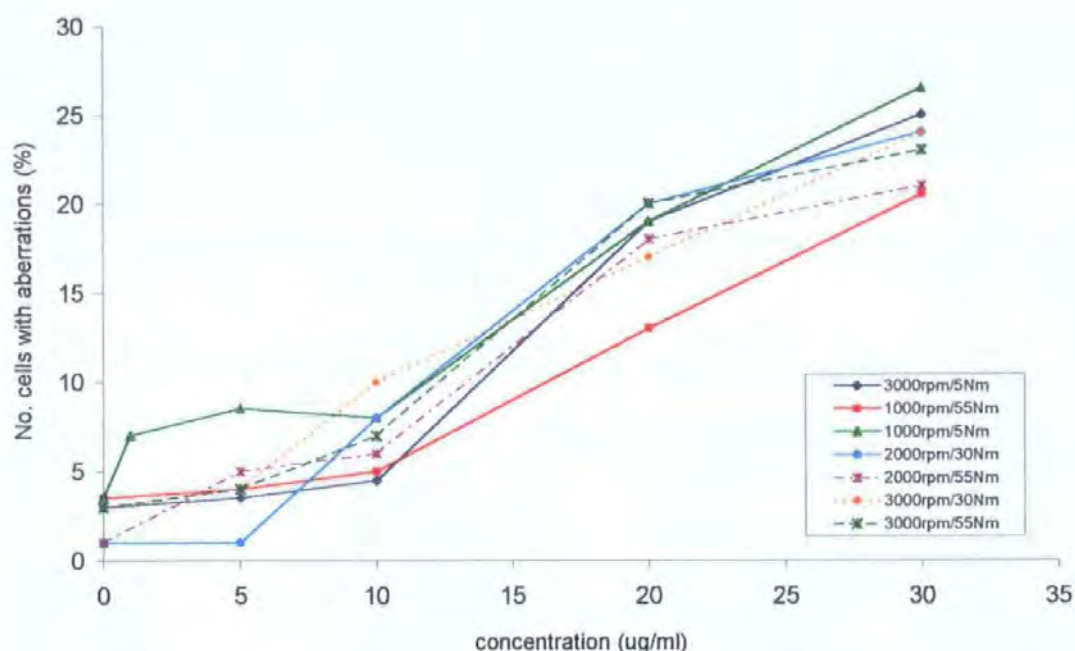


Figure 70. Number of chromosome aberrations induced in Chinese hamster ovary CHO-K1 cells after exposure without metabolic activation to the polar fractions of seven engine emission samples collected over a range of engine conditions of speed and load

To summarise, all seven polar fractions from engine runs at different speeds and loads were assayed for their direct-acting mutagenicity in the chromosome aberration assay. The effect on mitotic rate followed a similar pattern for each fraction. There was little or no reduction in mitotic index at the lower concentrations, followed by a sharper fall at the higher concentrations. At 30 $\mu\text{g/ml}$, the mitotic index averaged 43 % of the control mitotic index, although within this were two extremes – 16 % of control for polar fraction ES 51+54 (1000 rpm/5 Nm) and 69 % of control for ES 116 (2000 rpm/55 Nm). The effect of exposure to the polar fractions on the percentage of cells with chromosome aberrations is shown in Figure 70, above. The traces for fractions from engine emissions collected at widely differing conditions of speed and load are very similar to each other in most cases. At the highest concentration assayed, a slightly greater number of aberrations were observed after exposure to fractions from emission samples collected at low engine load (5 Nm). The only outlying curve is that for ES 45+48 (1000 rpm/55 Nm), which appears to exhibit a marginally less mutagenic effect than the other fractions.

3.8.6.3 The polar fractions assayed with metabolic activation

The polar fraction of the three total emission samples collected during the engine run series of June 1996 were assayed for mutagenicity in the chromosome aberration assay with rat liver S9. Cytotoxicity assays in the presence of metabolic activation showed each fraction to have an inconsistent effect on cell viability. The fractions were therefore assayed for aberrations over a wider range of concentrations: 25, 50, 100, and 150 µg/ml. Because of a small initial sample mass, fraction ES 51+54 (from the emission sample collected at 1000 rpm and 5 Nm) was assayed to a maximum concentration of 100 µg/ml only.

There was no effect on mitotic rate of the cultured cells after exposure to the polar fraction ES 39+42 (3000 rpm/5 Nm) with S9 at 25 µg/ml. At subsequent higher doses, the mitotic rate fell in a dose dependant manner, to 54 % of the control mitotic index at the highest concentration of 150 µg/ml (Figure 71). The number of chromosome aberrations scored was within normal spontaneous rates at concentrations of 25 and 50 µg/ml (and therefore non-significant, $P > 0.05$). At 100 µg/ml the total number of aberrations rose to 23 (from 200 metaphases), and a further increase to 36 (again from 200 metaphases) was seen at 150 µg/ml (Figure 3.7.14). The corresponding increase in the percentage of cells with aberrations was highly significant ($P < 0.01$) at both higher doses when compared to controls (Table 51). The polar fraction of ES 39+42 was therefore designated as clastogenic in the *in vitro* chromosome aberration assay with metabolic activation.

There was a gradual fall in mitotic rate in cultures exposed to polar fraction ES 45+48 (1000 rpm/55 Nm) with increasing fraction dose in the presence of S9. At the highest dose of 150 µg/ml, the mitotic index of treated cells was reduced to 49 % of the control rate (Figure 72). The number of chromosome aberrations scored after exposure to polar fraction ES 45+48 rose above background levels from 16 in 200 cells at concentration 100 µg/ml to 26 in 200 cells at 150 µg/ml. The increases in the percentage

of cells with aberrations were statistically significant at 100 µg/ml ($P < 0.05$), and highly significant at 150 µg/ml ($P < 0.01$). With two clear positive dose levels (Table 52), the polar fraction of the engine emission collected at 1000 rpm and 55 Nm was classified as clastogenic when assayed in the presence of metabolic activation.

A dose dependant reduction in mitotic index was observed in cultures exposed to the polar fraction ES 51+54 (1000 rpm/5 Nm) from a concentration of 50 µg/ml in the presence of S9. At 100 µg/ml, the highest concentration assayed, the number of mitoses had fallen to 50 % of the control level (Figure 73). The number of chromosome aberrations was increased to 29 out of 200 cells at 100 µg/ml, a highly significant increase over the control level ($P < 0.01$, Table 53). At lower concentrations assayed, the number of aberrations remained within expected background values, with no significant increases. Although this polar fraction was positive at only one concentration, as the percentage of cells with total aberrations was increased above 10 %, it was classified as clastogenic. The testing at a higher concentration was not possible because of restricted sample mass available. Repeat engine sampling and fractionation rounds would enable testing at higher concentrations to provide a more conclusive data set.

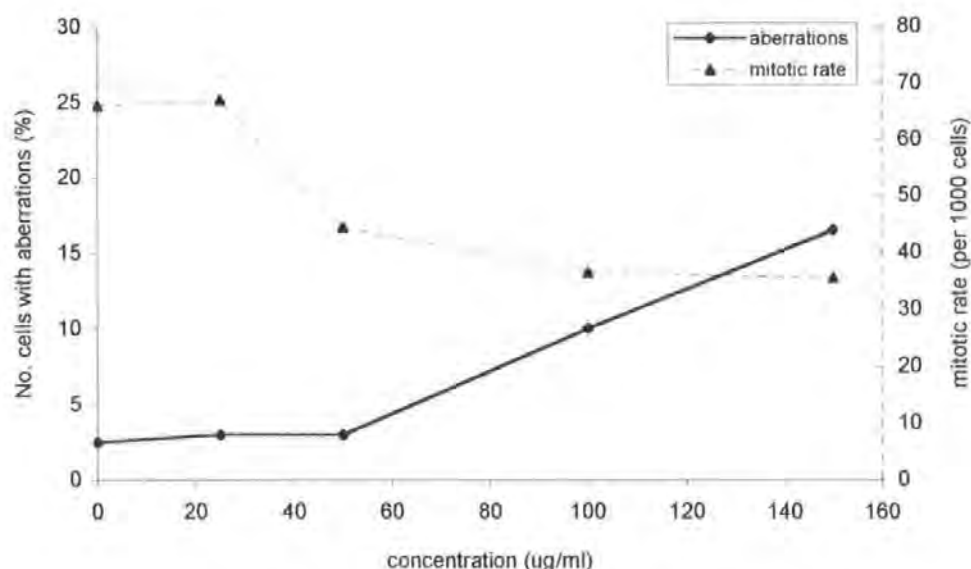


Figure 71. Mitotic rate and number of chromosome aberrations induced in Chinese hamster ovary CHO-K1 cells after exposure with metabolic activation (rat liver S9 fraction) to the polar fraction of the diesel engine emission sample collected at 3000 rpm and 5 Nm (ES 39+42)

concentration (ug/ml)	no. cells with total aberrations /cells scored	probability P^1	number of doses significant ($P \leq 0.0125$) ²	clastogenicity of sample ³
0	5/ 200			
25	6/ 200	0.386		
50	6/ 200	0.386		
100	20/ 200	9.361×10^{-4}		
150	33/ 200	4.156×10^{-7}		
			2	positive

¹ Fisher's exact test (Richardson *et al.*, 1990), comparison to DMSO control (concentration zero above)

² probability testing at 5 % significance level using Bonferroni correction for multiple dose comparisons (0.05/4 doses)

³ criteria based on Galloway *et al.* (1997), section 2.9.2.

Table 51. Chromosome aberrations induced in Chinese hamster ovary CHO-K1 cells exposed with metabolic activation (rat liver S9 fraction) to the polar fraction of the diesel engine emission sample collected at 3000 rpm and 5 Nm (ES 39+42)

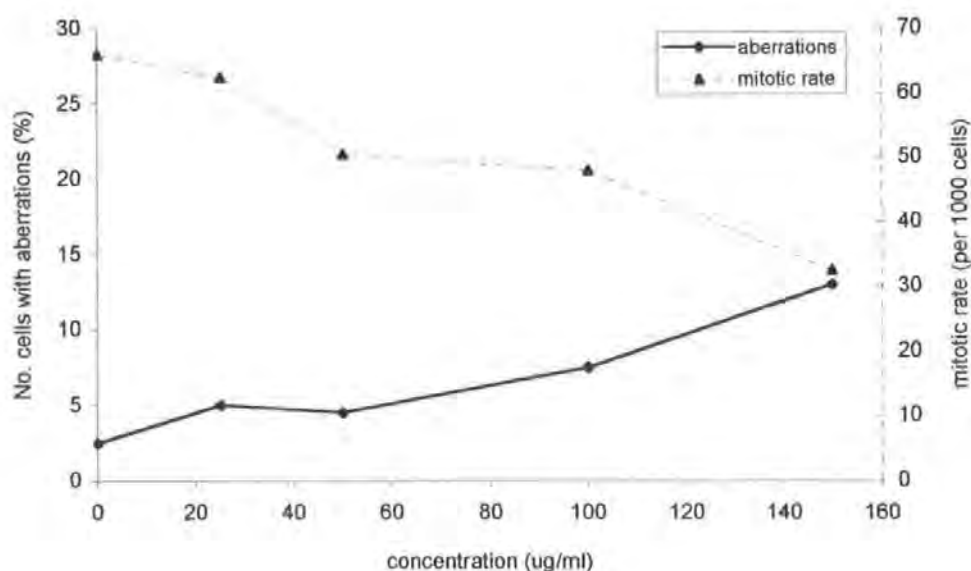


Figure 72. Mitotic rate and number of chromosome aberrations induced in Chinese hamster ovary CHO-K1 cells after exposure with metabolic activation (rat liver S9 fraction) to the polar fraction of the diesel engine emission sample collected at 1000 rpm and 55 Nm (ES 45+48)

concentration (µg/ml)	no. cells with total aberrations /cells scored	probability P^1	number of doses significant ($P \leq 0.0125$) ²	clastogenicity of sample ³
0	5/ 200			
25	10/ 200	0.101		
50	9/ 200	0.147		
100	15/ 200	0.012		
150	26/ 200	3.117×10^{-5}	2	positive

¹ Fisher's exact test (Richardson *et al.*, 1990), comparison to DMSO control (concentration zero above)

² probability testing at 5 % significance level using Bonferroni correction for multiple dose comparisons (0.05/4 doses)

³ criteria based on Galloway *et al.* (1997), section 2.9.2

Table 52. Chromosome aberrations induced in Chinese hamster ovary CHO-K1 cells exposed with metabolic activation (rat liver S9 fraction) to the polar fraction of the diesel engine emission sample collected at 1000 rpm and 55 Nm (ES 45+48)

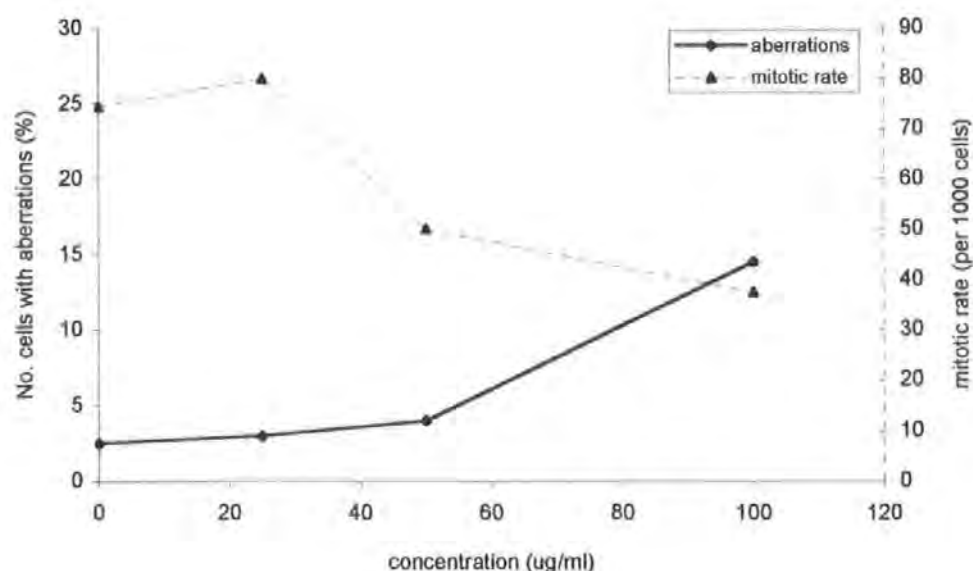


Figure 73. Mitotic rate and number of chromosome aberrations induced in Chinese hamster ovary CHO-K1 cells after exposure with metabolic activation (rat liver S9 fraction) to the polar fraction of the diesel engine emission sample collected at 1000 rpm and 5 Nm (ES 51+54)

concentration ($\mu\text{g/ml}$)	no. cells with total aberrations /cells scored	probability P^1	number of doses significant ($P \leq 0.0167$) ²	clastogenicity of sample ³
0	5/ 200			
25	6/ 200	0.386		
50	8/ 200	0.208		
100	29/ 200	5.118×10^{-6}	1	positive

¹ Fisher's exact test (Richardson *et al.*, 1990), comparison to DMSO control (concentration zero above)

² probability testing at 5 % significance level using Bonferroni correction for multiple dose comparisons (0.05/3 doses)

³ criteria based on Galloway *et al.* (1997), section 2.9.2

Table 53. Chromosome aberrations induced in Chinese hamster ovary CHO-K1 cells exposed with metabolic activation (rat liver S9 fraction) to the polar fraction of the diesel engine emission sample collected at 1000 rpm and 5 Nm (ES 51+54)

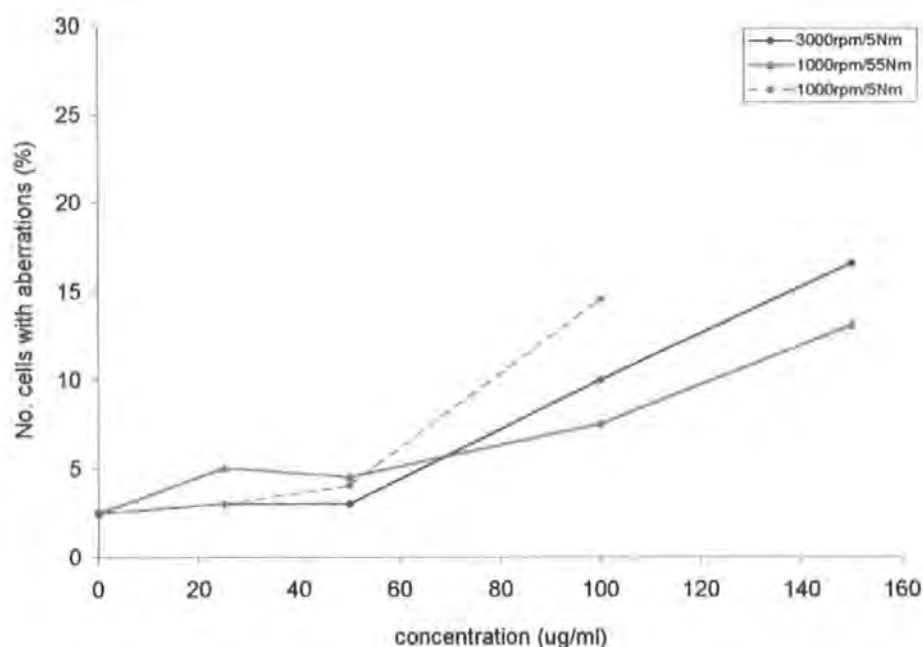


Figure 74. Number of chromosome aberrations induced in Chinese hamster ovary CHO-K1 cells after exposure with metabolic activation (rat liver S9 fraction) to the polar fractions of three diesel engine emission samples collected at 3000 rpm/5 Nm, 1000 rpm/55 Nm, and 1000 rpm/5 Nm

To summarise, the polar fractions of all three engine emissions assayed caused a dose dependant reduction in mitotic rate over a range of concentrations when tested in the presence of metabolic activation. A fall to an approximate 50 % of the control mitotic index was exhibited at the highest concentrations tested. The effect of exposure on the number of aberrations is shown together in Figure 74, above. The increase in the number of aberrations scored at the highest dose was highly significant in each case. For ES 39+42 and ES 45+48, there were significant increases at two or more doses, and both were therefore classified as clastogenic in the presence of metabolic activation. Testing of ES 51+54 was restricted due to its sample mass, although the graph clearly shows that the increase in aberrations seen at 100 μ g/ml exceeds that of the other two polar fractions.

3.9 Summary of diesel engine emission fraction clastogenicity in CHO-K1 cells

A summary table of all diesel emission sample fractions assayed and their clastogenic potential observed in Chinese hamster ovary CHO-K1 cells is shown in Figure 75. Fraction types in which no clastogenicity was observed are unshaded (for example aliphatic fractions of both diesel fuel and emission samples). Fractions types where some weak clastogenic activity was observed are lightly shaded (for example 3+ -ring fractions assayed without metabolic activation), and full shading is given in areas where a clearly positive clastogenic activity was observed (for example polar fractions).

3.10 Overview of chromosome aberration type observed in CHO-K1 cells in response to diesel emission fraction exposure

The number and type of chromosome aberrations observed in CHO-K1 cells after exposure to the fractions of diesel emissions were identified and recorded following the classification given by Dean and Danford (1984, section 2.6.4), and are given in full in Appendix B. Photographs of the type of simple aberrations (including gaps and breaks) and complex aberrations (dicentric chromosomes and exchanges) that were observed are shown in Section 3.4. A comparison of the ratios of simple to complex aberrations observed in positive emission samples is shown in section 3.10.1. Finally, as well as the standard types of simple and complex chromosomal aberrations, aberrant cells were observed showing evidence of centromeric disruption after exposure to polar fractions of diesel engine emissions, which is discussed in section 3.10.2.

		WITHOUT S9				WITH S9				
		fuel	5 Nm	30 Nm	55 Nm	fuel	5 Nm	30 Nm	55 Nm	
ALIPHATIC	fuel									
	1000rpm									
	2000rpm									
	3000rpm	-				-				
AROMATIC	fuel	-				-				
	1000rpm	-			-	+	-			
	2000rpm									
	3000rpm	+				-				
	1-RING	fuel	-				-			
		1000rpm				-	-			
		2000rpm								
		3000rpm	-				-			
	2-RING	fuel	-				++			
		1000rpm				+	++			
		2000rpm								
		3000rpm	-				-			
	3+ -RING	fuel	+				++			
		1000rpm								
		2000rpm								
		3000rpm	+				++			
POLAR	fuel									
	1000rpm	++			++	++	++			
	2000rpm			++	++					
	3000rpm	++	++	++	++					

key

- non-clastogenic
- + weak clastogen, or
> 5 but < 10 % aberrations
- ++ strong clastogen

shading

- no evidence of clastogenicity
- contains some clastogenic or weak clastogenic fractions
- contains fractions with clear clastogenic activity

Figure 75. Summary of diesel fuel and engine emission samples assayed and their resultant clastogenic activity in the chromosome aberration assay in Chinese hamster ovary CHO-K1 cells, assayed both with and without metabolic activation (rat liver S9 fraction)

3.10.1 Aberration types observed in clastogenic fractions

The proportion of simple type to complex type chromosome aberrations in the diesel fuel and engine emission fractions found to be clastogenic was examined. Although numbers in some fractions were small, the proportions within each group of compounds was relatively consistent, for example the three polar fractions assayed produced an average of 1.5 : 1 simple aberrations to complex aberrations, with a range of 1.3 : 1 to 1.7 : 1. Distinctive differences between proportions produced by the alternate groups of compounds were revealed (Figure 76). The figure shows that for the polar group of compounds, there was a clear excess of simple type aberrations to the complex type (1.6:1). This was also true for the polar fractions when assayed with metabolic activation, although to a slightly lesser extent (1.5:1).

In contrast to the clastogenic effect of the polar fractions, the 2-ring group compounds effected an excess of complex type aberrations when assayed with S9. The complex aberrations were more than twice the number of simple aberrations for the 2-ring fractions (1:2.1 simple:complex). The clastogenic 3+ -ring fractions, when assayed with S9, produced almost equal numbers of simple to complex aberrations (1:1.1), a differing ratio again to those already described.

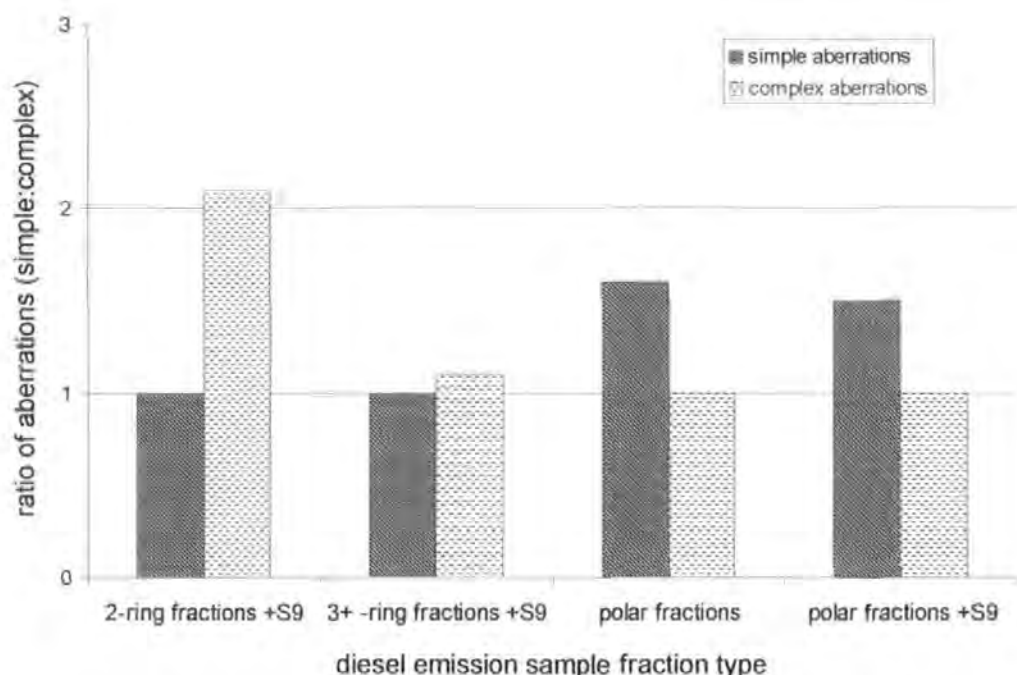
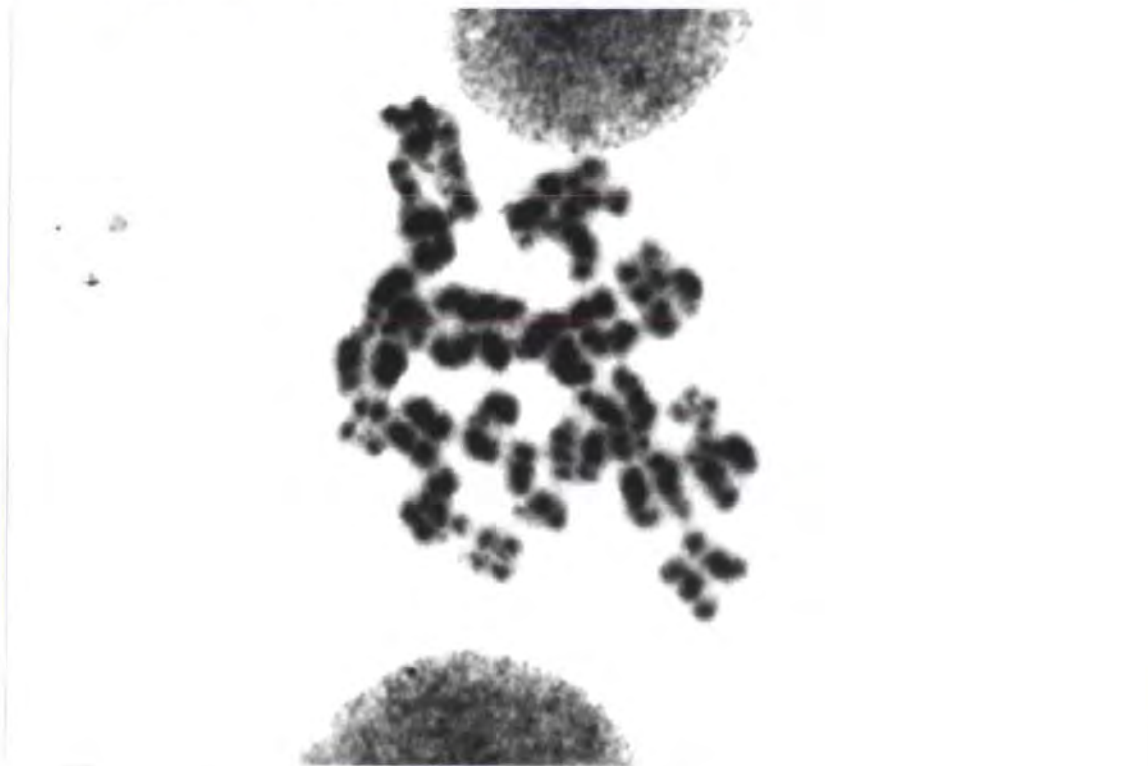


Figure 76. The ratios of simple to complex chromosome aberrations induced in Chinese hamster ovary CHO-K1 cells after exposure to clastogenic fractions of diesel engine fuel and emission samples (polar group compounds, polar group compounds with rat liver S9 metabolic activation, 2-ring aromatic group compounds with S9, and 3+ -ring aromatic group compounds with S9)

3.10.2 Centromeric disruption after exposure to the polar fractions of diesel engine emissions

Each of the polar fractions of the diesel engine emission samples, when assayed without S9, caused a breakdown of the chromosome structure to varying degrees in up to 5 % of cells. This was termed centromeric disruption of the CHO-K1 cell chromosomes. A range of cells were visible over a single slide showing DNA and associated chromosomal proteins with progressive disruption of chromosome architecture (Figures 77a to 78b). In what appeared to be the latter stages of separation, chromosomes could not be identified, the remains appearing to be fragments of DNA and associated proteins. A similar effect has been observed in Chinese hamster ovary chromosome exposed to sodium arsenite (Radha and Natarajan, 1998).

(a) stage 1 centromeric disruption



(b) stage 2 centromeric disruption



Figure 77. Centromeric disruption of Chinese hamster ovary CHO-K1 cells after exposure to the polar fraction of diesel engine emission samples collected over a range of engine speed and load conditions. Apparently sequential disruption of the chromosome architecture is shown through Figure 77(a) to 78(b).

(a) stage 3 centromeric disruption



(b) stage 4 centromeric disruption



Figure 78. Centromeric disruption of Chinese hamster ovary CHO-K1 cells after exposure to the polar fraction of diesel engine emission samples collected over a range of engine speed and load conditions. Apparently sequential disruption of the chromosome architecture is shown through Figure 77(a) to 78(b).

4. DISCUSSION

4.1 Methodology variations and issues raised during the investigation

4.1.1 The diesel engine emission sampling method

There have been a number of different systems developed to sample diesel exhaust emissions. The choice of sampling system is important in that the method of collection may produce samples with different composition, for example through preferential collection of certain diesel group compounds or through artefact formation. The Total Exhaust Solvent Scrubbing Apparatus (TESSA), used in this study, was originally designed to aid in the determination of the origin of the components of diesel engine exhaust emissions. The design therefore necessitates the sampling apparatus being as close to the combustion chamber as possible (Trier, 1988). The rapid removal of the solvent from the exhaust stream is designed to prevent artefact formation. One possible criticism of this system is that emission samples collected may not therefore be representative of the emissions actually expelled from exhaust pipes of diesel powered vehicles, which are diluted with air as they pass along the exhaust. During the developmental work for TESSA, Trier (1988) did find that extension of the sample transfer tube length to simulate an exhaust system lead to alteration of the emission sample collected. Whilst the aromatic and polar groups of compounds appeared largely unchanged, there was a 40 % reduction in aliphatic compounds. Hayano *et al.* (1985) observed a similar reduction in aliphatic compounds sampled from the combustion chamber directly in comparison to aliphatic compounds sampled from the exhaust. Reduction in the aliphatic fraction does not necessarily detract from suitability of the TESSA sampling method for genotoxicity testing of diesel emissions. The aliphatic fraction of diesel exhaust emissions has been suggested to have little mutagenicity associated with it when assayed in bacteria (Lewtas, 1988; Schuetzle *et al.*, 1980). This has been confirmed by the present study for mammalian cells (section 3.8.1), at least for the aliphatic fraction from an engine running at 3000 rpm speed and under 5 Nm load. Therefore an increase in the aliphatic component post combustion

chamber may not be significant in assessing genotoxicity of diesel emissions. It would seem to be more important that the biologically significant fractions of aromatic and polar group compounds are largely unaltered (Trier, 1988), although a full characterisation has not been performed. Characterisation and comparison of near combustion chamber and exhaust pipe expelled aromatic and polar group compounds would be an important area of further work.

In the major alternative to TESSA, the United States Environmental Protection Agency dilution tunnel sampling system, an attempt is made to mimic the natural dilution and cooling of exhaust as it leaves the exhaust tailpipe. Sampling by this method, however, is not without significant drawbacks. The filter used for collection at the end of the tunnel fails to efficiently collect hydrocarbons and Polycyclic Aromatic Compounds (PAC) that have remained in the vapour phase (Petch *et al.*, 1987). In addition, the long sampling times required to collect adequate sample mass for genotoxicity testing leads to artefact formation on the carbon particles collected on filters by the continuous stream passing over compounds that have already settled (Lach and Winkler, 1988). HNO_3 and NO_2 for example, present in the exhaust stream, have been shown to cause significant degradation of PAH adsorbed onto particulate matter, and a subsequent increase in mutagenicity of the solvent extracts of these particulates (Linskog, 1983).

The concentration of 1-nitropyrene in emission samples collected by TESSA was found to be lower than those generally quoted in the literature (Collier, 1995). Thus the dilution of diesel emissions in the exhaust may account for greater nitration of PAH compared with nitration of PAH within the combustion chamber, leading to the potential under representation of biologically significant nitro-PAH in samples collected from TESSA. However, it has to be considered that the mechanism of post combustion nitro-PAH formation may be over estimated because of the documented liability of dilution

tunnels for artefact nitro-PAH (Lach & Winkler, 1988). Further clarification of the nitro-PAH component of diesel engine emissions expelled from the exhaust is needed.

The work up procedure of emission samples collected from TESSA was devised and has been developed to facilitate maximum extraction of emission organics with minimal artefact formation. Radiochemical precursors spiked into the fuel have been used to assess percentage recoveries (Collier, 1995; Pemberton, 1997). Early evaluation by Trier showed recoveries in excess of 90 % for most PAH species (Trier, 1988), with factors such as solubility in water (used during liquid-liquid separation) affecting individual compound recovery. More recently, Collier (1995) showed that laboratory losses of nitro-PAH were low with 80 – 90 % of nitro-PAH species recovered. Identification of the most genotoxic components of the diesel exhaust, followed by quantification of their losses during sample work up, will provide a better picture of the contribution of certain compounds to diesel genotoxicity.

As the dilution tunnel system has been the most widely adopted for sampling of diesel emissions, there is a lack of published data for direct comparison of TESSA or TESSA-like emission samples, especially with respect to genotoxicity. The more recent use of specially designed sampling devices to collect the semivolatile phase compounds (for example Andersson *et al.*, 1998) in addition to the standard filter collection of particulate adsorbed organic emissions from the dilution tunnel (Schuetzle *et al.*, 1980; Enya *et al.*, 1997; Bunger *et al.*, 1998) provides a more complete picture of complete engine emissions, and therefore is more directly comparable to TESSA samples. Further information is required to completely evaluate two different sampling systems and will come as more of the chemical data is published on the components of their emissions.

The TESSA has provided a reliable method for collecting sufficient emission sample masses for *in vitro* genotoxicity testing. It has advantages over other sampling systems, not least of which is the minimal artefact formation discussed. Several potential drawbacks of the TESSA sampling system, in particular those that would affect the genotoxicity of the emissions, appear to have been minimised by careful checking procedures (such as the spiking of the fuel and subsequent recovery). Further evaluation on the affect of the dilution of the exhaust stream after it leaves the combustion chamber would be advantageous/informative.

4.1.2 Emission sample work up and collection during this study

For the first engine run series (ES 3 to 7, 3500 rpm/ 75 Nm), the 2 minute sample masses (Table 7, section 2.1.4) were low and apparently inconsistent with sample masses from other engine conditions which generally increased with increasing speed and load. For this reason samples from this series were used for trial fractionations, cytotoxicity and chromosome aberrations assays only. The low mass samples achieved may have been a reflection of inexperience in the chemical techniques. Consultation of manufacturer's engine emission maps (summarised in Appendix D) shows 3500 rpm and 75 Nm to be a particular low spot for hydrocarbon emissions, which may also be contributory to the low masses achieved.

The use of liquid-liquid partition during emission sample work up resulted in contamination of the total emission sample with water, which occurred in less than 10 % of samples. This was removed by re-partitioning once the sample had been rotary evaporated to less than 20 ml. If the second separation was not successful in removing all traces of water, the problem was recorded and the sample was not used for further testing. It was

possible to discard samples because 6 repeats of each 2 minute sample were collected at each speed and load, and only a maximum of four samples were used for genotoxicity testing. Repeated separation rounds resulted in small losses of the total emission sample, with the concern that these losses would alter the complex balance of chemicals in the sample.

During silica-gel column chromatography, the final elution with methanol removed trace amounts of silica from the column along with the polar group compounds, as observed previously (Kingston, 1994). Pre-mixing of methanol with the preceding elutant (DCM) reduced the 'shock' to the column and therefore the stripping of silica fragments. Polar fractions with visible silica-gel contamination were not used for aberration assay testing.

4.1.3 Chinese hamster ovary CHO-K1 cell line freezing

Stocks of cells purchased from the ECACC (European Collection of Animal Cell Cultures) were frozen upon receipt and regularly throughout the study to maintain a frozen stock (Section 2.4.2). Cells were divided each time and half frozen in medium containing 91 % foetal calf serum and 9 % cryoprotectant, the other half in medium containing 20 % foetal calf serum and 20 % cryoprotectant. The former was recommended by the ECACC to promote maximal cell survival, which was found to be the case particularly after 12 months or more in storage. The latter medium is used regularly in the Department and was adequate for medium term storage, and had the advantage of reduced cost as the foetal calf serum was the most expensive component.

4.1.4 Cytotoxicity assay methodology

During the neutral red dye assay to assess cytotoxicity, absorbance readings for the uptake of neutral red into control Chinese Hamster Ovary cells which were treated with DMSO solvent (or with DMSO plus S9 mix) exhibited wide variation between assays (control absorbance values of 0.2245 to 1.156 units, Appendix A). Control values with S9 mix were generally marginally lower than without S9, and this would initially point to a toxic effect of the S9 mix on the cells. The contribution of physical shock to the cells which occurs during the rounds of cell medium changes and monolayer washing, together with alterations in culture environment during these processes (in particular temperature) cannot, however, be underestimated. The small surface area of each well in the multi-well vessel used during cytotoxicity assays gives a less robust cell monolayer making cells more susceptible to physical stress than during aberration assays (25 cm² flasks). The age of the neutral red dye, variation in absorbance of disposable cuvettes, and critically dispensing of cells during set up were also possibly contributory to variation within and between assays. The neutral red dye was controlled to some extent by storing at the recommended 4°C in the dark for a maximum of 1 week prior to use (recommended maximum 3 weeks, Fiennes *et al.*, 1987), after which time a fresh stock was prepared. Such variation is commonly observed, with cytotoxicity assays known as largely non-reproducible (Scott *et al.*, 1990). Patterns of dose-related reductions in cell viability from control levels were observed generally throughout the study and taken as confirmation of the procedure.

4.1.5 Chromosome aberration assay methodology

During the chromosome aberration assays, a period of recurrent problems with bacterial cell contamination occurred, which were not traced to one particular source. The

contamination coincided with major building works in the Department over several months, in the area around the cell culture rooms. After the completion of work, the area was thoroughly cleaned and CHO-K1 cells resuscitated from frozen stocks, which resolved the infection problem. Cells were routinely cultured and stored without antibiotics so that any contamination was easily detected (following the recommendations of the ECACC).

The karyotype of the CHO-K1 altered during the 3 years of the study so that the predominant cell line observed at the end was that with 20 chromosomes. As the CHO-K1 cell line with 20 chromosomes had been present in significant numbers at the start of the experiment (Figure 14, section 3.3.2), and the line with 19 chromosomes was still very much in evidence, this was not considered a problem. Karyotypic stability was generally maintained by not passaging the cells for more than 16 times, with replenishment from frozen stocks where necessary (following recommendations of Galloway *et al.*, 1985 and other authors). The sporadic high incidence of chromosome damage occasionally observed by other authors in cultures of some Chinese hamster lines (Tweats and Gatehouse, 1988), particularly when incubated with rat liver S9 (Kirkland *et al.*, 1989) was not observed here. There was a slight increase in the mean number of cells with aberrations in the control with S9 at 2.75 % compared to the control without S9 (2.61 %). This is less than the variation observed by other authors (Margolin *et al.*, 1986; Kingston, 1994).

In the absence of metabolic activation, cells were routinely exposed to the test sample for approximately 1.5 x the cell cycle time (around 18 hours in total) following the protocol of Galloway (1987). Following international collaboration and discussion, 'two phase' testing has been recommended where full testing of a sample (one test) would consist of 1 or 2 phases. The major difference is for 'Phase 1' where treatment with the test chemical is for 3-6 hours, with harvesting at 1.5 x normal cell cycle time as previously (OECD, 1996; Kirkland, 1998). This was brought about through analysis of available data

which showed that more clastogens are positive after short treatments than after continuous treatments. This is assumed to be because higher concentrations will be tolerated in the short treatments, and may also reflect the importance of a recovery period shown to be important for certain chemicals (Galloway *et al.*, 1997). 'Phase 2' testing, with continuous treatment with the test sample for 1.5 x the normal cell cycle time, is as used in this study and previously (Galloway *et al.*, 1987). Continuous exposure has been shown to be required for clastogenic assessment of certain compounds (Galloway *et al.*, 1997). Further work from this study could include a 3-6 hour pulse treatment of each diesel fraction when assaying without metabolic activation. This would potentially permit the testing of higher concentrations of diesel emission fractions and may uncover genotoxic responses presently masked by the cytotoxic effect of certain fractions on the CHO cells.

4.2 Overview of testing

This study adopted the use of bioassay directed fractionation in an attempt to unravel the very complex mixture of compounds that make up diesel emissions. Samples collected over the engines range of speed and load conditions were each separated into aliphatic, aromatic, and polar group fractions (section 2.2.1). The aromatic fraction was then further fractionated by HPLC into 1-ring, 2-ring, and 3+-ring group compounds (section 2.2.2). Nitro-PAH, a component of the aromatic fraction (Collier, 1995), has been proposed as the major mutagenic component of diesel engine emissions in assays in bacterial systems (Pederson and Siak, 1981; Nakagawa *et al.*, 1983; Strandell *et al.*, 1994; Enya *et al.*, 1997). The polar fraction of diesel emissions has also been shown to exhibit a significant proportion of the total direct-acting mutagenicity of diesel engine emissions (Nakagawa *et al.*, 1983; Hayakawa *et al.*, 1997). It was therefore in these areas that work was concentrated, with the aliphatic fraction of one engine emission sample assayed for clastogenicity for completeness.

4.3 Cytotoxicity of fuel and engine emission sample fractions

When assayed, the cytotoxicity of some of the fuel and engine emissions fractions were shown to be more closely related to the fraction type than to their source in terms of engine conditions of speed and load (Section 3.6). Polar emission sample fractions from all sources, for example, showed a more direct relationship to each other than to the engine conditions they were collected under (Figures 28 and 29, section 3.7.6 and 3.7.7). This is suggestive of each fraction being homogenous in nature in relation to its toxic effect on CHO cells, or that one or several compounds produced within that fraction being predominately responsible for toxicity. It is also possible that the combination of compounds within each fraction is the most important factor in its cytotoxicity, and that their synergistic and antagonistic effects within the fraction work to determine its effect irrespective of the masses of individual chemicals (which vary depending on the speed and load – section 4.4.4). Determination of synergistic and/or antagonistic effects within each fraction would be an informative area of further work.

The aliphatic fractions of the engine emission samples assayed showed no evidence of cytotoxicity up to concentrations of 200 $\mu\text{g/ml}$ with or without metabolic activation, and the fuel fraction showed a slight cytotoxic with S9 at 200 $\mu\text{g/ml}$ (section 3.6.1). Therefore the types of compounds typically found within this fraction, predominately straight chain hydrocarbons and PAH (Schuetzle *et al.*, 1980), are not toxic to cells *in vitro*. Some indication of toxicity is preferential prior to mutagenicity testing as many mutagenic compounds are only active at concentrations which induce some degree of cytotoxicity (Scott *et al.*, 1990). Repeated rounds of sampling and fractionation would provide sufficient mass of sample to assay up to the recommended maximum of 10 mM (Kirkland, 1998) or 2 to 3 mg/ml (Scott *et al.*, 1990) provided that the osmolarity of the culture medium remains unaffected. The practical upper limit for testing of 10mM was based upon the highest *in vitro* concentrations needed to detect *in vivo* clastogens. The further

work described would provide conclusive data to rule out completely any cytotoxic effect of the aliphatic fractions of diesel emissions from the engine conditions sampled during this study.

All of the aromatic fractions assayed for their cytotoxicity in CHO cells (both fuel and emission fraction) displayed significant toxicity at 50µg/ml without S9 (Section 3.6.2). The fuel aromatic fraction exhibited a slightly reduced effect on cell viability in comparison to the emission sample aromatic fractions. Whilst the aromatic fractions show comparative cytotoxicity at the same concentration, the actual mass of aromatic fraction produced per unit of time varies with the engine operating conditions of speed and load. Thus a snapshot of the toxicity of the emissions expelled from the engine at any one time will be dependant on the speed and load conditions the engine is operating under.

The high level of cytotoxicity exhibited by the whole aromatic fraction was postulated as a barrier to informative clastogenicity testing, with cytotoxicity masking genotoxicity. The breakdown of the aromatic fraction by HPLC into 1-, 2-, and 3+ -ring fractions enabled further investigation of cytotoxic effects within the aromatic fraction compounds. The ring fractions, when assayed for their effect on cell viability in the neutral red vital staining assay, each showed greater cytotoxicity than their respective aromatic fraction over the same range of concentrations (sections 3.6.3 to 3.6.5). This suggests that the ring fractions therefore exhibit antagonistic effects on each other when combined, making the aromatic fraction as a whole less toxic. The mass of each ring fraction contributing to the aromatic fraction may be important – the aromatic fraction is made up of mostly 1-ring compounds for the fuel aromatic fraction (62 %) and the aromatic emission sample collected at 1000 rpm/55 Nm (68 %), although the 3000 rpm/5 Nm aromatic emission sample is predominantly 2-ring (60%), with 1-ring 29 %.

Without S9, there was a correlation of increasing cytotoxicity with increasing ring size, hinting at the more mutagenic/toxic compounds thought to be present in the greater ring size fractions (e.g. 1,8-dinitropyrene, a 4-ring aromatic compound which exhibits one of the highest recorded mutagenicities in bacterial systems; Enya *et al.*, 1997). The uncombusted diesel fuel has comparable cytotoxicity to engine emission fractions, and thus PACs present in the fuel prior to combustion have a significant toxic effect, and supports the suggestion that majority of PAC survive combustion unaltered (Collier *et al.*, 1995). With S9, the ring fractions of the engine emissions collected at 1000 rpm and 55 Nm were more cytotoxic than the fuel or 3000 rpm and 5 Nm ring fractions. At 1000 rpm speed and 55 Nm load there appears to be a particular 'hotspot' for measured engine outputs of Bosch smoke, hydrocarbons, NO_x, and carbon monoxide. At this speed and load all four factors are greater than at any other speed and load conditions sampled in this series (Appendix D). This 'hotspot' of engine output may be contributory to the increased cytotoxicity of the 1000 rpm/55 Nm ring fractions over the fuel and other emission sample assayed. The effect in relation to genotoxicity is discussed in section 4.4.3.2.

All seven of the polar fractions tested exhibited almost identical direct-acting cytotoxic effects on CHO-K1 cells (sections 3.6.6 and 3.6.7), with significant direct-acting toxicity exhibited at 50 µg/ml (comparable to the cytotoxicity of the aromatic fractions). In the presence of S9, a severe cytotoxic effect was exhibited at 200 µg/ml for all three fractions assayed. Cytotoxic effects with metabolic activation were more evident in the aromatic fractions at lower concentrations. As discussed, variations of sample speed and load had minimal effect on the concentrations at which cytotoxicity was exhibited. Chemical analysis of the polar fractions would be required to determine if the similarities in cytotoxic effect were due to chemical homogeneity of samples collected at different speed and load conditions. Homogeneity of fractions collected at different speeds and loads is not suggested from the GC/MS analysis of ring aromatic fractions (section 3.2.2).

Chemical analysis is problematic because of the difficulty in analysing non-volatile polar compounds directly by GC/MS (discussed in section 1.10.4), but would be an area of further work.

4.4 Clastogenicity of diesel fuel and engine emission sample fractions

Previous genotoxicity testing of whole emission samples collected over a range of differing engine conditions using TESSA gave a variety of responses, some positive and some negative, with and without metabolic activation (Kingston, 1995). At the more extreme conditions of speed and load, many of the samples were cytotoxic which prevented analysis of clastogenic effects. One of the initial aims of this study was to repeat some of the engine sampling at the same engine conditions, fractionate and then assay the emission sample fractions produced to provide information about their chemical nature and to account for differences in clastogenicity between samples collected at different speeds and loads. The comparison of the results observed in this work to those of other authors working on the mutagenicity of diesel emissions has to take into account the variability in emission sample collection (section 1.10.3) which may contribute to differences in the chemical constituents of certain fractions.

4.4.1 The aliphatic fraction of diesel engine emissions

The aliphatic fraction of the engine emission sample collected at 3000 rpm and 5 Nm was not clastogenic with or without S9 up to 600 µg/ml, the maximum concentration possible within the scope of this study (Section 3.8.1). This is in line with previous findings in bacterial assays (Schuetzle *et al.*, 1980; Hayakawa *et al.*, 1997), and in brain lesions in the rat (Andersson *et al.*, 1998) and reflects the nature of chemicals known and assumed to be

found in this fraction which are non-carcinogenic (Grimmer *et al.*, 1987). There has, however, been a recent report of tubular necrosis and renal failure occurring twice in a patient overexposed to aliphatic hydrocarbons (Landry and Langlois, 1998). It would therefore be informative to repeat testing at concentrations up to the recommended maximum to rule out a clastogenic potential for the aliphatic fraction of diesel emissions at high concentrations. Testing of aliphatic emission samples collected at different speed and loads would be required for a complete investigation, as the aliphatic fractions of diesel emissions are not necessarily homogeneous when engine conditions are altered. As the fuel aliphatic fraction exhibited a slight toxic effect at 200 µg/ml in this study, this fraction is now suggestive of an important first fraction to eliminate by higher dose testing.

4.4.2 *The aromatic fractions of diesel engine emissions*

Although they showed clear evidence of direct acting cytotoxicity at 50 µg/ml, none of the three aromatic fractions assayed produced statistically significant increase in the number of aberrations at any concentration, with or without S9 (section 3.8.2). They were therefore all classified as non-clastogenic.

This is in contrast to mutagenicity work in bacterial assays where the aromatic fractions have been generally shown to exhibit a high degree of direct-acting mutagenicity (Schuetzle *et al.*, 1980; Hayakawa *et al.*, 1997; Ostby *et al.*, 1997). Indeed many authors have concluded that aromatic fraction of diesel emissions accounts for most of the direct-acting mutagenicity (40 to 61.5 %) of the crude extract (Schuetzle *et al.*, 1980; Strandell *et al.*, 1994; Hayakawa *et al.*, 1997). Several nitro-PAH, including dinitropyrenes (Nakagawa *et al.*, 1983; Tokiwa *et al.*, 1987) and 3-nitrobenzanthrone (Enya *et al.*, 1997), have been proposed as the major mutagenic species in diesel emissions. The aromatic

fraction of diesel emissions has been shown to contain nitro-PAC, for example, 1,6-dinitropyrene (Collier, 1995). Nitro-PAC are strong direct-acting mutagens in bacterial assays (section 1.10.6.3), a response ascribed to the inherent nitroreductase activity of the *Salmonella* bacteria used in Ames assays (Beland *et al.*, 1995; Fu, 1990), as nitroreductases are capable of activating nitro-PAC to reactive epoxides. Native nitroreductase activity is however minimal in mammalian cells in culture and *in vivo* (Nachtman and Wolff, 1982), which would explain the lack of direct-acting mutagenic potential of many nitro-PAC in CHO cells (Boyes *et al.*, 1991). This would therefore be a possible explanation for the non-clastogenic response of the CHO cells to the aromatic fractions of diesel emissions assayed here. The high levels of mutagenicity found by previous authors in the aromatic fractions of diesel emissions may also be artificially inflated due to artefact formation during dilution tunnel sampling as discussed (section 4.1.1). It is of course possible that the opposite is true - nitro-PAH compounds may be underrepresented in emission samples collected from TESSA (such as in this study), therefore reducing the mutagenicity that would be present in the aromatic fraction.

There was a lack of clastogenic activity for the aromatic fractions even in the presence of supplementary metabolic activation enzymes (rat liver S9 fraction), and therefore the aromatic fraction was not clastogenic in CHO-K1 cells (section 3.8.2.2). Nitroreductase enzymes in rat liver S9 may have been insufficient to activate potentially clastogenic nitro-PAH compounds. It is also possible that the clastogenic potential of the aromatic fractions assayed here was masked by the cytotoxic effects of the fraction as a whole. Thus the toxic effects of certain compounds within the fraction prohibited testing of mutagenic compounds at sufficiently high concentrations for them to exert an effect.

It may be important that after exposure to the 3000 rpm/5 Nm aromatic fraction without S9, greater than 5 % of cells with aberrations were observed at three

concentrations (all 7 %, not dose related; Table 21). Several possible intimations can be made – the fraction may be clastogenic over a narrow concentration range which was just touched upon, or it may be again that cytotoxicity is masking genotoxicity, or that a cell cycle delaying effect caused by this group of compounds made the standard sampling time sub-optimal. It is also possible that there are genotoxic compounds present within the aromatic fraction but their effect is largely masked by the presence of other inhibitory PAC compounds. For example, several PAC have been shown to exhibit antagonistic effects on benzo[a]pyrene and 1-nitropyrene (mutagenic compounds previously identified in the aromatic fraction of diesel engine emissions) (Hermann, 1981; Cherng *et al.*, 1996). To try and unravel this question, and following the scheme of bioassay directed fractionation, the aromatic fraction was further separated by HPLC into groups of aromatic rings.

4.4.3 Aromatic ring fractions

The fractionation of the aromatic diesel engine fuel and emission samples into 1-ring, 2-ring, and 3+ -ring fractions, and subsequent assay for genotoxicity is novel and therefore direct comparison to the work of other workers is not possible. References are therefore made to related work on known or suspected compounds present in the fractions.

4.4.3.1 1-ring aromatic diesel emission sample fractions

All three 1-ring aromatic fractions, derived from the fuel and two diesel emission samples (1000 rpm/55 Nm and 3000 rpm/5 Nm), were negative in the chromosome aberration assay when assayed with or without S9 (section 3.8.3). Benzene, a typical 1-ring aromatic compound identified in diesel emissions (Scheepers and Boss, 1992), has been shown to be clastogenic when metabolically activated (Ishidate, 1988). It has also been classified as carcinogenic (IARC, 1989). The combination of chemicals that make up the 1-ring

fractions tested here exhibited significant cytotoxic effects at low concentrations without S9 (>50 % cell killing at 20 µg/ml) in all three cases, and the possibility of toxicity masking any genotoxic effects remains. Further fractionation and chemical classification of the 1-ring aromatic samples is required to fully study their genotoxicity.

4.4.3.2 2-ring aromatic diesel emission sample fractions

Without S9, the 2-ring fractions of the fuel and the two diesel emission samples exhibited no clastogenic effects on CHO cells (section 3.8.4.1). As with the 1-ring fractions, toxicity was significant at low concentrations, although in this case even more severe (minimal cell survival at 20 µg/ml). As well as further fractionation as a key to understanding the nature of the 2-ring fraction, one approach for further investigation may be to repeat the assay with a shorter pulse exposure time (3-6 hours), in line with recent recommendations for the chromosome aberration assay (Kirkland, 1998). In the presence of supplementary metabolic activation, the fuel and the 1000 rpm/55 Nm emission sample 2-ring fractions were clastogenic, with statistically significant increases in chromosome aberrations at at least one concentration (section 3.8.4.2). This finding is consistent with the presence of indirect-acting mutagens in the 2-ring group of compounds. Napthalene, a 2-ring aromatic compound, is an example of an indirect-acting clastogen (Ishidate, 1988) which has been detected in diesel emissions (Schuetzle *et al.*, 1980). Assay of the third 2-ring sample with metabolic activation (from emission sample collected at 3000 rpm/5 Nm) did not result in a significant increase in chromosome aberrations and was therefore not clastogenic.

The opposing results from the 2-ring samples was the first real indication that although the fractions contained the same type of compounds, their actual chemical make-up differed. The emission sample collected at 1000 rpm/55 Nm clearly contains indirect-

acting genotoxic compounds, whilst at the same concentration the 2-ring fraction from an emission sample collected at a different speed and load (3000 rpm/5 Nm) was not clastogenic with S9. Thus this second fraction must contain less of the active genotoxic chemical compounds, or contain more of certain compounds that suppress the active compound's genotoxicity. Compounds in the fuel (for example PAC) may survive combustion unaltered, may be completely combusted under 'ideal' engine operating conditions, or they may be partially broken down and take part in pyrosynthetic reactions which may result in the formation of new PAC. As the uncombusted fuel 2-ring fraction was also clastogenic with S9, it suggests that genotoxic compounds present in the fuel survive the combustion process for an engine operating at 1000 rpm/55 Nm, although it is of course possible that it is different chemical compounds in these two fractions exhibiting a similar genotoxicity. The combustion efficiency of PAC in the fuel described above is related to conditions in the combustion chamber such as temperature, oxygen concentration, swirl, and the kinetics of the PAC reaction (Scheepers and Boss, 1992; Collier *et al.*, 1995; Pemberton *et al.*, 1997). Research suggests that at high speed and low load (for example 3000 rpm/5 Nm) pyrosynthetic reactions are more favoured, so that fuel PAC are pyrosynthesised in the combustion chamber to form altered PAC. At high engine loads, combustion efficiencies are greater so that for the 1000 rpm/55 Nm emission sample fuel PAC are more likely to be completely combusted, and those PAC not combusted are more likely to survive unaltered (Collier *et al.*, 1995).

The emission sample collected at 1000 rpm/55 Nm corresponds to a point in the combustion chamber where the four measured engine outputs of smoke, NO_x, hydrocarbons, and CO are greatest (a 'hotspot'), shown in Figure 124, Appendix D. The greater amounts of these four engine outputs at this speed and load may be related to the fraction's constituents and therefore its increased genotoxicity over the second 2-ring emission fraction (3000 rpm/5 Nm). It may be particularly significant that the NO_x

(oxides of nitrogen) content of the combustion chamber and the exhaust is thought to be a crucial factor in respect to the formation of mutagenic nitro-PAC emissions (Collier, 1995). NO_x measured at 1000 rpm/55 Nm is much greater at 1450 ppm compared to only 200 ppm at 3000 rpm/5 Nm. This is suggestive of the presence of higher levels of nitro-PAC in the 2-ring fraction collected at 1000 rpm/55 Nm. The presence of sufficient levels of nitro-PAC in this fraction may account for some of the indirect-acting genotoxicity observed here in this mammalian cell test system, because as discussed nitro-PAC are indirect-acting mutagens in mammalian systems (Boyes *et al.*, 1991; Nachtman and Wolff, 1982). The contrasting activity of nitro-PAH in bacterial to mammalian cell systems is thought to be due to the presence of nitroreductase and has been discussed. Increases in nitro-PAH formation would not, however, explain the observed clastogenicity of the fuel 2-ring aromatic fraction when assayed with metabolic activation as it has obviously not been subjected to NO_x in the exhaust. This may suggest therefore that in light of the combustion efficiency of the engine at 1000 rpm/55 Nm, the majority of PAC present in the sample are those that have survived from the fuel unaltered. Thus the genotoxic PAC in the 2-ring fuel sample are similar to those in the emission sample. Combustion efficiency is less at 3000 rpm/5 Nm, and therefore more PAC and related compounds are only partly combusted facilitating pyrosynthesis of new compounds. These new compounds would then have to be the significant portion of the sample and non-genotoxic at the concentrations assayed, or one or more particular pyrosynthesised compounds may be suppressing the activity of the fraction from this speed and load. As well as comparison of the chemical make up of the 2-ring fractions, genotoxicity testing of emission sample 2-ring fractions collected over a wider range of engine conditions where combustion efficiencies are known would be informative.

Another major difference between the emission samples collected at 1000 rpm/55 Nm and 3000 rpm/5 Nm was the relative percentages of ring fractions that made up the

aromatic fraction, as mentioned in section 4.3. Whilst the fuel and the 1000 rpm/55 Nm aromatic fractions are predominantly 1-ring compounds (62 – 68%), the 3000 rpm/5 Nm aromatic emission sample is mainly comprised of 2-ring aromatic compounds. This may be related to combustion efficiencies, but does clearly demonstrate the variation in the chemical structure of emission samples that are emitted depending upon the speed and load at which an engine is operating.

4.4.3.3 3+ -ring aromatic diesel emission sample fractions

Although without S9, there was no statistically significant increase in number of chromosome aberrations after exposure to the 3+ -ring fractions, the percentage of cells with aberrations was raised above the background 5 % rate (section 3.8.5.1). For the fuel 3+ -ring fraction, there were greater than 5% aberrations at one concentration (8 % at highest concentration), and greater than 5% aberrations at 3 concentrations for 3000 rpm/5 Nm emission sample fraction (8, 8, and 9 %). Direct-acting mutagens are either not present in the 3+ -ring fractions in amounts sufficient to result in statistically significant numbers of chromosome aberrations, or the activity of such compounds is reduced or masked by other compounds in the fraction. The rise in the number of aberrations above background rates may be an indication of direct-acting genotoxicity, where the exposure timing or the range of concentrations were not optimal for detecting clastogenicity of these samples, or as suggested genotoxicity is masked by cytotoxicity of other compounds within a fraction, or antagonistic effects of other compounds within a fraction.

With S9 supplementary activation, both 3+ -ring fractions assayed (fuel and emission sample collected at 3000 rpm/5 Nm) showed a statistically significant clastogenic effect in CHO cells (section 3.8.5.2). This confirms the presence of one or more indirect-

acting mutagens in this fraction. 1-nitropyrene, isolated from diesel exhaust emissions, is an example of a 4-ring aromatic compound which if present would therefore fall into this category. Although 1-nitropyrene has been shown to exhibit strong direct-acting mutagenicity in bacterial systems (Schuetzle, 1983; Tokiwa *et al.*, 1987), its mutagenicity in a variety of mammalian short term assays is dependant upon the presence of supplementary metabolic activation (Heflich *et al.*, 1985; Matsuoka *et al.*, 1991; Ensell *et al.*, 1998), which would explain the genotoxic activity here with S9. The 3+ -ring fuel and emission samples exhibited a similar clastogenic effect, but possibly for different reasons as an initial examination of the GC/MS traces provided shows that the chemical make-up of the two fractions is not identical (Figure 79 below and Appendix C). Compounds such as biphenylene, fluorene and methyl-fluorene are minimal in the fuel fraction and more abundant in the emission sample fraction, for example fluorene has an abundance of 400,000 units in the fuel fraction and a much greater 3,400,000 units in the emission sample fraction. Other compounds, such as trimethylphenanthrene, are more abundant in the fuel 3+ -ring fraction (1,900,000 units) compared to the emission sample fraction (1,200,000 units). This is as expected as one of the major reactions the combustion chamber is de-methylation.

The amount of 3+ -ring fraction within the aromatic fraction, and hence within the emission sample as a whole, is small. The relative contribution of the 3+ -ring fraction to the aromatic fraction is the least at 4.3 % of the fuel, 5.3 % of the 1000 rpm/55 Nm aromatic fraction, and 11.5 % of the 3000 rpm/5 Nm aromatic fraction. Antagonistic effects of compounds within the other two ring fractions (1-ring and 2-ring) may therefore be responsible for lack of genotoxic activity observed in the aromatic fractions as a whole.

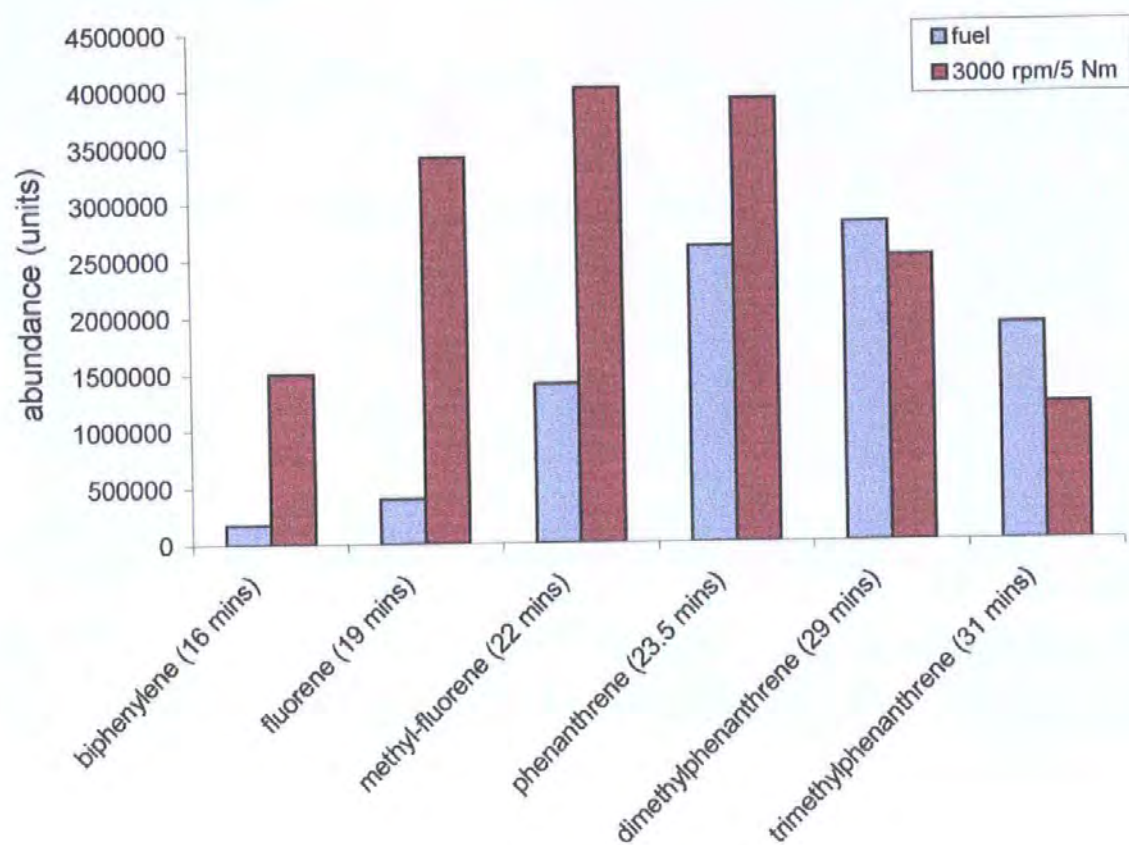


Figure 79. Relative abundance of selected aromatic compounds in the diesel fuel and engine emission 3+ -ring fractions detected by GC/MS (gas chromatography/ mass spectrometry)

4.4.4 The polar fractions of diesel engine emission samples

All of the polar emission sample fractions assayed exhibited significant clastogenicity both with and without metabolic activation (section 3.8.6). This suggests that the polar group of compounds is a mix of indirect and direct-acting mutagens, or that it is comprised of direct-acting mutagens unaffected by S9 mix. During bacterial testing of extracts diesel exhaust particulates, the addition of S9 has been shown to lower the genotoxic response (Wang *et al.*, 1981; Clark and Vigil, 1980; Bunger *et al.*, 1998). Genotoxic activity does

not appear to have been suppressed in this system although it is not possible to say with certainty as experimental conditions such as exposure time (2 hours versus 18 hours) and concentrations assayed (maximum 30 µg/ml versus 150 µg/ml) were different for assays with and without S9. The genotoxicity of each polar fraction did not differ significantly from other polar fractions collected at different speed and load conditions when assayed at the same concentration. This is generally suggestive of a relatively homogeneous mixture of chemicals in the polar fractions, or the presence of sufficient quantities of one or two highly genotoxic compounds sufficient to make the relative contributions of other polar compounds to the fraction unimportant.

Despite the generally homogeneous nature of the polar fractions, there was a slight increase in direct-acting clastogenicity for low engine load polar emission fractions at the highest concentration assayed of 30 µg/ml (Figure 70, section 3.8.6). With S9, the low load emission sample fraction (1000 rpm/5 Nm) showed a sharper increase in chromosome aberrations (Figure 74) than other emission sample polar fractions, although it could not be assayed at the full range of concentrations. At low engine load, the unburnt fuel zone in the combustion chamber is larger, leading to a greater survival and generation (pyrosynthesis) of PAC (Collier, 1995). It may be that PAC generated under low load conditions are more genotoxic, or that genotoxic compounds are favourably produced, increasing overall fraction genotoxicity. Collection and assay of a wider range of low load polar emission fractions would confirm this and highlight a major area of possible engine or vehicle design improvement.

The polar aberration assay results indicate that the polar fraction compounds are responsible for a significant contribution to the clastogenicity of diesel exhaust emissions. The polar fraction is 25 % by mass of the total emission sample collected at 3000 rpm and 5 Nm. Without metabolic activation, this polar fraction is responsible for the majority 68 %

of the direct acting genotoxicity, with the 3+ -ring fraction responsible for the remaining 32 % (despite being only 3.4 % of the total emission sample). This relationship is altered in the presence of S9, where the polar fraction is responsible for 33 % of the direct acting genotoxicity, and the majority due to the 3+ -ring fraction. This contribution of the polar fraction to the overall genotoxicity of diesel emission is in agreement with some authors (Crebelli *et al.*, 1995), but is inconsistent with the conclusions of others (Ostby *et al.*, 1997; Westerholm *et al.*, 1991; Hayakawa *et al.*, 1997). Direct comparison with my work and that of the latter 3 authors is not possible, however, because they describe the major mutagens in the aromatic fraction as nitro-PAH which, as stated, may be artificially inflated due to artefact formation during dilution tunnel sampling. The use of the Ames assay by these authors increases the significance of nitro-PAH genotoxicity because of their inherent nitroreductase activity. Crebelli *et al.* (1995) found mutagenic profiles of diesel emissions in nitroreductase deficient strains of TA98 suggested only a small contribution of the dinitropyrenes in particular to the responses observed, and importantly his direct sampling system was designed to include sampling of gas phase compounds and to minimise the chance of secondary transformations (which is more like the TESSA sampling system than the dilution tunnel). For some work, for example Schuetzle *et al.* (1980), comparison is again invalid as although they described the aromatic fractions as the most mutagenic, they did not assay the final, most polar fraction at that time. It is interesting and may be relevant that particulate matter samples from urban air show the polar fraction to exhibit the most mutagenicity without S9 (Schuetzle and Daisey, 1990; Helmig *et al.*, 1992; Enya *et al.*, 1997).

Regarding engine operating conditions, several studies have proposed a link between increased diesel engine emission mutagenicity in bacteria and NO_x emissions (Bechtold *et al.*, 1986; Courtois *et al.*, 1993; Kingston, 1994). As discussed, this would correspond to the results observed in this study of increased clastogenicity with S9 for the

1000 rpm/55 Nm 2-ring fraction (NO_x 1450 ppm) compared to the 3000 rpm/5 Nm 2-ring fraction (NO_x 200 ppm). The results of the polar fractions do not, however, follow through. They exhibit very similar levels of genotoxicity with no clear relationship between engine conditions and individual sample genotoxicity. As previous assays were of whole diesel emission samples, it may be that the increased NO_x affected only the aromatic compounds within the whole sample (increasing nitro-PAH formation) which could obviously not be discerned. Increased nitro-PAH would not be expected to be reflected by increased genotoxicity of polar group compounds. Emission sampling and assay of the aromatic ring fractions obtained over a wider engine range, with differing levels of NO_x emissions, would provide more conclusive information about the relationship between NO_x emissions, aromatic ring fractions, and nitro-PAH.

4.5 Mass of emission sample fraction obtained during standard sampling

Although many of the fractions exhibited cytotoxic or clastogenic effects at the same concentration, the engine conditions of speed and load are relevant and important to exposure risk. This can be illustrated clearly for the polar fractions, where all seven fractions assayed exhibited direct-acting clastogenicity at a concentration of 20 µg/ml. The mass of each polar fraction produced during each 2 minute sampling session is, however, not the same and is very dependant upon the engine speed and load as shown in Figure 80. As emission sampling is from one of the four cylinders only, mass obtained from TESSA sampling has been multiplied by four to represent the approximate mass that would be expelled from the exhaust each minute. At low engine speed and load the mass of polar fraction produced per minute is 23.4 mg (1000 rpm/5 Nm), at mid speed and load this is increased to 62.0 mg (2000 rpm/30 Nm), and at high speed and load (3000 rpm/55 Nm) a maximal 98.0 mg of polar fraction compounds is emitted. Thus when an engine is

operating at high engine speeds and loads, it is producing the greatest mass of these highly genotoxic polar compounds which are released into the atmosphere.

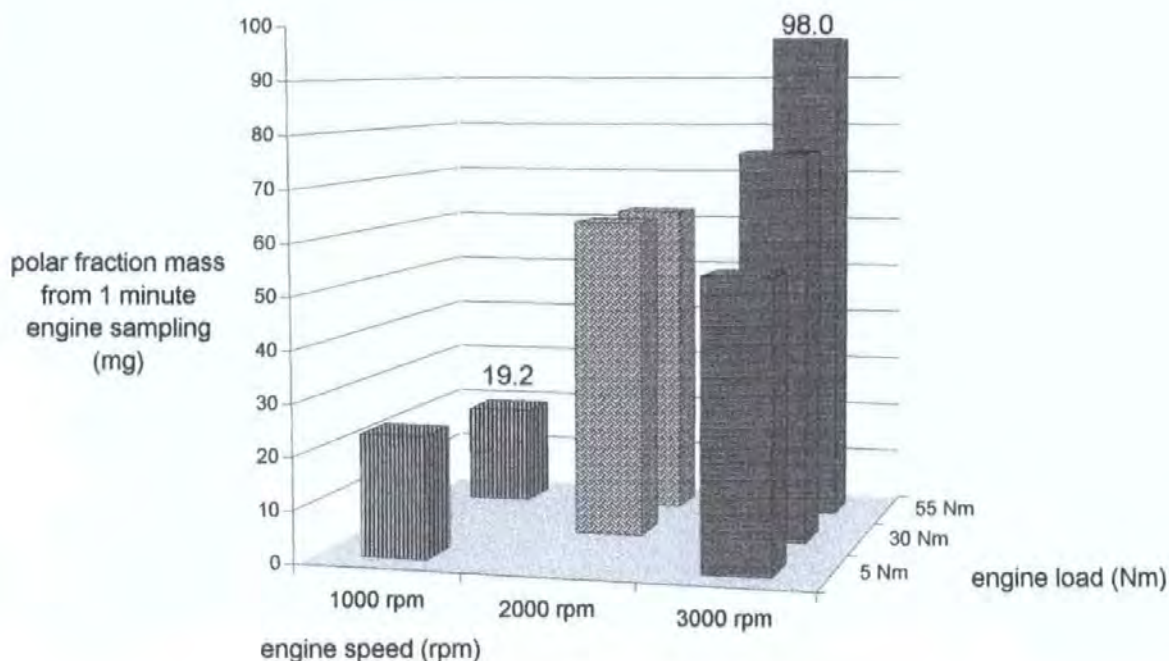


Figure 80. The extrapolated mass of polar fraction group compounds emitted per minute from the diesel test engine for various engine conditions of speed and load tested

4.6 Type of chromosome aberrations observed

The difference in ratios of simple to complex aberrations induced by the clastogenic fractions (section 3.10.1) may indicate different modes of action for clastogenic chemicals within each fraction. It has been shown, for example, that the processes leading to the formation of dicentrics and translocations are different (Natarajan *et al.*, 1994). Aberration assays of restriction endonucleases and ionizing radiations in CHO cells have shown breakpoints preferentially occurring in G-light bands (Folle *et al.*, 1998). PAC are all S-dependent mutagens, and therefore the formation of the initial DNA lesion is critical and

suggested as being dependent on the type of chemical compound. Further work in this area is required, especially to increase sample sizes and therefore statistical significance of differences in aberration types. Although specific sites of chromosomal attack were not noted, G-banding of the CHO-K1 cells may enable the detection of such sites and any relationship with compound type.

CHO cells exposed to higher concentrations of the polar fraction compounds were affected by loss of chromosome structure in approximately 3 % of cells (section 3.10.2). The affect on chromosome structure was similar to that observed after exposure to arsenite and sodium arsenite (Radha and Natarajan, 1998), and other chemicals such as mimosine (Jha *et al.*, 1995), where abnormal cells with pulverised chromosomes and decondensed chromatin are observed. This abnormal separation of the chromosomes and loss of chromosome structure may be important in the formation of aneuploid cells. In human cells, for example, precocious centromere separation has been proposed by Angell (1997) as a possible mechanism for the induction of aneuploidy after the finding of loss of sister chromatid cohesion in Meiosis I of oocytes. The observations here may also aid in the determination of compounds within the polar fraction, which has been hampered by the generally non-volatile nature of polar compounds which cannot be analysed by GC/MS without derivatization. It may be productive to look for compounds with structural similarity to arsenite.

4.7 Implications of the results for health and the environment

Although there have been conflicting reports about the potential health effects of diesel emissions (section 1.4), there is a consensus that at the very least the contribution of diesel to particulate load in urban air is resulting in premature death of susceptible individuals (DoE, 1996). Several authors have gone much further than this and suggested that

particulate exposure is affecting all people, particularly in urban areas, and reducing life-span (Pope *et al.*, 1995). A relationship between particulate emissions and lung (HEI, 1995; Bhatia *et al.*, 1998) and other types of cancer (IARC, 1989; Nielson *et al.*, 1996) have also been described.

This study has confirmed previous work in showing that the diesel particulates emitted have mutagenic compounds adsorbed onto them, even those compounds emitted from engines powered by modern fuels. A mode of action for diesel activity in humans has not yet been ascertained, although several studies have described increases in the activation of airway epithelial cells after exposure (Ohtoshi *et al.*, 1998; Takano *et al.*, 1998; Miyabara *et al.*, 1998), a potential model for the observed allergic airway response. Despite the concern over the potential health effects of diesel, and the implementation of emissions legislation, there has been a continued rise in the number of diesel cars sold. In some countries where diesel cars now account for 50 % of new car sales, implementation of tighter emissions controls has been negated by the maintenance of new car sales.

A mechanism of action for diesel emissions in humans is essential to prove the causation that is implied from epidemiological studies. Identification of mutagenic PAC may aid in the uncovering of a mode of action and this study has been a step in that direction by determination of fractions of diesel emissions that are highly mutagenic in mammalian cells.

4.8 Conclusions

As the majority of testing of fractionated diesel emissions has been performed in bacterial systems, the use of a mammalian cell system in this study was important to further our understanding of the complex area of diesel mutagenicity. The IARC (1989) suggested

that results on diesel emission testing from existing cytogenetic studies were inconclusive and that further work in this field was required. Despite this, there has remained a lack of *in vitro* testing of diesel emissions, particularly fractionated samples. The continued general movement to improve airborne pollution has lead to many recent advances in diesel technology, and therefore revised mutagenicity testing is appropriate. A relatively new low sulphur diesel fuel was therefore used in a modern diesel engine in this study.

One of the primary objectives of this investigation was to identify the most mutagenic components of diesel engine emissions through the use of bioassay directed fractionation. This has been achieved in a number of ways. The most mutagenic portion of the diesel emissions was identified as the polar fraction. In contrast to the different clastogenic responses of the ring fractions collected at different engine speeds and loads, the polar fractions were collected over a wide engine range and yet exhibited very similar strong genotoxic effects. A small correlation between increased clastogenicity and low engine load (5 Nm) was observed. The highly toxic response of the aromatic fractions assayed promoted isolation of aromatic ring fractions by HPLC, the assay of which showed increasing genotoxicity with increasing number of rings. The design of the study was also to test diesel fuel fractionated in the same way as emission samples to facilitate a pre- and post-combustion comparison, and this has revealed the fuel itself as a genotoxic mixture. It has also been shown that similar levels of clastogenicity may be observed when complex mixtures of differing chemical composition are assayed.

One of the main advantages of this study has been the ability to make direct comparisons between samples as the only variation between them should be the speed and load at which they were collected. This provides information about the engine conditions at which the majority of genotoxic compounds will be emitted into the atmosphere. For example for an engine operating at 3000 rpm and 55 Nm, 98 mg of highly genotoxic polar

group compounds, which are clastogenic to CHO cells at concentrations as low as 20 µg/ml, will be emitted into the atmosphere (section 4.5). This study has shown that the polar group compounds are of particular concern because of their strong direct-acting genotoxicity. The testing performed during this investigation has therefore shown that engine conditions of speed and load are important, for some fractions giving a greater clastogenic response, for example the increased genotoxicity of polar fractions collected at low engine loads. Such information can be used by engine manufactures and policy makers to aid in the reduction of airborne pollution. At 1000 rpm and 55 Nm, the 2-ring fraction of the diesel emission sample was clastogenic when assayed with S9. This corresponds to an area in the engine where NO_x emission are at their highest, because high temperatures promote the formation of NO_x from nitrogen and oxygen in the combustion chamber. Engine and fuel development could therefore work at reducing the effect of this engine 'hotspot', although more than a simple reduction in combustion chamber temperature is required as this would merely increase particulate emissions through the incomplete fuel combustion that takes place at lower temperatures. As the emission of particulates is a major area of public health concern (section 1.4), any increase in particulate emissions despite a reduction in the release of genotoxic compounds would not be beneficial.

The genotoxicity of diesel emissions will continue to be relevant for as long as there is an increased market penetration of diesel car sales, and increased car ownership and usage in general aggravating the particulate load in the atmosphere particularly in urban areas. The almost certain adverse effect of diesel particulate emissions on public health will promote the search for a mechanism of action for diesel particulates, for which one of the fundamental requirements is a better understanding of the chemical and mutagenic nature of the emissions.

APPENDIX A

CYTOTOXICITY ASSAYS

The cytotoxicity of all diesel fuel and engine emission sample fractions was assessed to indicate a range of concentrations suitable for chromosome aberration testing. The method followed was that of dye uptake by viable cells after Fiennes *et al.* (1987) as described in section 2.6.1. The cytotoxic effect of sample fractions was assessed after incubation of the test sample with Chinese hamster ovary CHO-K1 cells over the same time period as used in the aberration assay. Surviving cells were quantified spectrophotomertrically following incubation with neutral red dye for the final two hours. A minimal amount of neutral red dye was retained in wells that contained medium only (no cells), and therefore absorbance levels of less than 0.01 were regarded as representing no viable cells. Data from duplicate wells is presented as mean absorbance values with error bars representing ± 2 standard deviations.

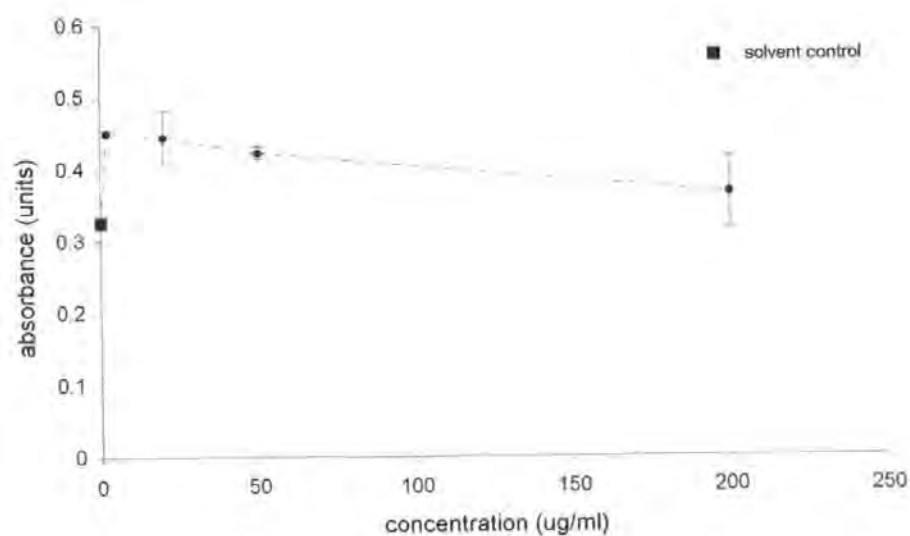


Figure 81. Cytotoxicity of the aliphatic fraction F 7 of the diesel fuel in the neutral red dye assay in Chinese hamster ovary CHO-K1 cells, without metabolic activation

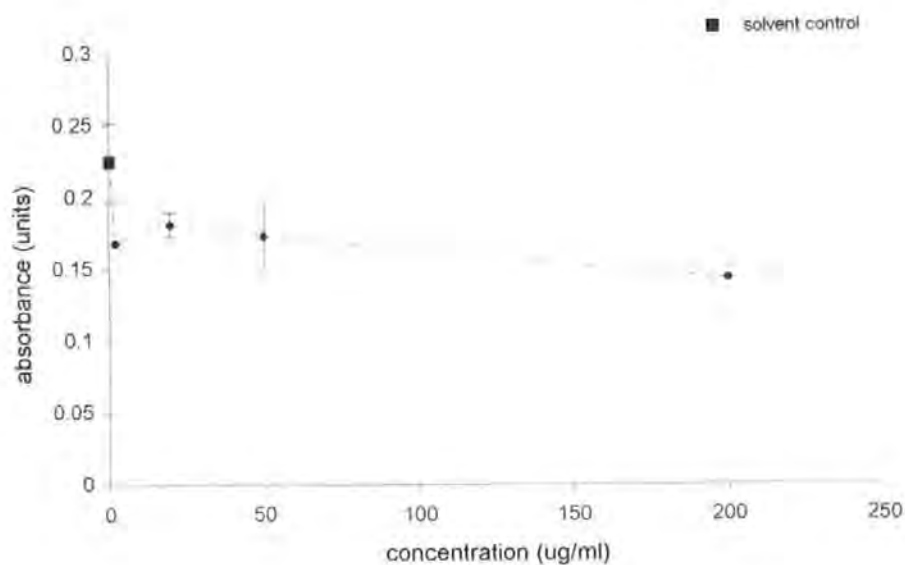


Figure 82. Cytotoxicity of the aliphatic fraction F 7 of diesel fuel in the neutral red dye assay in Chinese hamster ovary CHO-K1 cells, with metabolic activation (rat liver S9 fraction)

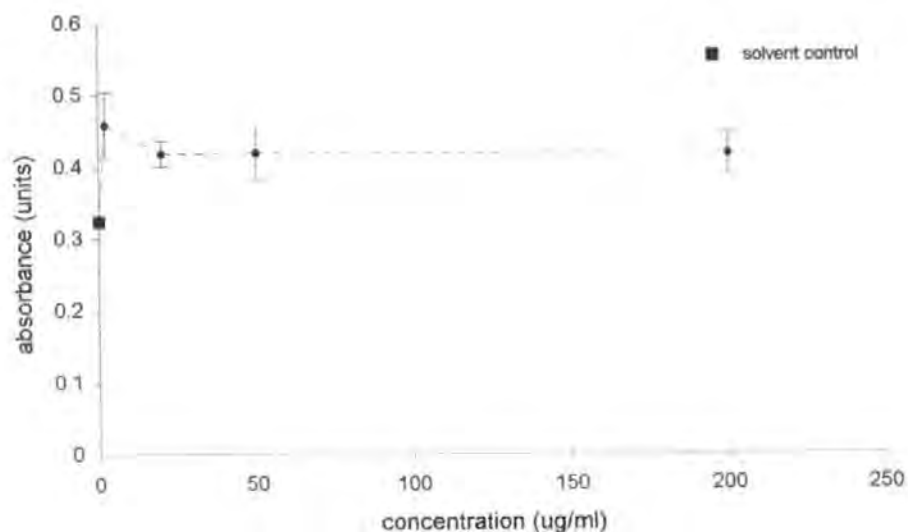


Figure 83. Cytotoxicity of the aliphatic fraction ES 37+40, from diesel engine emission sample collected at 3000 rpm/5 Nm, in the neutral red dye assay in Chinese hamster ovary CHO-K1 cells without metabolic activation

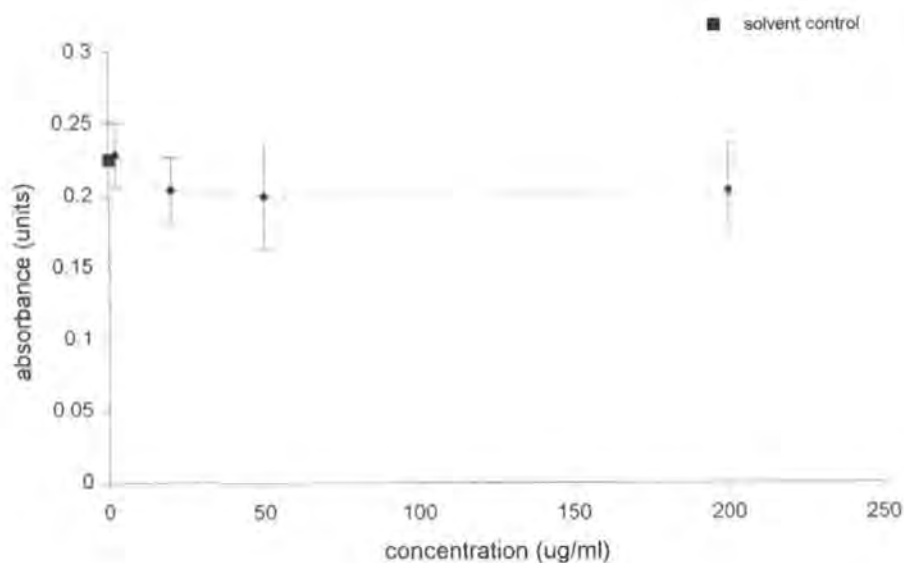


Figure 84. Cytotoxicity of the aliphatic fraction ES 37+40, from diesel engine emission sample collected at 3000 rpm/5 Nm, in the neutral red dye assay in Chinese hamster ovary CHO-K1 cells with metabolic activation (rat liver S9 fraction)

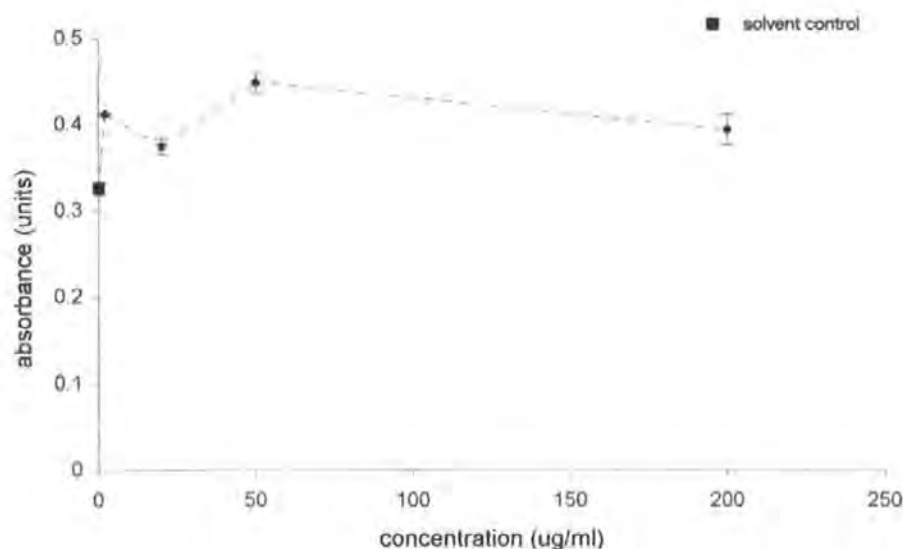


Figure 85. Cytotoxicity of the aliphatic fraction ES 43+46, from diesel engine emission sample collected at 1000 rpm/55 Nm, in the neutral red dye assay in Chinese hamster ovary CHO-K1 cells without metabolic activation

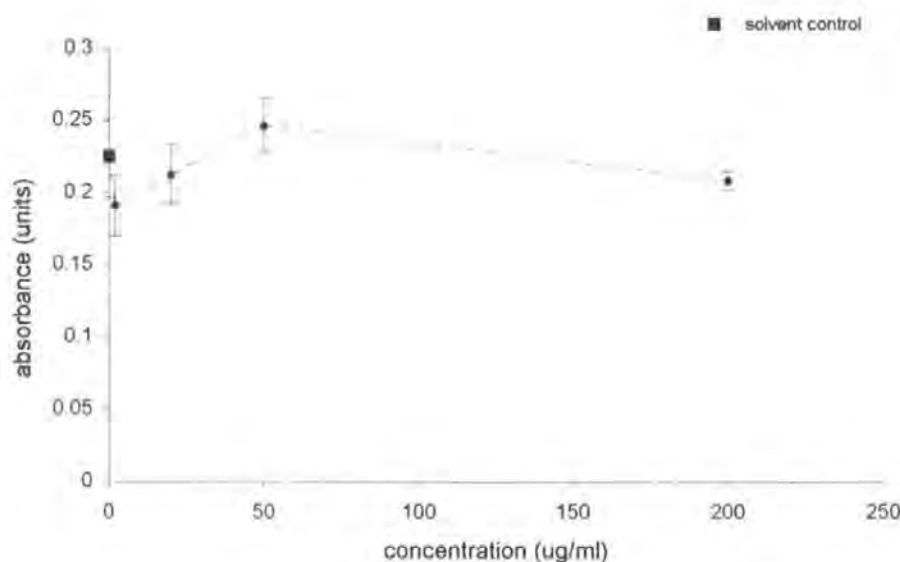


Figure 86. Cytotoxicity of the aliphatic fraction ES 43+46, from diesel engine emission sample collected at 1000 rpm/55 Nm, in the neutral red dye assay in Chinese hamster ovary CHO-K1 cells with metabolic activation (rat liver S9 fraction)

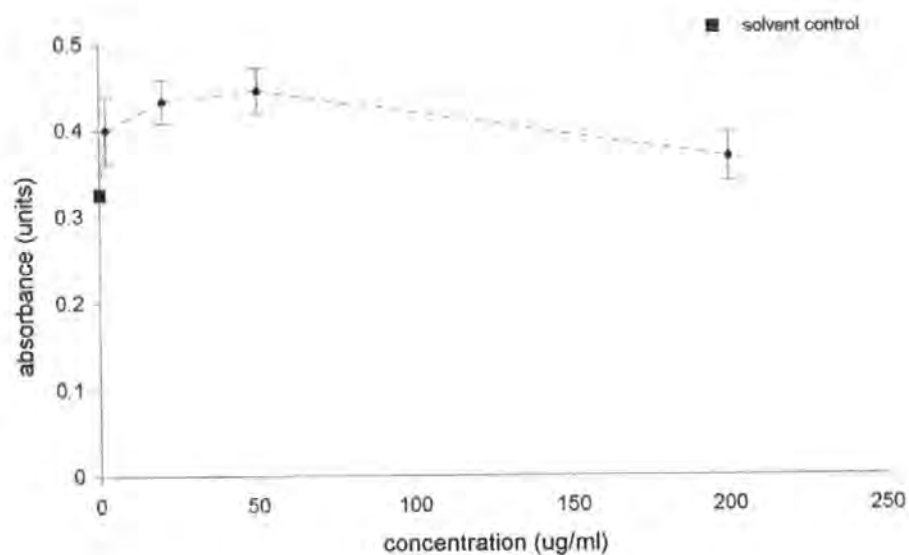


Figure 87. Cytotoxicity of the aliphatic fraction ES 49+52, from diesel engine emission sample collected at 1000 rpm/5 Nm, in the neutral red dye assay in Chinese hamster ovary CHO-K1 cells without metabolic activation

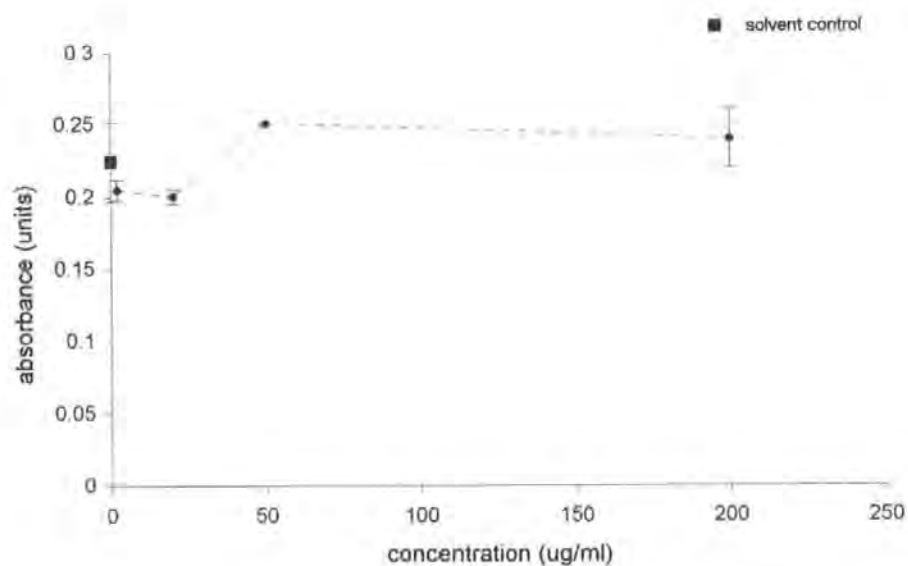


Figure 88. Cytotoxicity of the aliphatic fraction ES 49+52, from diesel engine emission sample collected at 1000 rpm/5 Nm, in the neutral red dye assay in Chinese hamster ovary CHO-K1 cells with metabolic activation (rat liver S9 fraction)

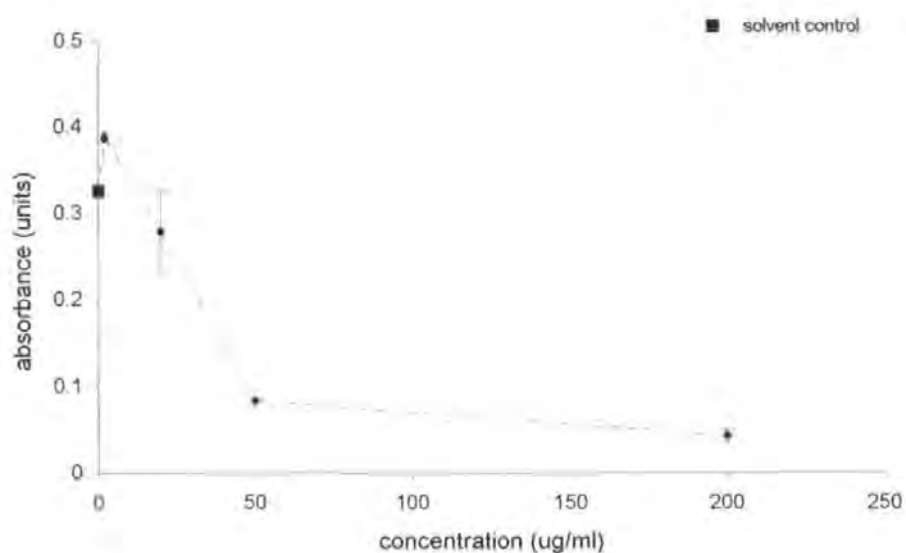


Figure 89. Cytotoxicity of the aromatic fraction F 8 of diesel fuel in the neutral red dye assay in Chinese hamster ovary CHO-K1 cells without metabolic activation

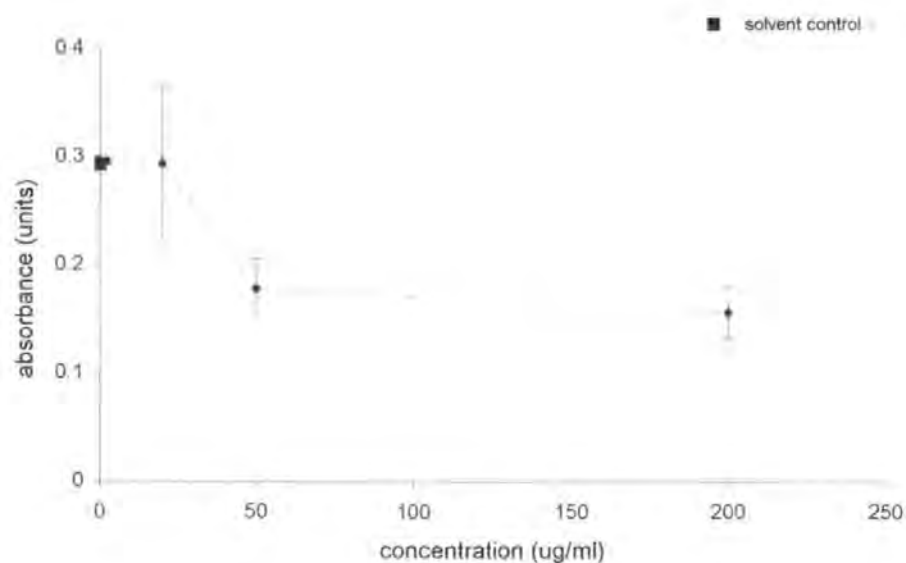


Figure 90. Cytotoxicity of the aromatic fraction F 8 of diesel fuel in the neutral red dye assay in Chinese hamster ovary CHO-K1 cells with metabolic activation (rat liver S9 fraction)

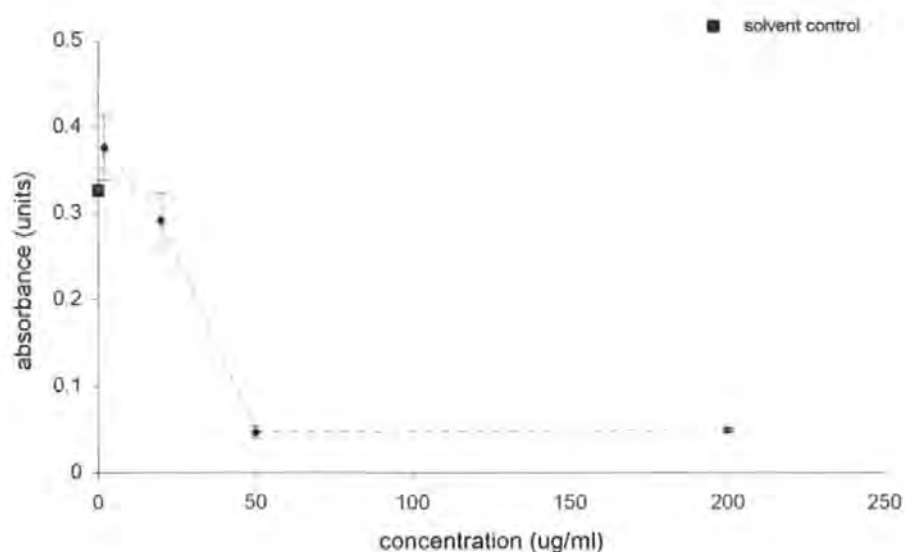


Figure 91. Cytotoxicity of the aromatic fraction ES 38+41, from diesel engine emission sample collected at 3000 rpm/5 Nm, in the neutral red dye assay in Chinese hamster ovary CHO-K1 cells without metabolic activation

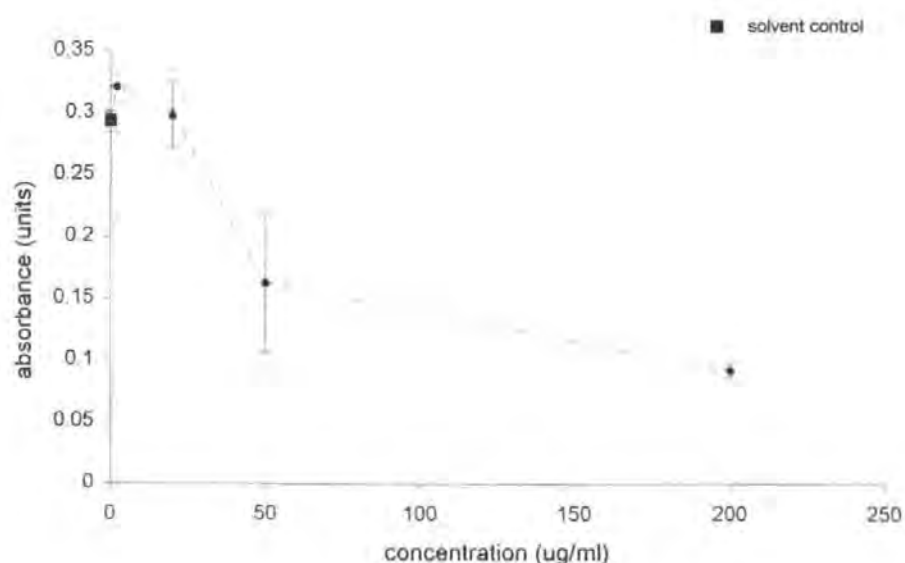


Figure 92. Cytotoxicity of the aromatic fraction ES 38+41, from diesel engine emission sample collected at 3000 rpm/5 Nm, in the neutral red dye assay in Chinese hamster ovary CHO-K1 cells with metabolic activation (rat liver S9 fraction)

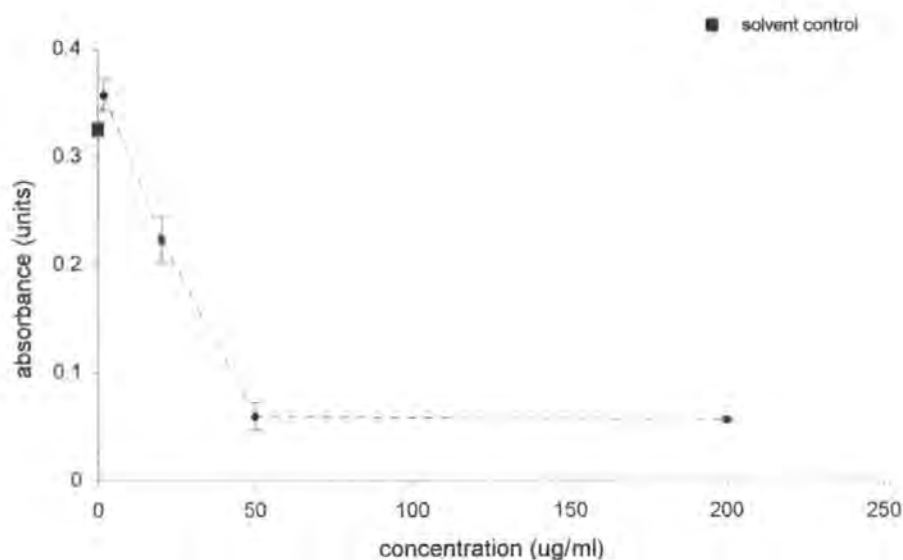


Figure 93. Cytotoxicity of the aromatic fraction ES 44+47, from diesel engine emission sample collected at 1000 rpm/55 Nm, in the neutral red dye assay in Chinese hamster ovary CHO-K1 cells without metabolic activation

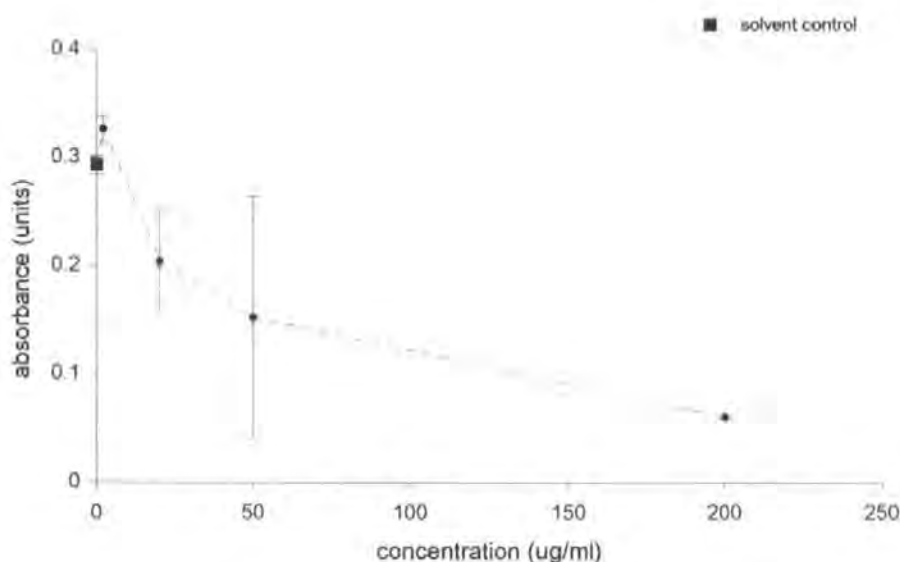


Figure 94. Cytotoxicity of the aromatic fraction ES 44+47, from diesel engine emission sample collected at 1000 rpm/55 Nm, in the neutral red dye assay in Chinese hamster ovary CHO-K1 cells with metabolic activation (rat liver S9 fraction)

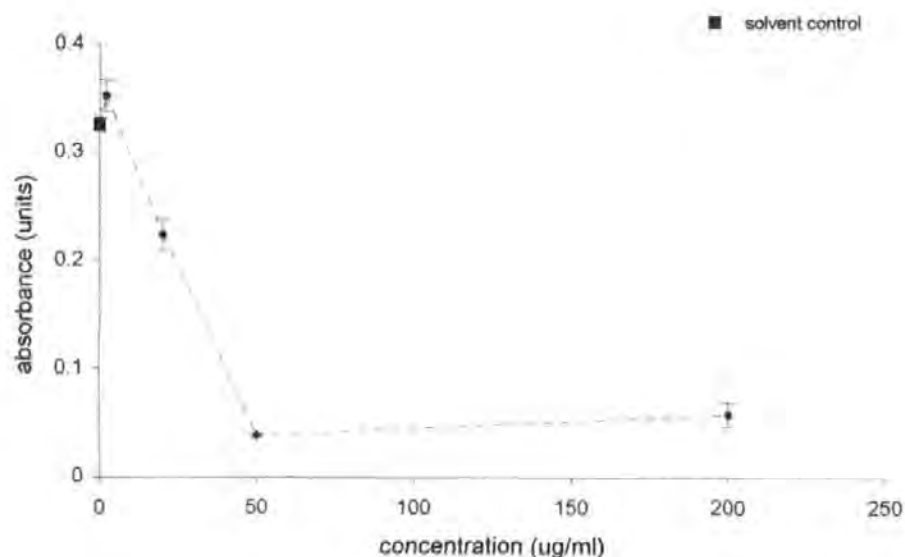


Figure 95. Cytotoxicity of the aromatic fraction ES 50+53, from diesel engine emission sample collected at 1000 rpm/5 Nm, in the neutral red dye assay in Chinese hamster ovary CHO-K1 cells without metabolic activation

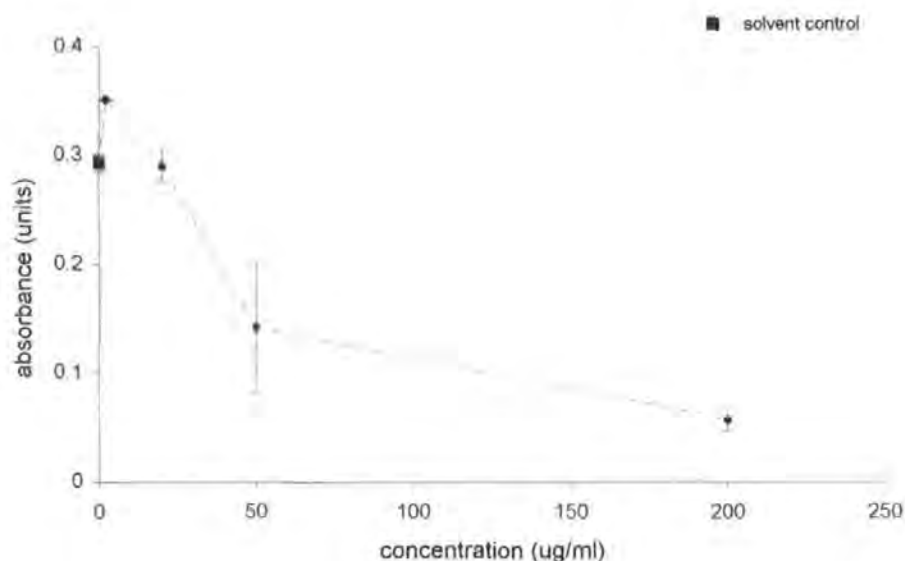


Figure 96. Cytotoxicity of the aromatic fraction ES 50+53, from diesel engine emission sample collected at 1000 rpm/5 Nm, in the neutral red dye assay in Chinese hamster ovary CHO-K1 cells with metabolic activation (rat liver S9 fraction)

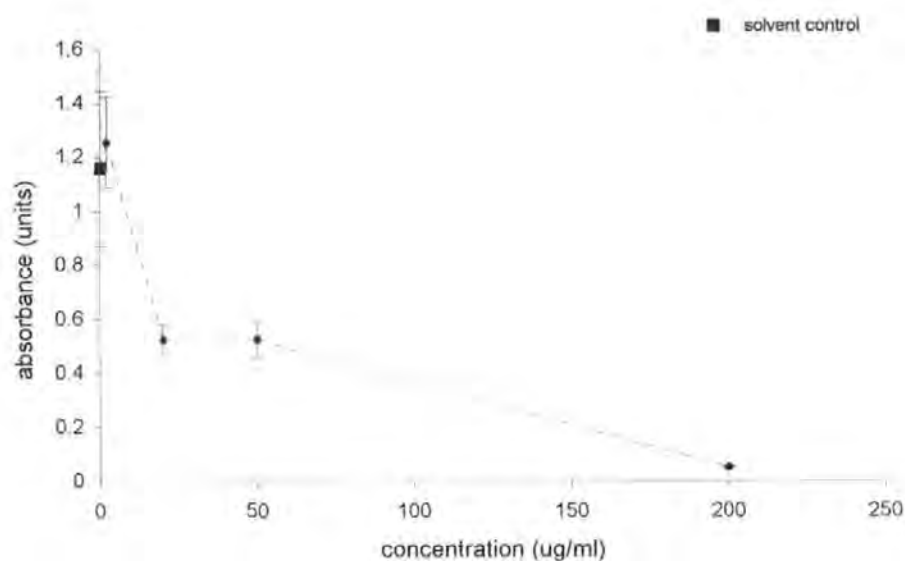


Figure 97. Cytotoxicity of the 1-ring aromatic fraction R 40 from diesel fuel in the neutral red dye assay in Chinese hamster ovary CHO-K1 cells, without metabolic activation

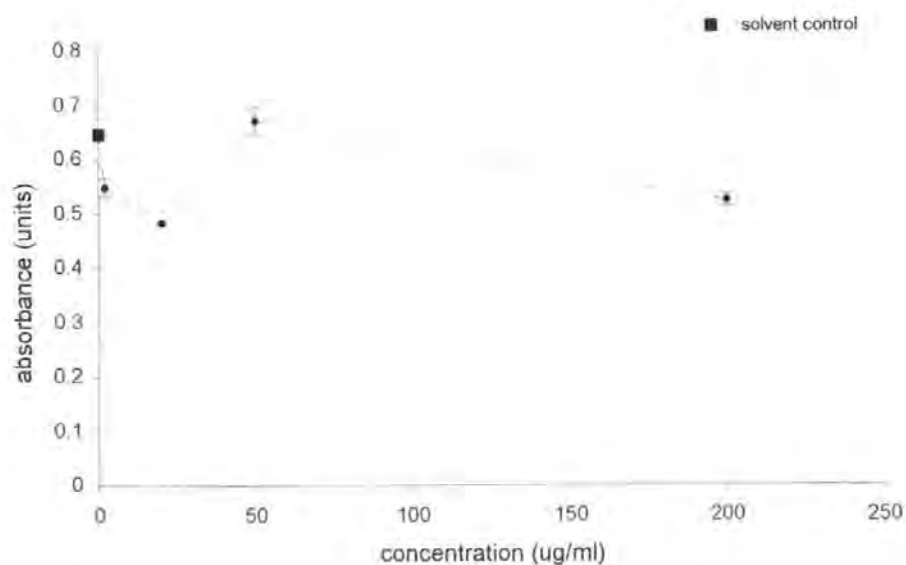


Figure 98. Cytotoxicity of the 1-ring aromatic fraction R 40 from diesel fuel in the neutral red dye assay in Chinese hamster ovary CHO-K1 cells, with metabolic activation (rat liver S9 fraction)

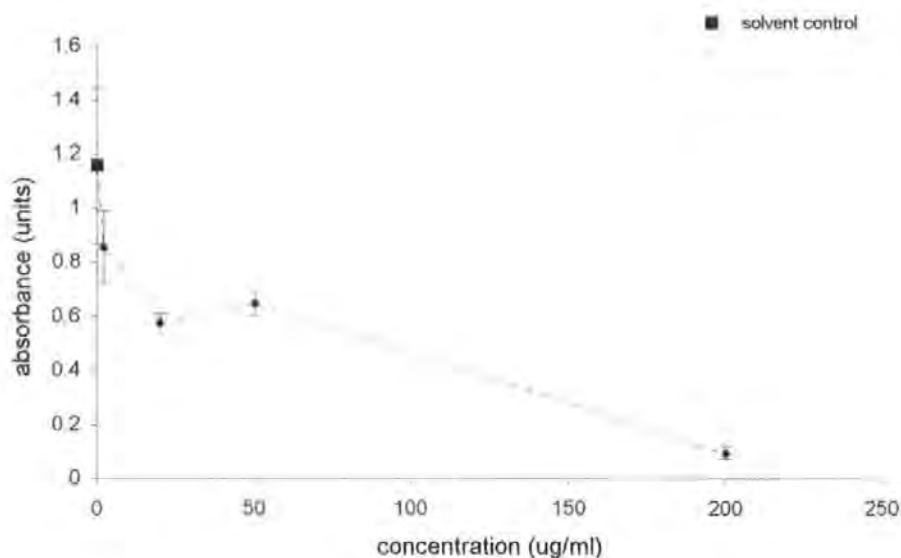


Figure 99. Cytotoxicity of the 1-ring aromatic fraction R 41, from diesel engine emission sample collected at 3000 rpm and 5 Nm, in the neutral red dye assay in Chinese hamster ovary CHO-K1 cells without metabolic activation

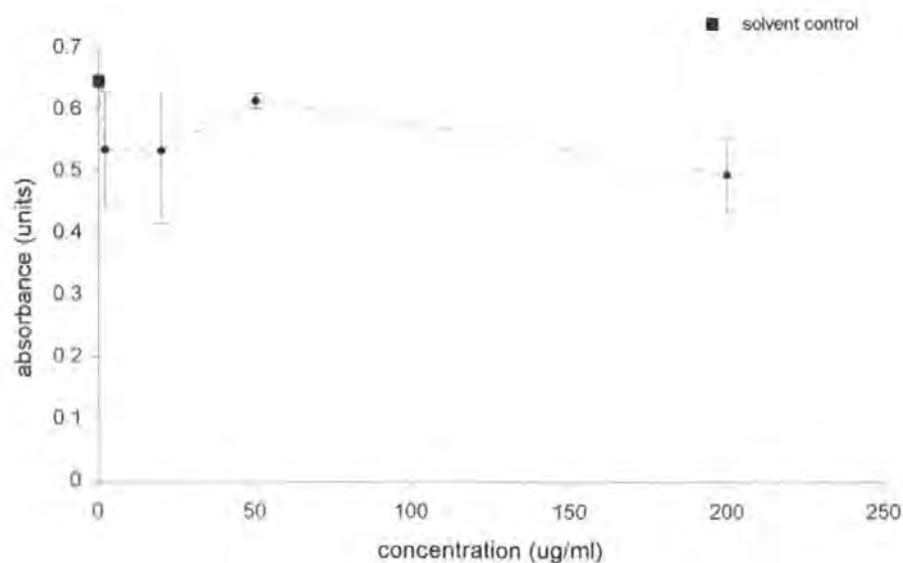


Figure 100. Cytotoxicity of the 1-ring aromatic fraction R 41, from diesel engine emission sample collected at 3000 rpm and 5 Nm, in the neutral red dye assay in Chinese hamster ovary CHO-K1 cells with metabolic activation (rat liver S9 fraction)

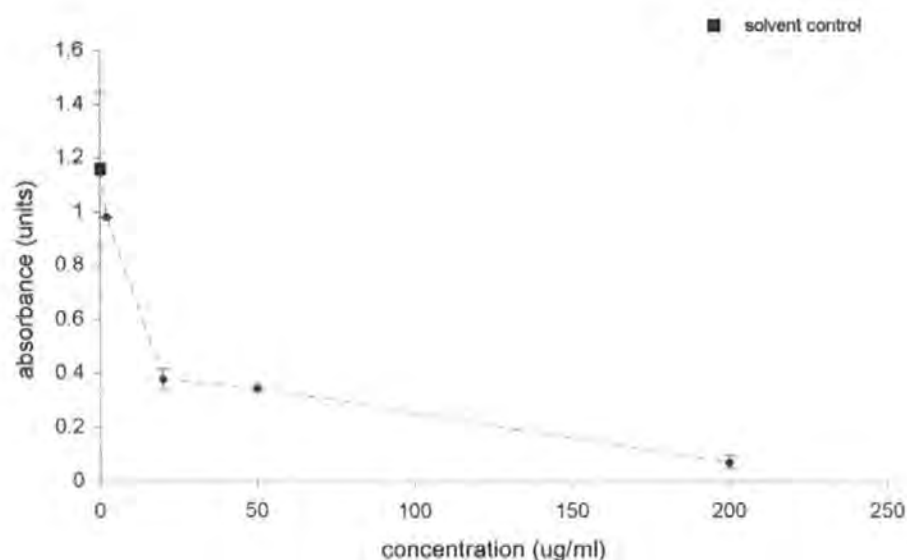


Figure 101. Cytotoxicity of the 1-ring aromatic fraction R 28+37, from diesel engine emission sample collected at 1000 rpm and 55 Nm, in the neutral red dye assay in Chinese hamster ovary CHO-K1 cells without metabolic activation

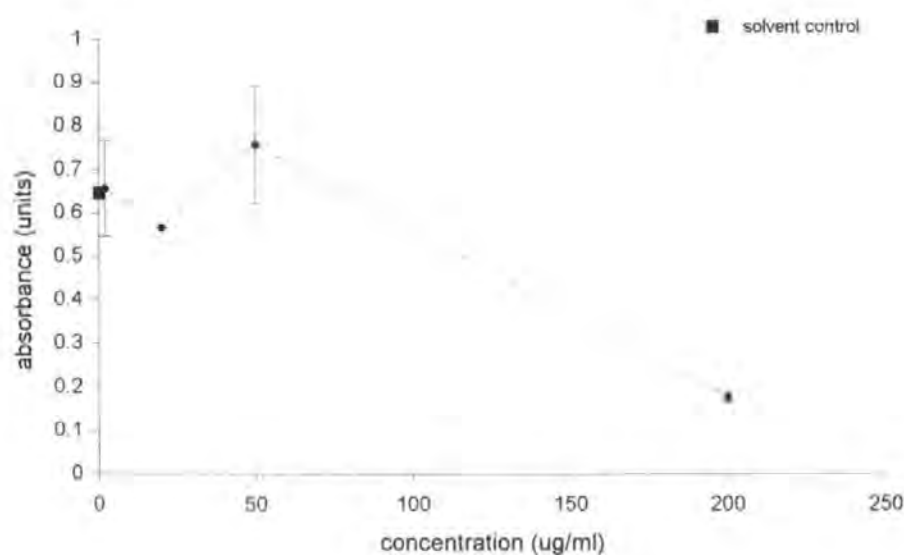


Figure 102. Cytotoxicity of the 1-ring aromatic fraction R 28+37, from diesel engine emission sample collected at 1000 rpm and 55 Nm, in the neutral red dye assay in Chinese hamster ovary CHO-K1 cells with metabolic activation (rat liver S9 fraction)

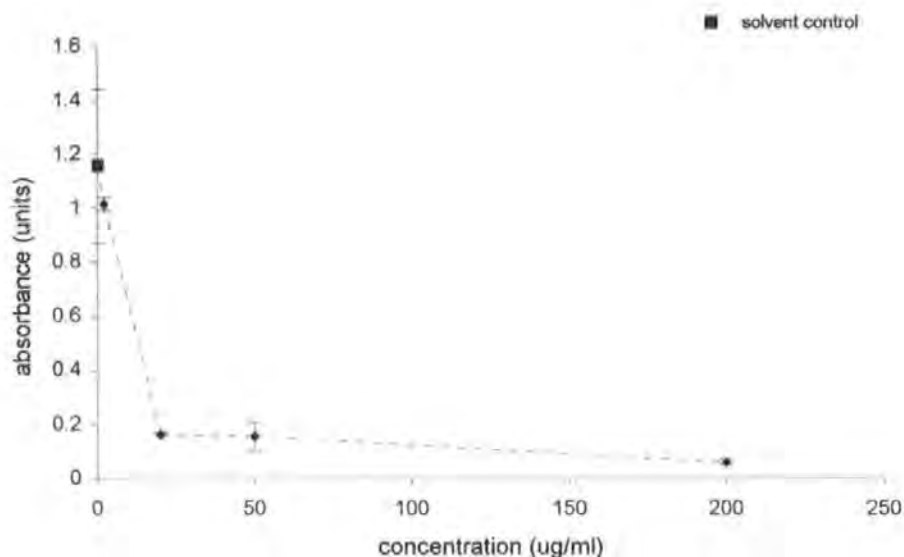


Figure 103. Cytotoxicity of the 2-ring aromatic fraction R 26 from diesel fuel in the neutral red dye assay in Chinese hamster ovary CHO-K1 cells, without metabolic activation

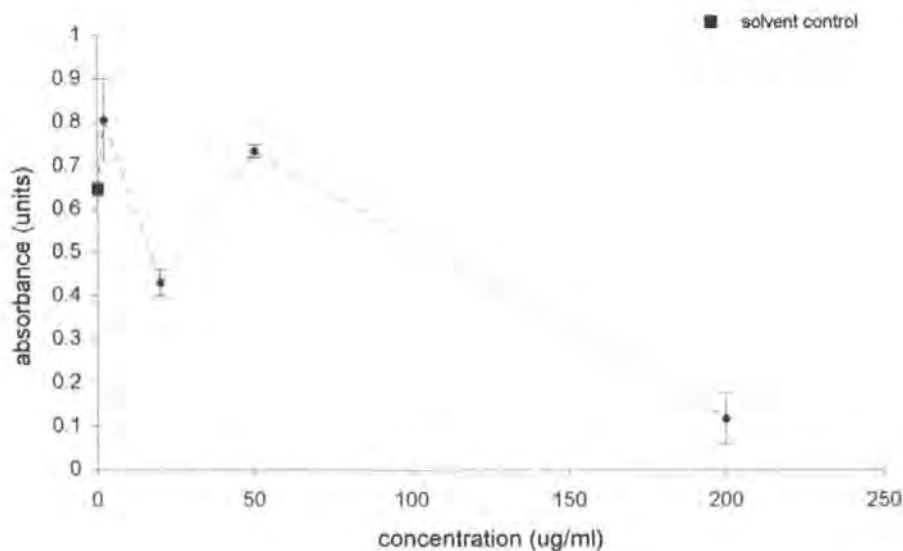


Figure 104. Cytotoxicity of the 2-ring aromatic fraction R 26 from diesel fuel in the neutral red dye assay in Chinese hamster ovary CHO-K1 cells, with metabolic activation (rat liver S9 fraction)

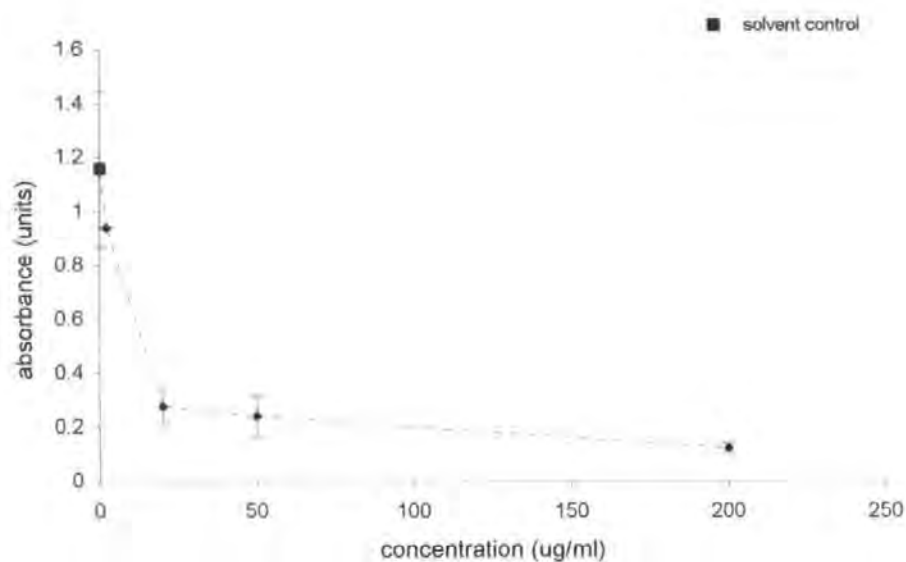


Figure 105. Cytotoxicity of the 2-ring aromatic fraction R 32, from diesel engine emission sample collected at 3000 rpm and 5 Nm, in the neutral red dye assay in Chinese hamster ovary CHO-K1 cells without metabolic activation

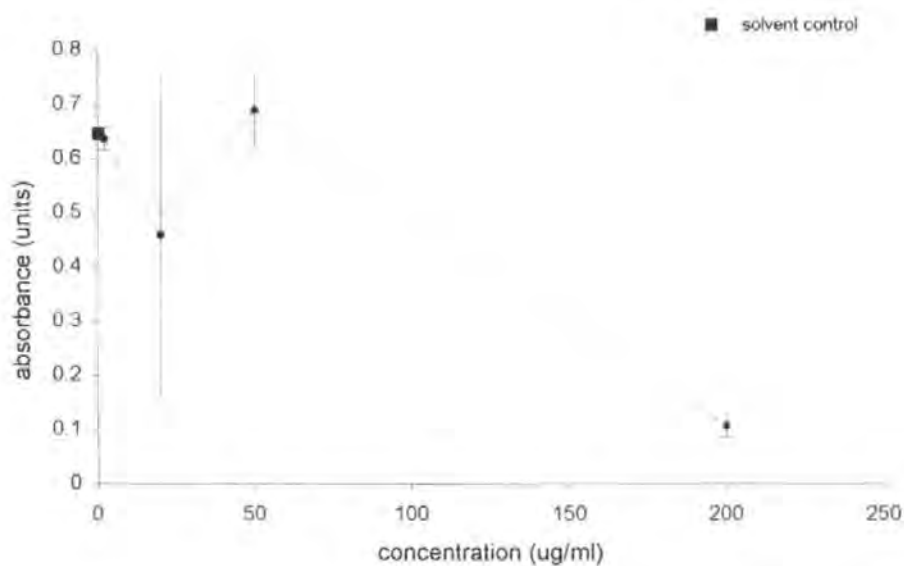


Figure 106. Cytotoxicity of the 2-ring aromatic fraction R 32, from diesel engine emission sample collected at 3000 rpm and 5 Nm, in the neutral red dye assay in Chinese hamster ovary CHO-K1 cells with metabolic activation (rat liver S9 fraction)

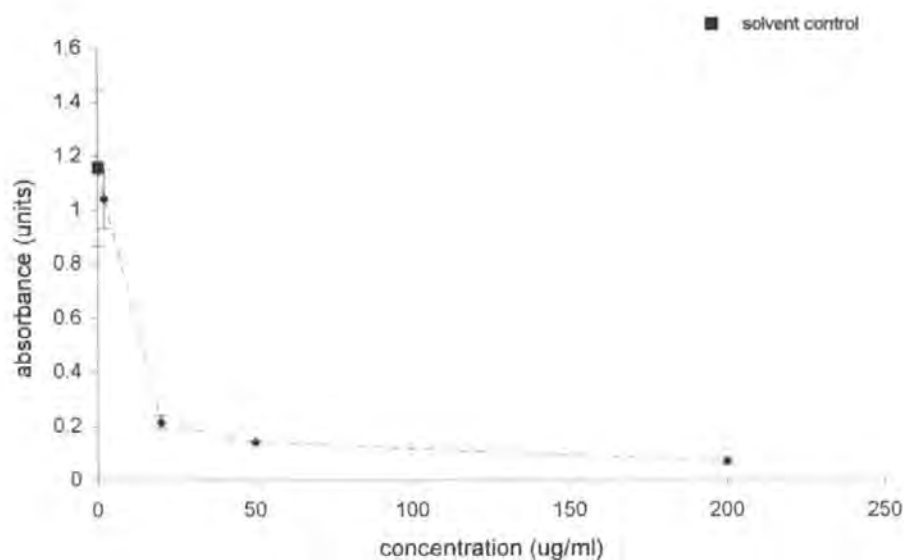


Figure 107. Cytotoxicity of the 2-ring aromatic fraction R 29+38, from diesel engine emission sample collected at 1000 rpm and 55 Nm, in the neutral red dye assay in Chinese hamster ovary CHO-K1 cells without metabolic activation

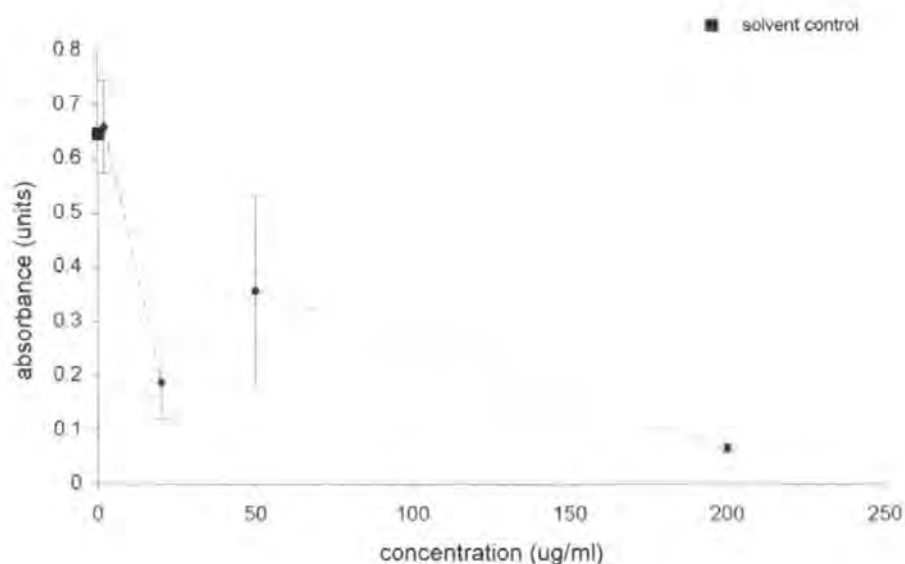


Figure 108. Cytotoxicity of the 2-ring aromatic fraction R 29+38, from diesel engine emission sample collected at 1000 rpm and 55 Nm, in the neutral red dye assay in Chinese hamster ovary CHO-K1 cells with metabolic activation (rat liver S9 fraction)

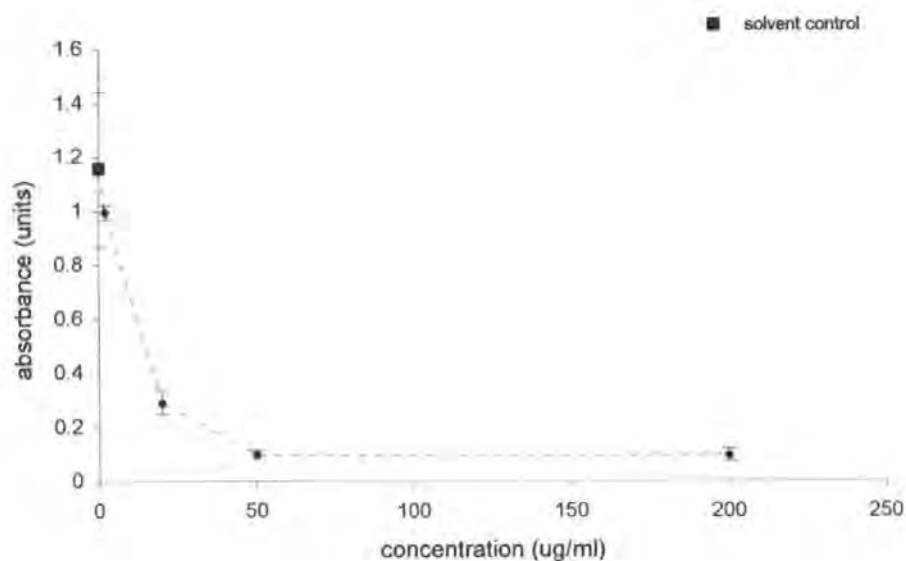


Figure 109. Cytotoxicity of the 3-ring aromatic fraction R 27 from diesel fuel in the neutral red dye assay in Chinese hamster ovary CHO-K1 cells, without metabolic activation

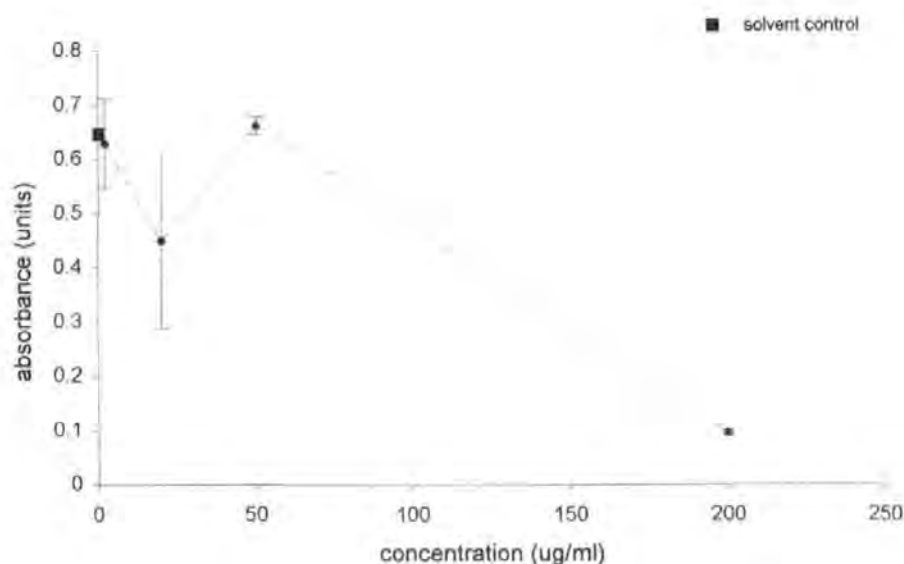


Figure 110. Cytotoxicity of the 3-ring aromatic fraction R 27 from diesel fuel in the neutral red dye assay in Chinese hamster ovary CHO-K1 cells, with metabolic activation (rat liver S9 fraction)

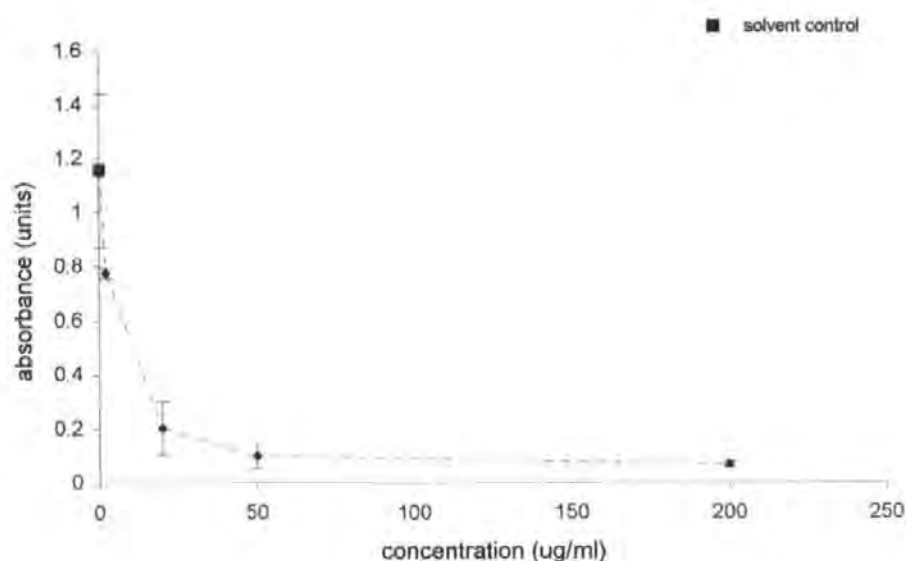


Figure 111. Cytotoxicity of the 3-ring aromatic fraction R 33, from diesel engine emission sample collected at 3000 rpm and 5 Nm, in the neutral red dye assay in Chinese hamster ovary CHO-K1 cells without metabolic activation

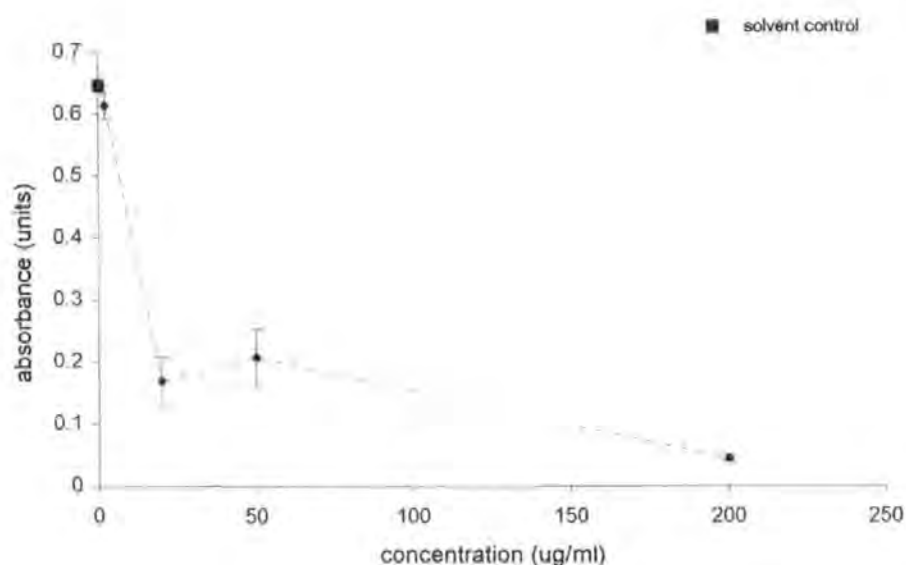


Figure 112. Cytotoxicity of the 3-ring aromatic fraction R 33, from diesel engine emission sample collected at 3000 rpm and 5 Nm, in the neutral red dye assay in Chinese hamster ovary CHO-K1 cells with metabolic activation (rat liver S9 fraction)

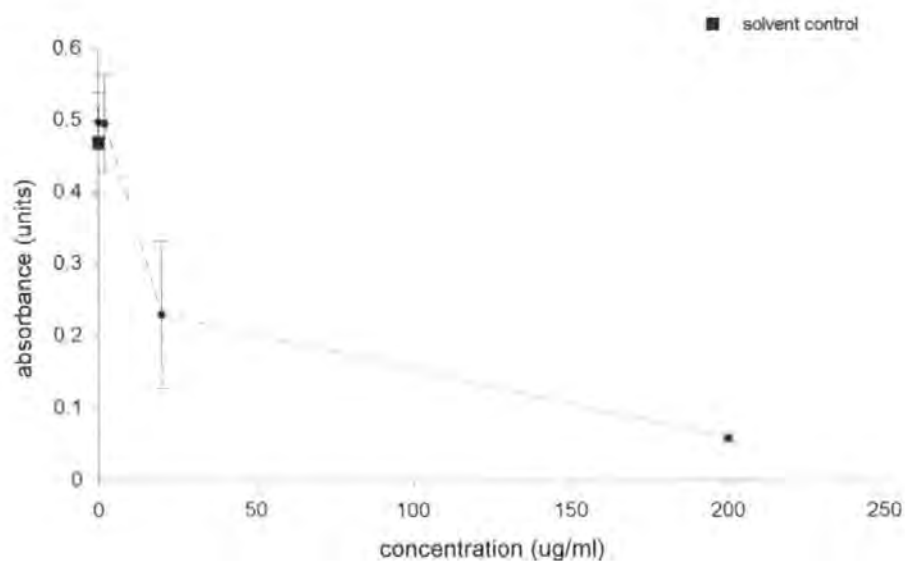


Figure 113. Cytotoxicity of the polar fraction ES 39+42, from diesel engine emission sample collected at 3000 rpm and 5 Nm, in the neutral red dye assay in Chinese hamster ovary CHO-K1 cells without metabolic activation

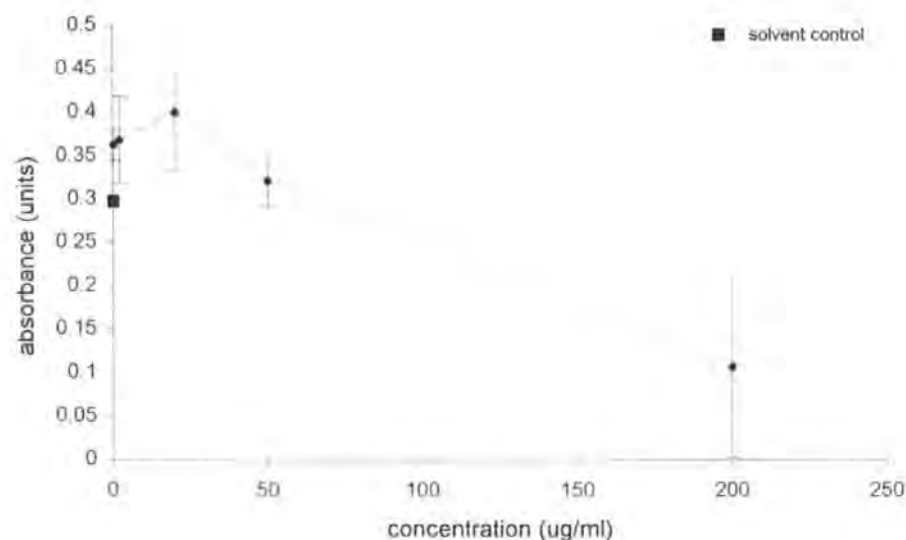


Figure 114. Cytotoxicity of the polar fraction ES 39+42, from diesel engine emission sample collected at 3000 rpm and 5 Nm, in the neutral red dye assay in Chinese hamster ovary CHO-K1 cells with metabolic activation (rat liver S9 fraction)

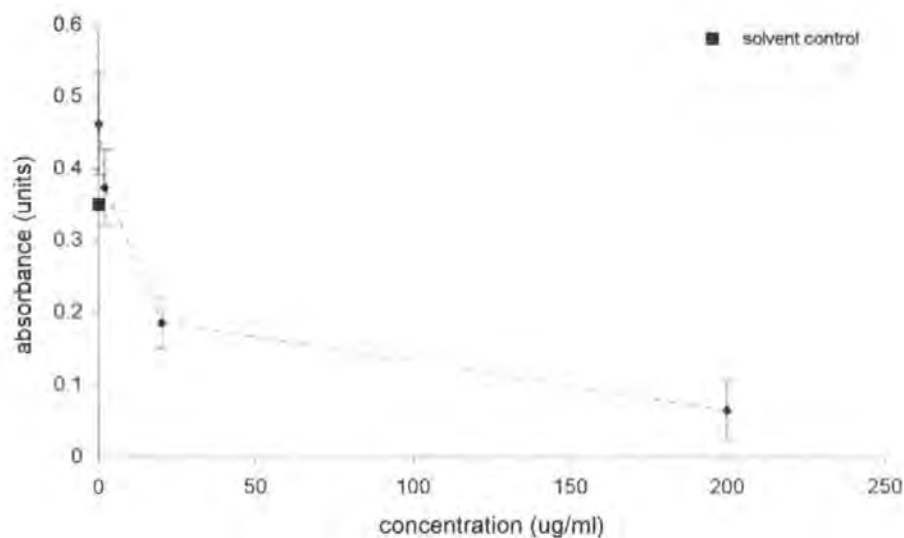


Figure 115. Cytotoxicity of the polar fraction ES 45+48, from diesel engine emission sample collected at 1000 rpm and 55 Nm, in the neutral red dye assay in Chinese hamster ovary CHO-K1 cells without metabolic activation

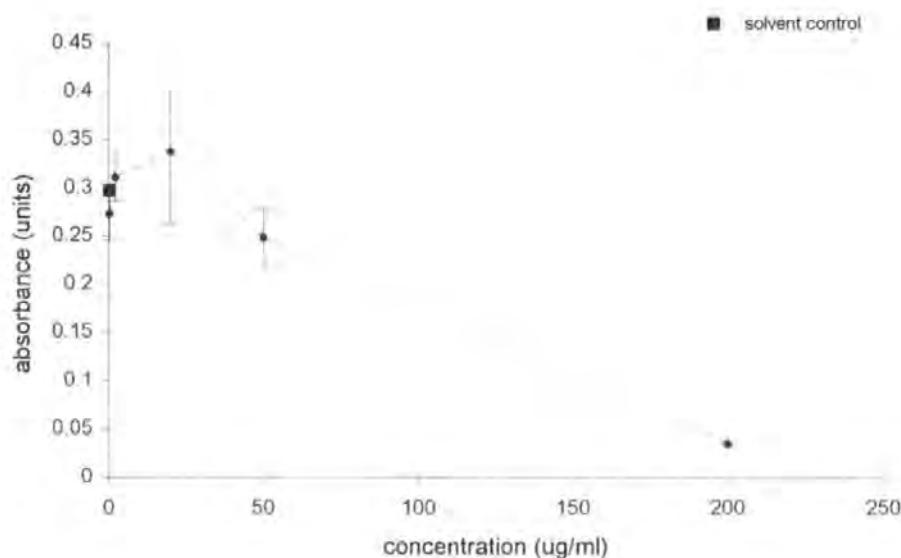


Figure 116. Cytotoxicity of the polar fraction ES 45+48, from diesel engine emission sample collected at 1000 rpm and 55 Nm, in the neutral red dye assay in Chinese hamster ovary CHO-K1 cells with metabolic activation (rat liver S9 fraction)

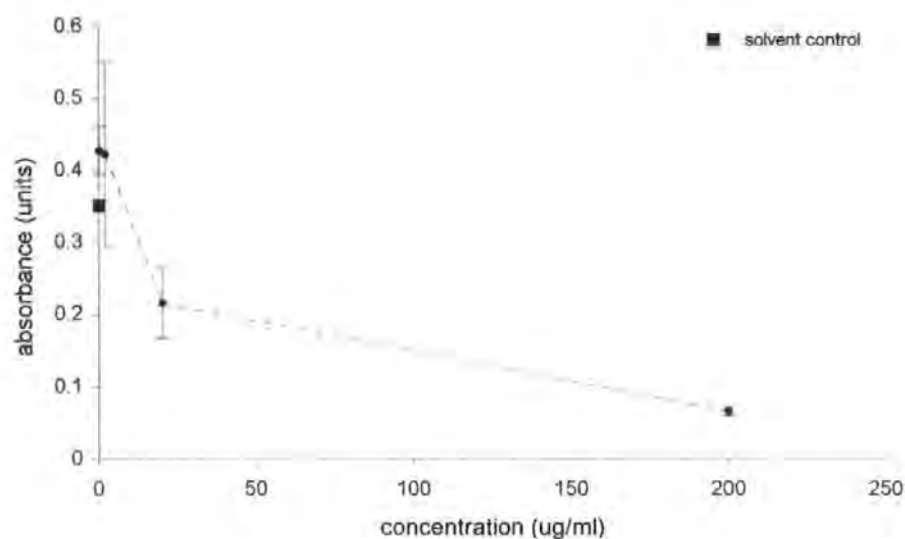


Figure 117. Cytotoxicity of the polar fraction ES 51+54, from diesel engine emission sample collected at 1000 rpm and 5 Nm, in the neutral red dye assay in Chinese hamster ovary CHO-K1 cells without metabolic activation

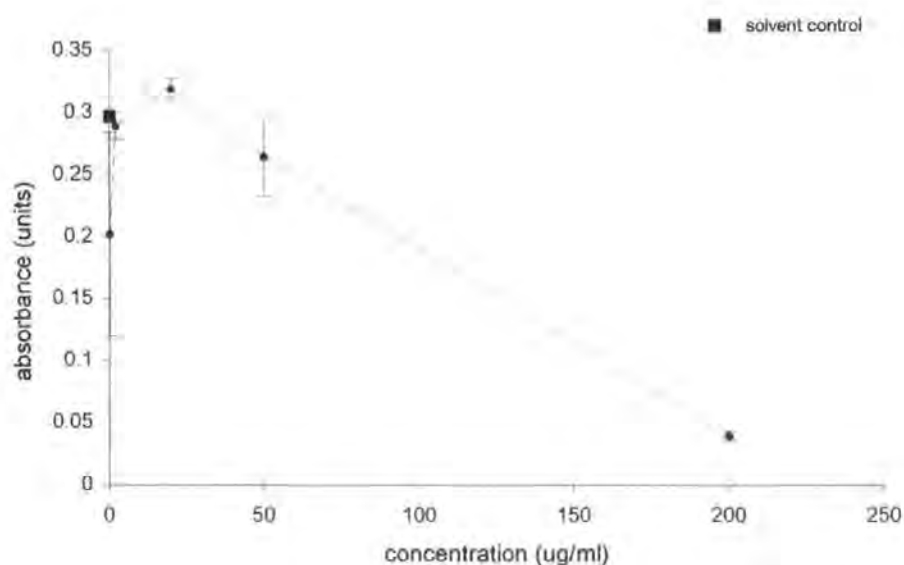


Figure 118. Cytotoxicity of the polar fraction ES 51+54, from diesel engine emission sample collected at 1000 rpm and 5 Nm, in the neutral red dye assay in Chinese hamster ovary CHO-K1 cells with metabolic activation (rat liver S9 fraction)

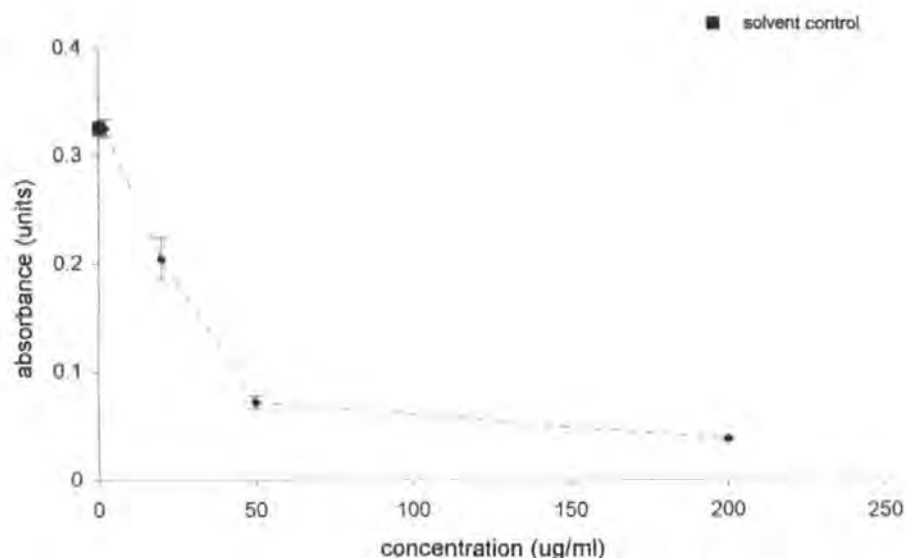


Figure 119. Cytotoxicity of the polar fraction ES 107, from diesel engine emission sample collected at 2000 rpm and 30 Nm, in the neutral red dye assay in Chinese hamster ovary CHO-K1 cells without metabolic activation

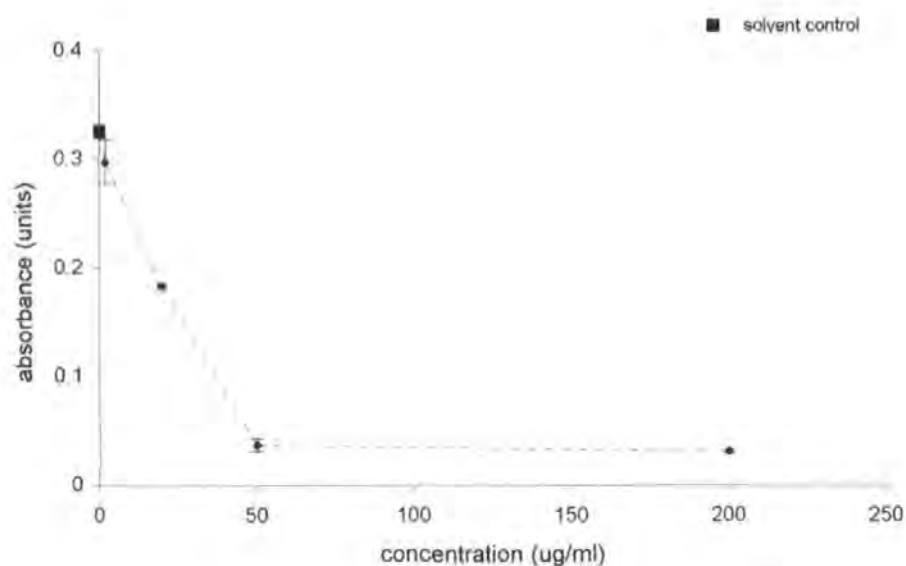


Figure 120. Cytotoxicity of the polar fraction ES 116, from diesel engine emission sample collected at 2000 rpm and 55 Nm, in the neutral red dye assay in Chinese hamster ovary CHO-K1 cells without metabolic activation

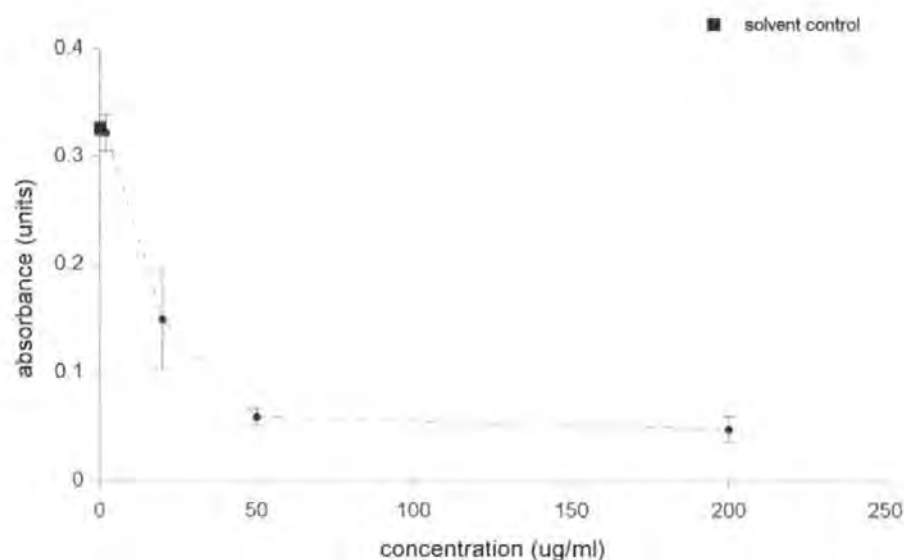


Figure 121. Cytotoxicity of the polar fraction ES 119, from diesel engine emission sample collected at 3000 rpm and 30 Nm, in the neutral red dye assay in Chinese hamster ovary CHO-K1 cells without metabolic activation

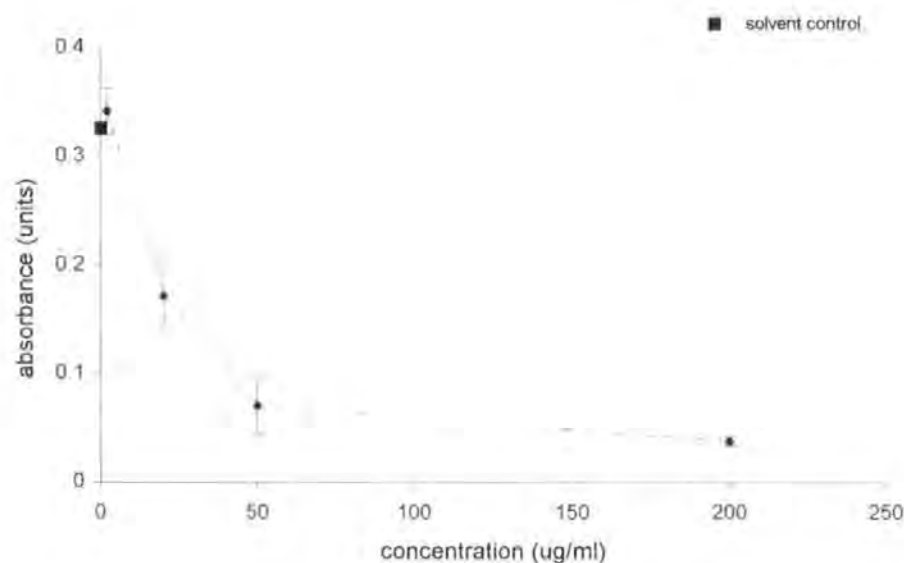


Figure 122. Cytotoxicity of the polar fraction ES 125, from diesel engine emission sample collected at 3000 rpm and 55 Nm, in the neutral red dye assay in Chinese hamster ovary CHO-K1 cells without metabolic activation

APPENDIX B

CHROMOSOME ABERRATION ASSAY DATA

Diesel fuel and engine emission sample fractions were exposed to Chinese hamster ovary CHO-K1 cells both in the presence and absence of metabolic activation (rat liver S9 fraction). Clastogenic response to sample exposure was recorded as the number of chromosomal aberrations observed in each category (simple, complex, total: section 2.6.4), and as the percentage of cells with chromosome aberrations at each concentration. Where replicate cultures have been scored they are recorded, together with the results of dispersion test calculations. The DMSO solvent control is represented as concentration zero. Aberration data for positive controls MNNG and CP are also given, together with mitotic rate at each sample concentration assayed.

concentration ($\mu\text{g/ml}$)	mitotic rate ¹	cells scored	simple aberrations		complex aberrations		total aberrations	
			number of aberrations	% cells	number of aberrations	% cells	number of aberrations	% cells
0	104	100	1	1	0	0	1	1
75	91	100	2	1	1	1	3	2
150	95	100	0	0	2	2	2	2
300	80	100	3	3	1	1	4	4
600	59	100	1	1	2	2	3	3
MNNG ²	39	100	9	8	6	6	15	14

¹ number of mitoses per 1,000 cells scored

² direct acting positive control MNNG, concentration 0.15 $\mu\text{g/ml}$

Table 54. Chromosome aberrations observed in Chinese hamster ovary CHO-K1 cells after exposure to aliphatic diesel emission sample ES 37+40 (3000 rpm speed/ 5 Nm load) without metabolic activation

concentration ($\mu\text{g/ml}$)	mitotic rate ¹	cells scored	simple aberrations		complex aberrations		total aberrations	
			number of aberrations	% cells	number of aberrations	% cells	number of aberrations	% cells
0	57	100	0	0	2	2	2	2
75	62	100	1	1	2	2	3	3
150	57	100	0	0	1	1	1	1
300	53	100	2	1	1	1	3	2
600	64	100	0	0	3	3	3	3
CP ³	38	100	10	8	12	10	22	17

¹ number of mitoses per 1,000 cells scored

³ indirect acting positive control cyclophosphamide, concentration 25 $\mu\text{g/ml}$

Table 55. Chromosome aberrations observed in Chinese hamster ovary CHO-K1 cells after exposure to aliphatic diesel emission sample ES 37+40 (3000 rpm speed/ 5 Nm load) with metabolic activation (rat liver S9 fraction)

concentration ($\mu\text{g/ml}$)	mitotic rate ¹	cells scored	simple aberrations		complex aberrations		total aberrations	
			number of aberrations	% cells	number of aberrations	% cells	number of aberrations	% cells
0	70	100	1	1	0	0	1	1
10	60	100	1	1	2	2	3	3
20	49	100	0	0	3	2	3	2
30	34	100	3	3	2	1	5	4
40	9	100	2	2	3	3	5	5
MNNG ²	29	100	5	5	5	5	10	10

¹ number of mitoses per 1,000 cells scored

² direct acting positive control MNNG, concentration 0.15 $\mu\text{g/ml}$

Table 56. Chromosome aberrations observed in Chinese hamster ovary CHO-K1 cells after exposure to the aromatic fraction F 8 of diesel fuel, without metabolic activation

concentration ($\mu\text{g/ml}$)	mitotic rate ¹	cells scored	simple aberrations		complex aberrations		total aberrations	
			number of aberrations	% cells	number of aberrations	% cells	number of aberrations	% cells
0	83	100	0	0	1	1	1	1
10	68	100	3	3	1	1	4	4
20	52	100	3	3	1	1	4	4
30	58	100	1	1	1	1	2	2
40	40	100	3	3	1	1	4	4
CP ³	8	100	8	7	6	6	14	13

¹ number of mitoses per 1,000 cells scored

³ indirect acting positive control cyclophosphamide, concentration 25 $\mu\text{g/ml}$

Table 57. Chromosome aberrations observed in Chinese hamster ovary CHO-K1 cells after exposure to the aromatic fraction F 8 of diesel fuel, with metabolic activation (rat liver S9 fraction)

concentration ($\mu\text{g/ml}$)	mitotic rate ¹	cells scored	simple aberrations		complex aberrations		total aberrations	
			number of aberrations	% cells	number of aberrations	% cells	number of aberrations	% cells
0	80	100	2	2	3	3	5	5
10	106	100	4	4	5	3	9	7
20	96	100	3	3	4	4	7	7
30	21	100	1	1	3	3	4	4
40	10	100	4	4	3	3	7	7
MNNG ²	90	100	5	5	5	5	10	10

¹ number of mitoses per 1,000 cells scored

² direct acting positive control MNNG, concentration 0.15 $\mu\text{g/ml}$

Table 58. Chromosome aberrations observed in Chinese hamster ovary CHO-K1 cells after exposure to aromatic diesel emission sample ES 38+41 (3000 rpm speed/ 5 Nm load), without metabolic activation

concentration ($\mu\text{g/ml}$)	mitotic rate ¹	cells scored	simple aberrations		complex aberrations		total aberrations	
			number of aberrations	% cells	number of aberrations	% cells	number of aberrations	% cells
0	68	100	3	3	1	1	4	4
10	68	100	0	0	0	0	0	0
20	87	100	3	3	2	2	5	5
30	112	100	3	3	2	2	5	5
40	75	100	1	1	4	4	5	5
CP ²	26	100	11	11	7	5	19	16

¹ number of mitoses per 1,000 cells scored

² indirect acting positive control cyclophosphamide, concentration 25 $\mu\text{g/ml}$

Table 59. Chromosome aberrations observed in Chinese hamster ovary CHO-K1 cells after exposure to aromatic diesel emission sample ES 38+41 (3000 rpm speed/ 5 Nm load), with metabolic activation (rat liver S9 fraction)

Concentration ($\mu\text{g/ml}$)	Mitotic rate ¹	Cells scored	Simple aberrations		Complex aberrations		Total aberrations	
			Number of aberrations	% cells	Number of aberrations	% cells	Number of aberrations	% cells
0	83	100	3	3	2	2	5	5
100	52	100	1	1	4	4	5	5
CP ²	31	100	10	9	7	7	17	16

¹ number of mitoses per 1,000 cells scored

² indirect acting positive control cyclophosphamide, concentration 25 $\mu\text{g/ml}$

³ rat liver S9 fraction increased to 6.7 % of the S9 mix, Section 2.7.5

Table 60. Chromosome aberrations observed in Chinese hamster ovary CHO-K1 cells after exposure to aromatic diesel emission sample ES 38+41 (3000 rpm speed/ 5 Nm load), with 2 x S9 mix metabolic activation (double concentration of rat liver S9 fraction)³

concentration ($\mu\text{g/ml}$)	mitotic rate ¹	cells scored	simple aberrations		complex aberrations		total aberrations	
			number of aberrations	% cells	number of aberrations	% cells	number of aberrations	% cells
0	70	100	2	2	1	1	3	3
10	68	100	1	1	3	2	4	3
20	54	100	3	3	1	1	4	4
30	27	100	3	2	3	3	6	5
40	8	100	2	2	2	2	4	4
MNNG ²	23	100	6	5	7	6	13	11

¹ number of mitoses per 1,000 cells scored

² direct acting positive control MNNG, concentration 0.15 $\mu\text{g/ml}$

Table 61. Chromosome aberrations observed in Chinese hamster ovary CHO-K1 cells after exposure to aromatic diesel emission sample ES 44+47 (1000 rpm speed/ 55 Nm load) without metabolic activation

concentration ($\mu\text{g/ml}$)	mitotic rate ¹	cells scored	simple aberrations		complex aberrations		total aberrations	
			number of aberrations	% cells	number of aberrations	% cells	number of aberrations	% cells
0	68	100	3	3	1	1	4	4
10	103	100	1	1	1	1	2	2
20	53	100	1	1	1	1	2	2
30	57	100	0	0	1	1	1	1
40	40	100	2	2	1	1	3	3
CP ³	26	100	11	11	7	5	19	16

¹ number of mitoses per 1,000 cells scored

³ indirect acting positive control cyclophosphamide, concentration 25 $\mu\text{g/ml}$

Table 62. Chromosome aberrations observed in Chinese hamster ovary CHO-K1 cells after exposure to aromatic diesel emission sample ES 44+47 (1000 rpm speed/ 55 Nm load) with metabolic activation (rat liver S9 fraction)

concentration ($\mu\text{g/ml}$)	mitotic rate ¹	cells scored	simple aberrations		complex aberrations		total aberrations	
			number of aberrations	% cells	number of aberrations	% cells	number of aberrations	% cells
0	72	100	2	2	2	1	4	3
10	76	100	3	3	1	1	4	4
20	49	100	1	1	2	2	3	3
30	25	100	1	1	1	1	2	2
40	11	100	1	1	2	2	3	3
MNNG ²	65	100	6	5	6	6	12	11

¹ number of mitoses per 1,000 cells scored

² direct acting positive control MNNG, concentration 0.15 $\mu\text{g/ml}$

Table 63. Chromosome aberrations observed in Chinese hamster ovary CHO-K1 cells after exposure to aromatic diesel emission sample ES 50+53 (1000 rpm speed/ 5 Nm load) without metabolic activation

concentration ($\mu\text{g/ml}$)	mitotic rate ¹	Cells scored	simple aberrations		complex aberrations		total aberrations	
			number of aberrations	% cells	number of aberrations	% cells	number of aberrations	% cells
0	53	100	0	0	0	0	0	0
10	61	100	5	5	2	2	7	7
20	47	100	0	0	1	1	1	1
30	56	100	1	1	2	2	3	3
40	23	100	1	1	1	1	2	2
CP ³	22	100	12	8	8	6	20	13

¹ number of mitoses per 1,000 cells scored

³ indirect acting positive control cyclophosphamide, concentration 25 $\mu\text{g/ml}$

Table 64. Chromosome aberrations observed in Chinese hamster ovary CHO-K1 cells after exposure to aromatic diesel emission sample ES 50+53 (1000 rpm speed/ 5 Nm load) with metabolic activation (rat liver S9 fraction)

concentration ($\mu\text{g/ml}$)	mitotic rate ¹	cells scored	simple aberrations		complex aberrations		total aberrations	
			number of aberrations	% cells	number of aberrations	% cells	number of aberrations	% cells
0	68	100	1	1	1	1	2	2
12.5	72	100	1	1	3	3	4	4
25	42	100	2	1	1	1	3	2
50	23	100	1	1	2	2	3	3
75	2	*						
MNNG ²	47	100	8	8	6	5	14	13

* mitotic rate too low to score aberrations

¹ number of mitoses per 1,000 cells scored

² direct acting positive control MNNG, concentration 0.15 $\mu\text{g/ml}$

Table 65. Chromosome aberrations observed in Chinese hamster ovary CHO-K1 cells after exposure to 1-ring aromatic fraction of diesel fuel (R 40) without metabolic activation

concentration ($\mu\text{g/ml}$)	mitotic rate ¹	cells scored	simple aberrations		complex aberrations		total aberrations	
			number of aberrations	% cells	number of aberrations	% cells	number of aberrations	% cells
0	42	100	2	2	1	1	3	3
25	37	100	2	2	3	3	5	5
50	39	100	2	2	0	0	2	2
100	41	100	2	2	1	1	3	3
200	28	100	1	1	3	2	4	3
CP ³	23	100	11	10	8	8	19	17

¹ number of mitoses per 1,000 cells scored

³ indirect acting positive control cyclophosphamide, concentration 25 $\mu\text{g/ml}$

Table 66. Chromosome aberrations observed in Chinese hamster ovary CHO-K1 cells after exposure to 1-ring aromatic fraction of diesel fuel (R 40) with metabolic activation (rat liver S9 fraction)

concentration ($\mu\text{g/ml}$)	mitotic rate ¹	cells scored	simple aberrations		complex aberrations		total aberrations	
			number of aberrations	% cells	number of aberrations	% cells	number of aberrations	% cells
0	68	100	1	1	1	1	2	2
12.5	65	100	2	1	2	2	4	3
25	45	100	2	2	1	1	3	3
50	37	100	0	0	2	2	2	2
75		*						
MNNG ²	47	100	8	8	6	5	14	13

* mitotic rate too low to score aberrations

¹ number of mitoses per 1,000 cells scored

² direct acting positive control MNNG, concentration 0.15 $\mu\text{g/ml}$

Table 67. Chromosome aberrations observed in Chinese hamster ovary CHO-K1 cells after exposure to 1-ring aromatic diesel emission fraction R 41 (3000 rpm speed/5 Nm load) without metabolic activation

concentration ($\mu\text{g/ml}$)	mitotic rate ¹	cells scored	simple aberrations		complex aberrations		total aberrations	
			number of aberrations	% cells	number of aberrations	% cells	number of aberrations	% cells
0	42	100	2	2	1	1	3	3
25	57	100	2	1	0	0	2	1
50	47	100	3	3	2	2	5	5
100	32	100	2	2	1	1	3	3
200	38	100	2	2	3	3	5	5
CP ³	23	100	11	10	8	8	19	17

¹ number of mitoses per 1,000 cells scored

³ indirect acting positive control cyclophosphamide, concentration 25 $\mu\text{g/ml}$

Table 68. Chromosome aberrations observed in Chinese hamster ovary CHO-K1 cells after exposure to 1-ring aromatic diesel emission fraction R 41 (3000 rpm speed/5 Nm load) with metabolic activation (rat liver S9 fraction)

concentration (µg/ml)	mitotic rate ¹	cells scored	simple aberrations		complex aberrations		total aberrations	
			number of aberrations	% cells	number of aberrations	% cells	number of aberrations	% cells
0	97	100	0	0	0	0	0	0
10	82	100	1	1	0	0	1	1
15	65	100	1	1	2	2	3	3
20	54	100	4	4	0	0	4	4
50	4	*						
MNNG ²	39	100	8	8	7	7	15	14

* mitotic rate too low to score aberrations

¹ number of mitoses per 1,000 cells scored

² direct acting positive control MNNG, concentration 0.15 µg/ml

Table 69. Chromosome aberrations observed in Chinese hamster ovary CHO-K1 cells after exposure to 1-ring aromatic diesel emission fraction R 28+37 (1000 rpm speed/55 Nm load) without metabolic activation

concentration (µg/ml)	mitotic rate ¹	cells scored	simple aberrations		complex aberrations		total aberrations	
			number of aberrations	% cells	number of aberrations	% cells	number of aberrations	% cells
0	42	100	2	2	1	1	3	3
25	61	100	2	2	1	0	3	2
50	53	100	1	1	0	0	1	1
100	61	100	3	2	1	1	4	3
150	39	100	2	2	2	1	4	3
200	20	100	1	1	2	2	3	3
CP ³	24	100	11	10	8	8	19	17

¹ number of mitoses per 1,000 cells scored

³ indirect acting positive control cyclophosphamide, concentration 25 µg/ml

Table 70. Chromosome aberrations observed in Chinese hamster ovary CHO-K1 cells after exposure to 1-ring aromatic diesel emission fraction R 28+37 (1000 rpm speed/55 Nm load) with metabolic activation (rat liver S9 fraction)

concentration ($\mu\text{g/ml}$)	mitotic rate ¹	cells scored	simple aberrations		complex aberrations		total aberrations	
			number of aberrations	% cells	number of aberrations	% cells	number of aberrations	% cells
0	75	100	1	1	2	2	3	3
5	58	100	1	1	3	3	4	4
10	72	100	1	1	2	2	3	3
15	62	100	1	1	2	2	3	3
20	29	100	2	2	2	2	4	4
40	*							
MNNG ²	49	100	5	5	9	8	14	13

* mitotic rate too low to score aberrations

¹ number of mitoses per 1,000 cells scored

² direct acting positive control MNNG, concentration 0.15 $\mu\text{g/ml}$

Table 71. Chromosome aberrations observed in Chinese hamster ovary CHO-K1 cells after exposure to the 2-ring aromatic fraction R 26 of diesel fuel without metabolic activation

concentration ($\mu\text{g/ml}$)	mitotic rate ¹	cells scored	simple aberrations		complex aberrations		total aberrations	
			number of aberrations	% cells	number of aberrations	% cells	number of aberrations	% cells
0	45	100	2	2	0	0	2	2
25	52	100	6	6	5	5	11	11
50	38	100	5	5	8	8	13	12
100	41	100	4	3	13	11	17	13
150 ⁴	26	100						
200	25	100	2	2	12	12	14	14
CP ³	38	100	7	7	5	5	12	11

¹ number of mitoses per 1,000 cells scored

³ indirect acting positive control cyclophosphamide, concentration 25 $\mu\text{g/ml}$

⁴ aberrations not scored at this concentration as higher concentration suitable for scoring

Table 72. Chromosome aberrations observed in Chinese hamster ovary CHO-K1 cells after exposure to the 2-ring aromatic fraction R 26 of diesel fuel with metabolic activation (rat liver S9 fraction)

concentration ($\mu\text{g/ml}$)	mitotic rate ¹	cells scored	simple aberrations		complex aberrations		total aberrations	
			number of aberrations	% cells	number of aberrations	% cells	number of aberrations	% cells
0	75	100	1	1	2	2	3	3
5	82	100	1	1	1	1	2	2
10	51	100	3	2	0	0	3	2
15	30	100	2	2	0	0	2	2
20	25	*						
40	3	*						
MNNG ²	49	100	5	5	9	8	14	13

* mitotic rate too low to score aberrations

¹ number of mitoses per 1,000 cells scored

² direct acting positive control MNNG, concentration 0.15 $\mu\text{g/ml}$

Table 73. Chromosome aberrations observed in Chinese hamster ovary CHO-K1 cells after exposure to the 2-ring aromatic diesel emission fraction R 32 (3000 rpm speed/5 Nm load) without metabolic activation

concentration ($\mu\text{g/ml}$)	mitotic rate ¹	cells scored	simple aberrations		complex aberrations		total aberrations	
			number of aberrations	% cells	number of aberrations	% cells	number of aberrations	% cells
0	45	100	2	2	0	0	2	2
25	46	100	3	3	2	2	5	5
50	29	100	3	3	2	2	5	4
100	23	100	3	3	2	2	5	5
150	26	100	2	2	3	3	5	5
200	12	*						
CP ³	38	100	7	7	5	5	12	11

* mitotic rate too low to score aberrations

¹ number of mitoses per 1,000 cells scored

³ indirect acting positive control cyclophosphamide, concentration 25 $\mu\text{g/ml}$

Table 74. Chromosome aberrations observed in Chinese hamster ovary CHO-K1 cells after exposure to the 2-ring aromatic diesel emission fraction R 32 (3000 rpm speed/5 Nm load) with metabolic activation (rat liver S9 fraction)

concentration ($\mu\text{g/ml}$)	mitotic rate ¹	cells scored	simple aberrations		complex aberrations		total aberrations	
			number of aberrations	% cells	number of aberrations	% cells	number of aberrations	% cells
0	75	100	1	1	2	2	3	3
5	69	100	2	1	2	2	4	3
10	63	100	1	1	3	3	4	4
15	28	100	3	3	3	3	6	6
20	19	*						
40	9	*						
MNNG ²	49	100	5	5	9	8	14	13

* mitotic rate too low to score aberrations

¹ number of mitoses per 1,000 cells scored

² direct acting positive control MNNG, concentration 0.15 $\mu\text{g/ml}$

Table 75. Chromosome aberrations observed in Chinese hamster ovary CHO-K1 cells after exposure to the 2-ring aromatic diesel emission fraction R 29+38 (1000 rpm speed/ 55 Nm load) without metabolic activation

concentration ($\mu\text{g/ml}$)	mitotic rate ¹	cells scored	simple aberrations		complex aberrations		total aberrations	
			number of aberrations	% cells	number of aberrations	% cells	number of aberrations	% cells
0	42	100	2	2	1	1	3	3
10	39	100	3	3	5	5	8	8
20	46	100	3	3	8	8	11	11
40	25	100	5	5	7	5	12	9
100	7	*						
CP ³	23	100	11	10	8	8	19	17

* mitotic rate too low to score aberrations

¹ number of mitoses per 1,000 cells scored

³ indirect acting positive control cyclophosphamide, concentration 25 $\mu\text{g/ml}$

Table 76. Chromosome aberrations observed in Chinese hamster ovary CHO-K1 cells after exposure to the 2-ring aromatic diesel emission fraction R 29+38 (1000 rpm speed/ 55 Nm load) with metabolic activation (rat liver S9 fraction)

concentration ($\mu\text{g/ml}$)	mitotic rate ¹	cells scored	simple aberrations		complex aberrations		total aberrations	
			number of aberrations	% cells	number of aberrations	% cells	number of aberrations	% cells
0	67	100	1	1	3	2	4	3
5	54	100	1	1	3	3	4	4
10	33	100	1	1	3	3	4	4
20	26	100	2	2	6	6	8	8
40	0	*						
MNNG ²	41	100	7	5	7	7	14	12

* mitotic rate too low to score aberrations

¹ number of mitoses per 1,000 cells scored

² direct acting positive control MNNG, concentration 0.15 $\mu\text{g/ml}$

Table 77. Chromosome aberrations observed in Chinese hamster ovary CHO-K1 cells after exposure to the 3-ring aromatic fraction R 27 from diesel fuel without metabolic activation

concentration ($\mu\text{g/ml}$)	mitotic rate ¹	cells scored	simple aberrations		complex aberrations		total aberrations	
			number of aberrations	% cells	number of aberrations	% cells	number of aberrations	% cells
0	37	100	4	4	0	0	4	4
25	38	100	7	7	8	8	15	13
50	25	100	7	6	11	11	18	16
100	25	101	13	13	8	8	21	21
200	0	*						
CP ³	28	100	6	5	9	8	15	12

* mitotic rate too low to score aberrations

¹ number of mitoses per 1,000 cells scored

³ indirect acting positive control cyclophosphamide, concentration 25 $\mu\text{g/ml}$

Table 78. Chromosome aberrations observed in Chinese hamster ovary CHO-K1 cells after exposure to the 3-ring aromatic fraction R 27 from diesel fuel with metabolic activation (rat liver S9 fraction)

concentration ($\mu\text{g/ml}$)	mitotic rate ¹	cells scored	simple aberrations		complex aberrations		total aberrations	
			number of aberrations	% cells	number of aberrations	% cells	number of aberrations	% cells
0	67	100	1	1	3	2	4	3
2.5 ⁴	57							
5	38	100	6	6	3	3	9	8
10	37	100	2	2	6	6	8	8
20	25	100	6	6	4	4	10	9
40	6	*						
MNNG ²	41	100	7	5	7	7	14	12

* mitotic rate too low to score aberrations

¹ number of mitoses per 1,000 cells scored

² direct acting positive control MNNG, concentration 0.15 $\mu\text{g/ml}$

⁴ aberrations not scored at this concentration as other concentrations tested more suitable for scoring

Table 79. Chromosome aberrations observed in Chinese hamster ovary CHO-K1 cells after exposure to the 3-ring aromatic diesel emission fraction R 33 (3000 rpm speed/ 5 Nm load) without metabolic activation

concentration ($\mu\text{g/ml}$)	mitotic rate ¹	cells scored	simple aberrations		complex aberrations		total aberrations	
			number of aberrations	% cells	number of aberrations	% cells	number of aberrations	% cells
0	37	100	4	4	0	0	4	4
25	41	100	5	5	5	5	10	9
50	30	100	7	7	12	12	19	18
100	19	100	10	10	10	10	20	20
150	0	*						
200	0	*						
CP ³	28	100	6	5	9	8	15	12

* mitotic rate too low to score aberrations

¹ number of mitoses per 1,000 cells scored

³ indirect acting positive control cyclophosphamide, concentration 25 $\mu\text{g/ml}$

Table 80. Chromosome aberrations observed in Chinese hamster ovary CHO-K1 cells after exposure to the 3-ring aromatic diesel emission fraction R 33 (3000 rpm speed/ 5 Nm load) with metabolic activation (rat liver S9 fraction)

concentration ($\mu\text{g/ml}$)	mitotic rate ¹	cells scored	simple aberrations		complex aberrations		total aberrations	
			number of aberrations	% cells	number of aberrations	% cells	number of aberrations	% cells
0	56	100	0	0	3	3	3	3
0	51	100	2	2	1	1	3	3
5	46	100	0	0	3	2	3	2
5	49	100	2	2	3	3	5	5
10	47	100	2	2	2	2	4	4
10	45	100	2	2	3	3	5	5
20	39	100	10	10	10	9	20	19
20	35	100	10	9	14	10	24	19
30	24	100	23	19	9	8	32	27
30	23	100	22	17	7	7	29	23
MNNG ²	24	100	9	7	5	5	14	12
MNNG ²	31	100	10	10	4	4	14	14

¹ number of mitoses per 1,000 cells scored

² direct acting positive control MNNG, concentration 0.15 $\mu\text{g/ml}$

Table 81. Chromosome aberrations observed in Chinese hamster ovary CHO-K1 cells after exposure to the polar diesel emission fraction ES 39+42 (3000 rpm speed/5 Nm load), without metabolic activation

calculated test statistic (X^2) ¹	degrees of freedom	critical X^2 value (upper 5 % point)	test outcome
1.875	5	11.070	no evidence of heterogeneity between cultures

¹ method of Richardson *et al.*, 1990

Table 82. Binomial dispersion test calculated for replicate cultures of the polar emission fraction ES 39+42 (3000 rpm speed/5 Nm load) when assayed in the chromosome aberration assay in CHO-K1 cells without metabolic activation

concentration ($\mu\text{g/ml}$)	mitotic rate ¹	cells scored	simple aberrations		complex aberrations		total aberrations	
			number of aberrations	% cells	number of aberrations	% cells	number of aberrations	% cells
0	63	100	1	1	1	1	2	2
0	69	100	1	1	2	2	3	3
25	64	100	3	3	0	0	3	3
25	70	100	1	1	2	2	3	3
50	48	100	4	4	0	0	4	4
50	41	100	0	0	2	2	2	2
100	36	100	8	8	4	3	12	11
100	37	100	7	6	4	4	11	9
150	36	100	9	8	7	7	16	15
150	35	100	13	11	7	7	20	18
CP ²	56	100	8	8	8	8	16	15
CP ²	54	100	6	6	9	9	15	15

¹ number of mitoses per 1,000 cells scored

² indirect acting positive control cyclophosphamide, concentration 25 $\mu\text{g/ml}$

Table 83. Chromosome aberrations observed in Chinese hamster ovary CHO-K1 cells after exposure to the polar diesel emission fraction ES 39+42 (3000 rpm speed/5 Nm load), with metabolic activation (rat liver S9 fraction)

calculated test statistic (χ^2) ¹	degrees of freedom	critical χ^2 value (upper 5 % point)	test outcome
1.441	5	11.070	no evidence of heterogeneity between cultures

¹ method of Richardson *et al.*, 1990

Table 84. Binomial dispersion test calculated for replicate cultures of the polar emission fraction ES 39+42 (3000 rpm speed/5 Nm load) when assayed in the chromosome aberration assay in CHO-K1 cells with metabolic activation (rat liver S9 fraction)

concentration ($\mu\text{g/ml}$)	mitotic rate ¹	cells scored	simple aberrations		complex aberrations		total aberrations	
			number of aberrations	% cells	number of aberrations	% cells	number of aberrations	% cells
0	90	100	0	0	4	4	4	4
0	101	100	1	1	2	2	3	3
5	104	100	2	2	2	2	4	4
5	95	100	1	1	3	3	4	4
10	63	100	1	1	4	4	5	5
10	72	100	3	3	2	2	5	5
20	55	100	5	5	6	6	11	11
20	57	100	8	8	8	8	16	15
30	32	100	14	14	7	6	21	19
30	29	100	19	17	7	6	26	22
MNNG ²	33	100	10	10	4	4	14	14
MNNG ²	36	100	10	9	2	2	12	11

¹ number of mitoses per 1,000 cells scored

² direct acting positive control MNNG, concentration 0.15 $\mu\text{g/ml}$

Table 85. Chromosome aberrations observed in Chinese hamster ovary CHO-K1 cells after exposure to the polar diesel emission fraction ES 45+48 (1000 rpm speed/55 Nm load), without metabolic activation

calculated test statistic (X^2) ¹	degrees of freedom	critical X^2 value (upper 5 % point)	test outcome
1.131	5	11.070	no evidence of heterogeneity between cultures

¹ method of Richardson *et al.*, 1990

Table 86. Binomial dispersion test calculated for replicate cultures of the polar emission fraction ES 45+48 (1000 rpm speed/55 Nm load) when assayed in the chromosome aberration assay in CHO-K1 cells without metabolic activation

concentration ($\mu\text{g/ml}$)	mitotic rate ¹	cells scored	simple aberrations		complex aberrations		total aberrations	
			number of aberrations	% cells	number of aberrations	% cells	number of aberrations	% cells
0	69	100	1	1	1	1	2	2
0	63	100	1	1	2	2	3	3
25	60	100	3	3	2	2	5	5
25	65	100	4	4	1	1	5	5
50	53	100	2	2	4	3	6	5
50	48	100	2	2	2	2	4	4
100	46	100	6	6	3	3	9	9
100	50	100	2	2	5	4	7	6
150	34	100	10	10	4	4	14	14
150	31	100	6	6	6	6	12	12
CP ²	56	100	8	8	8	8	16	15
CP ²	54	100	6	6	9	9	15	15

¹ number of mitoses per 1,000 cells scored

² indirect acting positive control cyclophosphamide, concentration 25 $\mu\text{g/ml}$

Table 87. Chromosome aberrations observed in Chinese hamster ovary CHO-K1 cells after exposure to the polar diesel emission fraction ES 45+48 (1000 rpm speed/55 Nm load), with metabolic activation (rat liver S9 fraction)

calculated test statistic (X^2) ¹	degrees of freedom	critical X^2 value (upper 5 % point)	test outcome
1.147	5	11.070	no evidence of heterogeneity between cultures

¹ method of Richardson *et al.*, 1990

Table 88. Binomial dispersion test calculated for replicate cultures of the polar emission fraction ES 45+48 (1000 rpm speed/55 Nm load) when assayed in the chromosome aberration assay in CHO-K1 cells with metabolic activation (rat liver S9 fraction)

concentration ($\mu\text{g/ml}$)	mitotic rate ¹	cells scored	simple aberrations		complex aberrations		total aberrations	
			number of aberrations	% cells	number of aberrations	% cells	number of aberrations	% cells
0	90	100	0	0	4	4	4	4
0	101	100	1	1	2	2	3	3
1	95	100	3	3	3	3	6	6
1	90	100	4	4	4	4	8	8
5	88	100	6	6	1	1	7	7
5	94	100	7	7	4	3	11	10
10	87	100	5	4	4	4	9	8
10	88	100	4	4	4	4	8	8
20	30	100	18	16	3	3	21	19
20	35	100	15	14	6	6	21	19
30	11	100	20	19	11	10	31	26
30	19	100	19	16	13	12	32	27
MNNG ²	33	100	10	10	4	4	14	14
MNNG ²	36	100	10	9	2	2	12	11

¹ number of mitoses per 1,000 cells scored

² direct acting positive control MNNG, concentration 0.15 $\mu\text{g/ml}$

Table 89. Chromosome aberrations observed in Chinese hamster ovary CHO-K1 cells after exposure to the polar diesel emission fraction ES 51+54 (1000 rpm speed/5 Nm load), without metabolic activation

calculated test statistic (X^2) ¹	degrees of freedom	critical X^2 value (upper 5 % point)	test outcome
1.060	6	12.592	no evidence of heterogeneity between cultures

¹ method of Richardson *et al.*, 1990

Table 90. Binomial dispersion test calculated for replicate cultures of the polar emission fraction ES 51+54 (1000 rpm speed/5 Nm load) when assayed in the chromosome aberration assay in CHO-K1 cells without metabolic activation

concentration ($\mu\text{g/ml}$)	mitotic rate ¹	cells scored	simple aberrations		complex aberrations		total aberrations	
			number of aberrations	% cells	number of aberrations	% cells	number of aberrations	% cells
0	77	100	2	2	0	0	2	2
0	72	100	2	2	1	1	3	3
25	78	100	2	2	1	1	3	3
25	82	100	1	1	2	2	3	3
50	53	100	2	2	2	2	4	4
50	47	100	3	3	1	1	4	4
100	39	100	12	10	6	6	18	14
100	36	100	8	8	9	9	17	15
CP ²	56	100	8	8	8	8	16	15
CP ²	54	100	6	6	9	9	15	15

¹ number of mitoses per 1,000 cells scored

² indirect acting positive control cyclophosphamide, concentration 25 $\mu\text{g/ml}$

Table 91. Chromosome aberrations observed in Chinese hamster ovary CHO-K1 cells after exposure to the polar diesel emission fraction ES 51+54 (1000 rpm speed/5 Nm load), with metabolic activation (rat liver S9 fraction)

calculated test statistic (χ^2) ¹	degrees of freedom	critical χ^2 value (upper 5 % point)	test outcome
0.245	4	9.488	no evidence of heterogeneity between cultures

¹ method of Richardson *et al.*, 1990

Table 92. Binomial dispersion test calculated for replicate cultures of the polar emission fraction ES 51+54 (1000 rpm speed/5 Nm load) when assayed in the chromosome aberration assay in CHO-K1 cells with metabolic activation (rat liver S9 fraction)

concentration ($\mu\text{g/ml}$)	mitotic rate ¹	cells scored	simple aberrations		complex aberrations		total aberrations	
			number of aberrations	% cells	number of aberrations	% cells	number of aberrations	% cells
0	42	100	0	0	1	1	1	1
5	41	100	2	1	0	0	2	1
10	44	100	3	3	5	5	8	8
20	30	100	10	9	12	11	21	20
30	22	100	15	14	14	12	29	24
MNNG ²	30	100	8	8	8	7	16	14

¹ number of mitoses per 1,000 cells scored

² direct acting positive control MNNG, concentration 0.15 $\mu\text{g/ml}$

Table 93. Chromosome aberrations observed in Chinese hamster ovary CHO-K1 cells after exposure to the polar diesel emission fraction ES 107 (2000 rpm speed/ 30 Nm load), without metabolic activation

concentration ($\mu\text{g/ml}$)	mitotic rate ¹	cells scored	simple aberrations		complex aberrations		total aberrations	
			number of aberrations	% cells	number of aberrations	% cells	number of aberrations	% cells
0	42	100	0	0	1	1	1	1
5	53	100	5	5	2	2	7	5
10	47	100	4	4	2	2	6	6
20	31	100	10	10	9	9	19	18
30	29	100	20	17	6	6	26	21
MNNG ²	30	100	8	8	8	7	16	14

¹ number of mitoses per 1,000 cells scored

² direct acting positive control MNNG, concentration 0.15 $\mu\text{g/ml}$

Table 94. Chromosome aberrations observed in Chinese hamster ovary CHO-K1 cells after exposure to the polar diesel emission fraction ES 116 (2000 rpm speed/ 55 Nm load), without metabolic activation

concentration ($\mu\text{g/ml}$)	mitotic rate ¹	cells scored	simple aberrations		complex aberrations		total aberrations	
			number of aberrations	% cells	number of aberrations	% cells	number of aberrations	% cells
0	66	100	2	2	1	1	3	3
5	68	100	3	3	1	1	4	4
10	63	100	6	6	5	5	11	10
20	38	100	10	9	11	8	21	17
30	27	100	22	17	10	9	32	24
MNNG ²	41	100	9	7	6	6	15	13

¹ number of mitoses per 1,000 cells scored

² direct acting positive control MNNG, concentration 0.15 $\mu\text{g/ml}$

Table 95. Chromosome aberrations observed in Chinese hamster ovary CHO-K1 cells after exposure to the polar diesel emission fraction ES 119 (3000 rpm speed/ 30 Nm load), without metabolic activation

concentration ($\mu\text{g/ml}$)	mitotic rate ¹	cells scored	simple aberrations		complex aberrations		total aberrations	
			number of aberrations	% cells	number of aberrations	% cells	number of aberrations	% cells
0	66	100	2	2	1	1	3	3
5	60	100	4	4	0	0	4	4
10	54	100	5	5	3	3	8	7
20	35	100	15	13	9	9	24	20
30	29	100	21	18	8	7	29	23
MNNG ²	41	100	9	7	6	6	15	13

¹ number of mitoses per 1,000 cells scored

² direct acting positive control MNNG, concentration 0.15 $\mu\text{g/ml}$

Table 96. Chromosome aberrations observed in Chinese hamster ovary CHO-K1 cells after exposure to the polar diesel emission fraction ES 125 (3000 rpm speed/ 55 Nm load), without metabolic activation

APPENDIX C

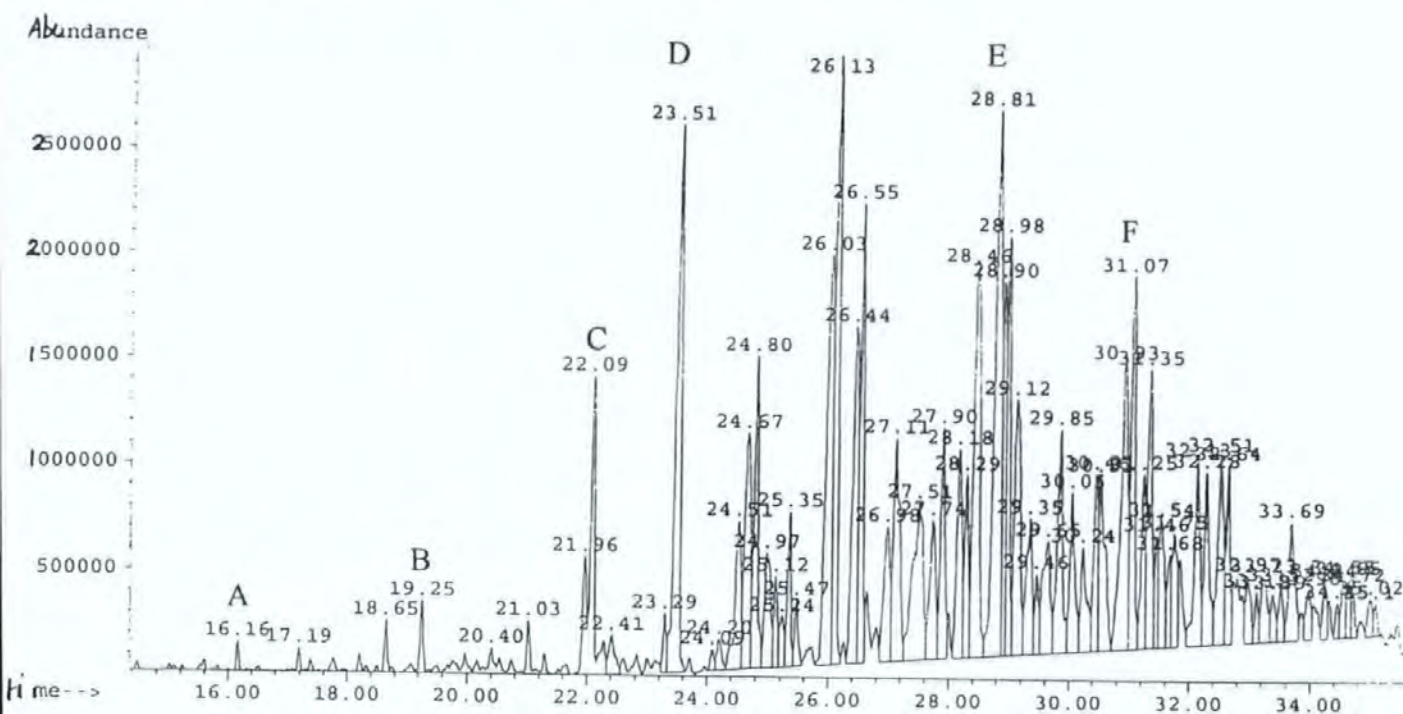
GC/MS TRACES FOR AROMATIC 3+ -RING FRACTIONS

GC/MS (gas chromatography/mass spectrometry) was used to assess the success of HPLC fractionation of the aromatic fraction of diesel fuel and engine emission samples into ring fraction groups. GC/MS traces for the 3+ -ring fractions of the fuel and of the emission sample collected at 3000 rpm and 5 Nm were provided and are shown here. Selected peaks have been identified and the compounds and their relative abundance's are given.

(a) 3+ -ring aromatic fraction of the diesel fuel

A biphenylene (16 min)
B fluorene (19 min)
C methylfluorene (22 min)

D phenanthrene (23.5 min)
E dimethylphenanthrene (29 min)
F trimethylphenanthrene (31 min)



(b) 3+ -ring aromatic fraction of the diesel engine emission sample collected at 3000 rpm and 5 Nm

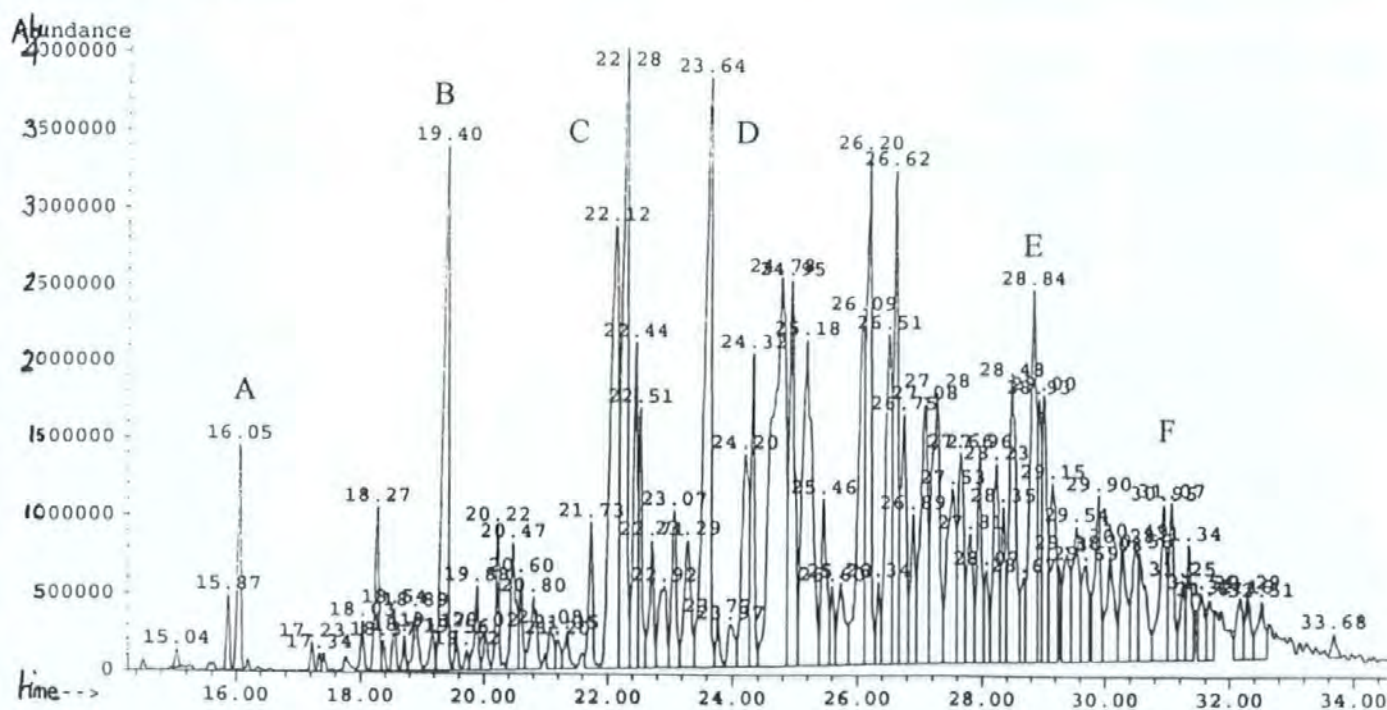


Figure 123. GC/MS trace for the 3+ -ring aromatic fractions, obtained by HPLC fractionation of the diesel fuel and engine emission sample collected at 3000 rpm and 5 Nm, showing relative abundance of peak compounds

APPENDIX D

DIESEL ENGINE OUTPUT MEASUREMENTS

Specified diesel engine outputs including Bosch smoke, hydrocarbon production, NOx emissions, and carbon monoxide are regularly assessed on site at Plymouth by the engine manufacturers. Engine outputs measured at each speed and load that emission samples were collected under during this study are given in graphical form.

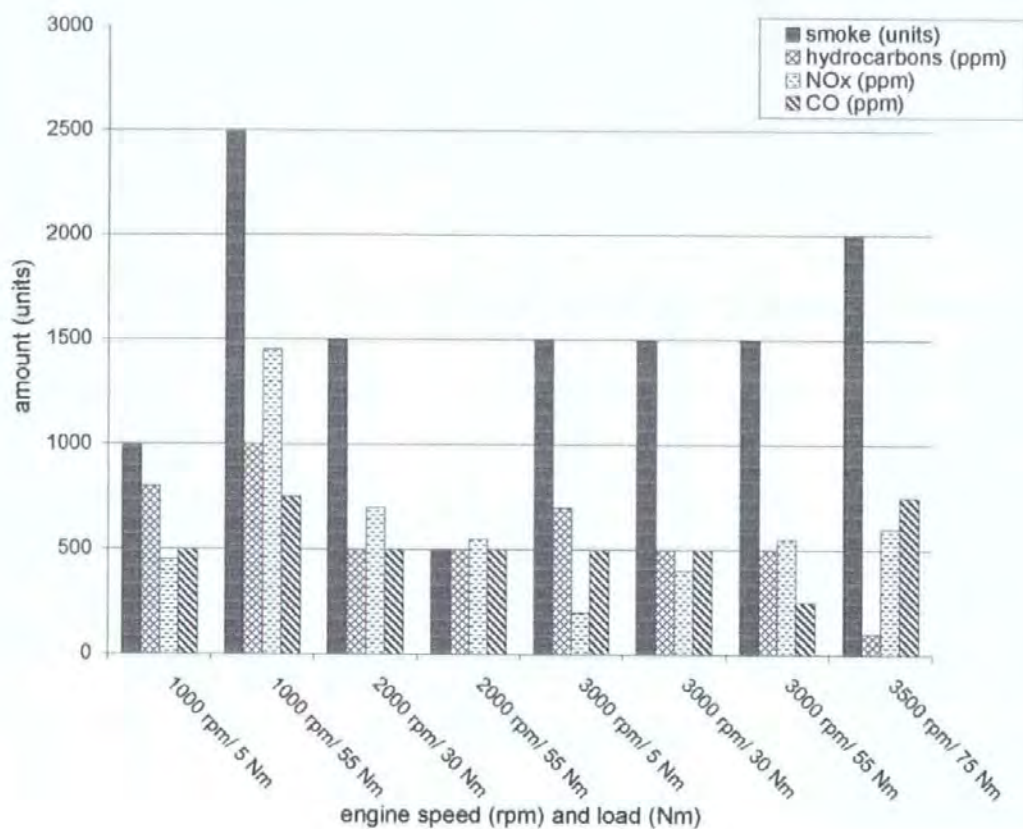


Figure 124. Measured outputs of smoke, hydrocarbons, NOx, and carbon monoxide for the diesel test engine used during this study measured at each condition of speed and load used for emission sampling

References

- Ames, B.N., McCann, J., Yamasaki, E. (1975) Methods for detecting carcinogens and mutagens with the *Salmonella*/mammalian microsome mutagenicity test. *Mutation Research*, **31**, 347-64.
- Anderson, H.R., Limb, E.S., Bland, J.M., Deleon, A.P., Strachan, D.P., Bower, J.S. (1995) Health effects of an air pollution episode in London, December 1991. *Thorax*, **50** (11), 1188-93.
- Andersson, H., Lindqvist, E., Westerholm, R., Gragg, K., Almen, J., Olson, L. (1998) Neurotoxic effects of fractionated diesel exhausts following microinjections in rat hippocampus and striatum. *Environmental Research*, **76** (1), 41-51.
- Angel, R. (1997) First meiotic division nondisjunction in human oocytes. *American Journal of Human Genetics*, **61** (1), 23-32.
- Arey, J., Zielinska, B., Harger, W.P., Atkinson, R., Winer, A.M. (1988) The contribution of nitrofluoranthenes and nitropyrenes to the mutagenic activity of ambient particulate organic matter collected in southern California. *Mutation Research*, **207** (2), 45-51.
- Ashby, J. (1995) Druckrey's definition of 'genotoxic'. *Mutation Research*, **329**, 225.
- Balajee, A.S., Oh, H.J., Natarajan, A.T. (1994) Analysis of restriction enzyme-induced chromosome aberrations in the interstitial telomeric sequences of CHO and CHE cells by FISH. *Mutation Research*, **307**, 307-13.
- Beland, F.A., Heflich, R.H., Howard, P.C. (1985) The *in vitro* metabolic activation of nitro polycyclic aromatic hydrocarbons. In: R.G. Harvey (Ed.), *Polycyclic Hydrocarbons and Carcinogenesis*. American Chemical Society, Washington D.C., 371-96.
- Bender, M.A., Griggs, H.G., Bedford, J.S. (1974) Mechanisms of chromosomal aberration production. III. Chemicals and ionising radiation. *Mutation Research*, **23**, 197-212.

Benford, D.J., Hubbard, S.A. (1987) Preparation and culture of mammalian cells. In: K. Snell & B. Mullock (Eds.), *Biochemical Toxicology: A Practical Approach*. IRL Press, Oxford, 57-82.

Bhatia, R., Lopipero, P., Smith, A.H. (1998) Diesel exhaust exposure and lung cancer. *Epidemiology*, **9** (1), 84-91.

Bown W. (1994) Forum: How green were our hopes for diesel? - William Bown roots for the man with all the dirt about diesels. *New Scientist*, Reed Business Information Ltd., London.

Boyes, B.G., Rogers, C.G., Stapley, R. (1991) Genotoxicity of 1-nitronaphthalene in Chinese hamster V79 cells. *Mutation Research*, **259**, 111-21.

Brennan-Craddock, W.E., Rowland, I.R., Mallett, A.K., Neale, S. (1987) Age-dependent changes in activation of dietary mutagens by mouse hepatic fractions. *Mutagenesis*, **2**, 301-2.

Bryant, P.J. (1993) Towards the cellular functions of tumour suppressors. *Trends in Cell Biology*, **3**, 31-5.

Bunger, J., Krah, J., Franke, H., Munack, A., Hallier, E. (1998) Mutagenic and cytotoxic effects of exhaust particulate matter of biodiesel compared to fossil diesel fuel. *Mutation Research*, **415**, 13-23.

Chandley, A.C. (1981) The origin of chromosomal aberrations in man and their potential for survival and reproduction in the adult human population. *Annals of Genetics*, **24**, 5-11.

Chang, T.Y., Hammerle, R., Japar, S.M., Saleem, I.T. (1991) Alternative transportation fuels and air quality. *Environmental Science and Technology*, **25**, 1190-3.

Cherng, S.-H., Lin, S.T., Lee, H. (1996) Modulatory effects of polycyclic aromatic hydrocarbons on the mutagenicity of 1-nitropyrene: a structure-activity relationship study. *Mutation Research*, **367**, 177-85.

Chu, E.H.Y. (1983) Mutation systems in cultured mammalian cells. In: G.M. Williams, V.C. Dunkel, V.A. Ray, (Eds.), *Cellular systems for toxicity testing*. The New York Academy of Sciences, New York, 221-30.

Clark, C.R., and Vigil, C.L. (1980) Influence of rat lung and liver homogenates on the mutagenicity of diesel exhaust particulate extracts. *Toxicol Appl Pharmacol*, **56**, 100-15.

Cole, J., McGregor, D.B., Fox, M., Thacker, J., Garner, R.C. (1990) Gene mutation assays in cultured mammalian cells. In: D.J. Kirkland (Ed.) *Basic mutagenicity tests: UKEMS recommended procedures*, Cambridge University Press, Cambridge, 87-114.

Collier, A.R. (1995) Profiling the organic emissions from a light-duty direct-injection diesel engine over a range of speeds and loads. Ph.D. Thesis, University of Plymouth.

Collier, A.R., Rhead, M.M., Trier, C.J., Bell, M.A. (1995) Polycyclic aromatic compound profiles from a light-duty direct-injection diesel engine. *Fuel*, **74** (3), 362-7.

Courtois, Y., Molinier, B., Pasquereau, M., Degobert, P., Festy, B. (1993) Influence of the operating conditions of a diesel engine on the mutagenicity of its emissions. *Science of the Total Environment*, **134** (1-3), 61-70.

Crebelli, R., Conti, L., Crochi, B., Carere, A., Bertoli, C., Del Giacomo, N. (1995) The effect of fuel composition on the mutagenicity of diesel engine exhaust. *Mutation Research*, **346**, 167-72.

Croner (1999) Croner's Environmental Management: Current Proposals January 1999.

Croner Publications Ltd.

Croxford, B., Penn, A., Hillier, B. (1996) Spatial distribution of urban pollution: civilizing urban traffic. *The Science of the Total Environment*, **189/190**, 3-9.

Cummings, M.R. (1990) *Human Heredity: Principles and Issues*. West Publishing Co., Eagan.

De Fre, R., Bruynseraede, P., Kretzschmar, J.G. (1994) Air pollution measurement in traffic tunnels. *Environmental Health Perspectives*, **102** (Suppl 4), 31-7.

De Serres, F.J., and Hollaender, A. Eds. (1980) *Chemical Mutagens: Principles and Methods for their Detection*. Plenum Press, New York.

Dean, B.J., Danford, N. (1984) Assays for the detection of chemically-induced chromosome damage in cultured mammalian cells. In: S. Venitt, J.M. Parry (Eds.), *Mutagenicity Testing: A Practical Approach*. IRL Press, Oxford, 187-232.

Deaven, L.L., Petersen, D.F. (1973) The chromosomes of CHO, an aneuploid Chinese hamster cell line: G-band, C-band, and autoradiographic analyses. *Chromosoma*, **41**, 129-44.

Delgado-Rodriguez, A., Ortiz-Martelo, R., Graf, U., Villalobos-Pietrini, R., Gomez-Arroyo, S. (1995) Genotoxic activity of environmentally important polycyclic aromatic hydrocarbons and their nitro derivatives in the wing spot test of *Drosophila melanogaster*. *Mutation Research*, **341**, 235-47.

Dipple, A. (1985) Polycyclic aromatic hydrocarbon carcinogenesis: An introduction. In: R.G. Harvey (Ed.), *Polycyclic Hydrocarbons and Carcinogenesis*. American Chemical Society, Washington D.C., 1-17.

DoE (1996) The United Kingdom National Air Quality Strategy: Consultation draft. Department of the Environment, London.

Druckrey, H. (1973) Specific carcinogenic and teratogenic effects of indirect acting alkylating methyl and ethyl compounds, and their dependency on stages of ontogenic developments. *Xenobiotica*, **3**, 271-303.

DuBridge, R.B., Calos, M.P. (1987) Molecular approaches to the study of gene mutation in human cells. *Trends in Genetics*, **3** (10), 293-7.

Dunkel, V.C. (1983) Biological significance of end points. In: G.M. Williams, V.C. Dunkel, V.A. Ray (Eds.) *Cellular systems for toxicity testing*. The New York Academy of Sciences, New York, 34-41.

Edwards, M.J., Parry, J.M., Batmanghelich, S., Smith, K. (1986) Toxicity and DNA damage induced by 1-nitropyrene and derivatives in Chinese hamster lung fibroblasts. *Mutation Research*, **163**, 81-9.

Ensell, M.-X., Whong, W.-Z., Heng, Z.-C., Nath, J., Ong, T. (1998) *In vitro* and *in vivo* transformation in rat tracheal epithelial cells exposed to diesel emission particles and related compounds. *Mutation Research*, **412**, 283-91.

Enya, T., Suzuki, H., Watanabe, T., Hirayama, T., Hisamatsu, Y. (1997) 3-nitrobenzanthrone, a powerful bacterial mutagen and suspected human carcinogen found in diesel exhaust and airborne particulates. *Environmental Science and Technology*, **31** (10), 2772-6.

Evans, H.J. (1983) Cytogenetic methods for detecting effects of chemical mutagens. In: G.M. Williams, V.C. Dunkel, V.A. Ray (Eds.), *Cellular systems for toxicity testing*. The New York academy of sciences, New York, 131-41.

Fahrig, R. (1984) Genetic mode of action of cocarcinogens and tumor promoters in yeast and mice. *Molecular and General Genetics*, **194** (1-2), 7-14.

Fearon, E.R., and Vogelstein, B. (1990) A genetic model for colorectal tumorigenesis. *Cell*, **61**, 759-67.

Fiennes, A.G.T.W., Walton, J., Winterbourne, D., McGlashan, D., Hermon-Taylor, J. (1987) Quantitative correlation of neutral red dye uptake with cell number in human cancer cell cultures. *Cell Biology International Reports*, **11** (5), 373-8.

Folle, G.A., Martinez, L.W., Boccardo, E., Obe, G. (1998) Localization of chromosome breakpoints: implication of the chromatin structure and nuclear architecture. *Mutation Research*, **404** (1-2), 17-26.

Fox, M. (1985) Assay of colony forming ability in established cell lines. In: C.S. Potten, J.H. Hendry (Eds.), *Cell Clones*. Churchill Livingstone, 185-95.

Fu, P.P. (1990) Metabolism of nitro-polycyclic aromatic hydrocarbons. *Drug Metabolism Reviews*, **22** (2&3), 209-68.

Fu, P.P., Herreno-Saenz, D., Von Tungeln, L.S., Lay, J.O., Wu, Y.-S., Lai, J., Evans, F.E. (1994) DNA adducts and carcinogenicity of nitro-polycyclic aromatic hydrocarbons. *Environmental Health Perspectives*, **102** (Suppl 6), 177-84.

Gallagher, J., George, M., Kohan, M., Thompson, C., Shank, T., Lewtas, J. (1993) Detection and comparison of DNA adducts after in vitro and in vivo diesel emission exposures. *Environmental Health Perspectives*, **99**, 225-8.

Galloway, S.M., Bloom, A.D., Resnick, M.A., Margolin, B.H., Nakamura, F., Archer, P., Zeiger, E. (1985) Development of a standard protocol for *in vitro* cytogenetic testing with Chinese hamster ovary cells: comparison of results for 22 compounds in two laboratories. *Environmental Mutagenesis*, **7**, 1-51.

Galloway, S.M., Armstrong, M.J., Reuben, C., Colman, S., Brown, B., Cannon, C., Bloom, A.D., Nakamura, F., Ahmed, M., Duk, S., *et al.* (1987) Chromosome aberrations and sister chromatid exchanges in Chinese hamster ovary cells: evaluations of 108 chemicals. *Environmental and Molecular Mutagenesis*, **10** (S10), 1-35.

Galloway, S.M., Sofuni, T., Shelby, M.D., Thilagar, A., Kumaroo, P.V., Kaur, P., Gulati, D., Putman, D.L., Murli, H., Marshall, R., *et al.* (1997) Multilaboratory comparison of *in vitro* tests for chromosome aberrations in CHO and CHL cells tested under the same protocols. *Environmental and Molecular Mutagenesis*, **29**, 189-207.

Gatehouse, D.G., Wilcox, P., Forster, R., Rowland, I.R., Callander, R.D. (1990) Bacterial mutation assays. In: D.J. Kirkland (Ed.), *Basic mutagenicity tests: UKEMS recommended procedures*, Cambridge University Press, Cambridge, 13-61.

Gilmour, P., Brown, D.M., Beswick, P.H., Benton, E., MacNee, W., Donaldson, K. (1997) Surface free radical activity of PM10 and ultrafine titanium dioxide: A unifying factor in their toxicity? *Annals of occupational Hygiene*, **41** (Suppl 1), 32-8.

Grimmer, G., Brune, H., Deutsch-Wenzel, R., Dettbarn, G., Jacob, J., Naujack, K.W., Mohr, U., Ernst, H. (1987) Contribution of polycyclic aromatic hydrocarbons and nitro-

derivatives to the carcinogenic impact of diesel engine exhaust condensate, evaluated by implantation into the lungs of rats. *Cancer Letters*, **37** (2), 173-80.

Gu, Z.W., Zhong, B.Z., Nath, B., Whong, W.Z., Wallace, W.E., Ong, T.M. (1992) Micronucleus induction and phagocytosis in mammalian cells treated with diesel emission particles. *Mutation Research*, **279**, 55-60.

Hammerle, R., Schuetzle, D., Adams, W. (1994) A perspective on the potential development of environmentally acceptable light-duty diesel vehicles. *Environmental Health Perspectives*, **102** (supplement 4), 25-30.

Hammond, S.K., Smith, T.J., Woskie, S.R., Braun, A.G., Lafleur, A., Liber, H., Garshick, E., Schenker, M.B., Speizer, F.E. (1993) Railroad diesel exhaust: Concentration and mutagenicity. *Appl Occup Environ Hyg*, **8** (11), 955-63.

Hansen, M.F., Cavenee, W.K. (1988) Retinoblastoma and the progression of tumor genetics. *Trends in Genetics*, **4** (5), 125-8.

Hartman, P.E. (1983) Mutagens: some possible health impacts beyond carcinogenesis. *Environmental Mutagenesis*, **5**, 139-52.

Hasegawa, M.M., Nishi, Y., Tsuda, H., Inui, N., Morimoto, K. (1988) Effects of diesel exhaust particles on chromosome aberration, sister chromatid exchange and morphological transformation in cultured mammalian cells. *Cancer Letters*, **42**, 61-6.

Hayakawa, K., Nakamura, A., Terai, N., Kizu, R., Ando, K. (1997) Nitroarene concentrations and direct-acting mutagenicity of diesel exhaust particulates fractionated by silica-gel column chromatography. *Chem Pharm Bull*, **45** (11), 1820-2.

Hayano, S., Furuya, A., Kikuchi, T., Someya, T., Oikawa, C., Iida, Y., Matsushita, H., Kinouchi, T., Manabe, Y., Ohnishi, Y. (1985) Formation of hazardous substances and mutagenicity of PAH produced during the combustion process in a diesel engine. *Atmospheric Environment*, **19** (6), 1009-15.

Heddle, J.A. Ed. (1982) *Mutagenicity. New Horizons in Genetic Toxicology*. Academic Press, New York.

Heflich, R.H., Fifer, E.K., Djuric, Z., Beland, F.A. (1985) DNA adduct formation and mutation induction by nitropyrenes in *Salmonella* and Chinese hamster ovary cells: relationships with nitroreduction and acetylation. *Environmental Health Perspectives*, **62**, 135-43.

HEI. (1995) *Diesel Exhaust: A critical analysis of emissions, exposure, and health effects. A summary of the special report of the Institute's diesel working group*. Health Effects Institute. Cambridge, MA.

Hellou, J. (1996) Polycyclic aromatic hydrocarbons in marine mammals, finfish, and molluscs. In: W. Nelson Beyer, G.H. Heinz, A.W. Redmon-Norwood (Eds.) *Environmental contaminants in wildlife: Interpreting tissue concentrations*. CRC Lewis Publishers, New York, 229-50.

Helmig, D., Arey, J., Harger, W.P., Atkinson, R., Lopezcancio, J. (1992) Formation of mutagenic nitrodibenzopyranones and their occurrence in ambient air. *Environmental Science and Technology*, **26** (3), 622-4.

Hermann, M. (1981) Synergistic effects of individual polycyclic aromatic hydrocarbons on the mutagenicity of their mixtures. *Mutation Research*, **90**, 399-409.

Heyder, J. (1993) Regional deposition of inhaled particles in the human respiratory tract. In: U. Mohr (Ed.), *Advances in Controlled Clinical Inhalation Studies*, Springer Verlag, Berlin,

Hollaender, A. Ed. (1971) *Chemical Mutagens: Principles and Methods for their Detection*. Plenum Press, New York.

Horiuchi, M., Koichi, S., Ichihara, S. (1990) The effects of flow-through type oxidation catalysts on the particulate reduction of 1990s diesel engines. *Society of Automotive Engineers Transactions*, **99** (3), 1268-78.

Hornberg, C., Maciuleviciute, L., Seemayer, N.H. (1997) Genotoxic effects induced by airborne particulates on tracheobronchial epithelial cells *in vitro*. *Ann occup Hyg*, **41** (Suppl 1), 24-31.

IARC (1983) *Polynuclear Aromatic Compounds. Part 1. Chemical, Environmental and Experimental Data*. International Agency for Research on Cancer. Lyon.

IARC (1989) *Monographs on the evaluation of carcinogenic risks to humans: Diesel and gasoline engine exhausts and some nitroarenes*. International Agency for Research on Cancer. Lyon.

King, C.M., Romano, L.J., and Schuetzle, D. Eds. (1988) Tumor induction by nitropyrenes in the female CD rat. *Carcinogenic and Mutagenic Responses to Aromatic Amines and Nitroarenes*, Elsevier; New York.

Ishidate, M.J. (1988) *Data Book of Chromosomal Aberration Test In Vitro. Revised Edition*, Elsevier, Amsterdam.

Ishidate, M.J. (1990) *In vitro* chromosomal aberration test - current status. In: Obe G, Natarajan AT (Eds.), *Chromosomal aberrations: Basic and Applied Aspects*, Springer-Verlag, Berlin, 260-72.

Ishidate, M.J., Harnois, M.C., Sofuni, T. (1988) A comparative analysis of data on the clastogenicity of 951 chemical substances tested in mammalian cell cultures. *Mutation Research*, **195**, 151-213.

Ishidate, M.J., Sofuni, T., Yoshikawa, K., Hayashi, M., Nohmi, T., Sawada, M., Matsuoka, A. (1984) Primary mutagenicity screening of food additives currently used in Japan. *Food and Chemical Toxicology*, **22**, 623-36.

Jha, A.N., Hande, P.M., Mullenders, L.H.F., Natarajan, A.T. (1995) Mimosine is a potent clastogen in primary and transformed hamster fibroblasts but not in primary or transformed human lymphocytes. *Mutagenesis*, **10** (5), 385-91.

Jongeneelen, F.J., Leijdekkers, C.M., Henderson, P.T. (1984) Urinary excretion of 3-hydroxy-benzo[a]pyrene after percutaneous penetration and oral absorption of benzo[a]pyrene in rats. *Cancer Letters*, **25**, 195-201.

- Kamens, R., Bell, D., Dietrich, A., Perry, J., Goodman, R., Claxton, L., Tejada, S. (1985) Mutagenic transformations of dilute wood smoke systems in the presence of ozone and nitrogen dioxide - analysis of selected HPLC fractions from wood smoke particle extracts. *Environmental Science and Technology*, **19** (1), 63-9.
- Kao, F., and Puck, T.T. (1970) Genetics of somatic mammalian cells: Linkage studies with human-Chinese hamster cell hybrids. *Nature*, **228**, 329-32.
- Kingston, S.T. (1994) Genotoxicology of diesel engine exhaust emissions in cultured mammalian cells. Ph.D Thesis, University of Plymouth.
- Kirkland, D.J. Ed. (1990) *Basic Mutagenicity Tests: UKEMS Recommended Procedures*. Cambridge University Press, Cambridge.
- Kirkland, D.J. (1998) Chromosome aberration testing in genetic toxicology - past, present and future. *Mutation Research*, **404**, 173-85.
- Kirkland, D.J., and Fox, M. Eds. (1993) *Supplementary Mutagenicity Tests: UKEMS Recommended Procedures*. Cambridge University Press, Cambridge.
- Kotin, P., Falk, H.L., Thomas, M. (1955) Aromatic hydrocarbons. III Presence in the particulate phase of diesel engine exhausts and the carcinogenicity of exhaust extracts. *Archives of Industrial Health*, **11**, 113-20.
- Lafon, D., Chini, C., Auburtin, G., Ould Elkhim, M., Nonat, A. (1994) Are diesel particulate emissions a threat to public health? *J Aerosol Sci*, **25** (S1), S507-8.
- Lake, B.G. (1987) Preparation and characterisation of microsomal fractions for studies of xenobiotic metabolism. In: K. Snell, B. Mullock (Eds.) *Biochemical Toxicology: A Practical Approach*, IRL Press, Oxford, 183-213.
- Landry, J.F., Langlois, S. (1998) Acute exposure to aliphatic hydrocarbons: an unusual case of acute tubular necrosis. *Archives of Internal Medicine*, **158** (16), 1821-3.

Langsrud, O. (1999) Fisher's Exact Test.

Internet site <http://www.matsfork.no/ola/fisher.htm>. [Unpublished]

Lee, H.K., Kim, Y., Roh, J.K. (1994) Clastogenicity of methapyrilene hydrochloride in cultured Chinese hamster cells. *Mutation Research*, **341**, 77-82.

Lewtas, J. (1988) Genotoxicity of complex mixtures: strategies for the identification and comparative assessment of airborne mutagens and carcinogens from combustion sources. *Fundamental and Applied Toxicology*, **10** (4), 571-89.

Lindskog, A. (1983) Transformation of polycyclic aromatic hydrocarbons during sampling. *Environmental Health Perspectives*, **47**, 81-4.

Lloyd, D.C., and Edwards, A.A. (1983) Chromosome aberrations in human lymphocytes: Effect of radiation quality, dose, and dose rate. *Radiation-Induced Chromosome Damage in Man*, Alan R Liss, New York, 23-49.

Loveday, K.S., Lugo, M.H., Resnick, M.A., Anderson, B.E., Zeiger, E. (1989) Chromosome aberration and sister chromatid exchange tests in Chinese hamster ovary cells *in vitro*: II. Results with 20 chemicals. *Environmental and Molecular Mutagenesis*, **13**, 60-94.

Margolin, B.H., Resnick, M.A., Rimpo, J.Y., Archer, P., Galloway, S.M., Bloom, A.D., Zeiger, E. (1986) Statistical analyses for *in vitro* cytogenetic assays using Chinese hamster ovary cells. *Environmental Mutagenesis*, **8**, 183-204.

Matsumoto, K., Ohta, T. (1991) Rotenone induces aneuploidy, polyploidy and endoreduplication in cultured Chinese hamster cells. *Mutation Research*, **263**, 173-7.

Matsuoka, A., Sofuni, T., Miyata, N., Ishidate, M.J. (1991) Clastogenicity of 1-nitropyrene, dinitropyrenes, fluorene and mononitrofluorenes in cultured Chinese hamster cells. *Mutation Research*, **259**, 103-10.

Mauderly, J.L. (1992) Diesel exhaust. In: Lippmann M (Ed.) *Environmental Toxicants: Human Exposures and their Health Effects*, Van Nostrand Reinhold, New York, 119-62.

Mauderly, J.L. (1993) Toxicological approaches to complex mixtures. *Environmental Health Perspectives*, **101**, (Suppl. 4), 155-65.

Mauderly, J.L. (1994) Toxicological and epidemiological evidence for health risks from inhaled engine emissions. *Environmental Health Perspectives*, **102**, (S4), 165-71.

McCann, J., Choi, E., Yamasaki, E., Ames, B.N. (1975) Detection of carcinogens as mutagens in the *Salmonella*/microsome test: assay of 300 chemicals. *Proc Natl Acad Sci USA*, **72**, 5135-9.

McClellan, R.O. (1986) Health effects of diesel exhaust: a case study in risk assessment. *Am Ind Hyg Assoc J*, **47**, 1-13.

Minden, M.D. (1987) Oncogenes. In: I.F. Tannock, R.P. Hill (Eds.) *The Basic Science of Oncology*, Pergamon Press, New York, 72-88.

Miyabara, Y., Ichinose, T., Takano, H., Sagai, M. (1998) Diesel exhaust inhalation enhances airway hyperresponsiveness in mice. *International Archives of Allergy and Immunology*, **116** (2), 124-31.

Morgan, W.K.C., Reger, R.B., Tucker, D.M. (1997) Health effects of diesel emissions. *Ann occup Hyg*, **41** (6), 643-58.

Morimoto, K., Kitamuri, S., Kondo, H., Koizumi, A. (1986) Genotoxicity of diesel exhaust emissions in a battery of *in vitro* short term and *in vivo* bioassays. *Dev. Toxicol. Environ. Sci.*, **13**, 85-101.

Morita, T., Watanabe, Y., Takeda, K., Ukumura, K. (1989) Effects of pH in the *in vitro* chromosomal aberration test. *Mutation Research*, **225**, 55-60.

Nachtman, J.P., and Wolff, S. (1982) Activity of nitro-polynuclear aromatic hydrocarbons in the sister chromatid exchange assay with and without metabolic activation. *Environmental Mutagenesis*, **4**, 1-5.

Nakagawa, R., Kitamori, S., Horikawa, K., Nakashima, K., Tokiwa, H. (1983) Identification of dinitropyrenes in diesel-exhaust particles: Their probable presence as the major mutagens. *Mutation Research*, **124**, 201-11.

Natarajan, A.T., Balajee, A.S., Boei, J.J.W.A., Chatterjee, S., Darroudi, F., Grigorova, M., Noditi, M., Oh, H.J., Slijepcevic, P., Vermeulen, S. (1994) Recent developments in the assessment of chromosomal damage. *Int J Radiat Biol*, **66**, 615-23.

Natarajan, A.T., Vyas, R.C., Darroudi, F., Mullenders, L.H.F., Zdzienicka, M.Z. (1990) DNA lesions, DNA repair, and chromosomal aberrations. In: G. Obe, A.T. Natarajan (Eds.), *Chromosomal Aberrations: Basic and Applied Aspects*, Springer Verlag, Berlin, 31-40.

Nielsen, P.S., Andreasson, A., Farmer, P.B., Ovrebo, S., Autrup, H. (1996) Biomonitoring of diesel exhaust-exposed workers: DNA and hemoglobin adducts and urinary 1-hydroxypyrene as markers of exposure. *Toxicology Letters*, **86**, 27-37.

Nielsen, P.S., De Pater, N., Okkels, H. (1996) Environmental air pollution and DNA adducts in Copenhagen bus drivers - effect of GSTM1 and NAT2 genotypes on adduct levels. *Carcinogenesis*, **17**, 1021-7.

Nielsen, P.S., Jorgensen, H.E., Larsen, J.C., Poulsen, M. (1996) City air pollution of polycyclic aromatic hydrocarbons and other mutagens: occurrence, sources and health effects. *The Science of the Total Environment*, **189/190**, 41-9.

Nishioka, M.G., Howard, C.C., Contos, D.A., Ball, L.M., Lewtas, J. (1988) Detection of hydroxylated nitro aromatic and hydroxylated nitro polycyclic aromatic compounds in an ambient air particulate extract using bioassay directed fractionation. *Environmental Science and Technology*, **22** (8), 908-15.

OECD (1988) Introduction to the OECD guidelines on genetic toxicology testing and guidance on the selection and application of assays, genetic toxicology. Organisation for Economic Cooperation and Development, Paris.

OECD (1996) Guidelines for Testing of Chemicals. Updated Guideline 473, Genetic Toxicology: In vitro Mammalian Chromosome Aberration Test. Organisation for Economic Cooperation and Development, Paris.

Ohe, T. (1984) Mutagenicity of photochemical reaction products of polycyclic aromatic hydrocarbons with nitrite. *Science of the Total Environment*, **39** (1-2), 161-75.

Ohtoshi, T., Takizawa, H., Okazaki, H., Kawasaki, S., Takeuchi, N., Ohta, K., Ito, K. (1998) Diesel exhaust particles stimulate human airway epithelial cells to produce cytokines relevant to airway inflammation *in vitro*. *Journal of Allergy and Clinical Immunology*, **101** (6-1), 778-85.

Ong, T., Whong, W.Z., Xu, J., Burcheu, B., Green, F.H.Y., Lewis, T. (1985) Genotoxicity studies of rodents exposed to coal dust and diesel emission particulates. *Environmental Research*, **37**, 399-409.

Ostby, L., Engen, S., Melbye, A., Eide, I. (1997) Mutagenicity testing of organic extracts of diesel exhaust particles after fractionation and recombination. *Arch Toxicol*, **71**, 314-9.

Pahlman, R., and Pelkonen, O. (1987) Mutagenicity studies of different polycyclic aromatic hydrocarbons: the significance of enzymatic factors and molecular structure. *Carcinogenesis*, **8** (6), 773-8.

Palitti, F. (1998) Mechanisms of the origin of chromosomal aberrations. *Mutation Research*, **404**, 133-7.

Patel T. (1995) France counts the cost of cheap diesel. *New Scientist* 1974 (146), Reed Business Information Ltd., London.

Pearce F. (1997) Devil in the diesel. *New Scientist* 25th Oct (10-13), Reed Business Information Ltd., London.

Pedersen, T.C., and Siak, J.S. (1981) The role of nitroaromatic compounds in the direct-acting mutagenicity of diesel particle extracts. *J Appl Toxicol*, **1**, 54-60.

Pemberton, R. (1996) The fate of naphthalene and n-alkylnaphthalenes during combustion, and an evaluation of the sources of these compounds in diesel exhaust emissions. Ph.D Thesis, University of Plymouth.

Pemberton, R., Tancell, P., Rhead, M., Braven, J. (1997) The effect of driving conditions on the emissions of naphthalene from a direct injection diesel engine. *4th Symposium on Transport and Air Pollution*, Avignon, 165-72.

Petch, G.S., Trier, C.J., Rhead, M.M., Fussey, D.E., Millward, G.E. (1987) The development of a novel exhaust gas sampling technique with particular relevance to polycyclic aromatic hydrocarbons. Institute of Mechanical Engineers; London. C340/87

Phillips, R.A. (1987) The genetic basis of cancer. In: I.F. Tannock, R.P. Hill (Eds.) *The Basic Science of Oncology*, Pergamon Press, New York, 24-51.

Pointet, K., RenouGonnord, N.F., Milliet, A., Jaudon, P. (1997) Quantification of polycyclic aromatic hydrocarbons (PAHs) in diesel engine combustion by GC/MS. *Bulletin de la Societe Chimique de France*, **134** (2), 133-40.

Pope, C.A., Schwartz, J., Ransom, M. (1992) Daily mortality and PM10 pollution in the Utah valley. *Archives of Environmental Health*, **42**, 211-7.

Pope, C.A.I., Bates, D.V., Raizenne, M.E. (1995) Health effects of particulate air pollution: time for reassessment? *Environmental Health Perspectives*, **103**, 472-80.

Puck, T.T., Cieciura, S.J., Robinson, A. (1958) Genetics of somatic mammalian cells. *Journal of Experimental Medicine*, **108**, 945-56.

QUARG (1993a) *Urban Air Quality in the United Kingdom. First report of the Quality of Urban Air Review Group*. Department of the Environment, London.

QUARG (1993b) *Diesel Vehicle Emissions and Urban Air Quality. Second report of the Quality of Urban Air Review Group*. Department of the Environment, London.

QUARG (1996) *Airborne Particulate Matter in the United Kingdom. Third report of the Quality of Urban Air Review Group*. Department of the Environment. London.

- Radha, S., and Natarajan, A.T. (1998) Sodium arsenite-induced chromosomal aberrations in the Xq arm of Chinese hamster cell lines. *Mutagenesis*, **13** (3), 229-34.
- Raineri, R., Andrew, A.W., Poiley, J.A. (1986) Effect of donor age on the levels of activity of rat, hamster, and human liver S9 preparations in the *Salmonella* mutagenicity assay. *Journal of Applied Toxicology*, **6**, 101-8.
- Ray, M., and Mohandas, T. (1976) Proposed banding nomenclature for the Chinese hamster chromosomes. In: Hamerton J.L. (Ed.) *Birth Defects: Original Article Series*, The National Foundation, New York, 83-91.
- Reichhardt, T. (1995) Weighing the health risks of airborne particulates. *Environmental Science & Technology*, **29** (8), 360-4.
- Repace, J.L. (1982) Indoor air pollution. *Environ. Int.*, **8**, 21-36.
- Rhead, M.M., and Trier, C.J. (1992) Fuel residues and organic combustion products in diesel exhaust emissions: sources, sampling and analysis. *Trends in Analytical Chemistry*, **11** (7), 255-9.
- Richardson, C., Williams, D., Allen, J.A., Amphlett, G., Chanter, D.O., Phillips, B. (1989) Analysis of data from *in vitro* cytogenetic assays. In: D.J. Kirkland (Ed.) *Statistical evaluation of mutagenicity test data*, Cambridge University Press, Cambridge, 141-54.
- Richold, M., Chandley, A., Ashby, J., Gatehouse, D.G., Bootman, J., Henderson, L. (1990) *In vivo* cytogenetics assays. In: D.J. Kirkland (Ed.), *Basic mutagenicity tests: UKEMS recommended procedures*, Cambridge University Press, Cambridge, 115-42.
- Rinkus, S.J., and Legator, M.S. (1980) The need for both *in vitro* and *in vivo* systems in mutagenicity screening. In: F.J. De Serres, A. Hollaender, (Eds.) *Chemical Mutagens: Principles and Methods for their Detection*, Plenum Press, New York, 365-456.
- Rosenkranz, H.S. (1987) Diesel emissions revisited: is the carcinogenicity due to a genotoxic mechanism? *Mutation Research*, **182**, 1-4.

- Savage, J.R.K., and Harvey, A.N. (1991) Revell revisited. *Mutation Research*, **250**, 307-17.
- Scheepers, P.T.J., Bos, R.P. (1992a) Combustion of diesel fuel from a toxicological perspective I. Origin of incomplete combustion products. *International Archives of Occupational and Environmental Health*, **64** (3), 149-61.
- Scheepers, P.T.J., and Bos, R.P. (1992b) Combustion of diesel fuel from a toxicological perspective II. Toxicity. *International Archives of Occupational and Environmental Health*, **64**, 163-77.
- Schlesinger, R.B. (1995) Toxicological evidence for health effects from inhaled particulate pollution: does it support the human experience? *Inhalation Toxicology*, **7**, 99-109.
- Schuetzle, D. (1983) Sampling of vehicle emissions for chemical analysis and biological testing. *Environmental Health Perspectives*, **47**, 65-80.
- Schuetzle, D., and Daisey, J.M. (1990) Identification of genotoxic agents in complex mixtures of air pollutants. In: M.D. Waters (Ed.) *Genetic Toxicology of Complex Mixtures*, Plenum Press, New York, 11-32.
- Schuetzle, D., Lee, F.S.-C., Prater, T.J., Tejada, S.B. (1980) The identification of polynuclear aromatic hydrocarbon (PAH) derivatives in mutagenic fractions of diesel particulate extracts. In: R.W. Frei, U.A.T. Brinkman (Eds.), *Mutagenicity Testing and Related Analytical Techniques*, Gordon and Breach Science Publishers, London, 193-244.
- Schuetzle, D., and Lewtas, J. (1986) Bioassay directed chemical analysis in environmental research. *Analytical Chemistry*, **58** (11), 1061A-75A.
- Scott, D., Danford, N., Dean, B.J., Kirkland, D.J., and Richardson, C. (1983) Report of the UKEMS Sub-committee on Guidelines for Mutagenicity Testing. United Kingdom Environmental Mutagen Society, Cambridge.

Scott, D., Dean, B.J., Danford, N., Kirkland, D.J. (1990) Metaphase chromosome aberration assays *in vitro*. In: D.J. Kirkland (Ed.), *Basic mutagenicity tests: UKEMS recommended procedures*, Cambridge University Press, Cambridge, 62-86.

Seaton, A., MacNee, W., Donaldson, K., Godden, D. (1995) Particulate air pollution and acute health effects. *The Lancet*, **345**, 176-8.

Seller, M.J. (1982) Ethical aspects of genetic counselling. *Journal of Medical Ethics*, **8**, 185-8.

Shelby, M.D., and Stasiewicz, S. (1984) Chemicals showing no evidence of carcinogenicity in long-term, two-species rodent studies: the need for short-term test data. *Environmental Mutagenesis*, **6**, 871-8.

Slijepcevic, P., and Natarajan, A.T. (1994) Distribution of radiation-induced G₁ exchange and terminal deletion breakpoints in Chinese hamster chromosomes as detected by G banding. *International Journal of Radiation Biology*, **66** (6), 747-55.

Slijepcevic, P., and Natarajan, A.T. (1994) Distribution of X-ray induced G₂ chromatid damage among Chinese hamster chromosome: influence of chromatin configuration. *Mutation Research*, **323**, 113-9.

Sofuni, T., Matsuoka, A., Sawada, M., Ishidate, M.J., Zeiger, E., Shelby, M.D. (1990) A comparison of chromosome aberration induction by 25 compounds tested by two Chinese hamster cell (CHL and CHO) systems in culture. *Mutation Research*, **241**, 175-213.

Strandell, M., Zakrisson, S., Alsberg, T., Westerholm, R., Winquist, L., Rannug, U. (1994) Chemical analysis and biological testing of a polar fraction of ambient air, diesel engine, and gasoline engine particulate extracts. *Environmental Health Perspectives*, **102** (Supp 4), 85-92.

Takano, H., Ichinose, T., Miyabara, Y., Yoshikawa, T., Sagai, M. (1998) Diesel exhaust particles enhance airway responsiveness following allergen exposure in mice. *Immunopharmacology and Immunotoxicology*, **20** (2), 329-36.

Tepper, J.S., Lehmann, J.R., Winsett, D.W., Costa, D.L., Ghio, A.J. (1994) The role of surface complexed iron in the development of acute lung inflammation and airway hyperresponsiveness. *Am J Resp Crit Care Med*, **149**, A839

Thompson, E.D. (1986) Comparison of *in vivo* and *in vitro* cytogenetic assay results. *Environmental Mutagenesis*, **8**, 753-67.

Tokiwa, H., Kitamori, S., Nakagawa, R., Horikawa, K., Matamala, L. (1983) Demonstration of a powerful mutagenic dinitropyrene in airborne particulate matter. *Mutation Research*, **121**, 107-16.

Tokiwa, H., Nakagawa, R., Horikawa, K., Ohkubo, A. (1987) The nature of the mutagenicity and carcinogenicity of nitrated, aromatic compounds in the environment. *Environmental Health Perspectives*, **73**, 191-9.

Topinka, J., Schwarz, L.R., Kiefer, F., Wiebel, F.J., Gajdos, O., Vidova, P., Dobias, L., Fried, M., Sram, R.J., Wolff, T. (1998) DNA adduct formation in mammalian cell cultures by polycyclic aromatic hydrocarbons (PAH) and nitro-PAH in coke oven emission extract. *Mutation Research*, **419**, 91-105.

Trier, C.J. (1988) The origin of the organic species of diesel exhaust. Ph.D Thesis, Plymouth Polytechnic.

Tweats, D.J., and Gatehouse, D.G. (1988) Further debate of testing strategies. *Mutagenesis*, **3**, 95-102.

Veigl, E., Posch, W., Linder, W., Tritthart, P. (1994) Selective and sensitive analysis of 1-nitropyrene in diesel exhaust particulate extract by multidimensional HPLC. *Chromatographia*, **38** (3-4), 199-206.

Venitt, S., Crofton-Sleigh, C., Forster, R. (1984) Bacterial mutation assays using reverse mutation. In: S. Venitt, J.M. Parry (Eds.), *Mutagenicity Testing: A Practical Approach*, IRL Press, Oxford,

Wade III, J.F., Newman, L.S. (1993) Diesel asthma: reactive airways disease following overexposure to locomotive exhaust. *Journal of Occupational Medicine*, **35** (2), 149-54.

Walker, A. (1996) Environment - a new key area for Health of the Nation? *British Medical Journal*, **313**, 1197-9.

Wang, Y.Y., Talcott, R.E., Seid, D.A., Wei, E.J. (1981) Antimutagenic properties of liver homogenate protein and glutathione on diesel exhaust particulates. *Cancer Letters*, 265-75.

Westerholm, R., Almen, J., Hang, L., Rannug, U., Egeback, K.E., Gragg, K. (1991) Chemical and biological characterisation of particulate, semi volatile phase associated compounds in diluted heavy-duty diesel exhausts: a comparison of three different semi volatile phase samplers. *Environmental Science and Technology*, **25**, 332-8.

Westerholm, R., and Egeback, K.E. (1994) Exhaust emissions from light- and heavy-duty vehicles: Chemical composition, impact of exhaust after treatment, and fuel parameters. *Environmental Health Perspectives*, **102** (supplement 4), 13-23.

White, K.L. (1986) An overview of immunotoxicology and carcinogenic polycyclic aromatic hydrocarbons. *Environ Carcinogen Rev*, **4**, 163-202.

Wilson, A.P. (1992) Cytotoxicity and viability assays. In: R.I. Freshney (Ed.) *Animal Cell Culture: A Practical Approach*, 2nd Edn. Oxford University Press, Oxford.

Wong, D., Mitchell, C.E., Wolff, R.K., Mauderly, J.L., Jeffrey, A.M. (1986) Identification of DNA damage as a result of exposure of rats to diesel engine exhaust. *Carcinogenesis*, **7**, 1595-7.

Zimmerman, F.K., and Taylor-Mayer, R.E., Eds. (1985) *Mutagenicity Testing in Environmental Pollution Control*. Ellis Horwood Ltd, Chichester.